STRUCTURE-ACTIVITY CHARACTERIZATION OF NITRIC OXIDE-RELEASING DENDRIMERS AS DUAL-ACTION ANTIBACTERIAL AGENTS

Brittany Virginia Worley

A dissertation submitted to the faculty at the University of North Carolina at Chapel Hill in partial fulfillment of the requirements for the degree of Doctor of Philosophy in the Department of Chemistry (Analytical Chemistry)

Chapel Hill
2016

Approved by:

Mark H. Schoenfisch

James W. Jorgenson

Matthew R. Lockett

James F. Cahoon

Patricia A. Miguez

ABSTRACT

Brittany Virginia Worley: Structure-Activity Characterization of Nitric Oxide-Releasing Dendrimers as Dual-Action Antibacterial Agents
(Under the direction of Mark Schoenfisch)

The increasing prevalence of antibiotic-resistant bacteria coupled with the inherent resistance of biofilm-based infections have necessitated the development of new antibacterial agents capable of eradicating biofilms without fostering resistance. Nitric oxide (NO), an endogenously produced free radical, holds great promise as an antibacterial agent due to its broad-spectrum antimicrobial action. Combining NO with contact-based biocides on a macromolecular scaffold should further enhance bactericidal action. Herein, the synthesis of NO-releasing antibacterial dendrimers and their anti-biofilm capabilities as a function of exterior modification are described.

Dual-action antibacterial agents were synthesized through the functionalization of poly(amidoamine) dendrimer scaffolds with contact-based biocides and subsequent modification with *N*-diazeniumdiolate NO donors. Quaternary ammonium- and alkyl chain-modified dendrimers were designed with a range of generations and alkyl chain lengths. Nitric oxide storage was turned so that each set of modified dendrimers exhibited similar NO totals, allowing for the evaluation of antibacterial action independent of NO-release payloads.

The antibacterial action of dual-action dendrimer biocides proved dependent on dendrimer generation, alkyl chain length, and bacterial Gram class. Longer alkyl chain modifications were significantly more bactericidal than both unmodified scaffolds and shorter alkyl chains. Efficacy

of the shorter chains was improved with higher dendrimer generations and the addition of NO release. Long alkyl chain dendrimers did not benefit from NO release due to the significant membrane damage they induced precluding intracellular NO buildup. The anti-biofilm action of alkyl chain-modified dendrimers was dependent on the biocide's ability to penetrate into the biofilm and compromise cell membranes, with longer alkyl chains improving biofilm eradication due to greater membrane intercalation. The addition of NO release enhanced the efficacy of dendrimer biocides incapable of good biofilm penetration, indicating the utility of dual-action dendrimers as broad-spectrum anti-biofilm agents.

Electrospun polyurethane fibers capable of delivering NO-releasing dendrimers were fabricated by doping dendrimers into polyurethane solutions prior to electrospinning. The electrospun fiber mats were semi-porous and exhibited sufficient water uptake, demonstrating promise as potential wound dressing materials. Dendrimer- and NO-release rates were tunable by altering the dendrimer modification and polyurethane composition. Nitric oxide-releasing fibers exhibited moderate to high antibacterial activity against planktonic bacteria with minimal cytotoxic effects.

To my family –
for your love, support, and encouragement to dream big and succeed

ACKNOWLEDGEMENTS

This dissertation was only made possible with the help of many people. First, I would like to thank my advisor, Dr. Mark Schoenfisch, for giving me the opportunity to work with him and always pushing me to grow and better myself as a scientist. I'd also like to thank him for providing both personal and professional support, especially over these last few months as I figured out my next step after grad school. Additionally, I would like to thank my undergraduate advisor, Dr. Mark Meyerhoff, for taking me into his lab and sparking my interest in analytical chemistry, as well as his continued support through both my undergraduate and graduate studies.

I have to acknowledge the entire Schoenfisch lab, both past and present, for providing a positive work environment, including their assistance with experiments, critical evaluations of my research, and general support throughout my time here. Specifically, I would like to thank Dr. Alexis Carpenter, Dr. Yuan Lu, and Dr. Danielle Slomberg, who trained me when I joined the lab and helped me develop my first research projects. I would also like to thank Dr. Wesley Storm and Dr. Chris Backlund, who were not only great friends and colleagues, but were also great mentors who continued to support my science well after their defense dates. I also need to send a huge thanks to Robert Soto, whose knowledge and expertise were critical in helping me complete some of this work. Robert is an amazing scientist and friend, and I'd like to thank him specifically for his SEM imaging, electrospinning, polymer knowledge, and general advice on life and science. Finally, I would like to thank my undergraduate researchers, Kelci Schilly and Blake Schofield, whose hard work is evidenced in several chapters of this dissertation. In particular, I'd like to acknowledge Kelci's dedication to her research project, working long hours that included

weekends and snow days. She was a fantastic undergraduate researcher, and I wish her the best of luck in the future!

I would next like to acknowledge some of the amazing facilities we have at UNC. First, all of the individuals from Chapel Hill Analytical and Nanofabrication Lab (CHANL), including Dr. Carrie Donley (XPS), Dr. Amar Kumbhar (TEM), and Dr. Wallace Ambrose (microscopy). I would also like to thank Dr. Michael Chua and Dr. Neal Kramacy at the (now defunct) Michael Hooker Microscopy Facility for their assistance with confocal microscopy.

Finally, I need to thank my family and friends, without whom I never would have made it this far. My amazing friends Elise Brown, Kelsey Clancy Dzwilewski, and Jeannie Lieder, whose love and support know no distance. To the friends I made along the way – Matt Jackson, Allan Bunch, Stephanie Moore, Emilie Mainz, and Erin Redman. No one else can quite understand the crazy life that is grad school, and I'm thankful I had all of you with me as we moved through it. I would like to thank my entire extended family, who have supported me with kind words, care packages, and free dinners throughout my entire undergraduate and graduate careers. I especially need to thank my parents, Keith and Sara, and my brother, Eric, for their continued love and encouragement. You have been wonderful and supportive parents, and I am eternally grateful for you believing in me even when I didn't believe in myself. Thank you for helping me become who I am today. Finally, I need to thank my amazing partner Josh for standing by me through my craziest moments and always making me smile. Your patience, love, and support pulled me through each pitfall and made each success brighter, and I'm thankful every day I didn't have to do this without you. To my entire family, thank you and I love you.

TABLE OF CONTENTS

LIST OF TABLES

LIST OF SCHEMES

LIST OF FIGURES

LIST OF ABBREVIATIONS AND SYMBOLS

~	approximately
°C	degree(s) Celsius
>	greater than
≥	greater than or equal to
<	less than
≤	less than or equal to
$[NO]_{max}$	maximum NO flux
%	percent
±	standard deviation of the mean
×*g*	times the force of gravity
µg	microgram(s)
µL	microliter(s)
μm^2	micrometers squared
µM	micromolar
µmol	micromole(s)
Abs	absorbance
Ag	silver
Ag^+	silver ion(s)
AHAP3	*N*-(6-aminohexyl)amino-propyltrimethoxysilane
AMP	antimicrobial peptide
Ar	argon
BP	band-pass

Ca^{2+}	calcium ion(s)
cfu	colony forming units
cGMP	cyclic guanosine monophosphate
Cl	chlorine atom(s)
Cl^{+}	oxidative chlorine
CO_2	carbon dioxide
cm	centimeter(s)
cm^{-1}	wavenumber(s)
cm^2	centimeters squared
cNOS	constitutive nitric oxide synthase
CVC	critical vesicle concentration
d	day(s)
Da	Daltons
DAF-2	4,5-diaminofluorescein
DAF-2 DA	4,5-diaminofluorescein diacetate
DETA/NO	*N*-diazeniumdiolate-modified diethylenetriamine
DMEM	Dulbecco's modified Eagle's medium
DMF	*N*,*N*-dimethylformamide
DNA	deoxyribonucleic acid
E. coli	*Eschericia coli*
E. faecalis	*Enterococcus faecalis*
EDA	ethylene diamine
e.g.	exempli gratia (for example)

et al.	et alia (and others)
eNOS	endothelial nitric oxide synthase
EPS	exopolysaccharide
eV	electron volts
FBC_{24h}	24 h fractional bactericidal concentration index
FBS	fetal bovine serum
Fe^{3+}	iron ion(s)
FISH	fluorescent in situ hybridization
FTIR	Fourier transform infrared spectroscopy
Ga	gallium
G1	generation 1
G2	generation 2
G3	generation 3
G4	generation 4
GSNO	*S*-nitroso-L-glutathione
h	hour(s)
^{1}H NMR	proton nuclear magnetic resonance
HCl	hydrochloric acid
HP 93A	Tecophilic
IC_{50}	inhibitory concentration at 50% viability
i.e.	id est (that is)
iNOS	inducible nitric oxide synthase
K. pneumonia	*Klebsiella pneumoniae*

KOH	potassium hydroxide
kV	kilovolt(s)
LB	Luria-Bertani
MAP3	*N*-methylaminopropyltrimethoxysilane
MBC_{4h}	4 h minimum bactericidal concentration
MBC_{24h}	24 h minimum bactericidal concentration
$MBEC_{24h}$	24 h minimum biofilm eradication concentration
MeOH	methanol
min	minute(s)
mg	milligram(s)
mL	milliliter(s)
mS	millisiemen(s)
mm	millimeter(s)
mM	millimolar
mmol	millimole(s)
MRSA	methicillin-resistant *Staphylococcus aureus*
MTS	3-(4,5-dimethylthiazol-2-yl)-5-(3-carboxymethoxyphenyl)-2-(4-sulfophenyl)-2H-tetrazolium inner salt
mW	milliwatt(s)
MWCO	molecular weight cutoff
n	number of dendrimer terminal end groups
N_2	nitrogen gas
N_2O_3	dinitrogen trioxide
N.A.	numerical aperature

NaOMe	sodium methoxide
nm	nanometer(s)
nM	nanomolar
NO	nitric oxide
NOA	nitric oxide analyzer
NOS	nitric oxide synthase
nNOS	neuronal nitric oxide synthase
O_2	oxygen
O_2^-	superoxide
$ONOO^-$	peroxynitrite
P. aeruginosa	*Pseudomonas aeruginosa*
PAMAM	poly(amidoamine)
PBS	phosphate buffered saline
PCR	polymerase chain reaction
PEG	poly(ethylene glycol)
pH	-log of proton concentration
PI	propidium iodide
PIA	polysaccharide intercellular adhesion
PLGA	poly(lactic-co-glycolic acid)
PLGH	poly(lactic-co-glycolic-co-hydroxymethyl propionic acid)
pM	picomolar
pmol	picomole(s)
PMS	phenazine methosulfate

ppb	parts per billion
PPI	polypropylenimine
ppm	parts per million
PROLI/NO	*N*-diazeniumdiolate-modified L-proline
PS	penicillin streptomycin
QA	quaternary ammonium
QS	quorum sensing
RIP	RNA III inhibiting peptide
RITC	rhodamine b isothiocyanate
RNA	ribonucleic acid
RSNO	*S*-nitrosothiol
s	second(s)
S. aureus	*Staphylococcus aureus*
S. epidermidis	*Staphylococcus epidermidis*
SEM	scanning electron microscope
SG 80A	Tecoflex
SNAP	*S*-nitroso-*N*-acetylpenicillamine
STAMP	selectively targeted antimicrobial peptide
$t_{1/2}$	half-life
t[NO]	total NO release
$t[NO]_{2h}$	2 h total NO release
$t[NO]_{4h}$	4 h total NO release
$t[NO]_{HCl}$	total NO release in 50 mM HCl

t_d	duration of NO release
t_{max}	time required to reach maximum NO flux
TEA	triethylamine
TEM	transmission electron microscopy
THF	tetrahydrofuran
TI	therapeutic index
TP 470	Tecoplast
TSA	tryptic soy agar
TSB	tryptic soy broth
UV	ultraviolet
v/v	volume to volume ratio
v/v/v	volume to volume to volume ratio
vis	visible
vol%	percent by volume
W_D	weight of dry fiber mat
W_H	weight of hydrated fiber mat
wt%	percent by weight
XPS	x-ray photoelectron spectroscopy
Zn^{2+}	zinc ion(s)
ZOI	zone of inhibition

CHAPTER 1:

Designing Novel Antibacterial Agents for Enhanced Biofilm Eradication

Biofilm-based infections, especially those caused by the opportunistic pathogens *Pseudomonas aeruginosa* and *Staphylococcus aureus*, continue to pose a tremendous challenge to the medical field.[1-3] Biofilms are bacterial communities encased in a protective exopolysaccharide matrix that demonstrate a variety of protective mechanisms, allowing for their persistence despite treatment with antibiotics or antiseptics.[4-6] The inability of current therapeutics to effectively eradicate biofilms promotes bacterial resistance. Nitric oxide is an endogenously produced free radical that plays a central role in the host immune response to infection, exhibits broad-spectrum antibacterial action, and is unlikely to foster resistance, making it an ideal candidate for the development of novel biocidal agents.[7-10] This chapter will describe the formation and protective mechanisms of biofilm-based infections, current research into more effective anti-biofilm therapeutics, the existing state of macromolecular scaffolds for controlled nitric oxide release, and the emergence of dual-action nitric oxide-releasing dendrimers as novel antibacterial agents.

1.1 Biofilm-based infections

Traditionally, planktonic (i.e., free-floating) bacteria have been used to evaluate antibiotic susceptibility; however, the majority of bacterial infections are believed to be caused by communities of bacteria called biofilms.[4, 11-13] As opposed to their free-floating counterparts, biofilm-based bacteria are encased in a complex exopolymeric matrix that tethers the biofilm to a surface, protecting it from invasion by antimicrobial agents (e.g., antibiotics, antiseptics).[4, 12, 14] Biofilms are significantly more difficult to treat, often requiring therapeutic doses 3–4 orders of

magnitude greater than those required to eradicate planktonic bacteria.[6, 15] It is thus important to examine the formation of these biofilm communities and the protective mechanisms that allow them to persist when designing new antibacterial agents.

1.1.1 Biofilm formation

Biofilm-based bacterial infections have been observed on most, if not all, implanted medical devices.[2, 11, 14] The formation of a biofilm is initiated by the irreversible attachment of planktonic bacteria to both living and inanimate surfaces, including human tissue and medical implants (Figure 1.1).[4-6, 11, 13, 14, 16, 17] Both the chemical properties of the underlying surface and the identity of colonizing bacterial cells impact the rate and extent of biofilm formation.[6] While biofilms have been observed on both rough and smooth surfaces ranging from very hydrophobic (e.g., Teflon, silicone) to charged and hydrophilic (e.g., glass, metal) materials, rougher and more hydrophobic materials develop biofilms more rapidly.[4] Bacterial appendages such as flagella or pili increase the rate of microbial attachment to surfaces, allowing bacteria to overcome repulsive or removal forces and remain attached.[4]

After irreversible attachment, bacteria begin to form microcolonies and secrete an exopolysaccharide (EPS) matrix that both surrounds and protects the biofilm.[4, 6, 11, 13] Although the specific composition of the EPS is dictated by the bacterial species it encloses, the matrix is generally composed of a combination of polysaccharides, proteins, glycoproteins, and DNA.[2, 4, 17] The EPS matrix provides the structural integrity critical for biofilm formation and survival.[4] During biofilm maturation, EPS synthesis is up-regulated and develops the complex biofilm

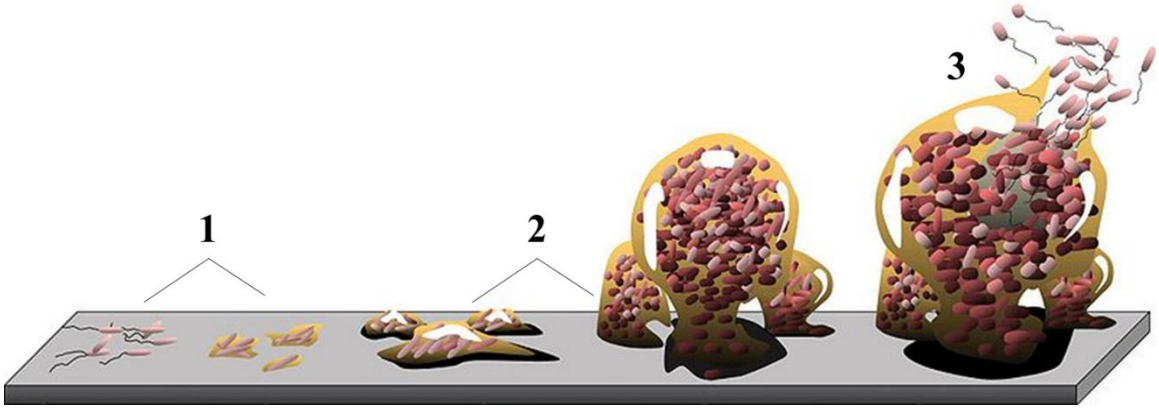

Figure 1.1 Stages of pathogenic biofilm formation: 1) initial and irreversible attachment of planktonic bacteria; 2) biofilm maturation and exopolysaccharide matrix production; 3) dispersion of planktonic cells to further infection. The biofilm community is protected from antimicrobial agents and the host immune response. Figure adapted from Monroe et al.[14] (Copyright 2007)

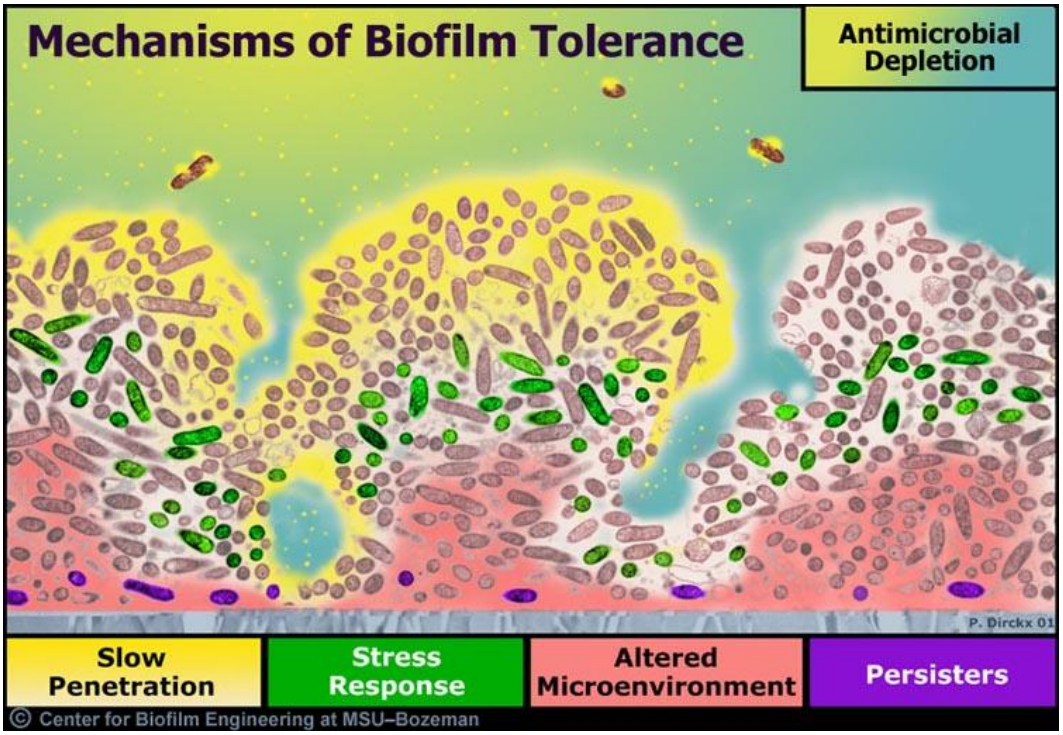

Figure 1.2 Schematic representation of biofilm protection mechanisms, including the inability of antimicrobial agents to penetrate into the biofilm (yellow), the extreme chemical microenvironment at the biofilm depths (pink), and the presence of surviving "persister" cells (purple). Reprinted with permission from the Center for Biofilm Engineering (Montana State University, Copyright 2001, www.biofilm.montana.edu).

architecture that protects the bacterial community from the immune response and antimicrobial agents.[17] The protective mechanisms of the EPS matrix will be described in detail in Section 1.1.2. The resulting EPS-confined biofilms are highly hydrated (98% water), persistently bound to the underlying surface, and heterogeneous in space, time, and bacterial composition.[4] Although *P. aeruginosa* and *S. aureus* are two of the most commonly isolated species in clinical infections, a more complex bacterial microflora has been observed with improvements in bacterial isolation techniques.[2, 18, 19] Consequently, the accumulation of a complex biofilm composed of a diverse bacterial community is considered to be responsible for promoting systemic infection via the detachment of cells and aggregates from the parent biofilm.[4]

1.1.2 Protective mechanisms of biofilms

In addition to the increasing prevalence of antibiotic resistant bacteria,[20-22] biofilm-based bacterial infections are notoriously resistant to standard antimicrobial treatment.[4-6, 23, 24] Antibiotic treatments that are effective at killing planktonic bacteria are often ineffective against biofilms, with biofilm eradication often requiring a 1,000–10,000-fold increase in therapeutic dose.[6, 15] Of importance, the common mechanisms of antibiotic resistance, including expression of efflux pumps, modified enzymes and target sites, and production of alternative metabolic pathways, are not necessarily responsible for the protection of these bacterial communities.[22, 24] Biofilms instead exhibit several unique protective mechanisms that contribute to their overall robustness (Figure 1.2).[4, 5, 24]

The first of these protective mechanisms is the inability of antimicrobial agents to penetrate beyond the surface layers of the biofilm.[5, 24] Diffusion through a biofilm may be slowed or completely prevented by charge interactions between antimicrobial agents and the EPS matrix, size exclusion by the matrix architecture, and/or reduced motility due to EPS viscosity.[5, 13] In vitro

measurements of antibiotic penetration in biofilms have exhibited a wide variation in permeation rates through such matrices, dependent on both the antibiotic structure and biofilm architecture.[23, 24] Significant limitations in biofilm penetration have been reported for beta-lactams and aminoglycosides.[23] In particular, positively-charged aminoglycosides are believed to bind to the negatively charged polymers within the biofilm, leading to antibiotic adsorption to the biofilm matrix and inhibited biofilm penetration.[24] In addition to restricted penetration, antimicrobial agents may be deactivated through reaction with or binding to the biofilm EPS matrix.[23, 25] For example, Nichols et al. demonstrated that the addition of alginate during biofilm formation reduced inhibition zones for tobramycin against *Escherichia coli* and *S. aureus*, suggesting the EPS matrix either interferes with antimicrobial action of tobramycin or inhibits its diffusion through the biofilm.[26] In a similar study, Coquet et al. observed a decrease in antimicrobial action for both tobramycin and imipenem against alginate-embedded *P. aeruginosa* biofilms compared to planktonic bacteria.[27] While the combination of tobramycin and imipenem was synergistic against planktonic cultures of *P. aeruginosa*, no synergy was displayed for the biofilm cultures.

The extreme chemical microenvironment within the biofilm further contributes to the decreased activity of antimicrobial agents.[5] Available oxygen is often consumed at the biofilm surface layers, leading to anaerobic pockets in the biofilm depths.[24] Additionally, the accumulation of acidic waste products may lead to pH gradients (>1 pH unit) between the EPS matrix and the biofilm interior.[23, 24] The pH, oxygen, and carbon dioxide gradients contribute to undesirable antibiotic effects within the deepest layers of the biofilm, where the acidic and anaerobic conditions are most dramatic.[6] In particular, aminoglycosides have demonstrated decreased efficacy against the same bacteria strains in anaerobic as opposed to aerobic conditions,[23, 24] and both aminoglycosides and tetracyclines are less effective under acidic

conditions.[6] These chemical gradients also lead to heterogeneity within the bacterial community with respect to growth states, with populations ranging from the continuously proliferating to the metabolically inactive.[5, 23, 24] The depletion of nutrients may cause bacteria to enter a slow- or non-growing state where they are protected from killing. The varied rates of bacterial growth dramatically dictate the effectiveness of antibiotics, many of which only target rapidly growing bacteria.[6, 23, 24]

Quorum sensing (QS) is a method of cell-to-cell communication between bacterial cells that allows for cell density and/or population-based gene regulation.[28, 29] Individual bacterial cells produce and release small QS signaling molecules to detect and relay information on the characteristics of the surrounding environment. The development of antibiotic and biocide tolerance or resistance phenotypes in biofilms is thought to be partially regulated by QS, although the exact mechanism is unknown.[28, 30] The dense, confined biofilm environment enables the accumulation of QS signaling molecules, triggering QS-regulated gene expression and affecting the host immune response.[28] For example, the release of various virulence factors by pathogenic bacteria is regulated by QS processes.[2, 31] In the case of *P. aeruginosa*, production of the leukocidal toxin rhamnolipid B shields against invading neutrophils and other cellular components of the host response, contributing to the persistence of *P. aeruginosa* biofilms.[2, 30]

The final proposed mechanism for increased biofilm survival is the presence of a subpopulation of "persister" bacteria that form a unique and highly protected phenotypic state.[5, 23, 24] Cells in this persister phenotype are considered to be specialized survivor cells and are neither defective nor antibiotic-stimulated.[13] The hypothesized presence of persister bacteria is based on the survival of a small population (<1% of the original bacterial community) despite prolonged, continued exposure to antibiotics[32, 33] and is further supported by the ability of bacterial biofilms

to resist killing by chemical disinfectants (e.g., chlorine bleach, glutaraldehyde, hydrogen peroxide) and antibiotics.[23, 34] Further, this subpopulation of highly persistent bacteria is observed in newly formed biofilms that are too thin to provide an adequate barrier to antibiotic diffusion or metabolic gradients.[34, 35] The presence of a persister subpopulation within a bacterial biofilm may promote the longevity and wide-spread resistance of bacteria to antimicrobial agents and disinfectants comprised of varying chemistries.

1.2 Current research into anti-biofilm therapeutics

The protective mechanisms exhibited by biofilms contributes to their ability to withstand treatment with antibiotics or antiseptics. Further, the increased occurrence of antibiotic-resistant bacteria coupled with a decline in new antibiotic research has necessitated the development of novel therapies capable of lessening or completely eliminating biofilm-based infections. This section describes the ongoing research aimed at either disrupting biofilm formation or killing established biofilms to reduce the bacterial burden in clinical infections.

1.2.1 Prevention of initial biofilm attachment

The majority of research on minimizing biofilm attachment focuses on developing or modifying surfaces to either prevent the initial bacterial adhesion (i.e., antifouling) or kill adhered bacterial cells (i.e., antimicrobial) through both passive or active strategies.[4, 13, 36] Passive strategies rely on mechanisms intrinsic to the material itself to prevent fouling as opposed to actively releasing a biocidal agent.[37] Active-release antimicrobial materials can be engineered through covalently binding, non-covalently immobilizing, or doping antimicrobial agents on or within a material to facilitate release.[36] For example, antibiotics[38-42] and silver[43-47] have been incorporated into materials to allow for localized release, which advantageously avoids large, systemic doses and maintains antimicrobial action close to the potential infection site.

As microbial cell membranes tend to be hydrophobic and negatively-charged, antifouling properties are often imparted to surfaces through chemical modification with hydrophilic or negatively charged functional groups.[48] Poly(ethylene glycol) (PEG) is one of the most highly investigated hydrophilic polymers for antifouling biomedical applications. The utility of PEG stems from reducing protein adsorption and bacterial attachment through hydration and steric effects.[49, 50] Unfortunately, resisting protein adhesion alone does not necessarily correlate with reduced bacterial adhesion due to adhesion mechanisms that do not rely on proteins and the instability of PEG coatings in physiological solutions.[51, 52] The use of negatively charged polymer coatings (e.g., heparin, albumin) has resulted in significant reductions in catheter-related infections.[53, 54] For example, a recent study demonstrated reduced adhesion of *Staphylococcus epidermidis* with a heparin-like polyurethane containing negatively charged sulfate groups.[55] Similarly, polycationic antimicrobial surfaces have been developed by tethering quaternary ammonium moieties to polymer coatings.[56-58] While the QA-modified surfaces effectively killed adhered bacteria, these immobilized antimicrobial or anti-infective agents are often only toxic to the first wave of incoming bacteria, providing little antimicrobial action once layers of dead bacterial cells accumulate.[11, 56]

Other research has focused on preventing bacterial attachment through an induced antibody response. The initial bacterial attachment is normally facilitated by adhesion proteins (adhesins), with interactions between bacterial adhesins and host tissue being critical for biofilm formation.[29] Thus, the development of antibodies for specific adhesins to inhibit bacterial adhesion and colonization was hypothesized to reduce infection.[59] Adhesins tend to be highly conserved proteins and lack major variation (~2% divergence) between similar bacterial strains, likely due to the required recognition of limited host receptors by all pathogenic strains.[59, 60] The lack in

variation between adhesins allows for the development of antibodies that should be effective against a wide range of bacterial strains. Langermann et al. reported antibodies against a single FimH adhesin protein with specificity for >90% of *E. coli* strains expressing the FimH adhesin.[61] This approach blocked the binding of *E. coli* to bladder cells in vitro. Vaccination of mice with the FimH adhesin vaccine reduced the in vivo colonization of bladder mucosa by *E. coli* by >99% and elicited a long-term immune response to FimH.[62]

Instead of studying individual adhesins, Schneewind and coworkers attempted to identify chemical reactions or binding steps that are shared by a large majority of surface proteins.[29, 63] Sortases are membrane enzymes present in many Gram-positive strains that catalyze the covalent anchoring of surface proteins to the outer peptidoglycan layer, making them an excellent target for anti-adhesion agents with broad clinical applications.[63-65] Several sortase inhibitors have been identified to date, including methane-thiosulfonate and mercurial p-hydroxymercuribenzoic acid, which block Cys184 residues in the active pocket of sortase A.[66, 67] However, these compounds exhibit poor therapeutic value due to their high toxicities.[29]

1.2.2 Exopolysaccharide matrix disruption

As the EPS matrix contributes significantly to the resistance of bacteria within biofilms to antimicrobial agents, strategies to enzymatically or chemically disrupt the biofilm matrix have become a popular approach for enhancing biofilm eradication.[13, 36] Hatch et al. demonstrated that although the production of alginate, a major component of the *P. aeruginosa* EPS matrix, inhibits the dissemination of antibiotics, treatment with the enzyme alginate lyase facilitated the diffusion of gentamicin and tobramycin through *P. aeruginosa* biofilms.[68] Similarly, Alipour et al. reported that the co-administration of alginate lyase with DNase enhanced the activity of aminoglycosides and reduced *P. aeruginosa* biofilm growth.[69] For many bacterial species (e.g., *S. epidermidis*, *S.*

aureus, *P. aeruginosa*, *E. coli*), iron (Fe^{3+}) is crucial for bacterial growth and metabolic enzyme function.[11] Gallium (Ga), alternatively, exhibits many similar features as Fe^{3+} (i.e., ionic radius) but does not perform the same functions critical for proper enzyme performance; as such, the uptake of Ga over Fe^{3+} by biological systems renders the enzymes non-functional.[11, 70] Kaneko et al. found that while *P. aeruginosa* grown in Ga concentrations >2 μM displayed a dose-dependent decrease in growth rate, sub-inhibitory Ga concentrations (1 μM) allowed for uninhibited *P. aeruginosa* growth but prevented biofilm formation.[71]

One of the most studied components of the Gram-positive EPS matrix is the polysaccharide intercellular adhesion (PIA) protein synthesized by the *icaADBC* operon in staphylococci, which is required for staphylococcal biofilm development.[36] The *ica* gene thus represents a viable potential target for the development of biofilm inhibitors. Sub-inhibitory concentrations of the common antibacterial agent povidone-iodine have exhibited anti-biofilm activity against *S. epidermidis* by reducing the transcription of the *icaADBC* operon through activation of the icaR transcriptional repressor.[72] The inhibition of PIA synthesis and staphylococcal biofilm disruption have also been demonstrated using the organosulfur compound allicin against *S. epidermidis* and sulfhydryl compounds (i.e., dithiothreitol, beta-mercaptoethanol, cysteine) against *S. aureus*.[36, 73, 74] As dimerization of specific protein domains in the presence of zinc (Zn^{2+}) are required for biofilm formation by both *S. epidermidis* and *S. aureus*, Zn^{2+} chelation was similarly shown to prevent biofilm formation by both staphylococcal bacteria, including antibiotic-resistant strains.[75]

1.2.3 Quorum sensing inhibition

Quorum sensing was introduced in Section 1.1.2 as a contributing factor in biofilm resistance to antimicrobial agents through the regulation of virulence factor release by effective cell-to-cell communication. As QS systems have been implicated in both biofilm formation and

infection, QS inhibitors have been developed to reduce bacterial pathogenicity.[28, 29] Quorum sensing inhibition is achieved through the binding of the inhibitor molecule to the QS receptor proteins, displacing the QS regulation center.[36]

Two of the leading classes of QS inhibitor candidates are furanones and RNA III inhibiting peptide (RIP).[29] Furanones in particular have been investigated for their broad-spectrum QS inhibitory mechanisms and ability to inhibit the QS centers in both Gram-negative and Gram-positive pathogens. Additionally, furanones incapable of QS inhibition have been determined to increase biofilm susceptibility to antibiotics and antiseptics. Hentzer et al. treated *P. aeruginosa* biofilms with several natural furanone compounds and found the furanones specifically targeted QS systems, inhibited virulence factor expression, and increased bacterial susceptibility to tobramycin and certain detergents.[76] The QS inhibitor RIP has also been shown to suppress pathogenic virulence, biofilm formation, and antibiotic resistance in certain staphylococcal strains.[77-80] Although RIP exhibited promising results as a QS inhibitor during studies with in vivo animal models, clinical applications have been limited due to concerns over in vivo stability and drug toxicity.[29] These concerns notwithstanding, several in vitro studies have established the potential of QS inhibitors as surface-immobilized anti-biofilm agents, qualifying their ability to disrupt biofilm formation on surfaces.[81, 82]

1.2.4 Development of novel anti-biofilm agents

Conventional therapies for eradicating bacterial biofilms are frequently ineffective, resulting in the persistence of bacterial subpopulations that exhibit increased resistance to antibacterial agents.[29, 36] Accordingly, new anti-biofilm strategies have been proposed to promote more complete killing of pathogenic biofilms. The encapsulation of traditional antibiotics within various delivery systems, including liposomes, micelles, and polymeric nanoparticles, represents

one such area.[25, 29, 36] While antibiotic delivery vehicles demonstrate several advantages, including more efficient antibiotic delivery, in vivo drug retention, and bacterial killing, fostering bacterial resistance continues to be a major drawback of these systems.

Ionic silver (Ag^+) has historically been used as an antimicrobial agent because it offers broad-spectrum activity at relatively low concentrations (0.05 ppm in PBS, ~50 ppm in biological fluids).[83-86] The antimicrobial activity of silver ions stems from a number of biocidal mechanisms, including surface binding to and damaging of bacterial cell membranes, interfering with DNA replication, poisoning respiratory enzymes, and denaturing proteins (including DNA and RNA).[83, 84, 87] Although wide-spread resistance to silver is unlikely due to its multi-mechanistic biocidal activity, bacterial resistance to silver has been observed clinically.[84, 86, 87] Several different types of silver-resistant clinical strains, mostly Gram-negative bacteria, have been recently isolated.[84-86, 88, 89] Bacterial resistance to silver is observed in two predominant forms: 1) the binding of silver by cells in the form of an intracellular complex; and, 2) the excretion of silver from microorganisms using cellular efflux pumps.[86, 89] In addition to potential bacterial resistance, silver use is associated with several clinical disadvantages. The use of silver products often leads to potential irritation or discoloration of the surrounding tissue (argyria), especially when using silver nitrate.[87] Silver-based products also poorly discriminate between healthy cells and pathogenic bacteria, resulting in toxicity to both keratinocytes and fibroblasts at bactericidal silver levels.[87, 89]

Antimicrobial peptides (AMPs) have recently been proposed as promising anti-biofilm agents. As fairly large, cationic macromolecules, AMPs exhibit broad-spectrum antimicrobial activity by binding to negatively-charged structural molecules on the microbial membrane, leading to membrane disruption and cell death.[29, 36] The ability of AMPs to permeate and damage cell

membranes makes them potentially effective against slow-growing or resistant bacteria embedded within biofilms; the development of resistance to this kind of mechanical disruption is rare.[90, 91] Unfortunately, AMPs are both difficult and expensive to synthesize in large quantities, have low specificity, and are sensitive to protease digestion, limiting current therapeutic utility.[29]

Modification of AMPs has led to the development of selectively targeted antimicrobial peptides (STAMPs), which represent a novel strategy for species-specific biofilm control. A typical STAMP contains a species-specific targeting peptide connected to an antimicrobial peptide via a 2 to 20 amino acid peptide chain.[29] This configuration allows for specific microbe targeting without reducing antibacterial activity. Eckert et al. first synthesized a *P. aeruginosa*-specific STAMP with increased bactericidal action and faster killing against *P. aeruginosa* than the non-targeted, general-killing peptide control.[92] The development of STAMPs has been extended to selectively remove both Gram-positive and Gram-negative bacterial strains from multi-species planktonic cultures.[92, 93] To date, however, the use of STAMPs alone has only resulted in inhibitory effects against *P. aeruginosa* and various cariogenic biofilms, though the co-administration of STAMPs with tobramycin has enhanced their biofilm eradication capabilities.[94]

1.3 Nitric oxide

Nitric oxide (NO) is an endogenously produced diatomic free radical that regulates several biological functions in the cardiovascular, respiratory, and nervous systems, including neurotransmission, angiogenesis, vasodilation, wound healing, and the immune response.[7, 95-103] The multifaceted roles of NO in the immune response to invading pathogenic bacteria, in particular, have led to countless investigations into the effects of exogenous NO delivery to promote bacteria killing and biofilm eradication, ultimately lessening the incidence of infection.

This section will consider the physiological roles of endogenously produced NO, including its innate antimicrobial action.

1.3.1 Physiological roles of nitric oxide

Nitric oxide is produced endogenously through the oxidation of L-arginine to L-citrulline via nitric oxide synthase (NOS).[9, 95, 96, 98] The three distinct isoforms of NOS are divided into two classes – constitutive (cNOS) and inducible (iNOS). The constitutive class encompasses the endothelial (eNOS) and neuronal (nNOS) isoforms with regulation by Ca^{2+} fluxes and binding to the messenger protein calmodulin.[95, 96] iNOS is present in epithelial, endothelial, and inflammatory cells (e.g., macrophages and neutrophils) and upregulates upon cytokine expression and/or inflammatory stimuli.[9, 95, 96] Although the three isoforms catalyze the same reaction to produce NO, they vary greatly with respect to regulation, concentration, and duration of NO production. The lowest levels of NO are produced by eNOS (pM), an enzyme located in the vascular endothelium, neurons, epithelial cells, and cardiac myocytes.[98] The low, intermittent levels of NO generated by eNOS help maintain basal vascular tone and proper blood flow and pressure.[95] Similarly, nNOS rapidly produces low, transient levels of NO (pM–nM) in neurons, skeletal muscle, and epithelial cells, allowing NO to function as a neurotransmitter in neuronal tissue.[95, 98] As might be expected, iNOS has the highest capacity for NO generation, yielding significantly greater quantities of NO (μM) per mole of enzyme per minute than either of the cNOS isoforms.[95, 98] The iNOS isoform is expressed in several cell types, particularly neutrophils and macrophages, as part of the innate immune response against invading pathogens and will be detailed further in Section 1.3.2.[95, 96, 98]

The low levels of NO produced by the cNOS isoforms readily diffuse across cell membranes to act as regulatory and signaling molecules. Within the vascular endothelium, NO

reacts with the iron center of guanylate cyclase, activating the production of cyclic guanosine monophosphate (cGMP).[95] The upregulation of cGMP leads to smooth muscle relaxation and vasodilation. Nitric oxide production in the cardiovascular system also regulates vascular tone, myocardial contractility, endothelial-leukocyte interactions, and antithrombotic effects, while NO deficiencies due to endothelium injury can lead to cardiovascular conditions such as atherosclerosis, hypertension, coronary heart disease, and stroke.[7, 95] Additionally, cNOS-derived NO acts as an intracellular messenger and neurotransmitter in the central nervous system through the stimulation of neuronal cGMP production.[97, 99] The cGMP-dependent nervous system functions of NO include regulating the firing of neurons in various areas of the brain and spinal cord, the release of specific neurotransmitters (e.g., acetylcholine, serotonin), and membrane depolarization.[99] The roles of endogenous NO span a wide range of functions in various biological systems, demonstrating its significance as a regulatory and signaling molecule.

1.3.2 Antimicrobial properties of nitric oxide

Nitric oxide production has been implicated in contributing to the innate host response to infectious pathogens.[8, 9, 96] Both iNOS and eNOS have been found in immune-system cells (e.g., macrophages, dendritic cells).[8] Infections in both humans and animal models are often associated with significant increases in endogenous NO.[96] The production of NO by iNOS is stimulated by the presence of pro-inflammatory cytokines as well as microbial byproducts (e.g., lipopolysaccharide, lipoteichoic acid).[8, 9] Low concentrations of NO (such as those released from macrophages after cytokine stimulation) upregulate the activation of iNOS, while substantially higher concentrations suppress iNOS and help prevent NO overproduction.[96] Nitric oxide demonstrates remarkably extensive antimicrobial activity with an ability to eradicate a broad range of pathogenic microorganisms, including both Gram-negative and Gram-positive bacteria, viruses,

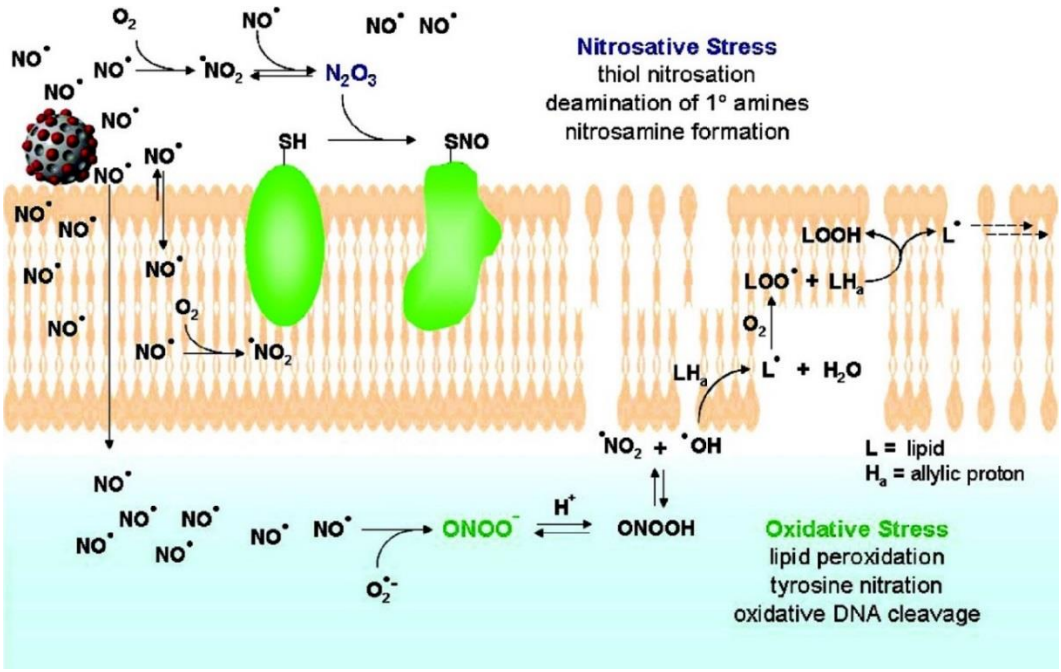

Figure 1.3 Schematic representation of the multi-mechanistic killing pathways of NO and its byproducts through the exertion of both nitrosative and oxidative stresses on bacteria. Reprinted with permission from Hetrick et al.[104] Copyright 2008, American Chemical Society.

fungi, and parasites.[8, 9, 105-107] The broad-spectrum antimicrobial action of NO is attributed to its multi-mechanistic killing pathways, exerting both nitrosative and oxidative stresses on pathogens through the formation of reactive nitrogen and oxygen intermediates (Figure 1.3).[7, 8, 104] Reactive nitrogen intermediates (e.g., N_2O_3) apply nitrosative stress to bacterial cells, modifying DNA, proteins, and lipids.[8] DNA targeting results in deamination, abasic sites, and strand breaks.[9] While nitrosation of protein thiols is one of the most important protein targets of NO, nitrosative stress can occur at heme groups, iron-sulfur clusters, or amines in addition to reactive thiols.[8, 9] Reaction of NO with superoxide (O_2^-) to form peroxynitrite ($ONOO^-$) leads to oxidative DNA and protein damage as well as lipid peroxidation.[8, 104, 108, 109] This multi-mechanistic action not only allows NO to exhibit broad-spectrum antimicrobial activity but also makes it unlikely to foster bacterial resistance.[7] Indeed, Gram-positive, Gram-negative, and antibiotic-resistant bacteria that survived exposure to lethal exogenous NO doses after several passages (20 d) demonstrated minimal increases in inhibitory NO concentrations, rendering the development of NO release a viable option for designing novel antibacterial agents that do not foster bacterial resistance.[10]

Along with potent antimicrobial action, NO shows selectivity towards invading pathogens over host mammalian cells due to their endogenous production of NO. Eukaryotic cells have developed several protective measures against NO's biocidal mechanisms at elevated concentrations. One notable means of protection is the production of metallothionein, which is upregulated by eukaryotic cells in response to oxidative stress, a major contributing mechanism to the bactericidal action of NO.[9] The expression of superoxide dismutase, an endogenously produced enzyme that removes superoxide (O_2^-) and limits peroxynitrite ($ONOO^-$) formation, also reduces the toxic side effects of NO in mammalian cells.[8, 110] However, superoxide dismutase is

less efficient than NO at scavenging superoxide, making it only partially effective at mitigating toxicity at high NO concentrations.[111]

1.4 Nitric oxide-releasing materials

Exogenous NO donors have displayed substantial antibacterial and anti-biofilm activity against a broad range of microorganisms. Indeed, applying gaseous NO to infected dermal wounds was found to reduce the microbial burden and improve wound healing.[112, 113] Both Gram-negative and Gram-positive bacteria, including antibiotic-resistant strains, have been found to be susceptible to gaseous NO.[114] Unfortunately, the rapid reactivity of gaseous NO makes its use impractical in a clinical setting, limiting any potential therapeutic utility. A number of NO donors have been developed to allow for the controlled storage and delivery of NO, with the hope of expanding the range of potential clinical applications. Several classes of NO donors exist, including metal nitrosyls, organic nitrites and nitrates, oximes, *S*-nitrosothiols (RSNOs), and *N*-diazeniumdiolates.[7, 115] To date, however, none have been translated to the clinic primarily due to challenging manufacturing issues.[7] *S*-nitrosothiol and *N*-diazeniumdiolate NO donors represent the most extensively researched NO-release agents with the greatest potential as therapeutics, though still only in the development stages.[115]

1.4.1 Nitric oxide donors

S-Nitrosothiols (RSNO) are the endogenous NO delivery vehicles within biological systems.[116, 117] On the bench, small molecule exogenous RSNO donors are synthesized through nitrosation of thiols with nitrous acid. Nitric oxide release is achieved through a number of decomposition pathways (Figure 1.4A), including homolytic cleavage of the S-NO bond by light or heat, copper ion-mediated catalytic decomposition, and reaction with reducing agents (e.g.,

ascorbate).[118] The multiple decomposition pathways and triggers to liberate NO results in certain stability issue in vivo, complicating the progression of RSNO-based therapies to the clinic.[115]

N-Diazeniumdiolate NO donors form on secondary amines under high pressures of NO gas in basic conditions to yield zwitterionic dialkylamino diazeniumdiolate salts (Figure 1.4B).[119-121] The resulting NO-releasing materials are generally stable in basic solutions or as solids at room temperature or below.[120] In aqueous solutions at neutral or acidic pH, protonation of the secondary amine nitrogen initiates NO donor breakdown, yielding two moles of NO for every mole of NO donor.[120, 122] As such, *N*-diazeniumdiolate moieties undergo spontaneous dissociation to yield biologically active NO under physiological conditions (i.e., pH 7.4), facilitating the therapeutic utility of this NO donor class. The rate of NO release is dependent on solution pH, with increasing solution acidity resulting in faster NO release.[122] Moreover, the rate and duration of NO release can be tuned by varying the identity of the amine precursor, allowing for chemical control of the NO-release kinetics.[121, 122] Similar to RSNO-based applications, no *N*-diazeniumdiolate-containing compounds have been clinically approved; however, a variety of animal studies have demonstrated the biomedical utility of *N*-diazeniumdiolate NO donors as a therapeutic source of NO.[115] Due to their increased stability and spontaneous NO release under physiological conditions, this work will primarily focus on *N*-diazeniumdiolate NO donor storage and delivery chemistries.

1.4.2 Macromolecular nitric oxide-release scaffolds

Initial investigations into the antibacterial action of NO donors were focused on the modification of low molecular weight small molecules. For example, the amino acid proline was modified with *N*-diazeniumdiolates to yield PROLI/NO, which is capable of storing large

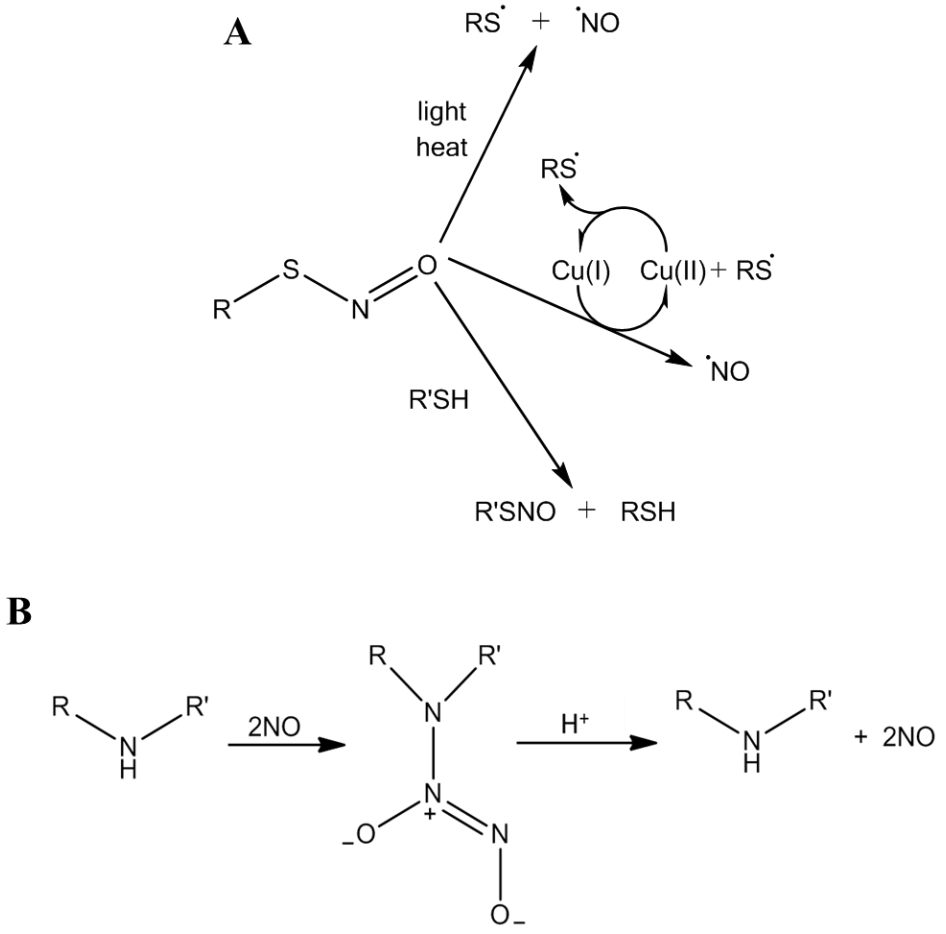

Figure 1.4 (A) Possible decomposition mechanisms for *S*-nitrosothiol (RSNO) NO donors, including heat, light, and copper-mediated decomposition. (B) Formation of *N*-diazeniumdiolate NO donors on secondary amines followed by proton-initiated decomposition to yield two moles of NO for every mole of NO donor.

quantities of NO (7.24 μmol/mg) due to the accessibility of secondary amines.[123] Poor NO donor stability triggers rapid NO release ($t_{1/2}$ = 1.8 s), however, resulting in NO liberation prior to association with bacteria and necessitating greater PROLI/NO doses for effective therapeutic action.[124] In contrast, the small molecule *N*-diazeniumdiolate-modified diethylenetriamine (DETA/NO) exhibits slower NO donor breakdown, allowing for greater broad-spectrum antibacterial activity.[125] Nevertheless, the antibacterial action of low molecular weight donors remains limited by uncontrolled NO release initiation and insufficient bacterial targeting, warranting the development of macromolecular scaffolds for NO delivery.

Modifying macromolecular scaffolds with NO-release capabilities has several advantages over small molecule NO donors, including more controllable NO payloads and release rates, modifiable surface chemistries, and reduced toxicity to mammalian cells. Several types of macromolecular scaffolds have been investigated for their NO-release capabilities, including liposomes,[126-129] metal nanoparticles,[130] metal organic frameworks,[126, 131-133] chitosan,[127, 134, 135] silica nanoparticles,[104, 136-140] and dendrimers.[141-143] The use of NO-releasing macromolecular vehicles improves both control over NO release and bacterial targeting/association. For example, the inhibitory concentration of *S*-nitrosated human serum albumin was decreased against bacteria by a factor of 5000 compared to two small molecule RSNO donors as a result of scaffold-bacteria association.[144] Hetrick et al. also observed that NO-releasing silica eradicated planktonic *P. aeruginosa* cultures at NO doses 20x lower than those required from the small molecule NO donor PROLI/NO.[104] The increase in bactericidal action was attributed to more efficient (targeted) NO delivery by the NO-releasing silica particles to the bacteria compared to PROLI/NO.

Bacterial targeting and bactericidal efficacy are also dependent on the structural characteristics of the macromolecular scaffold, including size, shape, and exterior

functionalization. Backlund and coworkers reported that NO-releasing silica nanoparticles with greater surface charge facilitated increased bacterial association, NO delivery efficiency, and bactericidal action over particles with lower zeta potential but similar NO totals and kinetics.[136] Carpenter et al. evaluated the ability of NO-releasing silica nanoparticles to reduce planktonic *P. aeruginosa* bacterial viability as a function of particle size through the synthesis of 50, 100, and 200 nm silica nanoparticles, independent of total NO payload.[137] Smaller (50 nm) particles were more effective at killing *P. aeruginosa* than larger (200 nm) particles, which was attributed to faster particle-bacteria association. In a similar study, Slomberg et al. found that 14 and 50 nm NO-releasing silica particles were more effective at killing planktonic *P. aeruginosa* than 150 nm particles.[140] Interestingly, the 50 and 150 nm NO-releasing particles exhibited similar action against planktonic Gram-positive *S. aureus* cultures, with increased bactericidal action observed for the 14 nm particles, demonstrating a dependence of Gram designation on NO antibacterial activity. Lu and coworkers expanded these studies to investigate the effects of particle shape on bactericidal activity. Nitric oxide-releasing silica nanorods were synthesized with varied aspect ratios, maintaining the same particle volume and NO release while increasing the rod length.[145] Greater antibacterial action against planktonic *P. aeruginosa* was observed with increasing aspect ratio due to more efficient NO delivery by the longer silica nanorods that associated with the bacteria longitudinally.

1.4.3 Effect of nitric oxide-releasing scaffold properties on biofilm eradication

Nitric oxide also exhibits anti-biofilm activity, including biofilm dispersion and eradication. Lancaster hypothesized that the rapid diffusion properties of NO may enhance penetration into biofilms, increasing the efficacy of NO against biofilm-encapsulated bacteria.[146] Barraud and coworkers demonstrated the ability of small molecule NO donors (i.e., sodium

nitroprusside, SNAP, GSNO) to disperse bacterial cells using *P. aeruginosa*, *E. coli*, *S. epidermidis*, and multi-species biofilms.[147, 148] To fully harness the anti-biofilm capabilities of NO, the development of NO-releasing scaffolds has focused on understanding the physicochemical properties of the scaffold with respect to enhanced biofilm eradication.

Hetrick et al. reported broad-spectrum anti-biofilm activity for NO-releasing MAP3 silica nanoparticles against Gram-negative, Gram-positive, and pathogenic fungus biofilms.[139] Further, the MAP3/NO silica nanoparticles demonstrated ~1000-fold greater efficacy against *P. aeruginosa* biofilms than the slower NO-releasing AHAP3/NO particles. This dramatic increase in anti-biofilm action was attributed to a combination of larger NO storage, faster NO-release kinetics, and the smaller size of the MAP3/NO scaffold. To further assess the effects of particle size on biofilm eradication, Slomberg et al. evaluated the anti-biofilm efficacy of NO-releasing silica nanoparticles as a function of particle size independent of NO payloads, with only a slight variation in release kinetics.[140] Smaller (14 nm) NO-releasing silica nanoparticles were more effective at eradicating both *P. aeruginosa* and *S. aureus* biofilms than larger (150 nm) particles. The greater anti-biofilm action observed for the 14 nm particles was attributed to faster association of the smaller particles with the biofilm leading to more efficient NO delivery. This study also evaluated the effects of particle shape on anti-biofilm action, with rod-like scaffolds being more effective at biofilm eradication versus the spherical particles.[140] Similar to planktonic studies, the longer, rod-shaped silica nanoparticles resulted in more efficient NO delivery and thus improved bactericidal action than spherical particles. Unfortunately, many of the NO-releasing silica scaffolds were toxic to L929 fibroblast cells at concentrations required to eradicate biofilms.[139, 140] However, the exhibited anti-biofilm efficacy of NO-releasing silica nanoparticles demonstrates the utility of NO for biofilm eradication.

1.5 Designing dual-action therapeutics

The use of antibiotic combinations has become common in clinical practice in efforts to increase the spectrum of antimicrobial activity, lower doses to circumvent toxicity, and minimize the likelihood of emerging bacterial resistance.[149] Combination therapies can be classified into four modes of action that allow for enhanced antimicrobial activity (Figure 1.5).[150] The first three modes combine a secondary adjuvant compound that augments activity of the primary drug by either 1) preventing its degradation or modification, 2) allowing for its accumulation and retention, or, 3) inhibiting the repair or tolerance mechanism of microbial cells to the primary drug. The fourth mode involves the combination of two or more mechanistically different biocides. Employing multiple compounds that work through different biocidal pathways should not only increase the bactericidal action and antibacterial sphere of influence, but also lessen the emergence of resistance due to the improbability of bacteria developing resistance to both biocidal mechanisms.[150, 151] Further, combining two or more antibacterial agents can result in synergy, where the bactericidal efficacy of the combination is more effective than their individual sums.[149, 150] As such, the design of dual-action therapeutics has become a viable option for the development of novel antibacterial agents.

Several antibiotic combinations have been successfully implemented to treat resistant bacterial infections.[150-152] A major category of combination therapy is the coupling of β-lactam class antibiotics with lactamase inhibitors (or inactivators), where the β-lactam targets the cell wall while the inhibitor prevents antibiotic degradation by the β-lactamase enzyme.[153] Combining the antibiotics trimethoprim and sulfamethoxazole, two inhibitors of folic acid metabolism, has been shown to promote synergistic bactericidal action as each inhibits a different step on the nucleotide biosynthesis pathway.[150] Other work has centered on developing compounds that render

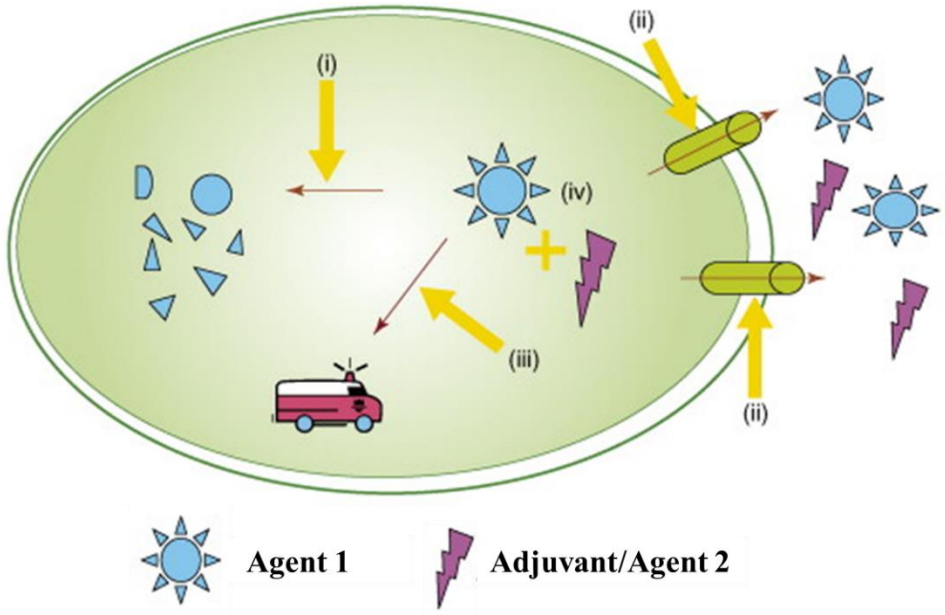

Figure 1.5 Modes of combination therapies. In the first three modes, the adjuvant (i) prevents degradation of the antibacterial agent, (ii) allows accumulation of the antibacterial agent by inhibiting efflux pumps, or (iii) inhibits cellular tolerance mechanisms. In the fourth mode (iv), both agents exhibit antibacterial activity through different biocidal mechanisms. Reprinted with permission from Cottarel et al.[150] Copyright 2007, Elsevier Ltd.

bacteriostatic drugs bactericidal. For example, the bactericidal drug Synercid (King Pharmaceuticals; Bristol, Tennessee) is the combination of two static antibacterial compounds.[152] More recent work has focused on the development of dual-action compounds on a single scaffold. For example, Oxaquin (BioVertis; Vienna, Austria) combines the therapeutic components of two different compounds in one molecule.[150, 154, 155]

The majority of dual-action antibacterial agents utilize a non-depleting, contact-based biocide as the base scaffold. Quaternary ammonium (QA) compounds are a popular non-depleting biocide due to their broad-spectrum efficacy and ability to kill bacteria without altering the QA structure, allowing for continued bactericidal activity.[156-158] The antibacterial action of QA compounds is derived from the attractive electrostatic interactions between the cationic QA group and the negatively charged bacterial cell membrane, in turn disrupting natural chemical balances by replacing essential metal cations (Figure 1.6).[156, 159] Adding alkyl chain groups to the QA moiety increases the biocidal action by promoting bacterial membrane penetration and disruption.[156, 157, 159, 160] Although their simple structure has allowed for the facile incorporation of QA moieties into a variety of systems (e.g., polymers, films, particles), tethering QAs to polymers or particles limits their action to only the bacteria that come into contact with the QA-modified surface. As a result, combining QA moieties with releasable antibacterial agents should increase the biocidal sphere of influence in addition to improving the overall bactericidal action.

To prevent biofilm formation on surfaces, Wong et al. developed layer-by-layer coatings comprised of a permanently biocidal QA-modified structure topped with hydrolytically-degradable films that allowed for the release of gentamicin.[161] Antibiotic release increased the zone of inhibition (ZOI) for the dual-functionalized films over the QA-modified base, while the biocidal QA structure resisted biofilm formation even after gentamicin depletion. In other work,

Hu et al. fabricated dual-action cellulose fibers by co-grafting *N*-halamine and QA salt monomers, allowing for the release of oxidative chlorine (Cl^+) from QA-modified cellulose.[162] The resulting dual-action fibers exhibited rapid and increased bactericidal action against Gram-negative and Gram-positive bacterial strains over the single-action QA-modified or Cl^+-releasing cellulose alone.

The efficacy of combining tethered QA moieties with releasable silver is another area of active research. Multi-layer antibacterial coatings capable of both release- and contact-based killing were produced by incorporating QA moieties and silver in a layer-by-layer method.[44, 163] For example, Grunlan et al. fabricated multi-layer films by dipping substrates into solutions containing either cetyltrimethylammonium bromide (QA moiety) or silver nitrite. The resulting dual-action films exhibited increased ZOIs against both *E. coli* and *S. aureus* versus the single-action silver-releasing films.[44] Alternatively, the antibacterial films developed by Li et al. were composed of a functional reservoir for silver ion release capped with QA-modified nanoparticles. The bactericidal action of the dual-action coatings was greater than the single-action films, with the QA nanoparticles allowing for retained antibacterial action even after silver depletion.[163] Similarly, Song et al. formed QA-modified polymer fibers doped with silver nanoparticles that were more bactericidal against *E. coli* and *S. aureus* than silver sulfadiazine.[164]

Carpenter et al. reported the synthesis of NO-releasing QA-functionalized silica nanoparticles containing methyl, butyl, octyl, or dodecyl alkyl chains.[138] All of the NO-releasing particles stored similar NO totals (~0.3 μmol NO/mg) regardless of QA modification, allowing for the evaluation of bactericidal action as a function of alkyl chain length independent of NO storage. Although the NO-releasing, QA-modified silica particles exhibited similar antibacterial action against planktonic cultures of *P. aeruginosa* as the single-action NO-releasing particles, the dual-

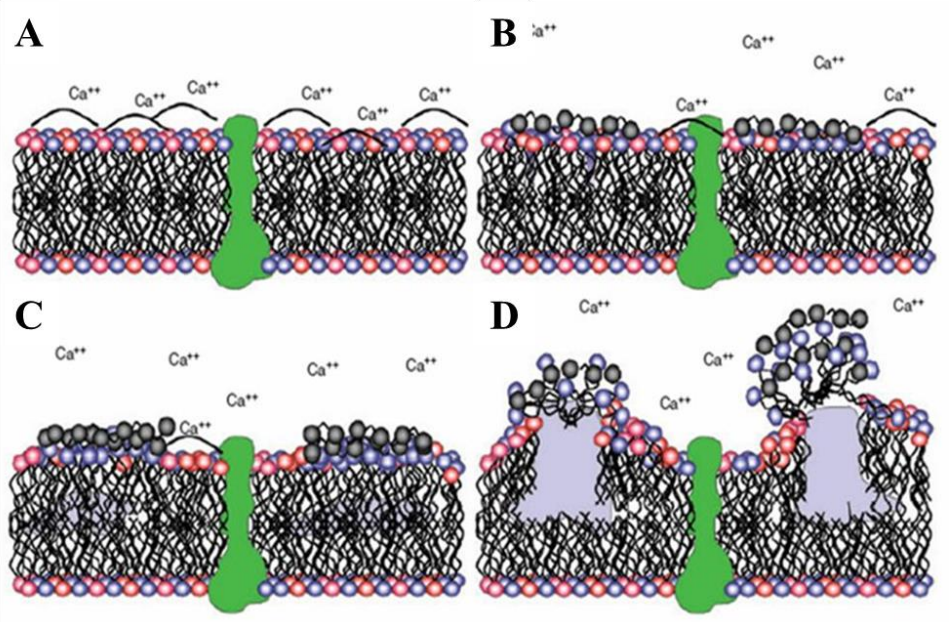

Figure 1.6 Mechanisms of action for quaternary ammonium (QA) compounds. (B, C) QA compound associate with the cell membrane, replacing essential metal cations at the cell surface. (D) Intercalation of long alkyl chains into the cell membrane leads to membrane disruption and cell death. Reprinted with permission from Gilbert et al.[159] Copyright 2005, John Wiley & Sons.

action particles were more effective at eradicating planktonic *S. aureus* than controls. Further, the bactericidal action of the NO-releasing, QA-modified particles against *S. aureus* increased with increasing alkyl chain length, establishing the benefit of combining biocidal moieties with NO release. Despite the improved antibacterial efficacy against Gram-positive bacteria, the NO-releasing, QA-modified silica particles demonstrated toxicity to L929 fibroblast cells at concentrations required to eradicate planktonic bacteria, necessitating the development of an alternative dual-action macromolecular scaffold with improved bactericidal action and negligible toxicity to mammalian cells.

1.6 Dendrimers as scaffolds for dual-action antibacterial agents

Dendrimers are a family of hyperbranched macromolecular scaffolds exhibiting unique multivalent architectures and modifiable exterior functional groups (Figure 1.7).[165, 166] Generally small in size (<5 nm) and monodisperse, dendrimers have recently been investigated as dual-action antibacterial scaffolds.[167-169] Increasing the dendrimer generation allows for synthetic control over size and the number of terminal functional groups.[170] Much work has focused on the modification of the dendrimer exterior with antibacterial functional groups, allowing for both the specific targeting of bacterial cell membranes and the combination of multiple biocides on a single scaffold.[167, 171] The ability of dendrimers to associate with, cross, or even disrupt bacterial cell membranes, combined with their small scaffold size, makes dendrimers an attractive scaffold for developing combination therapeutics.[172-174]

1.6.1 Antibacterial dendrimer scaffolds

The antibacterial action of dendrimer scaffolds is dependent on the number of bactericidal end groups and the dendrimer's ability to associate with and/or cross the bacterial cell membrane.[175] Both unmodified amino-terminated and modified (e.g., anionic, cationic, amphiphilic)

poly(amidoamine) (PAMAM) and poly(propyleneimine) (PPI) dendrimers have been shown to elicit antibacterial activity against Gram-negative and Gram-positive bacteria.[167, 168, 171-174] Xue et al. reported the ability of amino-terminated PAMAM dendrimers to inhibit the growth of *S. aureus* and *E. coli* as a function of dendrimer generation.[176] They found that the higher generations (generations 2 to 4) were more effective than the generation 1 (G1) scaffold. *S. aureus* bacteria that survived exposure to G2 PAMAM dendrimers after several passages (15 d) displayed minimal increases in inhibitory concentration, indicating a lack of induction of bacterial resistance by the dendrimer scaffold.

Amphiphilic compounds are known to perturb and disrupt bacterial cell membranes. Meyers et al. synthesized an anionic amphiphilic dendrimer scaffold that possessed efficient antibacterial activity against Gram-positive bacteria with minimal toxicity to eukaryotic cells.[171] Unfortunately, studies evaluating the effect of alkyl chain length on amphiphile bactericidal action resulted in no improvement in antimicrobial action with increasing alkyl chain length. Similarly, Tulu et al. observed antibacterial action against Gram-negative and Gram-positive pathogens with both anionic- and cationic-terminated PAMAM dendrimers, with the cationic dendrimers generally demonstrating greater bactericidal efficacy.[177]

As bacterial cell membranes are often hydrophobic and negatively charged, the use of cationic scaffolds allows for bacterial targeting leading to enhanced membrane disruption and permeation.[178] Chen et al. reported that PPI dendrimers modified with QA moieties containing alkyl chains of eight or more carbons displayed the greatest antibacterial action, with activity against *E. coli* being dependent on both dendrimer size (i.e., generation) and alkyl chain length.[160, 179] Similarly, Charles et al. observed an increased ZOI for dodecylQA-modified generation 3 (G3) PAMAM dendrimers against *E. coli* and *S. aureus* compared to butylQA and hexylQA

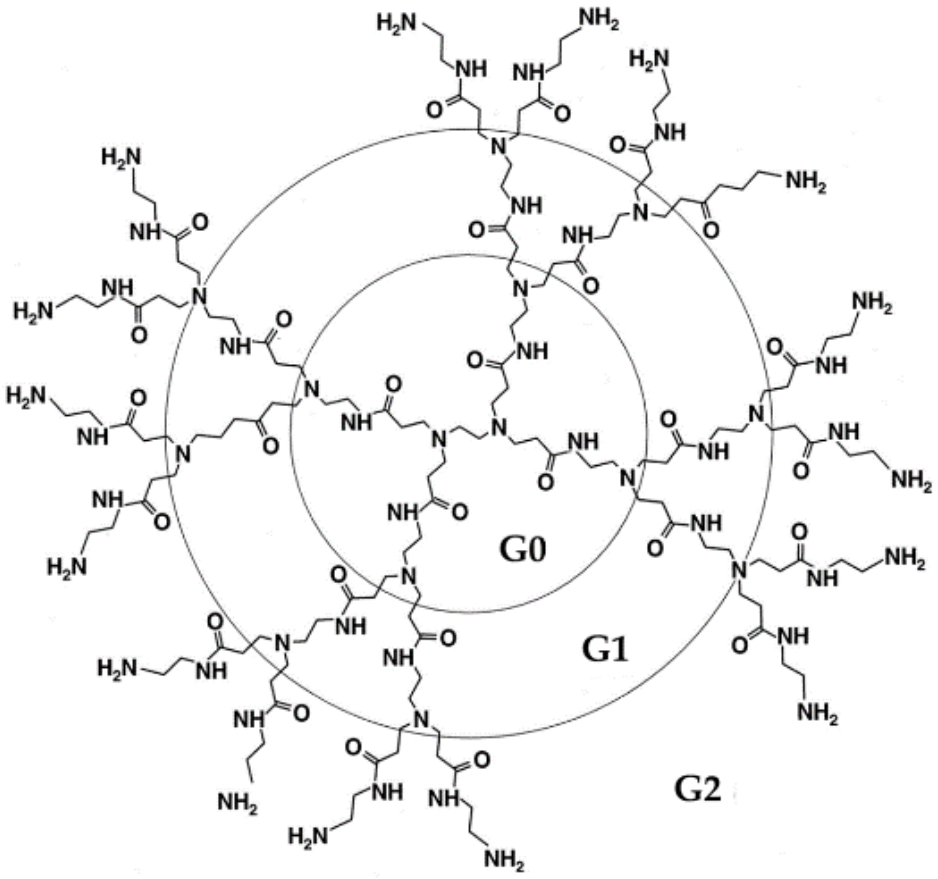

Figure 1.7 Structure of poly(amidoamine) (PAMAM) dendrimer scaffold. With each increase in generation (G0, G1, G2), dendrimer size increases linearly while the number of terminal functional groups (-NH_2) increases exponentially.

modifications, with the latter systems exhibiting negligible antibacterial action at the concentrations tested.[180] The antibacterial activity of cationic carbosilane dendrimers containing QA moieties was also reported by Javier de la Mata and coworkers.[181-183] Increasing the number of QA moieties at the exterior of the carbosilane dendrimer scaffold improved the bactericidal action against both Gram-negative and Gram-positive bacteria over amine- and single QA-functionalized dendrimers.[183] Despite establishing the potential of QA-modified dendrimers for use as antibacterial agents, these initial investigations lacked a mechanistic understanding of bactericidal efficacy as a function of bacterial Gram designation and QA alkyl chain length.

1.6.2 Nitric oxide-releasing dendrimers

Previous work in the Schoenfisch lab demonstrated the ability to modify both PPI and PAMAM dendrimers with *N*-diazeniumdiolate and *S*-nitrosothiol NO donors.[142, 143] Stasko et al. first reported the modification of PPI dendrimers with *N*-diazeniumdiolate moieties at primary amine sites.[143] Due to the instability of primary amine *N*-diazeniumdiolates, the dendrimers were further functionalized to impart secondary amines on the scaffold prior to NO donor formation. Functionalizing the dendrimer scaffold altered the NO-release kinetics, with the more hydrophobic modifications resulting in longer NO-release half-lives than their hydrophilic counterparts.[143] Increasing the dendrimer generation from G3 to G5 within the same exterior modification slightly extended the NO-release half-life, although the statistical significance is unclear.

These investigations were later expanded to include four PPI dendrimer generations (G2 – G5) and aromatic, hydrophilic, and hydrophobic functional groups.[141] Similar to the initial work, the NO-release storage and kinetics were highly dependent on exterior modification, with the more hydrophobic functional groups (e.g., benzene rings, long alkyl chains) exhibiting longer NO-release kinetics than the more hydrophilic functionalities (e.g., PEG, methyl groups). Increasing

the dendrimer generation had an indiscriminate effect on NO-release kinetics. While the more hydrophilic modifications demonstrated an increase in NO-release half-life at higher generations, little variance in the NO-release kinetics was observed for the hydrophobic groups; however, the statistical significance of these variations is again unclear.[141] Alternatively, Lu et al. modified G1 and G3 PAMAM scaffolds with a ratio of methyl and decene alkyl chains. The resulting amphiphilic dendrimers were then tuned to exhibit similar NO-release totals and half-lives regardless of the hydrophobicity ratio or dendrimer generation (though dendrimers containing only hydrophilic methyl groups still maintained slightly faster NO-release kinetics).[184] Based on these studies, the NO-release kinetics were observed to be more dependent on the hydrophobicity of the modification than the dendrimer generation.

Nitric oxide-releasing dendrimers have displayed antibacterial action against both Gram-negative and Gram-positive bacteria, including antibiotic-resistant strains. For example, Sun et al. reported the bactericidal action of G2 and G5 PPI dendrimers against planktonic cultures of *P. aeruginosa* and *S. aureus* as a function of dendrimer generation, exterior modification, and NO-release capabilities.[185] As expected, the more hydrophobic functionalities (e.g., benzene rings) were more effective at killing planktonic cultures than other modifications (e.g., PEG, methyl groups) due to increased association with the hydrophobic bacterial cell membrane. The addition of NO-release generally improved the antibacterial action of the dendrimer scaffolds against both bacterial strains. Additionally, the higher dendrimer generations exhibited greater bactericidal action than the lower generations, corresponding with more efficient NO delivery.

Lu et al. also reported on the antibacterial action of amphiphilic NO-releasing dendrimers against planktonic and biofilm-based cultures of *P. aeruginosa*.[184] Similar to previous observations, the dendrimers containing hydrophobic functional groups were more bactericidal

against planktonic *P. aeruginosa* than the hydrophilic methyl-modified dendrimers due to more rapid bacterial-association. The most hydrophobic amphiphilic compositions also resulted in greater biofilm eradication. Interestingly, the dendrimer structure exhibiting slight amphiphilicity (i.e., small ratio of hydrophilic side chains) was more effective than the purely hydrophobic-modified dendrimers at eradicating *P. aeruginosa* biofilms. This amphiphilic composition also resulted in faster and greater association of the dendrimer scaffold with the biofilm than the purely hydrophobic modification, suggesting that greater hydrophobicity may reduce the penetration of these scaffolds into the biofilm EPS matrix. Despite the greater biofilm eradication observed for the more hydrophobic long alkyl chain modifications, these dendrimers were highly toxic to L929 mouse fibroblast cells. In contrast, the less hydrophobic amphiphiles had lower toxicity to mammalian cells at their anti-biofilm concentrations, with NO release increasing the antibacterial action, highlighting the benefit of combining multiple biocides on a single dendrimer scaffold.

1.7 Summary of Dissertation Research

The goal of my dissertation research was to design NO-releasing therapeutics for the eradication of biofilm-based infections. First, I sought to develop dual-action antibacterial agents through the modification of poly(amidoamine) dendrimer scaffolds with various exterior functionalities and *N*-diazeniumdiolate NO donors. The antibacterial and anti-biofilm actions of the resulting scaffolds were next evaluated as a function of exterior modification, dendrimer generation, and NO-release capabilities. These dual-action antibacterial dendrimers were also incorporated into electrospun polyurethane fibers to produce polymers with potential utility as antibacterial wound dressings. In summary, my research aimed to:

1. Synthesize dual-action dendrimer biocides of varying dendrimer generation with distinct exterior modifications and tunable NO storage;

2. Assess the antibacterial action of dual-action dendrimers against planktonic bacteria as a function of dendrimer generation and exterior modification;
3. Evaluate the ability of dual-action dendrimers to eradicate pathogenic biofilms and determine the corresponding anti-biofilm mechanism; and,
4. Fabricate electrospun polyurethane fibers capable of antibacterial dendrimer and NO release as potential wound dressings.

In this introductory chapter, I sought to describe how the formation and protective mechanisms of bacterial biofilms allows for the persistence of infection despite treatment with antibiotics. The poor success of current anti-biofilm agents drives research related to the design of antibacterial agents capable of eradicating biofilms without fostering bacterial resistance. The synthesis and characterization of a wide range of dual-action antibacterial dendrimers exhibiting biocidal exterior modifications (i.e., quaternary ammonium moieties, alkyl chains) and tunable NO storage are described in Chapter 2. These dual-action, NO-releasing systems allowed for the detailed microbiological studies described in subsequent chapters. In Chapter 3, the antibacterial action of dual-action dendrimers was evaluated against planktonic cultures of pathogenic bacteria such as those commonly isolated in clinical infections. The ability of dual-action dendrimers to eradicate pathogenic biofilms, including *Pseudomonas aeruginosa*, *Staphylococcus aureus,* and methicillin-resistant *Staphylococcus aureus,* both alone and in concert with traditional antibiotics (i.e., vancomycin) is described in Chapter 4. Chapter 5 outlines the fabrication of single-component electrospun polyurethane fibers doped with antibacterial dendrimers modified with diverse exterior functionalities. Chapter 6 describes the study of electrospun composite polyurethane fibers as a function of polyurethane composition and dendrimer dopant. The resulting antibacterial action of these materials was evaluated against model Gram-negative and Gram-

positive pathogens. Lastly, Chapter 7 provides a final summary of my research and suggests future investigations for the further development and evaluation of NO-releasing, dual-action antibacterial agents.

REFERENCES

(1) James, G. A., Swogger, E., Wolcott, R., Secor, P., Sestrich, J., Costerton, J. W., and Stewart, P. S. "Biofilms in chronic wounds" *Wound Repair and Regeneration* **2008**, *16*, 37-44.

(2) Bjarnsholt, T., Kirketerp-Møller, K., Jensen, P. Ø., Madsen, K. G., Phipps, R., Krogfelt, K., Høiby, N., and Givskov, M. "Why chronic wounds will not heal: A novel hypothesis" *Wound Repair and Regeneration* **2008**, *16*, 2-10.

(3) Blakytny, R., and Jude, E. "The molecular biology of chronic wounds and delayed healing in diabetes" *Diabetic Medicine* **2006**, *23*, 594-608.

(4) Donlan, R. M. "Biofilm formation: A clinically relevant microbiological process" *Clinical Infectious Diseases* **2001**, *33*, 1387-1392.

(5) Donlan, R. M., and Costerton, J. W. "Biofilms: Survival mechanisms of clinically relevant microorganisms" *Clinical Microbiology Reviews* **2002**, *15*, 167-193.

(6) Dunne, W. M. "Bacterial adhesion: Seen any good biofilms lately?" *Clinical Microbiology Reviews* **2002**, *15*, 155-166.

(7) Carpenter, A. W., and Schoenfisch, M. H. "Nitric oxide release: Part II. Therapeutic applications" *Chemical Society Reviews* **2012**, *41*, 3742-3752.

(8) Fang, F. C. "Perspectives series: Host/pathogen interactions. Mechanisms of nitric oxide-related antimicrobial activity" *Journal of Clinical Investigation* **1997**, *99*, 2818.

(9) Jones, M. L., Ganopolsky, J. G., Labbé, A., Wahl, C., and Prakash, S. "Antimicrobial properties of nitric oxide and its application in antimicrobial formulations and medical devices" *Applied Microbiology and Biotechnology* **2010**, *88*, 401-407.

(10) Privett, B. J., Broadnax, A. D., Bauman, S. J., Riccio, D. A., and Schoenfisch, M. H. "Examination of bacterial resistance to exogenous nitric oxide" *Nitric Oxide* **2012**, *26*, 169-173.

(11) Bryers, J. D. "Medical biofilms" *Biotechnology and Bioengineering* **2008**, *100*, 1-18.

(12) Hall-Stoodley, L., Costerton, J. W., and Stoodley, P. "Bacterial biofilms: From the natural environment to infectious diseases" *Nature Reviews Microbiology* **2004**, *2*, 95-108.

(13) Lindsay, D., and Von Holy, A. "Bacterial biofilms within the clinical setting: What healthcare professionals should know" *Journal of Hospital Infection* **2006**, *64*, 313-325.

(14) Monroe, D. "Looking for chinks in the armor of bacterial biofilms" *PLoS Biology* **2007**, *5*, 2458-2461.

(15) Davis, S. C., Ricotti, C., Cazzaniga, A., Welsh, E., Eaglstein, W. H., and Mertz, P. M. "Microscopic and physiologic evidence for biofilm-associated wound colonization in vivo" *Wound Repair and Regeneration* **2008**, *16*, 23-29.

(16) Mustoe, T. "Understanding chronic wounds: A unifying hypothesis on their pathogenesis and implications for therapy" *The American Journal of Surgery* **2004**, *187*, S65-S70.

(17) Percival, S. L., Hill, K. E., Williams, D. W., Hooper, S. J., Thomas, D. W., and Costerton, J. W. "A review of the scientific evidence for biofilms in wounds" *Wound Repair and Regeneration* **2012**, *20*, 647-657.

(18) Altoparlak, U., Erol, S., Akcay, M. N., Celebi, F., and Kadanali, A. "The time-related changes of antimicrobial resistance patterns and predominant bacterial profiles of burn wounds and body flora of burned patients" *Burns* **2004**, *30*, 660-664.

(19) Percival, S. L., Thomas, J. G., and Williams, D. W. "Biofilms and bacterial imbalances in chronic wounds: Anti-koch" *International Wound Journal* **2010**, *7*, 169-175.

(20) Boucher, H. W., Talbot, G. H., Bradley, J. S., Edwards, J. E., Gilbert, D., Rice, L. B., Scheld, M., Spellberg, B., and Bartlett, J. "Bad bugs, no drugs: No eskape!" *Clinical Infectious Diseases* **2009**, *48*, 1-12.

(21) Nikaido, H. "Multidrug resistance in bacteria" *Annual Review of Biochemistry* **2009**, *78*, 119-146.

(22) Tenover, F. C. "Mechanisms of antimicrobial resistance in bacteria" *The American Journal of Medicine* **2006**, *119*, S3-S10.

(23) Stewart, P. S. "Mechanisms of antibiotic resistance in bacterial biofilms" *International Journal of Medical Microbiology* **2002**, *292*, 107-113.

(24) Stewart, P. S., and Costerton, J. W. "Antibiotic resistance of bacteria in biofilms" *The Lancet* **2001**, *358*, 135-138.

(25) Smith, A. W. "Biofilms and antibiotic therapy: Is there a role for combating bacterial resistance by the use of novel drug delivery systems?" *Advanced Drug Delivery Reviews* **2005**, *57*, 1539-1550.

(26) Nichols, W. W., Dorrington, S., Slack, M., and Walmsley, H. "Inhibition of tobramycin diffusion by binding to alginate" *Antimicrobial Agents and Chemotherapy* **1988**, *32*, 518-523.

(27) Coquet, L., Junter, G., and Jouenne, T. "Resistance of artificial biofilms of Pseudomonas aeruginosa to imipenem and tobramycin" *Journal of Antimicrobial Chemotherapy* **1998**, *42*, 755-760.

(28) Bjarnsholt, T., and Givskov, M. "Quorum-sensing blockade as a strategy for enhancing host defences against bacterial pathogens" *Philosophical Transactions of the Royal Society B: Biological Sciences* **2007**, *362*, 1213-1222.

(29) Chen, L., and Wen, Y. M. "The role of bacterial biofilm in persistent infections and control strategies" *International Journal of Oral Science* **2011**, *3*, 66-73.

(30) Kirketerp-Møller, K., Jensen, P. Ø., Fazli, M., Madsen, K. G., Pedersen, J., Moser, C., Tolker-Nielsen, T., Høiby, N., Givskov, M., and Bjarnsholt, T. "Distribution, organization, and ecology of bacteria in chronic wounds" *Journal of Clinical Microbiology* **2008**, *46*, 2717-2722.

(31) Rumbaugh, K. P., Diggle, S. P., Watters, C. M., Ross-Gillespie, A., Griffin, A. S., and West, S. A. "Quorum sensing and the social evolution of bacterial virulence" *Current Biology* **2009**, *19*, 341-345.

(32) Brooun, A., Liu, S., and Lewis, K. "A dose-response study of antibiotic resistance in Pseudomonas aeruginosa biofilms" *Antimicrobial Agents and Chemotherapy* **2000**, *44*, 640-646.

(33) Goto, T., Nakame, Y., Nishida, M., and Ohi, Y. "In vitro bactericidal activities of beta-lactamases, amikacin, and fluoroquinolones against Pseudomonas aeruginosa biofilm in artificial urine" *Urology* **1999**, *53*, 1058-1062.

(34) Cochran, W., McFeters, G., and Stewart, P. "Reduced susceptibility of thin Pseudomonas aeruginosa biofilms to hydrogen peroxide and monochloramine" *Journal of Applied Microbiology* **2000**, *88*, 22-30.

(35) Das, J., Bhakoo, M., Jones, M., and Gilbert, P. "Changes in the biocide susceptibility of Staphylococcus epidermidis and Escherichia coli cells associated with rapid attachment to plastic surfaces" *Journal of Applied Microbiology* **1998**, *84*, 852-858.

(36) Yang, L., Liu, Y., Wu, H., Song, Z., Høiby, N., Molin, S., and Givskov, M. "Combating biofilms" *FEMS Immunology & Medical Microbiology* **2012**, *65*, 146-157.

(37) Hetrick, E. M., and Schoenfisch, M. H. "Reducing implant-related infections: Active release strategies" *Chemical Society Reviews* **2006**, *35*, 780-789.

(38) Huang, Z. M., He, C. L., Yang, A., Zhang, Y., Han, X. J., Yin, J., and Wu, Q. "Encapsulating drugs in biodegradable ultrafine fibers through co- axial electrospinning" *Journal of Biomedical Materials Research Part A* **2006**, *77*, 169-179.

(39) Jannesari, M., Varshosaz, J., Morshed, M., and Zamani, M. "Composite poly (vinyl alcohol)/poly (vinyl acetate) electrospun nanofibrous mats as a novel wound dressing matrix for controlled release of drugs" *International Journal of Nanomedicine* **2011**, *6*, 993-1003.

(40) Said, S. S., Aloufy, A. K., El-Halfawy, O. M., Boraei, N. A., and El-Khordagui, L. K. "Antimicrobial PLGA ultrafine fibers: Interaction with wound bacteria" *European Journal of Pharmaceutics and Biopharmaceutics* **2011**, *79*, 108-118.

(41) Thakur, R., Florek, C., Kohn, J., and Michniak, B. "Electrospun nanofibrous polymeric scaffold with targeted drug release profiles for potential application as wound dressing" *International Journal of Pharmaceutics* **2008**, *364*, 87-93.

(42) Unnithan, A. R., Barakat, N. A., Pichiah, P. T., Gnanasekaran, G., Nirmala, R., Cha, Y.-S., Jung, C.-H., El-Newehy, M., and Kim, H. Y. "Wound-dressing materials with antibacterial activity from electrospun polyurethane–dextran nanofiber mats containing ciprofloxacin hcl" *Carbohydrate Polymers* **2012**, *90*, 1786-1793.

(43) Fong, J., and Wood, F. "Nanocrystalline silver dressings in wound management: A review" *International Journal of Nanomedicine* **2006**, *1*, 441-449.

(44) Grunlan, J. C., Choi, J. K., and Lin, A. "Antimicrobial behavior of polyelectrolyte multilayer films containing cetrimide and silver" *Biomacromolecules* **2005**, *6*, 1149-1153.

(45) Kostenko, V., Lyczak, J., Turner, K., and Martinuzzi, R. J. "Impact of silver-containing wound dressings on bacterial biofilm viability and susceptibility to antibiotics during prolonged treatment" *Antimicrobial Agents and Chemotherapy* **2010**, *54*, 5120-5131.

(46) Lo, S. F., Chang, C. J., Hu, W. Y., Hayter, M., and Chang, Y. T. "The effectiveness of silver- releasing dressings in the management of non-healing chronic wounds: A meta-analysis" *Journal of Clinical Nursing* **2009**, *18*, 716-728.

(47) Lo, S. F., Hayter, M., Chang, C. J., Hu, W. Y., and Lee, L. L. "A systematic review of silver- releasing dressings in the management of infected chronic wounds" *Journal of Clinical Nursing* **2008**, *17*, 1973-1985.

(48) Chen, S., Li, L., Zhao, C., and Zheng, J. "Surface hydration: Principles and applications toward low-fouling/nonfouling biomaterials" *Polymer* **2010**, *51*, 5283-5293.

(49) Chen, S., Yu, F., Yu, Q., He, Y., and Jiang, S. "Strong resistance of a thin crystalline layer of balanced charged groups to protein adsorption" *Langmuir* **2006**, *22*, 8186-8191.

(50) Sheth, S., and Leckband, D. "Measurements of attractive forces between proteins and end-grafted poly (ethylene glycol) chains" *Proceedings of the National Academy of Sciences* **1997**, *94*, 8399-8404.

(51) Ostuni, E., Chapman, R. G., Liang, M. N., Meluleni, G., Pier, G., Ingber, D. E., and Whitesides, G. M. "Self-assembled monolayers that resist the adsorption of proteins and the adhesion of bacterial and mammalian cells" *Langmuir* **2001**, *17*, 6336-6343.

(52) Wei, J., Ravn, D. B., Gram, L., and Kingshott, P. "Stainless steel modified with poly (ethylene glycol) can prevent protein adsorption but not bacterial adhesion" *Colloids and Surfaces B: Biointerfaces* **2003**, *32*, 275-291.

(53) Abdelkefi, A., Achour, W., Ben Othman, T., Ladeb, S., Torjman, L., Lakhal, A., Ben Hassen, A., Hsairi, M., and Ben Abdeladhim, A. "Use of heparin-coated central venous lines to prevent catheter-related bloodstream infection" *J Supportive Oncology* **2007**, *5*, 273-278.

(54) Jain, G., Allon, M., Saddekni, S., Barker, J.-F., and Maya, I. D. "Does heparin coating improve patency or reduce infection of tunneled dialysis catheters?" *Clinical Journal of the American Society of Nephrology* **2009**, *4*, 1787-1790.

(55) Francolini, I., Donelli, G., Vuotto, C., Baroncini, F. A., Stoodley, P., Taresco, V., Martinelli, A., D'Ilario, L., and Piozzi, A. "Antifouling polyurethanes to fight device-related Staphylococcal infections: Synthesis, characterization, and antibiofilm efficacy" *Pathogens and Disease* **2014**, *70*, 401-407.

(56) Mukherjee, K., Rivera, J. J., and Klibanov, A. M. "Practical aspects of hydrophobic polycationic bactericidal “paints”" *Applied Biochemistry and Biotechnology* **2008**, *151*, 61-70.

(57) Tiller, J. C., Lee, S. B., Lewis, K., and Klibanov, A. M. "Polymer surfaces derivatized with poly (vinyl- n- hexylpyridinium) kill airborne and waterborne bacteria" *Biotechnology and Bioengineering* **2002**, *79*, 465-471.

(58) Tiller, J. C., Liao, C.-J., Lewis, K., and Klibanov, A. M. "Designing surfaces that kill bacteria on contact" *Proceedings of the National Academy of Sciences* **2001**, *98*, 5981-5985.

(59) Wizemann, T. M., Adamou, J. E., and Langermann, S. "Adhesins as targets for vaccine development" *Emerging Infectious Diseases* **1999**, *5*, 395-403.

(60) Sokurenko, E. V., Courtney, H. S., Ohman, D. E., Klemm, P., and Hasty, D. L. "Fimh family of type 1 fimbrial adhesins: Functional heterogeneity due to minor sequence variations among fimh genes" *Journal of Bacteriology* **1994**, *176*, 748-755.

(61) Langermann, S., Palaszynski, S., Barnhart, M., Auguste, G., Pinkner, J. S., Burlein, J., Barren, P., Koenig, S., Leath, S., and Jones, C. H. "Prevention of mucosal Escherichia coli infection by fimh-adhesin-based systemic vaccination" *Science* **1997**, *276*, 607-611.

(62) Palaszynski, S., Pinkner, J., Leath, S., Barren, P., Auguste, C., Burlein, J., Hultgren, S., and Langermann, S. "Systemic immunization with conserved pilus-associated adhesins protects against mucosal infections" *Developments in Biological Standardization* **1997**, *92*, 117-122.

(63) Maresso, A. W., and Schneewind, O. "Sortase as a target of anti-infective therapy" *Pharmacological Reviews* **2008**, *60*, 128-141.

(64) Marraffini, L. A., DeDent, A. C., and Schneewind, O. "Sortases and the art of anchoring proteins to the envelopes of gram-positive bacteria" *Microbiology and Molecular Biology Reviews* **2006**, *70*, 192-221.

(65) Mazmanian, S. K., Liu, G., Ton-That, H., and Schneewind, O. "Staphylococcus aureus sortase, an enzyme that anchors surface proteins to the cell wall" *Science* **1999**, *285*, 760-763.

(66) Ton-That, H., Mazmanian, S. K., Alksne, L., and Schneewind, O. "Anchoring of surface proteins to the cell wall of Staphylococcus aureus cysteine 184 and histidine 120 of sortase form a thiolate-imidazolium ion pair for catalysis" *Journal of Biological Chemistry* **2002**, *277*, 7447-7452.

(67) Ton-That, H., and Schneewind, O. "Anchor structure of staphylococcal surface proteins IV. Inhibitors of the cell wall sorting reaction" *Journal of Biological Chemistry* **1999**, *274*, 24316-24320.

(68) Hatch, R. A., and Schiller, N. L. "Alginate lyase promotes diffusion of aminoglycosides through the extracellular polysaccharide of mucoidpseudomonas aeruginosa" *Antimicrobial Agents and Chemotherapy* **1998**, *42*, 974-977.

(69) Alipour, M., Suntres, Z. E., and Omri, A. "Importance of dnase and alginate lyase for enhancing free and liposome encapsulated aminoglycoside activity against pseudomonas aeruginosa" *Journal of Antimicrobial Chemotherapy* **2009**, *64*, 317-325.

(70) Singh, P. K. "Iron sequestration by human lactoferrin stimulates P. aeruginosa surface motility and blocks biofilm formation" *Biometals* **2004**, *17*, 267-270.

(71) Kaneko, Y., Thoendel, M., Olakanmi, O., Britigan, B. E., and Singh, P. K. "The transition metal gallium disrupts Pseudomonas aeruginosa iron metabolism and has antimicrobial and antibiofilm activity" *The Journal of Clinical Investigation* **2007**, *117*, 877-888.

(72) Oduwole, K. O., Glynn, A. A., Molony, D. C., Murray, D., Rowe, S., Holland, L. M., McCormack, D. J., and O'Gara, J. P. "Anti- biofilm activity of sub- inhibitory povidone- iodine concentrations against Staphylococcus epidermidis and Staphylococcus aureus" *Journal of Orthopaedic Research* **2010**, *28*, 1252-1256.

(73) Cruz-Villalón, G., and Pérez-Giraldo, C. "Effect of allicin on the production of polysaccharide intercellular adhesin in Staphylococcus epidermidis" *Journal of Applied Microbiology* **2011**, *110*, 723-728.

(74) Wu, X., Wang, Y., and Tao, L. "Sulfhydryl compounds reduce Staphylococcus aureus biofilm formation by inhibiting pia biosynthesis" *FEMS Microbiology Letters* **2011**, *316*, 44-50.

(75) Conrady, D. G., Brescia, C. C., Horii, K., Weiss, A. A., Hassett, D. J., and Herr, A. B. "A zinc-dependent adhesion module is responsible for intercellular adhesion in staphylococcal biofilms" *Proceedings of the National Academy of Sciences* **2008**, *105*, 19456-19461.

(76) Hentzer, M., Wu, H., Andersen, J. B., Riedel, K., Rasmussen, T. B., Bagge, N., Kumar, N., Schembri, M. A., Song, Z., and Kristoffersen, P. "Attenuation of Pseudomonas aeruginosa virulence by quorum sensing inhibitors" *The EMBO Journal* **2003**, *22*, 3803-3815.

(77) Balaban, N., Cirioni, O., Giacometti, A., Ghiselli, R., Braunstein, J. B., Silvestri, C., Mocchegiani, F., Saba, V., and Scalise, G. "Treatment of Staphylococcus aureus biofilm infection by the quorum-sensing inhibitor rip" *Antimicrobial Agents and Chemotherapy* **2007**, *51*, 2226-2229.

(78) Balaban, N., Giacometti, A., Cirioni, O., Gov, Y., Ghiselli, R., Mocchegiani, F., Viticchi, C., Del Prete, M. S., Saba, V., and Scalise, G. "Use of the quorum-sensing inhibitor RNAIII-inhibiting peptide to prevent biofilm formation in vivo by drug-resistant Staphylococcus epidermidis" *Journal of Infectious Diseases* **2003**, *187*, 625-630.

(79) Balaban, N., Stoodley, P., Fux, C. A., Wilson, S., Costerton, J. W., and Dell'Acqua, G. "Prevention of staphylococcal biofilm-associated infections by the quorum sensing inhibitor RIP" *Clinical Orthopaedics and Related Research* **2005**, *437*, 48-54.

(80) Dell'Acqua, G., Giacometti, A., Cirioni, O., Ghiselli, R., Saba, V., Scalise, G., Gov, Y., and Balaban, N. "Suppression of drug-resistant staphylococcal infections by the quorum-sensing inhibitorRNAII-inhibiting peptide" *Journal of Infectious Diseases* **2004**, *190*, 318-320.

(81) Kim, J.-H., Choi, D.-C., Yeon, K.-M., Kim, S.-R., and Lee, C.-H. "Enzyme-immobilized nanofiltration membrane to mitigate biofouling based on quorum quenching" *Environmental Science & Technology* **2011**, *45*, 1601-1607.

(82) Ng, F. S., Wright, D. M., and Seah, S. Y. "Characterization of a phosphotriesterase-like lactonase from sulfolobus solfataricus and its immobilization for disruption of quorum sensing" *Applied and Environmental Microbiology* **2011**, *77*, 1181-1186.

(83) Lipsky, B. A., and Hoey, C. "Topical antimicrobial therapy for treating chronic wounds" *Clinical Infectious Diseases* **2009**, *49*, 1541-1549.

(84) Percival, S., Bowler, P., and Russell, D. "Bacterial resistance to silver in wound care" *Journal of Hospital Infection* **2005**, *60*, 1-7.

(85) Silver, S., Phung, L. T., and Silver, G. "Silver as biocides in burn and wound dressings and bacterial resistance to silver compounds" *Journal of Industrial Microbiology and Biotechnology* **2006**, *33*, 627-634.

(86) Dunn, K., and Edwards-Jones, V. "The role of Acticoat™ with nanocrystalline silver in the management of burns" *Burns* **2004**, *30*, S1-S9.

(87) Fonder, M. A., Lazarus, G. S., Cowan, D. A., Aronson-Cook, B., Kohli, A. R., and Mamelak, A. J. "Treating the chronic wound: A practical approach to the care of nonhealing wounds and wound care dressings" *Journal of the American Academy of Dermatology* **2008**, *58*, 185-206.

(88) Landsdown, A., and Williams, A. "Bacterial resistance to silver in wound care and medical devices" *Journal of Wound Care* **2007**, *16*, 15-19.

(89) Atiyeh, B. S., Costagliola, M., Hayek, S. N., and Dibo, S. A. "Effect of silver on burn wound infection control and healing: Review of the literature" *Burns* **2007**, *33*, 139-148.

(90) Park, S.-C., Park, Y., and Hahm, K.-S. "The role of antimicrobial peptides in preventing multidrug-resistant bacterial infections and biofilm formation" *International Journal of Molecular Sciences* **2011**, *12*, 5971-5992.

(91) Batoni, G., Maisetta, G., Lisa Brancatisano, F., Esin, S., and Campa, M. "Use of antimicrobial peptides against microbial biofilms: Advantages and limits" *Current Medicinal Chemistry* **2011**, *18*, 256-279.

(92) Eckert, R., Qi, F., Yarbrough, D. K., He, J., Anderson, M. H., and Shi, W. "Adding selectivity to antimicrobial peptides: Rational design of a multidomain peptide against pseudomonas spp" *Antimicrobial Agents and Chemotherapy* **2006**, *50*, 1480-1488.

(93) He, J., Anderson, M. H., Shi, W., and Eckert, R. "Design and activity of a 'dual-targeted'antimicrobial peptide" *International Journal of Antimicrobial Agents* **2009**, *33*, 532-537.

(94) Eckert, R. H., Yarbrough, D. K., Shi, W., Anderson, M. H., Qi, F., He, J., and McHardy, I. H. "Selectively targeted antimicrobial peptides and the use thereof", US Patent: US8680058 B2 **2014**.

(95) Loscalzo, J., and Welch, G. "Nitric oxide and its role in the cardiovascular system" *Progress in Cardiovascular Diseases* **1995**, *38*, 87-104.

(96) Bogdan, C. "Nitric oxide and the immune response" *Nature Immunology* **2001**, *2*, 907-916.

(97) Garthwaite, J., and Boulton, C. "Nitric oxide signaling in the central nervous system" *Annual Review of Physiology* **1995**, *57*, 683-706.

(98) Hill, B. G., Dranka, B. P., Bailey, S. M., Lancaster, J. R., and Darley-Usmar, V. M. "What part of no don't you understand? Some answers to the cardinal questions in nitric oxide biology" *Journal of Biological Chemistry* **2010**, *285*, 19699-19704.

(99) Prast, H., and Philippu, A. "Nitric oxide as modulator of neuronal function" *Progress in Neurobiology* **2001**, *64*, 51-68.

(100) Rizk, M., Witte, M. B., and Barbul, A. "Nitric oxide and wound healing" *World Journal of Surgery* **2004**, *28*, 301-306.

(101) Schäffer, M. R., Tantry, U., Gross, S. S., Wasserkrug, H. L., and Barbul, A. "Nitric oxide regulates wound healing" *Journal of Surgical Research* **1996**, *63*, 237-240.

(102) Schwentker, A., Vodovotz, Y., Weller, R., and Billiar, T. R. "Nitric oxide and wound repair: Role of cytokines?" *Nitric Oxide* **2002**, *7*, 1-10.

(103) Witte, M. B., and Barbul, A. "Role of nitric oxide in wound repair" *The American Journal of Surgery* **2002**, *183*, 406-412.

(104) Hetrick, E. M., Shin, J. H., Stasko, N. A., Johnson, C. B., Wespe, D. A., Holmuhamedov, E., and Schoenfisch, M. H. "Bactericidal efficacy of nitric oxide-releasing silica nanoparticles" *ACS Nano* **2008**, *2*, 235-246.

(105) Augusto, O., Linares, E., and Giorgio, S. "Possible roles of nitric oxide and peroxynitrite in murine leishmaniasis" *Brazilian Journal of Medical and Biological Research* **1996**, *29*, 853-862.

(106) Kawanishi, M. "Nitric oxide inhibits epstein-barr virus DNA replication and activation of latent ebv" *Intervirology* **1995**, *38*, 206-213.

(107) Vazquez-Torres, A., Jones-Carson, J., and Balish, E. "Peroxynitrite contributes to the candidacidal activity of nitric oxide-producing macrophages" *Infection and Immunity* **1996**, *64*, 3127-3133.

(108) Babbs, C. F., and Steiner, M. G. "Simulation of free radical reactions in biology and medicine: A new two-compartment kinetic model of intracellular lipid peroxidation" *Free Radical Biology and Medicine* **1990**, *8*, 471-485.

(109) Fukuto, J. M., Cho, J. Y., and Switzer, C. H. "The chemical properties of nitric oxide and related nitrogen oxides" *Nitric Oxide: Biology and Pathobiology* **2000**, 23-40.

(110) Beckman, J. S., Beckman, T. W., Chen, J., Marshall, P. A., and Freeman, B. A. "Apparent hydroxyl radical production by peroxynitrite: Implications for endothelial injury from nitric oxide and superoxide" *Proceedings of the National Academy of Sciences* **1990**, *87*, 1620-1624.

(111) Beckman, J. S., and Koppenol, W. H. "Nitric oxide, superoxide, and peroxynitrite: The good, the bad, and ugly" *American Journal of Physiology-Cell Physiology* **1996**, *271*, C1424-C1437.

(112) Shekhter, A. B., Serezhenkov, V. A., Rudenko, T. G., Pekshev, A. V., and Vanin, A. F. "Beneficial effect of gaseous nitric oxide on the healing of skin wounds" *Nitric Oxide* **2005**, *12*, 210-219.

(113) Stenzler, A., and Miller, C. C. "Device and method for treatment of wounds with nitric oxide", US Patent: US7520866 B2 **2009**.

(114) Ghaffari, A., Miller, C., McMullin, B., and Ghahary, A. "Potential application of gaseous nitric oxide as a topical antimicrobial agent" *Nitric Oxide* **2006**, *14*, 21-29.

(115) Jen, M. C., Serrano, M. C., van Lith, R., and Ameer, G. A. "Polymer-based nitric oxide therapies: Recent insights for biomedical applications" *Advanced Functional Materials* **2012**, *22*, 239-260.

(116) Martínez-Ruiz, A., Cadenas, S., and Lamas, S. "Nitric oxide signaling: Classical, less classical, and nonclassical mechanisms" *Free Radical Biology and Medicine* **2011**, *51*, 17-29.

(117) Stamler, J. S., Jaraki, O., Osborne, J., Simon, D. I., Keaney, J., Vita, J., Singel, D., Valeri, C. R., and Loscalzo, J. "Nitric oxide circulates in mammalian plasma primarily as an s-nitroso adduct of serum albumin" *Proceedings of the National Academy of Sciences* **1992**, *89*, 7674-7677.

(118) Hogg, N. "The biochemistry and physiology of s-nitrosothiols" *Annual Review of Pharmacology and Toxicology* **2002**, *42*, 585-600.

(119) Bohle, D. S., and Smith, K. N. "Kinetics and mechanism of nucleophilic addition to nitric oxide: Secondary amine diazeniumdiolation" *Inorganic Chemistry* **2008**, *47*, 3925-3927.

(120) Dutton, A. S., Fukuto, J. M., and Houk, K. "The mechanism of no formation from the decomposition of dialkylamino diazeniumdiolates: Density functional theory and cbs-qb3 predictions" *Inorganic Chemistry* **2004**, *43*, 1039-1045.

(121) Hrabie, J. A., and Keefer, L. K. "Chemistry of the nitric oxide-releasing diazeniumdiolate ("nitrosohydroxylamine") functional group and its oxygen-substituted derivatives" *Chemical Reviews* **2002**, *102*, 1135-1154.

(122) Davies, K. M., Wink, D. A., Saavedra, J. E., and Keefer, L. K. "Chemistry of the diazeniumdiolates. 2. Kinetics and mechanism of dissociation to nitric oxide in aqueous solution" *Journal of the American Chemical Society* **2001**, *123*, 5473-5481.

(123) Hunter, R. A., Storm, W. L., Coneski, P. N., and Schoenfisch, M. H. "Inaccuracies of nitric oxide measurement methods in biological media" *Analytical Chemistry* **2013**, *85*, 1957-1963.

(124) Keefer, L. K., and Saavedra, J. E. "Nitrogen-based diazeniumdiolates: Versatile nitric oxide-releasing compounds for biomedical research and potential clinical applications" *Journal of Chemical Education* **2002**, *79*, 1427-1434.

(125) Raulli, R., McElhaney-Feser, G., Hrabie, J., and Cihlar, R. "Antimicrobial properties of nitric oxide using diazeniumdiolates as the nitric oxide donor" *Recent Research Developments in Microbiology* **2002**, *6*, 177-83.

(126) Riccio, D. A., and Schoenfisch, M. H. "Nitric oxide release: Part I. Macromolecular scaffolds" *Chemical Society Reviews* **2012**, *41*, 3731-3741.

(127) Seabra, A. B., and Durán, N. "Nitric oxide-releasing vehicles for biomedical applications" *Journal of Materials Chemistry* **2010**, *20*, 1624-1637.

(128) Suchyta, D. J., and Schoenfisch, M. H. "Encapsulation of N-diazeniumdiolates within liposomes for enhanced nitric oxide donor stability and delivery" *Molecular Pharmaceutics* **2015**, *12*, 3569-3574.

(129) Tai, L.-A., Wang, Y.-C., and Yang, C.-S. "Heat-activated sustaining nitric oxide release from zwitterionic diazeniumdiolate loaded in thermo-sensitive liposomes" *Nitric Oxide* **2010**, *23*, 60-64.

(130) Rothrock, A. R., Donkers, R. L., and Schoenfisch, M. H. "Synthesis of nitric oxide-releasing gold nanoparticles" *Journal of the American Chemical Society* **2005**, *127*, 9362-9363.

(131) Liu, H. A., and Balkus Jr, K. J. "Novel delivery system for the bioregulatory agent nitric oxide" *Chemistry of Materials* **2009**, *21*, 5032-5041.

(132) Nguyen, J. G., Tanabe, K. K., and Cohen, S. M. "Postsynthetic diazeniumdiolate formation and no release from mofs" *CrystEngComm* **2010**, *12*, 2335-2338.

(133) Wheatley, P. S., Butler, A. R., Crane, M. S., Fox, S., Xiao, B., Rossi, A. G., Megson, I. L., and Morris, R. E. "NO-releasing zeolites and their antithrombotic properties" *Journal of the American Chemical Society* **2006**, *128*, 502-509.

(134) Lu, Y., Slomberg, D. L., and Schoenfisch, M. H. "Nitric oxide-releasing chitosan oligosaccharides as antibacterial agents" *Biomaterials* **2014**, *35*, 1716-1724.

(135) Reighard, K. P., Hill, D. B., Dixon, G. A., Worley, B. V., and Schoenfisch, M. H. "Disruption and eradication of P. aeruginosa biofilms using nitric oxide-releasing chitosan oligosaccharides" *Biofouling* **2015**, *31*, 775-787.

(136) Backlund, C., Worley, B., Sergesketter, A., and Schoenfisch, M. H. "Kinetic-dependent killing of oral pathogens with nitric oxide" *Journal of Dental Research* **2015**, *94*, 1092-1098.

(137) Carpenter, A. W., Slomberg, D. L., Rao, K. S., and Schoenfisch, M. H. "Influence of scaffold size on bactericidal activity of nitric oxide-releasing silica nanoparticles" *ACS Nano* **2011**, *5*, 7235-7244.

(138) Carpenter, A. W., Worley, B. V., Slomberg, D. L., and Schoenfisch, M. H. "Dual action antimicrobials: Nitric oxide release from quaternary ammonium-functionalized silica nanoparticles" *Biomacromolecules* **2012**, *13*, 3334-3342.

(139) Hetrick, E. M., Shin, J. H., Paul, H. S., and Schoenfisch, M. H. "Anti-biofilm efficacy of nitric oxide-releasing silica nanoparticles" *Biomaterials* **2009**, *30*, 2782-2789.

(140) Slomberg, D. L., Lu, Y., Broadnax, A. D., Hunter, R. A., Carpenter, A. W., and Schoenfisch, M. H. "Role of size and shape on biofilm eradication for nitric oxide-releasing silica nanoparticles" *ACS Applied Materials & Interfaces* **2013**, *5*, 9322-9329.

(141) Lu, Y., Sun, B., Li, C., and Schoenfisch, M. H. "Structurally diverse nitric oxide-releasing poly (propylene imine) dendrimers" *Chemistry of Materials* **2011**, *23*, 4227-4233.

(142) Stasko, N. A., Fischer, T. H., and Schoenfisch, M. H. "S-nitrosothiol-modified dendrimers as nitric oxide delivery vehicles" *Biomacromolecules* **2008**, *9*, 834-841.

(143) Stasko, N. A., and Schoenfisch, M. H. "Dendrimers as a scaffold for nitric oxide release" *Journal of the American Chemical Society* **2006**, *128*, 8265-8271.

(144) Ishima, Y., Sawa, T., Kragh-Hansen, U., Miyamoto, Y., Matsushita, S., Akaike, T., and Otagiri, M. "S-nitrosylation of human variant albumin liprizzi (r410c) confers potent antibacterial and cytoprotective properties" *Journal of Pharmacology and Experimental Therapeutics* **2007**, *320*, 969-977.

(145) Lu, Y., Slomberg, D. L., Sun, B., and Schoenfisch, M. H. "Shape- and nitric oxide flux-dependent bactericidal activity of nitric oxide-releasing silica nanorods" *Small* **2013**, *9*, 2189-2198.

(146) Lancaster, J. "A tutorial on the diffusibility and reactivity of free nitric oxide" *Nitric Oxide* **1997**, *1*, 18-30.

(147) Barraud, N., Hassett, D. J., Hwang, S.-H., Rice, S. A., Kjelleberg, S., and Webb, J. S. "Involvement of nitric oxide in biofilm dispersal of pseudomonas aeruginosa" *Journal of Bacteriology* **2006**, *188*, 7344-7353.

(148) Barraud, N., Storey, M. V., Moore, Z. P., Webb, J. S., Rice, S. A., and Kjelleberg, S. "Nitric oxide-mediated dispersal in single-and multi-species biofilms of clinically and industrially relevant microorganisms" *Microbial Biotechnology* **2009**, *2*, 370-378.

(149) Eliopoulos, G., and Eliopoulos, C. "Antibiotic combinations: Should they be tested?" *Clinical Microbiology Reviews* **1988**, *1*, 139-156.

(150) Cottarel, G., and Wierzbowski, J. "Combination drugs, an emerging option for antibacterial therapy" *Trends in Biotechnology* **2007**, *25*, 547-555.

(151) Fischbach, M. A. "Combination therapies for combating antimicrobial resistance" *Current Opinion in Microbiology* **2011**, *14*, 519-523.

(152) Jones, R. N., Ballow, C. H., Biedenbach, D. J., Deinhart, J. A., and Schentag, J. J. "Antimicrobial activity of quinupristin-dalfopristin (rp 59500, synercid®) tested against over 28,000 recent clinical isolates from 200 medical centers in the united states and canada" *Diagnostic Microbiology and Infectious Disease* **1998**, *31*, 437-451.

(153) Navarro, A. S. "New formulations of amoxicillin/clavulanic acid" *Clinical Pharmacokinetics* **2005**, *44*, 1097-1115.

(154) Bradbury, B. J., and Pucci, M. J. "Recent advances in bacterial topoisomerase inhibitors" *Current Opinion in Pharmacology* **2008**, *8*, 574-581.

(155) Fox, J. L. "The business of developing antibacterials" *Nature Biotechnology* **2006**, *24*, 1521-1528.

(156) Simoncic, B., and Tomsic, B. "Structures of novel antimicrobial agents for textiles-a review" *Textile Research Journal* **2010**, *80*, 1721-1737.

(157) Thorsteinsson, T., Másson, M., Kristinsson, K. G., Hjálmarsdóttir, M. A., Hilmarsson, H., and Loftsson, T. "Soft antimicrobial agents: Synthesis and activity of labile environmentally friendly long chain quaternary ammonium compounds" *Journal of Medicinal Chemistry* **2003**, *46*, 4173-4181.

(158) Xue, Y., Xiao, H., and Zhang, Y. "Antimicrobial polymeric materials with quaternary ammonium and phosphonium salts" *International Journal of Molecular Sciences* **2015**, *16*, 3626-3655.

(159) Gilbert, P., and Moore, L. "Cationic antiseptics: Diversity of action under a common epithet" *Journal of Applied Microbiology* **2005**, *99*, 703-715.

(160) Chen, C. Z., Beck-Tan, N. C., Dhurjati, P., van Dyk, T. K., LaRossa, R. A., and Cooper, S. L. "Quaternary ammonium functionalized poly (propylene imine) dendrimers as effective antimicrobials: Structure-activity studies" *Biomacromolecules* **2000**, *1*, 473-480.

(161) Wong, S. Y., Moskowitz, J. S., Veselinovic, J., Rosario, R. A., Timachova, K., Blaisse, M. R., Fuller, R. C., Klibanov, A. M., and Hammond, P. T. "Dual functional polyelectrolyte multilayer coatings for implants: Permanent microbicidal base with controlled release of therapeutic agents" *Journal of the American Chemical Society* **2010**, *132*, 17840-17848.

(162) Hu, B., Chen, X., Zuo, Y., Liu, Z., and Xing, X. "Dual action bactericides: Quaternary ammonium/n-halamine-functionalized cellulose fiber" *Journal of Applied Polymer Science* **2014**, *131*, 40070-40076.

(163) Li, Z., Lee, D., Sheng, X., Cohen, R. E., and Rubner, M. F. "Two-level antibacterial coating with both release-killing and contact-killing capabilities" *Langmuir* **2006**, *22*, 9820-9823.

(164) Song, J., Kang, H., Lee, C., Hwang, S. H., and Jang, J. "Aqueous synthesis of silver nanoparticle embedded cationic polymer nanofibers and their antibacterial activity" *ACS Applied Materials & Interfaces* **2011**, *4*, 460-465.

(165) Tomalia, D., Baker, H., Dewald, J., Hall, M., Kallos, G., Martin, S., Roeck, J., Ryder, J., and Smith, P. "A new class of polymers: Starburst-dendritic macromolecules" *Polymer Journal* **1985**, *17*, 117-132.

(166) Tomalia, D. A. "Birth of a new macromolecular architecture: Dendrimers as quantized building blocks for nanoscale synthetic polymer chemistry" *Progress in Polymer Science* **2005**, *30*, 294-324.

(167) Duncan, R., and Izzo, L. "Dendrimer biocompatibility and toxicity" *Advanced Drug Delivery Reviews* **2005**, *57*, 2215-2237.

(168) Malik, N., Wiwattanapatapee, R., Klopsch, R., Lorenz, K., Frey, H., Weener, J., Meijer, E., Paulus, W., and Duncan, R. "Dendrimers: Relationship between structure and biocompatibility in vitro, and preliminary studies on the biodistribution of 125I-labelled polyamidoamine dendrimers in vivo" *Journal of Controlled Release* **2000**, *65*, 133-148.

(169) Svenson, S. "Dendrimers as versatile platform in drug delivery applications" *European Journal of Pharmaceutics and Biopharmaceutics* **2009**, *71*, 445-462.

(170) Maiti, P. K., Cagin, T., Wang, G., and Goddard, W. A. "Structure of PAMAM dendrimers: Generations 1 through 11" *Macromolecules* **2004**, *37*, 6236-6254.

(171) Meyers, S. R., Juhn, F. S., Griset, A. P., Luman, N. R., and Grinstaff, M. W. "Anionic amphiphilic dendrimers as antibacterial agents" *Journal of the American Chemical Society* **2008**, *130*, 14444-14445.

(172) Jevprasesphant, R., Penny, J., Attwood, D., McKeown, N. B., and D'Emanuele, A. "Engineering of dendrimer surfaces to enhance transepithelial transport and reduce cytotoxicity" *Pharmaceutical Research* **2003**, *20*, 1543-1550.

(173) Mecke, A., Uppuluri, S., Sassanella, T. M., Lee, D.-K., Ramamoorthy, A., Baker, J. R., Orr, B. G., and Holl, M. M. B. "Direct observation of lipid bilayer disruption by poly (amidoamine) dendrimers" *Chemistry and Physics of Lipids* **2004**, *132*, 3-14.

(174) Wiwattanapatapee, R., Carreño-Gómez, B., Malik, N., and Duncan, R. "Anionic pamam dendrimers rapidly cross adult rat intestine in vitro: A potential oral delivery system?" *Pharmaceutical Research* **2000**, *17*, 991-998.

(175) Castonguay, A., Ladd, E., van de Ven, T. G., and Kakkar, A. "Dendrimers as bactericides" *New Journal of Chemistry* **2012**, *36*, 199-204.

(176) Xue, X., Chen, X., Mao, X., Hou, Z., Zhou, Y., Bai, H., Meng, J., Da, F., Sang, G., and Wang, Y. "Amino-terminated generation 2 poly (amidoamine) dendrimer as a potential broad-spectrum, nonresistance-inducing antibacterial agent" *The AAPS Journal* **2013**, *15*, 132-142.

(177) Tulu, M., Aghatabay, N. M., Senel, M., Dizman, C., Parali, T., and Dulger, B. "Synthesis, characterization and antimicrobial activity of water soluble dendritic macromolecules" *European Journal of Medicinal Chemistry* **2009**, *44*, 1093-1099.

(178) Mintzer, M. A., Dane, E. L., O'Toole, G. A., and Grinstaff, M. W. "Exploiting dendrimer multivalency to combat emerging and re-emerging infectious diseases" *Molecular Pharmaceutics* **2011**, *9*, 342-354.

(179) Chen, C. Z., Cooper, S. L., and Beck-Tan, N. C. "Incorporation of dimethyldodecylammonium chloride functionalities onto poly (propylene imine) dendrimers significantly enhances their antibacterial properties" *Chemical Communications* **1999**, 1585-1586.

(180) Charles, S., Vasanthan, N., Kwon, D., Sekosan, G., and Ghosh, S. "Surface modification of poly(amidoamine) (PAMAM) dendrimer as antimicrobial agents" *Tetrahedron Letters* **2012**, *53*, 6670-6675.

(181) Fuentes-Paniagua, E., Hernández-Ros, J. M., Sánchez-Milla, M., Camero, M. A., Maly, M., Pérez-Serrano, J., Copa-Patiño, J. L., Sánchez-Nieves, J., Soliveri, J., and Gómez, R. "Carbosilane cationic dendrimers synthesized by thiol–ene click chemistry and their use as antibacterial agents" *RSC Advances* **2014**, *4*, 1256-1265.

(182) Ortega, P., Cobaleda, B. M., Hernández-Ros, J. M., Fuentes-Paniagua, E., Sánchez-Nieves, J., Tarazona, M. P., Copa-Patiño, J. L., Soliveri, J., de la Mata, F. J., and Gómez, R. "Hyperbranched polymers versus dendrimers containing a carbosilane framework and terminal ammonium groups as antimicrobial agents" *Organic & Biomolecular Chemistry* **2011**, *9*, 5238-5248.

(183) Rasines, B., Hernández-Ros, J. M., de las Cuevas, N., Copa-Patiño, J. L., Soliveri, J., Muñoz-Fernández, M. A., Gómez, R., and de la Mata, F. J. "Water-stable ammonium-terminated carbosilane dendrimers as efficient antibacterial agents" *Dalton Transactions* **2009**, 8704-8713.

(184) Lu, Y., Slomberg, D. L., Shah, A., and Schoenfisch, M. H. "Nitric oxide-releasing amphiphilic poly (amidoamine)(PAMAM) dendrimers as antibacterial agents" *Biomacromolecules* **2013**, *14*, 3589-3598.

(185) Sun, B., Slomberg, D. L., Chudasama, S. L., Lu, Y., and Schoenfisch, M. H. "Nitric oxide-releasing dendrimers as antibacterial agents" *Biomacromolecules* **2012**, *13*, 3343-3354.

CHAPTER 2:

Dual-Action Nitric Oxide-Releasing Poly(amidoamine) Dendrimers

2.1 Introduction

Nitric oxide (NO) is an endogenously produced free radical that regulates several biological functions in the cardiovascular, respiratory, and nervous systems.[1, 2] Further, the up-regulation of NO production in activated macrophages and monocytes is associated with host defenses against foreign pathogens.[2-5] While the increased NO output in macrophages allows for a nonspecific defense mechanism to protect the host, the host cells themselves have evolved a detoxification mechanism against NO cytotoxicity.[6] The broad-spectrum antibacterial activity of NO is derived from the production of reactive byproducts (e.g., dinitrogen trioxide and peroxynitrite) that compromise the bacterial membrane and cell function through both nitrosative and oxidative stresses.[3, 7] The multi-mechanistic biocidal action of NO makes it effective against a multitude of infectious pathogens while minimizing its risk of fostering bacterial resistance.[8]

The potential antibacterial activity of NO in vivo calls for efficient methods to chemically store and controllably release NO due to its short half-life in physiological milieu. As such, several classes of NO donors have been developed to store and deliver NO, including organic nitrates, metal nitrosyls, *S*-nitrosothiols, and *N*-diazeniumdiolates.[9] Of these NO donors, *N*-diazeniumdiolates are well-suited for in vivo applications as they spontaneously dissociate under physiological conditions (pH 7.4, 37 °C) to produce two moles of NO for every mole of NO donor.[10] Several small molecule *N*-diazeniumdiolate NO donors have been developed yielding a range of NO-release half-lives (i.e., PROLI/NO $t_{1/2}$ ~ 1.8 s, DETA/NO $t_{1/2}$ ~ 20 h).[10]

Unfortunately, the large doses of low molecular weight NO donors generally required to kill bacteria due to inefficient bacterial-association combined with the toxicity of the parent amine to healthy mammalian cells necessitates the development of more efficient methods for NO delivery.[7]

Large molecular frameworks capable of storing and controllably releasing NO have been developed as novel antibacterial agents. For example, our laboratory has reported the synthesis and bactericidal efficacy of both NO-releasing silica nanoparticles and dendrimers against several strains of bacteria.[7, 11-13] Similar to small molecule NO donors, these scaffolds spontaneously release NO under physiological conditions; however, there are several advantages in using larger NO-release scaffolds over small molecules. First, the rate and duration of NO release can be controlled as a function of size, structure, composition, and/or surface hydrophobicity of the scaffold.[11, 13] These scaffolds can also be tailored using specific functional groups to target specific cells or reduce the toxicity of the scaffold while maintaining therapeutic levels of NO release.[7]

Of the NO-releasing macromolecular scaffolds pioneered by our lab, dendrimers are a particularly promising candidate for the development of novel antibacterial agents. Dendrimers are hyperbranched macromolecular polymers exhibiting unique multivalent architectures and modifiable peripheral functional groups, making them excellent scaffolds for drug delivery.[14-16] The chemical environment surrounding the dendrimer can be altered by modifying the terminal primary amines with various functional groups, allowing for specific targeting of bacterial cell membranes.[14, 17] Increasing the dendrimer generation allows for facile synthetic control over scaffold size and increases the number of terminal primary amines, resulting in greater functional group density.[15, 16] Combining these factors with their ability to associate with and/or cross bacterial cell membranes makes dendrimers ideal candidates for use as antibacterial agents.[18, 19]

Previous work in our lab has established the ability to modify both poly(amidoamine) (PAMAM) and poly(propylene imine) (PPI) dendrimers with *N*-diazeniumdiolate and *S*-nitrosothiol NO donors. Stasko et al. demonstrated the ability to tune NO-release characteristics by modifying the dendrimer scaffold with either primary or tertiary *S*-nitrosothiol donors.[20] Further work demonstrated the increased stabilization of *N*-diazeniumdiolate NO donors on secondary amine-functionalized PPI dendrimers over unmodified dendrimer primary amines.[21] Lu et al. expanded on this work through the modification of generation 2 (G2) through generation 5 (G5) PPI dendrimers with diverse exterior functionalities (e.g., aromatic, hydrophilic, hydrophobic) that were further modified with *N*-diazeniumdiolate NO donors on the resultant secondary amine sites.[22] It was found that both NO-release totals and kinetics were dependent on the exterior modification of the dendrimer scaffold, with hydrophobic modification resulting in slightly longer dendrimer NO-release half-lives than those functionalized with hydrophilic groups.

To further expand our toolbox of NO-releasing dendrimers capable of efficient antibacterial action, we modified PAMAM dendrimers with both biocidal functional groups and NO-release capabilities. Poly(amidoamine) dendrimers of varying generation were first modified with contact-based biocides (i.e., quaternary ammonium moieties or alkyl chains) before *N*-diazeniumdiolate modification. In this chapter, we describe the synthesis and characterization of these dual-action dendrimer biocides prior to antibacterial evaluation.

2.2 Materials and Methods

Triethylamine (TEA), trimethylsilanolate, glycidyltrimethylammonium chloride, epichlorohydrin, dimethylbutylamine, dimethyloctylamine, and dimethyldodecylamine, were purchased from Sigma-Aldrich (St. Louis, MO). Methyl acrylate, 1,2-epoxybutane, 1,2-epoxyhexane, 1,2-epoxyoctane, 1,2-epoxydodecane, and ethylenediamine (EDA) were purchased

from the Aldrich Chemical Company (Milwaukee, WI). Sodium methoxide (5.4 M solution in methanol) was purchased from Acros Organics (Geel, Belgium). Cellulose ester dialysis membranes (500-1000 MWCO) were purchased from Spectrum Laboratories, Inc. (Rancho Dominguez, CA). Common laboratory salts and solvents were purchased from Fisher Scientific (Fair Lawn, NJ). Nitrogen (N_2), argon (Ar), and nitric oxide (NO) calibration (25.87 PPM, balance N_2) gases were purchased from National Welders (Raleigh, NC). Pure nitric oxide (NO) gas (99.5%) was purchased from Praxair (Sanford, NC). Distilled water was purified using a Millipore Milli-Q UV Gradient A-10 system (Bedford, MA), resulting in a total organic content of ≤6 ppb and a final resistivity of 18.2 mΩ·cm. All materials were analytical-reagent grade and used as received without further purification.

2.2.1 Synthesis of quaternary ammonium-modified PAMAM dendrimers

Poly(amidoamine) **(**PAMAM) scaffolds were synthesized as described previously,[15, 16, 23] by repeated alkylation/amidation steps using methyl acrylate and EDA from an EDA core. The addition of QA functionalities to the dendrimer scaffold necessitated the synthesis of quaternary ammonium epoxides (QA-epoxides), as described previously.[11] Briefly, 0.04 mmol epichlorohydrin was reacted with 0.01 mmol *N*,*N*-dimethylbutylamine, *N*,*N*-dimethyloctylamine, or *N*,*N*-dimethyldodecylamine at room temperature overnight (~18 h). The mixture was then added dropwise to cold ether while sonicating, and the solid/viscous liquid QA-epoxides were collected via centrifugation (810×*g*, 5 min). The supernatant was decanted, and the QA-epoxides were washed with 50 mL of cold ether and sonicated extensively. This washing procedure was repeated three times before drying the product in vacuo.

A ring-opening reaction was then carried out between the QA-epoxides and the terminal primary amines of the PAMAM dendrimers. G1 or G4 PAMAM (50 mg) was dissolved in 5 mL

of methanol. One equivalent of triethylamine (e.g., with respect to the molar amount of primary amines) and 2.5 molar equivalents of QA-epoxide were then added to the vial. The solution was stirred at room temperature for 4 d. Solvent was then removed in vacuo. The dendrimers were subsequently dissolved in water and purified by dialysis against water overnight. The pure product was recovered via lyophilization.

Representative ^{1}H NMR data of QA-modified dendrimers via the reactions of G4 PAMAM with glycidyltrimethylammonium chloride (methylQA), glycidyldimethylbutylammonium chloride (butylQA), glycidyldimethyloctylammonium chloride (octylQA), and glycidyldimethyldodecylammonium chloride (dodecylQA) included the following peaks. G4 methylQA: ^{1}H NMR (400 MHz, D_2O, δ) 3.07 (s, $CH_2N^+(CH_3)_3$), 2.31 (s, $NCH_2CH_2C(O)NH$). G4 butylQA: ^{1}H NMR (400 MHz, CD_3OD, δ) 2.30 (s, $NCH_2CH_2C(O)NH$), 1.81 (s, $CH_2N^+(CH_3)_2CH_2$-$CH_2CH_2CH_3$), 1.36–1.30 (q, $CH_2N^+(CH_3)_2CH_2CH_2CH_2CH_3$), 0.93 (t, $CH_2N^+(CH_3)_2CH_2$-$CH_2CH_2CH_3$). G4 octylQA: ^{1}H NMR (400 MHz, CD_3OD, δ) 2.31 (s, $NCH_2CH_2C(O)NH$), 1.80 (s, $CH_2N^+(CH_3)_2CH_2CH_2(CH_2)_5CH_3$), 1.31–1.23 (m, $CH_2N^+(CH_3)_2CH_2CH_2(CH_2)_5CH_3$), 0.83 (t, $CH_2N^+(CH_3)_2CH_2CH_2(CH_2)_5CH_3$). G4 dodecylQA: ^{1}H NMR (400 MHz, CD_3OD, δ) 2.31 (s, $NCH_2CH_2C(O)NH$), 1.81 (s, $CH_2N^+(CH_3)_2CH_2CH_2(CH_2)_9CH_3$), 1.32–1.22 (m, $CH_2N^+(CH_3)_2CH_2CH_2(CH_2)_9CH_3$), 0.83 (t, $CH_2N^+(CH_3)_2CH_2CH_2(CH_2)_9CH_3$).

2.2.2 Synthesis of alkyl chain-modified PAMAM dendrimers

To form alkyl chain-functionalized dendrimers without a QA moiety, G1 PAMAM dendrimers were modified with butyl, hexyl, octyl, and dodecyl alkyl chains. Briefly, G1 PAMAM (100 mg) was dissolved in either 2 mL (butyl and hexyl modifications) or 5 mL (octyl and dodecyl modifications) methanol, and one equivalent of triethylamine (e.g., with respect to the molar amount of primary amines) and 1 molar equivalent of epoxide (i.e., epoxybutane, epoxyhexane,

epoxyoctane, or epoxydodecane) were then added to the vial. The solution was stirred at room temperature for 3 d. After reaction completion, solvent and excess epoxide was removed in vacuo. To ensure the removal of any unreacted epoxide, the single-action dendrimers were re-dissolved in 5 mL methanol and kept under vacuum overnight. Complete removal of the epoxide was verified via ^{1}H NMR spectroscopy.

To investigate the effects of dendrimer generation, a ring-opening reaction was carried out between either epoxybutane or epoxyhexane and the terminal primary amines of the PAMAM dendrimers to yield single-action butyl- or hexyl-modified dendrimers. Briefly, G2, G3, or G4 PAMAM (100 mg) was dissolved in 2 mL of methanol, and one equivalent of triethylamine (e.g., with respect to the molar amount of primary amines) and 1 molar equivalent of epoxide were then added to the vial. The solution was stirred at room temperature for 3 d. After reaction completion, excess epoxide was removed in vacuo. To ensure the removal of any unreacted epoxide, the single-action dendrimers were re-dissolved in 5 mL methanol before being kept under vacuum overnight. Complete removal of the epoxide was verified via ^{1}H NMR spectroscopy.

Representative ^{1}H NMR data of butyl- and hexyl-modified G4 PAMAM via the reaction of G4 PAMAM with epoxybutane and epoxyhexane included the following peaks. G4 butyl: ^{1}H NMR (400 MHz, MeOD, δ) 2.28 (s, $NCH_2\mathit{CH_2}C(O)NH$), 1.41–1.35 (m, $NHCH_2CH(OH)C\mathit{H_2}CH_3$), 0.87–0.85 (t, $NHCH_2CH(OH)CH_2C\mathit{H_3}$). G4 hexyl: ^{1}H NMR (400 MHz, MeOD, δ) 2.28 (s, $NCH_2\mathit{CH_2}C(O)NH$), 1.34–1.20 (m, $NHCH_2CH(OH)C(\mathit{H_2})_3CH_3$), 0.85–0.81 (t, $NHCH_2CH(OH)C(H_2)_3C\mathit{H_3}$).

2.2.3 N-Diazeniumdiolation of QA- and alkyl chain-modified PAMAM dendrimers

To form *N*-diazeniumdiolate NO donors on the QA-functionalized dendrimer scaffold, QA-modified G1 and G4 PAMAM (20 mg) were added to varying ratios of anhydrous methanol

(MeOH) to tetrahydrofuran (THF) (1.5 mL solvent) depending on QA modification as follows: 100% MeOH (methylQA, butylQA); 3:1 MeOH:THF (octylQA); 1:1 MeOH:THF (dodecylQA). Trimethylsilanolate was added in a 10-fold excess relative to secondary amines.

To form *N*-diazeniumdiolate NO donors on the alkyl chain-modified dendrimer scaffold, single-action alkyl chain-modified G1 – G4 PAMAM (30 mg) were added to varying ratios of anhydrous MeOH to THF (1 mL solvent) depending on the alkyl chain modification and dendrimer generation as follows: 100% MeOH (G1 butyl, G2 butyl); 9:1 MeOH:THF (G3 butyl, G2 hexyl, G3 hexyl); 8.5:1.5 MeOH:THF (G4 butyl, G1 hexyl); 8:2 MeOH:THF (G4 hexyl); 3:2 MeOH:THF (G1 octyl); 2:3 MeOH:THF (G1 dodecyl). The solutions were vortexed and then one molar equivalent (e.g., with respect to the molar amount of primary amines) of sodium methoxide was added.

The dendrimer solutions were placed in a stainless steel reactor with continuous magnetic stirring and connected to an in-house NO reactor. The vessel was flushed with Ar three times to a pressure of 7 bar, followed by three longer Ar purges (10 min) to remove trace oxygen from the solutions. Following deoxygenation, the reactor was then pressurized to 10 bar with NO gas purified over KOH. The pressure was maintained at 10 bar NO for 4 d, after which the solutions were again purged with Ar three times at short durations followed by extended purges (3 × 10 min) to remove unreacted NO. Solvent was removed in vacuo, and the resulting NO-releasing dendrimers were dissolved in anhydrous methanol in a 1 dram glass vial, capped and parafilmed, and stored at -20 °C.

2.2.4 Characterization of single- and dual-action PAMAM dendrimers

^{1}H nuclear magnetic resonance (^{1}H NMR) spectra were recorded on a Bruker (400 MHz) spectrometer. X-ray photoelectron spectroscopy (XPS) analysis was performed on a Kratos Axis

Ultra DLD X-ray Photoelectron Spectrometer with a monochromatic Al Kα X-ray source (150W). Electrons were collected at an angle of 90 degrees from the sample surface from a 300 x 700 μm^2 area on the sample. The pass energy was set to 20 eV to obtain high resolution spectra. All spectra were acquired with a step size of 0.1 eV and calibrated to the C1s peak at 284.6 eV. Surface tension measurements were made using an Attension Sigma 701 tensiometer with a standard Du Noüy ring. All UV measurements were obtained in methanol using an Evolution Array UV-Visible Spectrophotometer (Thermo Scientific, Waltham, MA). Infrared spectra were obtained using a Bruker Alpha FT-IR spectrometer operating in ATR mode and signal averaging over 18 spectra.

2.2.5 Characterization of NO storage and release

Real-time NO release in deoxygenated PBS (pH 7.4, 37 °C) was monitored using a Sievers NOA 280i chemiluminescence NO analyzer (NOA, Boulder, CO). Prior to analysis, the NO analyzer was calibrated with air passed through a NO zero filter (0 ppm NO) and a 25.87 ppm NO standard gas (balance N_2). One milligram aliquots (or 0.5 mg for G1 octyl and dodecyl) of *N*-diazeniumdiolate-functionalized PAMAM in methanol were added to 30 mL deoxygenated PBS to initiate NO release. Nitrogen was flowed through the solution at a flow rate of 80 mL/min to carry the liberated NO to the analyzer. Additional nitrogen flow was supplied to the flask to match the collection rate of the instrument at 200 mL/min. Nitric oxide analysis was terminated when NO levels decreased to below 10 ppb NO/mg dendrimer.

Scheme 2.1 Reaction of PAMAM scaffold with either (A) QA or (B) alkyl chain epoxides to yield single-action dendrimers, followed by reaction with high pressures of NO to yield dual-action, NO-releasing dendrimers.

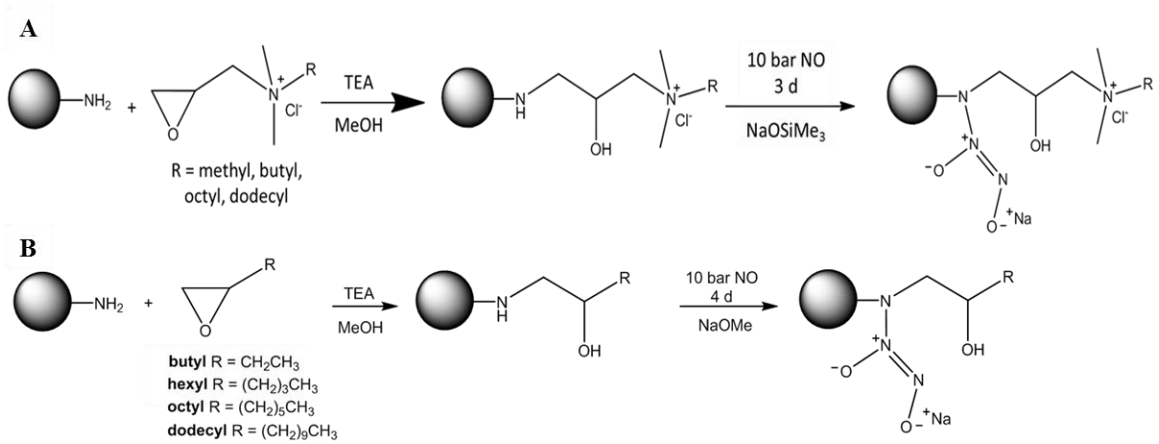

2.3 Results and Discussion

2.3.1 Synthesis and characterization of quaternary ammonium-modified PAMAM Dendrimers

Generation 1 (G1) and generation 4 (G4) PAMAM dendrimers were modified with QA moieties via a ring-opening reaction between the peripheral primary amines (*n*) and QA epoxides (Scheme 2.1 A). To investigate the role of QA alkyl chain length on NO release, PAMAM dendrimers were functionalized with QA moieties containing methyl, butyl, octyl, and dodecyl alkyl chains. While glycidyltrimethylammonium chloride (methylQA epoxide) is available commercially, butylQA, octylQA, and dodecylQA epoxides were synthesized through the reaction of epichlorohydrin with dimethylbutylamine, dimethyloctylamine, or dimethyldodecylamine, respectively.[11]

The resulting QA epoxides were reacted with G1 (*n*=8) and G4 (*n*=64) PAMAM dendrimers in a 2.5-fold excess to the number of peripheral primary amines in methanol. The number of QA moieties added to the dendrimer scaffold was determined using ^{1}H NMR spectroscopy. On average, 4 and 32 QA moieties were tethered to the G1 and G4 PAMAM scaffolds, respectively, resulting in approximately 50% functionalization of the peripheral primary amines (Table 2.1). The addition of the quaternary ammonium to the dendrimer scaffold was confirmed using IR spectroscopy and X-ray photoelectron spectroscopy (XPS). A weak IR stretch at 970 cm^{-1} indicative of the QA functional group was present for all QA-modified dendrimers (Figure 2.1 A).[24] The N 1s binding energies of the PAMAM dendrimer amines ranged from 397 – 399 eV, with an additional peak at 402 eV, corresponding to the quaternary ammonium group, present after modification with the QA moiety (Figure 2.1 B).[25] Additionally, a doublet at 198 eV, absent for the PAMAM scaffold, was observed for the QA-modified dendrimers, signifying the presence of the chloride counter ion (Figure 2.1 C).

Table 2.1 Percent functionalization and corresponding molecular weight for QA-modified G1 and G4 PAMAM dendrimers.

Dendrimer	Average # QAs	% Functionalized	Molecular Weight (Da)
G1 methylQA	4 ± 1	48	2006.2
G1 butylQA	4 ± 1	53	2243.5
G1 octylQA	4 ± 1	53	2479.2
G1 dodecylQA	5 ± 1	58	2867.7
G4 methylQA	35 ± 4	55	19522.1
G4 butylQA	35 ± 7	55	20994.5
G4 octylQA	30 ± 3	46	21709.0
G4 dodecylQA	36 ± 3	56	25227.4

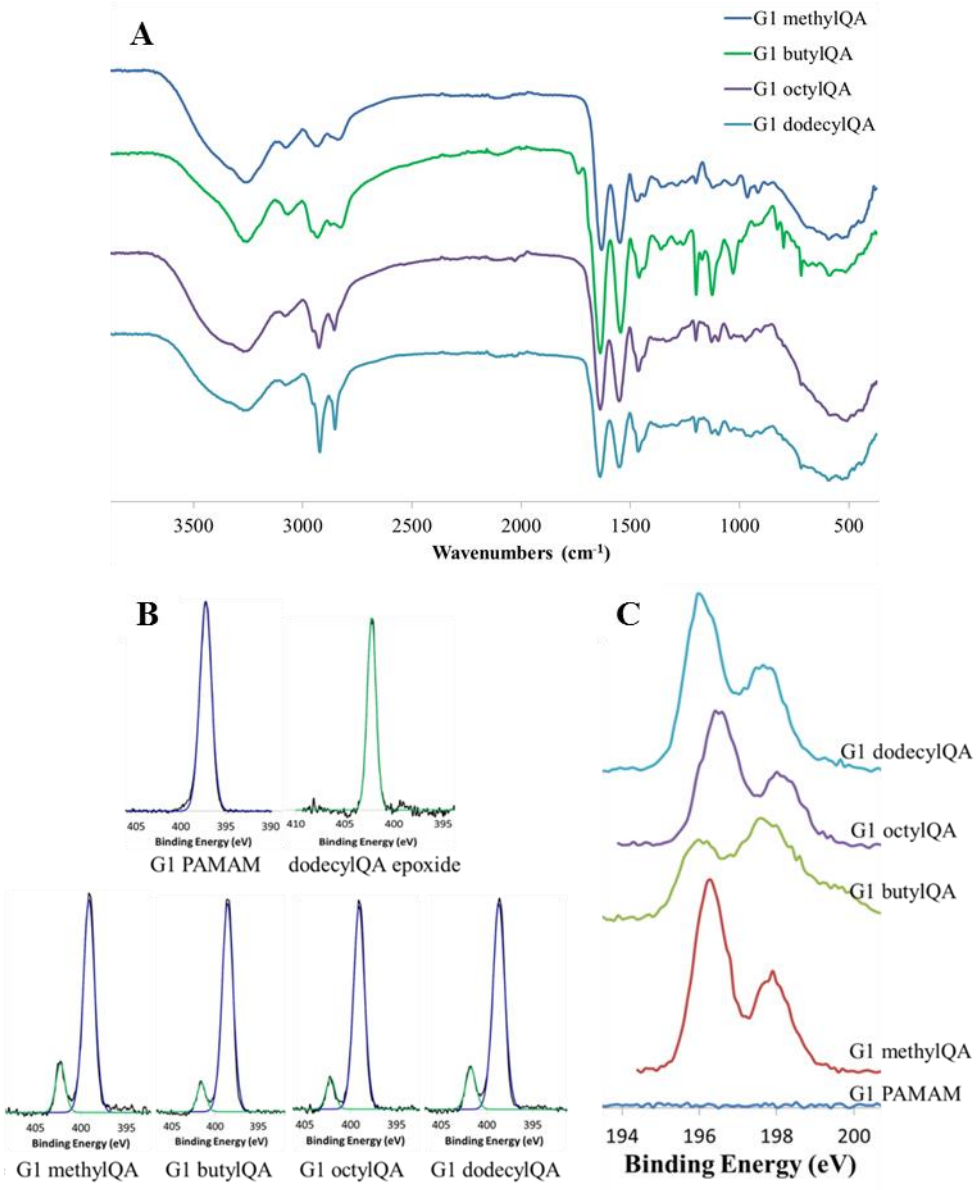

Figure 2.1 Representative (A) Fourier transform infrared spectra of G1 QA-modified dendrimers. Representative (B) N 1s and (C) Cl 2p XPS spectra for G1 QA-modified dendrimers.

Table 2.2 Nitric oxide-release properties for G1 and G4 QA-modified dendrimers in PBS (pH 7.4, 37 °C) as measured by a chemiluminescence NO analyzer.[a]

	$[NO]_{max}$[b] (ppb/mg)	t_{max}[c] (s)	t[NO][d] (μmol/mg)	$t[NO]_{4h}$[e] (μmol/mg)	$t_{1/2}$[f] (h)
G1 methylQA/NO	15000 ± 3372	48 ± 7	1.50 ± 0.11	0.73 ± 0.07	4.4 ± 1.1
G1 butylQA/NO	8675 ± 8182	61 ± 9	1.35 ± 0.30	0.78 ± 0.19	3.0 ± 0.5
G1 octylQA/NO	3400 ± 1249	64 ± 5	1.30 ± 0.05	0.69 ± 0.06	3.6 ± 0.9
G1 dodecylQA/NO	5016 ± 1379	71 ± 8	1.07 ± 0.16	0.72 ± 0.12	1.9 ± 0.8
G4 methylQA/NO	5170 ± 252	52 ± 4	1.69 ± 0.22	0.77 ± 0.08	4.9 ± 0.6
G4 butylQA/NO	4550 ± 3097	62 ± 13	1.48 ± 0.32	0.78 ± 0.18	3.8 ± 1.2
G4 octylQA/NO	7721 ± 5372	62 ± 10	1.49 ± 0.41	0.86 ± 0.23	2.9 ± 0.4
G4 dodecylQA/NO	3550 ± 1909	84 ± 4	1.17 ± 0.11	0.78 ± 0.06	1.9 ± 0.1

[a]For all measurements, $n \geq 3$ pooled experiments. [b]Maximum flux of NO release. [c]Time required to reach maximum flux. [d]Total NO payload released. [e]NO payload released after 4 h. [f]NO release half-life.

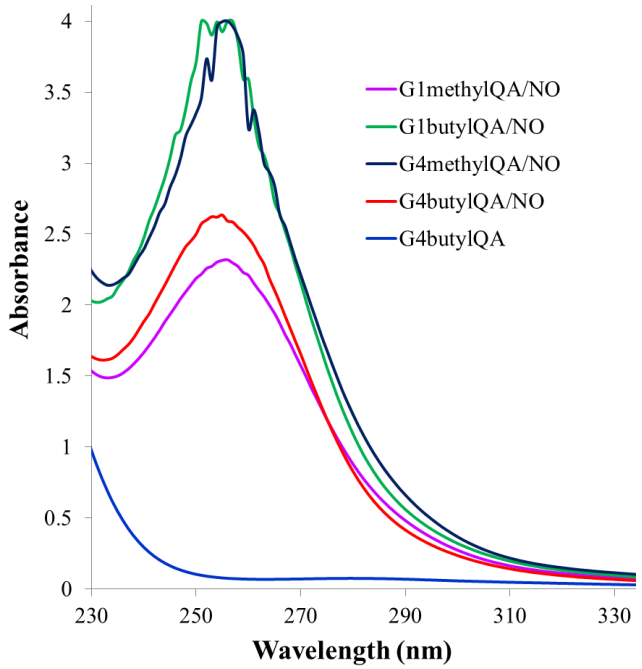

Figure 2.2 Representative UV-vis spectra for NO-releasing QA-modified dendrimers. Absorbance peak at ~253 nm is indicative of *N*-diazeniumdiolate NO donor.

Both G1 and G4 QA-modified dendrimers were exposed to high pressures of NO in the presence of a base to form *N*-diazeniumdiolate NO donors on secondary amines. *N*-diazeniumdiolate formation was confirmed by the presence of an absorbance maximum at 253 nm, a peak that was not observed in the absorbance spectra of QA-modified PAMAM dendrimer prior to diazeniumdiolate formation (Figure 2.2).[7] Nitric oxide storage was tunable by adjusting the polarity of the charging solvent (i.e., by increasing the ratio of THF:methanol with increasing alkyl chain length). The resulting NO-releasing QA-modified dendrimers exhibited similar 4 h NO payloads of approximately 0.76 μmol/mg (Table 2.2). In this regard, the effects of both dendrimer generation and QA alkyl chain length on bactericidal efficacy could be evaluated independent of NO release totals.

The *N*-diazeniumdiolated QA-modified dendrimers were characterized by an initial maximum burst of NO ($[NO]_{max}$) after introducing the dendrimers into solution, followed by a steady decline in NO release. For each generation, the time required to reach this maximum flux (t_{max}) increased as the QA alkyl chain length increased from methyl to dodecyl, with a concomitant decrease in the $[NO]_{max}$ values. The increase in t_{max} with increasing alkyl chain length is attributed to the presence of the hydrophobic QA alkyl chains that decrease the rate of water diffusion to the secondary amine-bound NO donors.[11] However, a decrease in NO-release half-life was also observed with increasing alkyl chain length, an opposite phenomenon than what might be expected from reduced water diffusion. The observed decrease in half-life for longer (i.e., octylQA and dodecylQA) QA alkyl chains is likely due to the formation of dendrimer vesicles in aqueous solution, in which the hydrophobic alkyl chains of neighboring dendrimers face inwards (i.e., towards each other), exposing the portion of the dendrimer scaffold containing the *N*-diazeniumdiolate to aqueous solution (Figure 2.3). Indeed, Schenning et al. reported the formation

of dendrimer bilayers at pH 7.4 for hydrophobic alkyl chain-modified scaffolds.[26] In this scenario, the hydrophobic alkyl chains align perpendicularly to the dendrimer scaffold, which faces the aqueous phase.[26] To determine if the QA-modified dendrimers were in fact forming supramolecular structures in aqueous solution, the surface tension of phosphate buffered saline (pH 7.4) solutions with increasing concentrations of QA-modified dendrimers was measured to determine the critical vesicle concentration (CVC) for the dendrimer biocides (Figure 2.4 A-B). The CVCs of G4 octylQA and G4 dodecylQA were determined to be 29 ± 11 and 22 ± 4 μg/mL, respectively, suggesting the formation of vesicles in solution above these concentrations. In comparison, the CVC of G4 butylQA was > 5 mg/mL due to the inability of the shorter QA alkyl chains to readily form vesicles at the concentrations employed herein. Transmission electron microscopy further confirmed the formation of G4 dodecylQA vesicles (Figure 2.4 C).

2.3.2 Synthesis and characterization of alkyl chain-modified PAMAM dendrimers

Due to the inherent cationic nature of PAMAM dendrimers and their natural ability to associate with bacteria, we hypothesized that alkyl chain modification without QA moieties would reduce the synthetic burden to produce dual-action dendrimer biocides while still allowing us to evaluate the effects of alkyl chain length. Thus, PAMAM dendrimers were functionalized with alkyl chains via a ring-opening reaction at the peripheral primary amines (Scheme 2.1 B). We first synthesized single- and dual-action G1 PAMAM dendrimers modified with butyl, hexyl, octyl, or dodecyl alkyl chains to investigate the effects of alkyl chain length on NO release and bactericidal action without the presence of a quaternary ammonium. To further evaluate the effects of dendrimer generation (i.e., size and functional group density) on antibacterial activity, we prepared

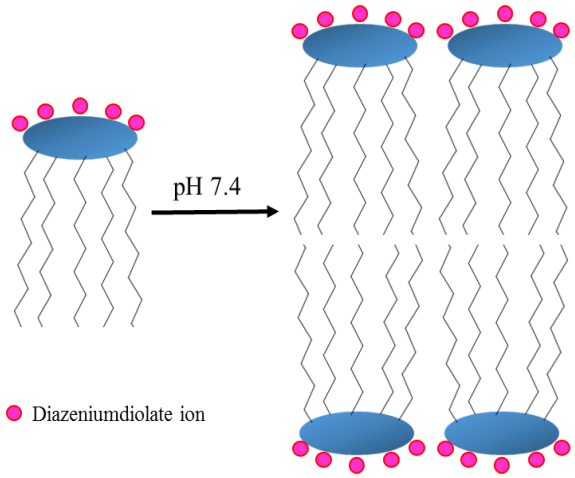

Figure 2.3 Formation of dendrimer vesicles at pH 7.4. The hydrophobic alkyl chains of neighboring dendrimers face towards each other, exposing the *N*-diazeniumdiolate ions to aqueous solution.

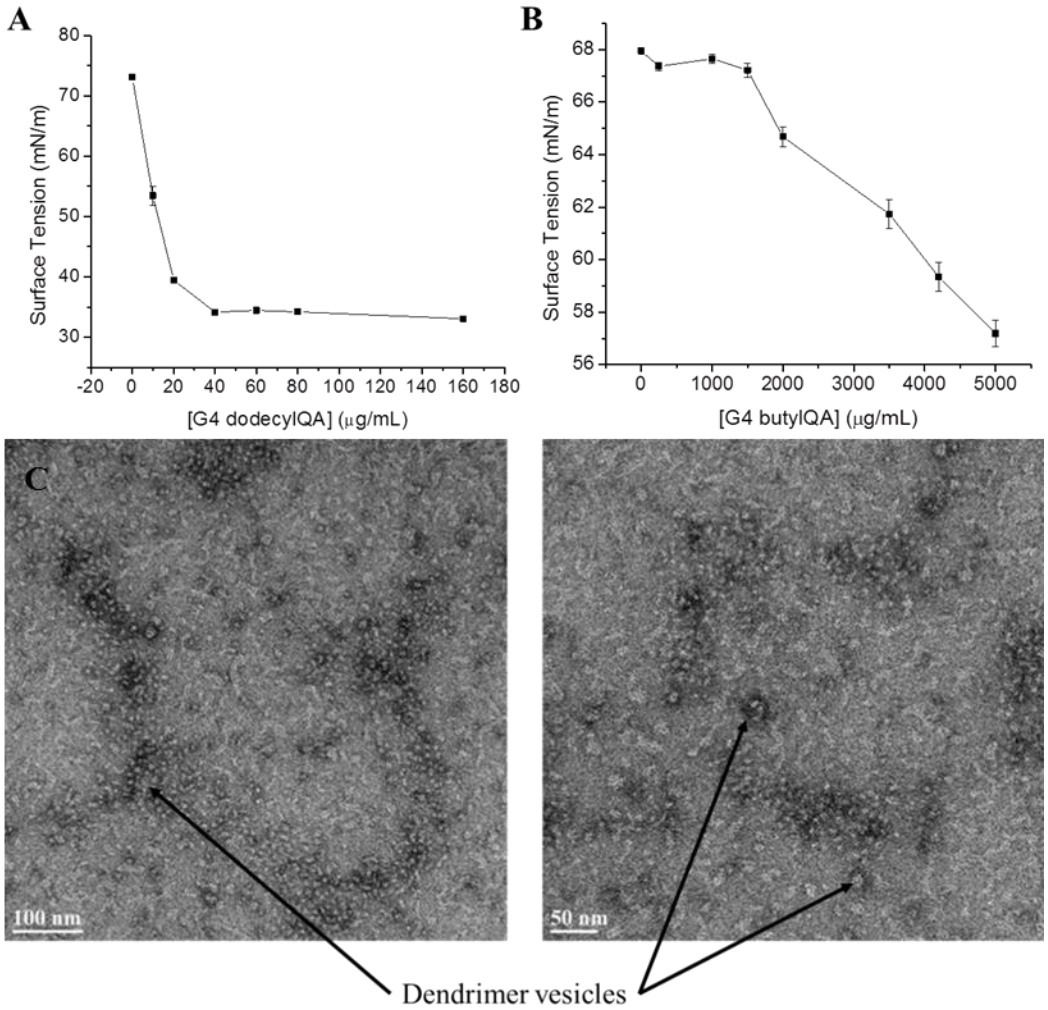

Figure 2.4 Surface tension plots for (A) G4 dodecylQA and (B) G4 butylQA, demonstrating the decrease in surface tension with increasing dendrimer concentration. Plot (A) indicates the leveling off of surface tension indicative of the CVC. Error bars represent standard deviation of the mean. Transmission electron microscopy images (C) of G4 dodecylQA dendrimer vesicles (500 μg/mL in milli-Q water).

G1 (n = 8), G2 (n = 16), G3 (n = 32), and G4 (n = 64) butyl- and hexyl-modified PAMAM dendrimers with and without NO-release capabilities.

After modification, the number of alkyl chains added to the G1 dendrimer scaffold was determined using ^{1}H NMR spectroscopy. On average, 5–6 functional groups were tethered to the G1 scaffold, resulting in approximately 65% functionalization (Table 2.3). The addition of the alkyl chain modification was further verified with IR spectroscopy with a stronger IR stretch observed at 2900 cm^{-1} with increasing alkyl chain length, corresponding to the greater number of C–H bonds in the alkyl chain (Figure 2.5). As longer alkyl chains resulted in vesicle formation for the QA-modified dendrimers, CVC values were also determined for each of the alkyl chain-modified G1 PAMAM dendrimers by measuring the surface tension of solutions containing increasing concentrations of dendrimer.[27] As expected, lower CVC values were measured for the longer chain G1 octyl and dodecyl dendrimers than the shorter G1 butyl or hexyl dendrimers (Table 2.3), indicating the formation of dendrimer vesicles at significantly lower concentrations. As such, chemiluminescent NO analysis for G1 octyl and dodecyl dendrimers was performed at concentrations below these CVC values to prevent vesicle formation from influencing the NO-release kinetics.

Alkyl chain-modified G1 dendrimers were exposed to high pressures of NO under basic conditions to form *N*-diazeniumdiolate NO donors on secondary amines. Nitric oxide storage was tuned by increasing the ratio of THF:methanol with increasing alkyl chain length, resulting in similar NO payloads of ~1 μmol/mg. The *N*-diazeniumdiolated alkyl chain-modified dendrimers were characterized by an initial maximum burst of NO after introducing the dendrimers into solution, followed by a steady decline in NO release. Contrary to the QA-modified dendrimers, the time to reach this maximum flux was relatively constant regardless of alkyl chain length (Table

Table 2.3 Percent functionalization, corresponding molecular weight, and critical vesicle concentrations for alkyl chain-modified PAMAM dendrimers.

	No. Modified End Groups	%	Molecular Weight (Da)	CVC (μg/mL)
G1 butyl	5 ± 1	60	1776.1	3193 ± 3
G1 hexyl	6 ± 1	73	2010.9	553 ± 11
G1 octyl	5 ± 1	61	2058.3	31 ± 7
G1 dodecyl	5 ± 1	63	2351.6	28 ± 7
G2 butyl	11 ± 1	67	4026.4	3604 ± 2
G2 hexyl	11 ± 1	69	4359.4	661 ± 5
G3 butyl	24 ± 3	76	8667.3	2979 ± 3
G3 hexyl	25 ± 2	78	9423.0	725 ± 4
G4 butyl	43 ± 4	68	17330.2	3066 ± 2
G4 hexyl	51 ± 4	80	19323.2	653 ± 10

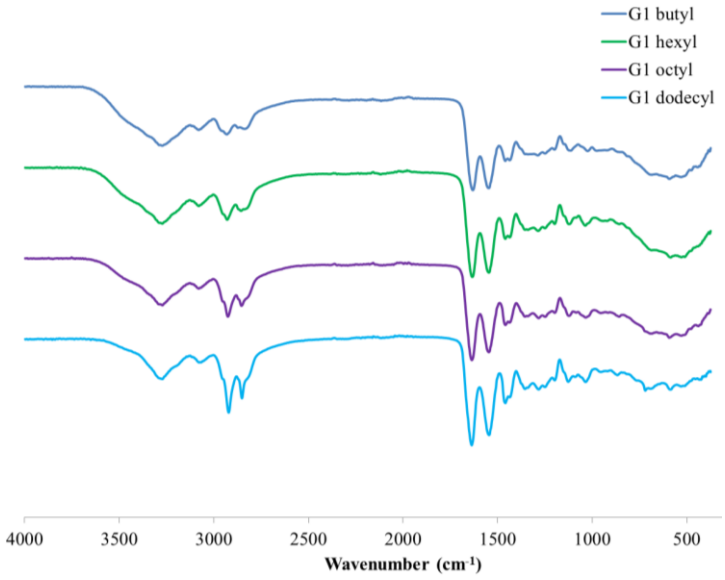

Figure 2.5 Fourier transform infrared spectra of G1 alkyl chain-modified dendrimers.

2.4). Further, a slight increase in NO-release half-life was observed for the longer octyl- and dodecyl-modified G1 dendrimers than the shorter butyl and hexyl chains (~21 to 37 min), indicating that the longer alkyl chains slightly impede water diffusion to the proton-labile *N*-diazeniumdiolate NO donors. Of note, the half-lives observed for the alkyl chain modifications were substantially lower than those of the QA-modified dendrimers (~0.5 h versus 2–5 h), suggesting that the quaternary ammonium group plays a significant role in determining NO-release kinetics. Indeed, the presence of the permanent positive charge of the QA moiety may stabilize the *N*-diazeniumdiolate group, extending NO release.[7, 22]

To evaluate the effects of dendrimer generation on NO release and bactericidal efficacy, epoxybutane or epoxyhexane was reacted with G1–G4 PAMAM dendrimers to yield butyl- and hexyl-modified PAMAM dendrimers. The number of alkyl chains added to the dendrimer scaffold was determined using ^{1}H NMR spectroscopy. For each generation, approximately 70% of the terminal primary amines were modified with either butyl or hexyl chains (Table 2.3). The surface tension of phosphate buffered saline (pH 7.4) solutions with increasing concentrations of alkyl chain-modified dendrimers were again measured to examine vesicle formation by the butyl- and hexyl-modified dendrimers at each generation.[26] The CVCs of the butyl- and hexyl-modified dendrimers were ~3 mg/mL and ~650 μg/mL, respectively, with no dependence on dendrimer generation. Based on these results, we concluded that vesicle formation does not occur at the concentrations required for NO release analysis. As such, any differences in NO-release kinetics are solely due to dendrimer generation or alkyl chain length.

Butyl- and hexyl-modified dendrimers were exposed to high pressures of NO under basic conditions to form *N*-diazeniumdiolate NO donors at secondary amines sites. Nitric oxide storage was tunable by adjusting the ratio of THF to methanol in the *N*-diazeniumdiolate modification

Table 2.4. Nitric oxide-release properties of alkyl chain-modified dendrimers in PBS (pH 7.4, 37 °C) as measured by a chemiluminescence NO analyzer.[a]

	t[NO][b] (μmol/mg)	t_{max}[c] (min)	$t_{1/2}$[d] (min)	t_d[e] (h)
G1 butyl/NO	1.06 ± 0.10	1.9 ± 0.4	21 ± 5	7 ± 2
G1 hexyl/NO	0.98 ± 0.11	2.0 ± 0.8	24 ± 6	7 ± 1
G1 octyl/NO	1.07 ± 0.13	2.8 ± 0.6	30 ± 5	9 ± 2
G1 dodecyl/NO	1.12 ± 0.10	1.8 ± 0.4	37 ± 6	9 ± 1
G2 butyl/NO	1.07 ± 0.15	1.2 ± 0.1	31 ± 5	10 ± 1
G2 hexyl/NO	1.04 ± 0.12	1.3 ± 0.1	31 ± 8	10 ± 2
G3 butyl/NO	0.93 ± 0.11	1.4 ± 0.6	26 ± 3	9 ± 1
G3 hexyl/NO	0.90 ± 0.11	1.5 ± 0.4	25 ± 4	9 ± 1
G4 butyl/NO	0.91 ± 0.09	1.5 ± 0.5	20 ± 3	8 ± 4
G4 hexyl/NO	0.94 ± 0.07	1.3 ± 0.3	20 ± 1	10 ± 4

[a]For all measurements, $n \geq 3$ pooled experiments. [b]Total NO payload released. [c]Time required to reach maximum flux. [d]NO release half-life. [e]Duration of NO release.

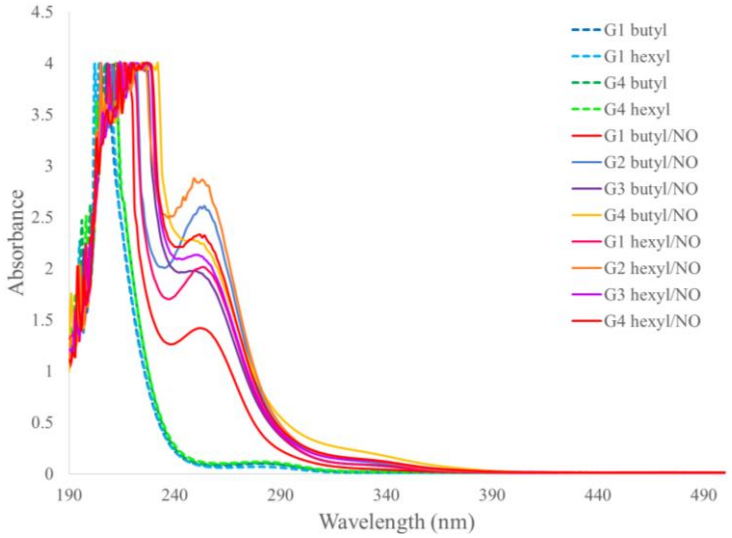

Figure 2.6 Representative UV-vis spectra for NO-releasing alkyl chain-modified dendrimers. Absorbance peak at ~253 nm is indicative of *N*-diazeniumdiolate NO donor.

solvent. *N*-diazeniumdiolate formation was confirmed by UV-vis spectroscopy with the presence of an absorbance maximum at 253 nm (Figure 2.6).[7] Of note, little to no nitrosamine formation was observed after NO exposure, as evidenced by no absorbance maximum at 350 nm.[28]

Chemiluminescence was used to evaluate real-time NO release in PBS (pH 7.4). The alkyl chain-modified dendrimers released NO for approximately 10 h, yielding total NO payloads of ~1 μmol/mg (Table 2.4). Proton-initiated NO release was characterized by an initial burst of NO upon dendrimer introduction into aqueous solution, followed by a steady decline in NO release. The time required to reach the maximum NO flux (t_{max}) was similar for both the butyl- and hexyl-modified dendrimers regardless of generation, indicating that the butyl and hexyl chains do not greatly influence water diffusion to the scaffold or *N*-diazeniumdiolate dissociation to NO. Similarly, each dendrimer system exhibited similar NO-release kinetics, with NO-release half-lives ($t_{1/2}$) of 20–30 min. In this regard, the effects of generation and alkyl chain modification on antibacterial and anti-biofilm action could be evaluated independent of both NO-release totals and kinetics.

2.4 Conclusions

Poly(amidoamine) dendrimers of varying generation were successfully modified with either QA moieties or alkyl chains of varying length. Nitric oxide-release kinetics were dependent on the type of modification (e.g., QA moiety or alkyl chain) and alkyl chain length but independent of dendrimer generation. Quaternary ammonium-modified PAMAM dendrimers exhibited much longer NO-release half-lives than their alkyl chain-modified counterparts, suggesting the presence of the cationic QA moiety stabilizes the diazeniumdiolate and extends NO-release kinetics. While the alkyl chain-modified G1 PAMAM dendrimers exhibited a slight increase in half-life with increasing alkyl chain length, the formation of vesicles at lower concentrations for the QA-

modified dendrimers resulted in a significant decrease in NO-release half-life for the longer dodecylQA modifications at each generation. Despite these differences in NO-release kinetics, altering the NO donor modification conditions allowed the total NO payloads to be tuned for each modification. As such, bactericidal action can be evaluated independent of NO-release totals (QA modifications) and both NO-release totals and kinetics (alkyl chain modifications).

REFERENCES

(1) Marletta, M., Tayeh, M., and Hevel, J. "Unraveling the biological significance of nitric oxide" *BioFactors* **1990**, *2*, 219-225.

(2) Moncada, S., Higgs, E., Hodson, H., Knowles, R., López-Jaramillo, P., McCall, T., Palmer, R., Radomski, M., Rees, D., and Schulz, R. "The L-arginine: Nitric oxide pathway" *Journal of Cardiovascular Pharmacology* **1991**, *17*, S1-S9.

(3) Fang, F. C. "Perspectives series: Host/pathogen interactions. Mechanisms of nitric oxide-related antimicrobial activity" *Journal of Clinical Investigation* **1997**, *99*, 2818.

(4) Fang, F. C. "Antimicrobial reactive oxygen and nitrogen species: Concepts and controversies" *Nature Reviews Microbiology* **2004**, *2*, 820-832.

(5) MacMicking, J., Xie, Q.-w., and Nathan, C. "Nitric oxide and macrophage function" *Annual Review of Immunology* **1997**, *15*, 323-350.

(6) Ghaffari, A., Miller, C., McMullin, B., and Ghahary, A. "Potential application of gaseous nitric oxide as a topical antimicrobial agent" *Nitric Oxide* **2006**, *14*, 21-29.

(7) Hetrick, E. M., Shin, J. H., Stasko, N. A., Johnson, C. B., Wespe, D. A., Holmuhamedov, E., and Schoenfisch, M. H. "Bactericidal efficacy of nitric oxide-releasing silica nanoparticles" *ACS Nano* **2008**, *2*, 235-246.

(8) Privett, B. J., Broadnax, A. D., Bauman, S. J., Riccio, D. A., and Schoenfisch, M. H. "Examination of bacterial resistance to exogenous nitric oxide" *Nitric Oxide* **2012**, *26*, 169-173.

(9) Riccio, D. A., and Schoenfisch, M. H. "Nitric oxide release: Part I. Macromolecular scaffolds" *Chemical Society Reviews* **2012**, *41*, 3731-3741.

(10) Hrabie, J. A., and Keefer, L. K. "Chemistry of the nitric oxide-releasing diazeniumdiolate ("nitrosohydroxylamine") functional group and its oxygen-substituted derivatives" *Chemical Reviews* **2002**, *102*, 1135-1154.

(11) Carpenter, A. W., Worley, B. V., Slomberg, D. L., and Schoenfisch, M. H. "Dual action antimicrobials: Nitric oxide release from quaternary ammonium-functionalized silica nanoparticles" *Biomacromolecules* **2012**, *13*, 3334-3342.

(12) Privett, B. J., Deupree, S. M., Backlund, C. J., Rao, K. S., Johnson, C. B., Coneski, P. N., and Schoenfisch, M. H. "Synergy of nitric oxide and silver sulfadiazine against gram-negative, gram-positive, and antibiotic-resistant pathogens" *Molecular Pharmaceutics* **2010**, *7*, 2289-2296.

(13) Sun, B., Slomberg, D. L., Chudasama, S. L., Lu, Y., and Schoenfisch, M. H. "Nitric oxide-releasing dendrimers as antibacterial agents" *Biomacromolecules* **2012**, *13*, 3343-3354.

(14) Duncan, R., and Izzo, L. "Dendrimer biocompatibility and toxicity" *Advanced Drug Delivery Review* **2005**, *57*, 2215-2237.

(15) Tomalia, D., Baker, H., Dewald, J., Hall, M., Kallos, G., Martin, S., Roeck, J., Ryder, J., and Smith, P. "A new class of polymers: Starburst-dendritic macromolecules" *Polymer Journal* **1985**, *17*, 117-132.

(16) Tomalia, D. A. "Birth of a new macromolecular architecture: Dendrimers as quantized building blocks for nanoscale synthetic polymer chemistry" *Progress in Polymer Science* **2005**, *30*, 294-324.

(17) Meyers, S. R., Juhn, F. S., Griset, A. P., Luman, N. R., and Grinstaff, M. W. "Anionic amphiphilic dendrimers as antibacterial agents" *Journal of the American Chemical Society* **2008**, *130*, 14444-14445.

(18) Jevprasesphant, R., Penny, J., Attwood, D., McKeown, N. B., and D'Emanuele, A. "Engineering of dendrimer surfaces to enhance transepithelial transport and reduce cytotoxicity" *Pharmaceutical Research* **2003**, *20*, 1543-1550.

(19) Wiwattanapatapee, R., Carreño-Gómez, B., Malik, N., and Duncan, R. "Anionic pamam dendrimers rapidly cross adult rat intestine in vitro: A potential oral delivery system?" *Pharmaceutical Research* **2000**, *17*, 991-998.

(20) Stasko, N. A., Fischer, T. H., and Schoenfisch, M. H. "S-nitrosothiol-modified dendrimers as nitric oxide delivery vehicles" *Biomacromolecules* **2008**, *9*, 834-841.

(21) Stasko, N. A., and Schoenfisch, M. H. "Dendrimers as a scaffold for nitric oxide release" *Journal of the American Chemical Society* **2006**, *128*, 8265-8271.

(22) Lu, Y., Sun, B., Li, C., and Schoenfisch, M. H. "Structurally diverse nitric oxide-releasing poly(propylene imine) dendrimers" *Chemistry of Materials* **2011**, *23*, 4227-4233.

(23) Lu, Y., Slomberg, D. L., Shah, A., and Schoenfisch, M. H. "Nitric oxide-releasing amphiphilic poly (amidoamine)(PAMAM) dendrimers as antibacterial agents" *Biomacromolecules* **2013**, *14*, 3589-3598.

(24) Beyth, N., Houri-Haddad, Y., Baraness-Hadar, L., Yudovin-Farber, I., Domb, A. J., and Weiss, E. I. "Surface antimicrobial activity and biocompatibility of incorporated polyethylenimine nanoparticles" *Biomaterials* **2008**, *29*, 4157-4163.

(25) Shi, Z., Neoh, K., Kang, E., and Wang, W. "Antibacterial and mechanical properties of bone cement impregnated with chitosan nanoparticles" *Biomaterials* **2006**, *27*, 2440-2449.

(26) Schenning, A. P., Elissen-Roman, C., Weener, J.-W., Baars, M. W., van der Gaast, S. J., and Meijer, E. "Amphiphilic dendrimers as building blocks in supramolecular assemblies" *Journal of the American Chemical Society* **1998**, *120*, 8199-8208.

(27) Worley, B. V., Slomberg, D. L., and Schoenfisch, M. H. "Nitric oxide-releasing quaternary ammonium-modified poly(amidoamine) dendrimers as dual action antibacterial agents" *Bioconjugate Chemistry* **2014**, *25*, 918-927.

(28) Coneski, P. N., and Schoenfisch, M. H. "Competitive formation of N-diazeniumdiolates and N-nitrosamines via anaerobic reactions of polyamines with nitric oxide" *Organic Letters* **2009**, *11*, 5462-5465.

CHAPTER 3:

Antibacterial Action of Dual-Action Dendrimers against Planktonic Bacteria

3.1 Introduction

Although antibiotics remain the gold standard in the treatment of bacterial infections, the increased occurrence of antibiotic-resistant bacteria coupled with a decline in the development of new antibiotics necessitates the development of alternative antibacterial agents.[1] The co-administration of two mechanistically different biocides has been demonstrated to reduce the emergence of bacterial resistance and can be synergistic, where the bactericidal efficacy of the combination is more effective than their individual sums.[2, 3] Combining multiple biocides on a single macromolecular scaffold (e.g., nanoparticles, dendrimers) is expected to further increase bactericidal efficacy.[4] Importantly, enhancing the bactericidal efficacy of a scaffold should lower the required therapeutic dose and concomitantly reduce any toxicity to healthy cells and tissue. A promising option for multimodal therapeutics is to modify non-depleting, contact-based antibacterial agents with chemistries that allow for spontaneous release of a secondary biocide, therefore increasing the antibacterial sphere of influence. Further, the use of mechanistically different biocides reduces the emergence of resistance as bacteria are less likely to develop resistance to all of the employed mechanisms.[2]

Nitric oxide (NO) is an endogenously produced, reactive free radical that plays a central role in the host defense against microbial pathogens.[5, 6] The broad-spectrum antibacterial activity of NO is derived from the production of reactive byproducts (e.g., dinitrogen trioxide and peroxynitrite) that compromise the bacterial membrane and cell function through both nitrosative

and oxidative stresses.[5, 7] The ability of NO to act through more than one bactericidal mechanism makes it effective against a multitude of infectious pathogens. To harness the bactericidal actions of NO, large molecular frameworks capable of storing and controllably releasing NO have been developed as novel antibacterial agents. Our laboratory has reported the synthesis and bactericidal efficacy of both NO-releasing silica nanoparticles and dendrimers against several strains of bacteria, including antibiotic-resistant strains.[7-10] Benefits of these macromolecular scaffolds include controllable NO payloads and release rates, modifiable surface chemistries (e.g., to allow for the combination of multiple biocides on a single scaffold), and reduced toxicity to mammalian cells.[8, 10]

Quaternary ammonium (QA) compounds, widely used as antiseptic and disinfectant agents, are popular non-depleting biocides due to their broad-spectrum efficacy.[11] The bactericidal activity of QA compounds stems from the attractive electrostatic interactions between the cationic QA group and the negatively charged bacterial cell membrane, disrupting natural chemical balances by replacing essential metal cations.[11] The addition of long alkyl chains to the QA group promotes bacterial membrane penetration, further amplifying biocidal activity. The bactericidal efficacy of QA compounds is highly dependent on the length of this alkyl chain, with alkyl chains of at least eight carbon atoms demonstrating the greatest bactericidal activity due to increased penetration into the cell membrane.[11-13] The combination of long chain QA moieties with a releasable biocide such as nitric oxide would thus be anticipated to increase antibacterial action. For instance, it has been demonstrated that QA-functionalized polymers capable of releasing silver ions (Ag^+) exhibit a wider zone of inhibition than QA polymers alone.[14, 15] Carpenter et al. similarly reported on NO donor-modified QA-functionalized silica nanoparticles with enhanced bactericidal efficacy against both Gram-positive and Gram-negative bacteria.[8] Despite improved

antibacterial efficacy, however, the NO-releasing QA-modified silica particles demonstrated significant toxicity to mammalian cells at concentrations required to eradicate bacteria, motivating further development of these dual-action NO-releasing therapeutics.

Dendrimers are a family of macromolecular scaffolds with hyper-branched architecture and multivalent surfaces that have been widely investigated for use as drug delivery and therapeutic vehicles.[16, 17] The ability to functionalize the dendrimer exterior through straightforward chemical methods allows for their modification with specific biocidal end groups. This capability, combined with the ability of dendrimers to associate with and/or cross bacterial membranes, provides a potentially effective scaffold for the development of combination therapeutics.[18, 19] Cooper and co-workers demonstrated that PPI dendrimers modified with QA moieties containing alkyl chains of eight or more carbons exhibited antibacterial activity as a function of dendrimer size and QA alkyl chain length.[12, 20] Likewise, Charles et al. found that dodecylQA-modified G3 PAMAM dendrimers exhibited an increased zone of inhibition against Gram-negative *Escherichia coli* and Gram-positive *Staphylococcus aureus* compared to butylQA and hexylQA modifications.[21]

Herein, we report the antibacterial action of single- and dual-action generation 1 (G1) and generation 4 (G4) QA-modified PAMAM dendrimers against planktonic cultures of both Gram-negative and Gram-positive bacteria. The effects of QA alkyl chain length, dendrimer generation, and bacterial Gram designation on dendrimer bactericidal action were evaluated. To further elucidate the effects of alkyl chain length on antibacterial activity independent of a QA moiety, the bactericidal efficacies of G1 PAMAM dendrimers modified with butyl, hexyl, octyl, and dodecyl alkyl chains were also assessed. Finally, we report on the effects of dendrimer generation

on antibacterial action through the evaluation of G1–G4 butyl- and hexyl-modified PAMAM dendrimers against planktonic bacteria.

3.2 Materials and Methods

Phenazine methosulfate (PMS), fetal bovine serum (FBS), trypsin, 3-(4,5-dimethylthiazol-2-yl)-5-(3-carboxymethoxyphenyl)-2-(4-sulfophenyl)-2H-tetrazolium inner salt (MTS), penicillin streptomycin (PS), triethylamine (TEA), rhodamine B isothiocyanate (RITC), and propidium iodide (PI) were purchased from Sigma-Aldrich (St. Louis, MO). Dulbecco's modified Eagle's medium (DMEM) and Dulbecco's phosphate buffered saline (PBS) were obtained from Lonza Group (Basel, Switzerland). 4,5-Diaminofluorescein diacetate (DAF-2 DA) was purchased from Calbiochem (San Diego, CA). Tryptic soy broth (TSB) and tryptic soy agar (TSA) were obtained from Becton, Dickinson and Company (Franklin Lakes, NJ). *Pseudomonas aeruginosa* (*P. aeruginosa*; ATCC #19143), *Staphylococcus aureus* (*S.aureus*; ATCC #29213), and methicillin-resistant *S. aureus* (MRSA; ATCC #33591) were obtained from American Type Tissue Culture Collection (Manassas, VA). L929 mouse fibroblasts were obtained from the UNC Tissue Culture Facility (Chapel Hill, NC). Carbon dioxide (CO_2) was purchased from National Welders (Raleigh, NC). Glass bottom microscopy dishes were received from MatTek Corporation (Ashland, MA). Common laboratory salts and solvents were purchased from Fisher Scientific (Fair Lawn, NJ). Distilled water was purified using a Millipore Milli-Q UV Gradient A-10 system (Bedford, MA), resulting in a total organic content of ≤6 ppb and a final resistivity of 18.2 mΩ·cm. Unless noted otherwise, these and all other materials were analytical-reagent grade and used as received without further purification.

3.2.1 Planktonic bactericidal assays

Lyophilized *P. aeruginosa*, *S. aureus*, and MRSA were reconstituted in tryptic soy broth (TSB) and cultured overnight at 37 °C. A 0.5 mL aliquot of culture was grown in 50 mL TSB to a concentration of 10^8 colony forming units per mL (cfu/mL), collected by centrifugation (2355×*g*), resuspended in 15% glycerol (v/v in PBS), and stored at -80 °C in 1 mL aliquots. For daily experiments, colonies of bacteria culture were inoculated in 2 mL TSB overnight at 37 °C and recultured in fresh TSB (50 mL) the next day.

To assess the antibacterial action of QA-modified dendrimers, *P. aeruginosa* and *S. aureus* were cultured in tryptic soy broth to a concentration of 10^8 cfu/mL, collected by centrifugation (2355×*g*), resuspended in sterile phosphate buffered saline (PBS, pH 7.4), and diluted to 10^6 cfu/mL. Premeasured samples of QA-modified or NO-releasing QA-modified dendrimer in methanol were added to a 1 dram glass vial and dried under vacuum for 2 h prior to the bacteria assays. Corresponding volumes of 10^6 cfu/mL bacteria were added to obtain a range of dendrimer concentrations (37 °C). Untreated controls (blanks) were included in each experiment to ensure the bacteria remained viable (at 10^6 cfu/mL) over the 4 h assay. The blanks and dendrimer-treated bacteria were then spiral-plated at 10- and 100-fold dilutions on tryptic soy agar plates using an Eddy Jet spiral plater (IUL; Farmingdale, NY). Bacterial viability was assessed by counting the number of colonies formed on the agar plate using a Flash & Go colony counter (IUL; Farmingdale, NY). Minimum bactericidal concentrations (MBC_{4h}) were determined to be the minimum concentration of dendrimer that resulted in a 3-log reduction in bacterial viability compared to untreated cells after 4 h (i.e., reduced bacterial counts from 10^6 to 10^3 cfu/mL). Of note, the plate counting method used has an inherent limit of detection of 2.5 x 10^3 cfu/mL.[22]

To test the antibacterial action of the alkyl chain-modified dendrimers, *P. aeruginosa*, *S. aureus*, and MRSA were cultured in TSB to a concentration of 10^8 colony forming units per mL (cfu/mL), collected by centrifugation (2355×*g*), resuspended in sterile PBS, and diluted to 10^6 cfu/mL in pH 7.4 PBS. For *S. aureus* and MRSA assays, the 10^6 cfu/mL solution in PBS was supplemented with 1% glucose and 0.5% TSB to ensure bacteria viability throughout the assay duration. Of note, the addition of TSB did not influence the NO-release totals (i.e., NO totals were 4.5 ± 1.8% lower in TSB-supplemented PBS; $n \geq 3$). Premeasured samples of single- or dual-action dendrimer in methanol were added to a 1 dram glass vial and dried under vacuum for 2 h prior to the bacteria assays. Corresponding volumes of 10^6 cfu/mL bacteria were added to obtain a range of dendrimer concentrations. Untreated controls (blanks) were included in each experiment to ensure the bacteria remained viable (at 10^6 cfu/mL) over the 24 h assay at 37 °C. The blanks and dendrimer-treated bacteria were then spiral-plated at 10- and 100-fold dilutions on tryptic soy agar plates using an Eddy Jet spiral plater. Bacterial viability was assessed by counting the number of colonies formed on the agar plate using a Flash & Go colony counter. Minimum bactericidal concentrations (MBC_{24h}) were determined to be the minimum concentration of dendrimer that resulted in a 3-log reduction in bacterial viability compared to untreated cells after 24 h (i.e., reduced bacterial counts from 10^6 to 10^3 cfu/mL).

3.2.2 Confocal microscopy to assess dendrimer-bacteria association

Fluorescently-tagged G4 PAMAM dendrimers were synthesized as described previously.[10, 23, 24] Briefly, 100 mg G4 PAMAM were added to a vial containing one molar equivalent of RITC (3.8 mg) in 2 mL methanol. One equivalent of triethylamine (with respect to the molar amount of primary amines) was then added to the vial. The solution was stirred for 24 h in the dark, after which solvent was removed in vacuo. Dendrimers were dissolved in water,

dialyzed against water (3 d), and then lyophilized. The procedure for QA functionalization described in Section 2.2.1 was performed in the dark to modify the fluorescently-tagged G4 PAMAM with methylQA, butylQA, and dodecylQA moieties. *P. aeruginosa* and *S. aureus* were cultured as described above and diluted to 10^6 cfu/mL. Aliquots of the bacteria solutions were incubated in a glass bottom confocal dish for 45 min at 37 °C. A Zeiss 510 Meta inverted laser scanning confocal microscope with a 543 nm HeNe excitation laser (1.0 mW, 25.0% intensity) and a 560 – 615 nm band pass (BP) filter was used to obtain fluorescence images of the RITC-modified dendrimers. Both bright field and fluorescence images were collected using an N.A. (numerical aperature) 1.2 C-apochromat water immersion lens with a 40× objective. Solutions of RITC-tagged dendrimers (100 μg/mL) in PBS (1.5 mL) were added to 1.5 mL of the bacteria solution in the glass confocal dish to achieve a final concentration of 50 μg/mL. Images were collected every 2 min to temporally monitor association of the dendrimers with the bacteria.

3.2.3 Confocal microscopy for detection of intracellular NO and cell death

P. aeruginosa and *S. aureus* were cultured as described above and diluted to 10^6 cfu/mL in PBS containing 10 μM DAF-2 DA and 30 μM PI. Aliquots of the bacteria solution were incubated in a glass bottom confocal dish for 45 min at 37°C. A Zeiss 510 Meta inverted laser scanning confocal microscope with a 488 nm Ar excitation laser (30.0 mW, 2.0% intensity) and a BP 505 – 530 nm filter was used to obtain DAF-2 (green) fluorescence images. A 543 nm HeNe exciation laser (1.0 mW, 25.0% intensity) with a BP 560 – 615 nm filter was used to obtain PI (red) fluorescence images. Both bright field and fluorescence images were collected using an N.A. 1.2 C-apochromat water immersion lens with a 40× objective. Solutions of G4 methylQA/NO, G4 butylQA/NO, G4 octylQA/NO, or G4 dodecylQA/NO (40 μg/mL) in 1.5 mL PBS (containing 10 μM DAF-2 DA and 30 μM PI) were added to 1.5 mL of the bacteria solution in the glass confocal

dish to achieve a final concentration of 20 μg/mL. Images were collected every 5 min to temporally observe intracellular NO concentrations and bacteria cell death.

3.2.4 In vitro cytotoxicity

L929 mouse fibroblasts were grown in DMEM supplemented with 10 vol% FBS and 1 wt% PS and incubated in 5 vol% CO_2 under humidified conditions at 37 °C. After reaching 80% confluency, the cells were trypsinized, seeded onto tissue culture-treated polystyrene 96-well plates at a density of 2 x 10^4 cells/mL, and incubated at 37 °C for 72 h. The supernatant was then aspirated and replaced with 200 μL of fresh growth medium and either 50 μL of QA-modified dendrimer in PBS at the determined MBC_{4h} against *P. aeruginosa* or *S. aureus* or 50 μL of alkyl chain-modified dendrimer in PBS at the lowest and highest planktonic MBC_{24h} values. Dimethyl sulfoxide (10%) and 50 μL PBS were used as positive and negative controls, respectively. After incubation for 4 or 24 h at 37 °C, the supernatant was aspirated and 120 μL of a mixture of DMEM/MTS/PMS (105/20/1, v/v/v) was added to each well. After 1.5 h incubation at 37 °C, the absorbance of the colored solutions was quantified at 490 nm using a Thermoscientific Multiskan EX plate reader (Waltham, MA). The mixture of DMEM/MTS/PMS and untreated cells were used as a blank and control, respectively. Results were expressed as percentage of relative cell viability as follows:

$$\% \text{ Cell Viability} = [(Abs_{490} - Abs_{blank})/(Abs_{control} - Abs_{blank})] \times 100\% \qquad \textbf{Eq. 3.1}$$

3.3 Results and Discussion

3.3.1 Antibacterial action of QA-modified PAMAM dendrimers

As *P. aeruginosa* and *S. aureus* represent two of the most commonly isolated species in chronic wounds, they were selected to test the antibacterial efficacy of the QA-modified dendrimers.[25] Further, their use allowed us to examine the effect of Gram designation (i.e., Gram-

positive or Gram-negative) on the bactericidal efficacy of these antibacterial agents. Planktonic bacteria viability assays were performed under static conditions to determine the minimum dendrimer concentration required to elicit a 3-log reduction in bacterial viability over 4 h (MBC_{4h}). The bactericidal NO dose for the NO-releasing QA-modified dendrimers was determined by multiplying the 4 h NO payload ($t[NO]_{4h}$) by the corresponding MBC_{4h}.

The bactericidal efficacy of single-action (i.e., non-NO-releasing) QA-modified dendrimers was first assessed to determine the effects of QA alkyl chain length, dendrimer generation, and bacteria Gram designation on antibacterial activity prior to evaluating the effects of NO release. All QA alkyl chain lengths exhibited a generation dependence on bactericidal efficacy against *P. aeruginosa*, with G4 QA-modified dendrimers resulting in improved killing (i.e., decreased MBC_{4h} values) relative to their G1 counterparts (Table 3.1). The generation-dependent increase in antibacterial activity against *P. aeruginosa* is attributed to the greater alkyl chain density of the G4 scaffold over the more sparsely functionalized G1 dendrimers. Alternatively, only the methylQA-modified dendrimers exhibited a generation dependence against *S. aureus*. While the bactericidal concentration of G1 methylQA against *S. aureus* was greater than 8.0 mg/mL, G4 methylQA dendrimers resulted in complete bacterial killing at one-fourth that concentration (2.0 mg/mL). Although the shortest QA alkyl chain (methylQA) seemed to benefit from the increased functional group density of the G4 scaffold, no generation effect was observed for the remaining QA alkyl chain lengths, indicating that for antibacterials containing these longer QA alkyl chains (i.e., butylQA to dodecylQA), the mechanism of action against the Gram-positive pathogen *S. aureus* is not influenced by functional group density.

Both dendrimer generation and QA alkyl chain length influenced bactericidal efficacy and were dependent on bacterial Gram designation. While Gram-negative bacteria possess a lipid-rich

Table 3.1 Minimum bactericidal concentrations (MBC_{4h}) and bactericidal NO doses for single- and dual-action QA-modified dendrimers against *S. aureus* and *P. aeruginosa*.[a]

	S. aureus		*P. aeruginosa*	
	MBC_{4h} (μg/mL)	NO dose (μmol/mL)	MBC_{4h} (μg/mL)	NO dose (μmol/mL)
G1 PAMAM	>8000		250	
G4 PAMAM	1000		30	
G1 methylQA	>8000		1500	
G1 methylQA/NO	500	0.37	300	0.22
G1 butylQA	3500		1500	
G1 butylQA/NO	500	0.39	300	0.23
G1 octylQA	30		75	
G1 octylQA/NO	30	0.02	50	0.03
G1 dodecylQA	10		20	
G1 dodecylQA/NO	10	0.01	10	0.01
G4 methylQA	2000		500	
G4 methylQA/NO	300	0.23	250	0.19
G4 butylQA	3500		1000	
G4 butylQA/NO	500	0.39	250	0.20
G4 octylQA	30		30	
G4 octylQA/NO	20	0.02	30	0.03
G4 dodecylQA	10		10	
G4 dodecylQA/NO	10	0.01	10	0.01

[a]Each parameter was analyzed with multiple replicates ($n \geq 3$).

outer membrane and a thin peptidoglycan sheet, the outer wall of Gram-positive bacteria is comprised of a thicker and more resistant peptidoglycan layer.[26] For the short alkyl chains, both G1 and G4 scaffolds were more effective against Gram-negative *P. aeruginosa* than Gram-positive *S. aureus*. The antibacterial activity of the short alkyl chain QAs is attributed to positively charged ammonium groups interacting with the negatively charged bacterial cell membranes. Once associated, the QA functionality can induce cell death through a number of pathways, including disrupting membrane functions, replacing essential metal cations, interrupting protein activity, and damaging bacterial DNA.[11, 13] The increased bactericidal action toward *P. aeruginosa* indicates greater association of the dendrimers with the outer membrane layers present in the Gram-negative bacterium, while the thick peptidoglycan layer of Gram-positive *S. aureus* likely reduced associated and QA-induced cell death. Indeed, RITC-tagged G4 methylQA dendrimers associated with *P. aeruginosa* more rapidly than with *S. aureus* bacterial cells (Figures 3.1 and 3.2). While association with *P. aeruginosa* was noted at 10 min, G4 methylQA dendrimer association with *S. aureus* was not observed until after 28 min. In contrast, G1 dendrimers modified with longer QA alkyl chains more effectively killed *S. aureus* than *P. aeruginosa*, but neither modification demonstrated a Gram dependence with the G4 scaffold. We believe that the penetration of the longer QA alkyl chains tethered to the G1 scaffold exerts greater physical damage to the thicker peptidoglycan layer of *S. aureus* compared to the outer membrane of *P. aeruginosa*. This hypothesis, however, does not hold true for the G4 dendrimers, where the increased functional group densities afforded by the G4 scaffold result in similar killing against both strains of bacteria.

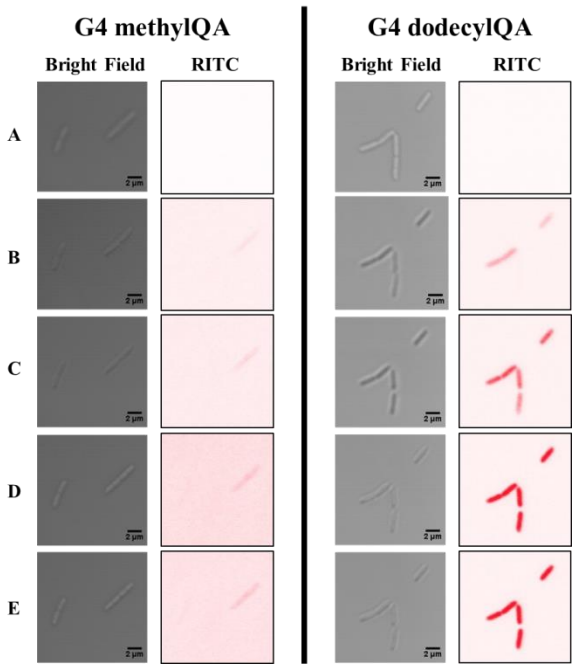

Figure 3.1. Confocal microscopy images of *P. aeruginosa* exposed to 50 µg/mL RITC-tagged G4 methylQA and G4 dodecylQA dendrimers at (A) 0, (B) 4, (C) 6, (D) 8, and (E) 10 min after dendrimer addition. Threshold reversed for clarity.

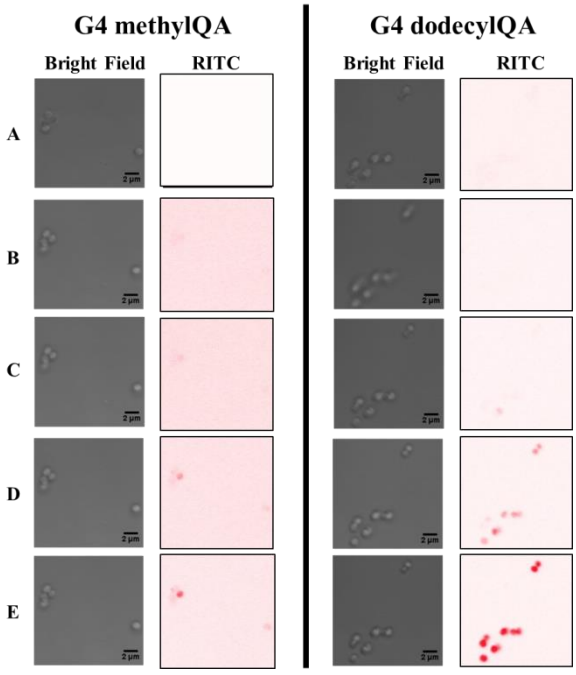

Figure 3.2. Confocal microscopy images of *S. aureus* exposed to 50 µg/mL RITC-tagged G4 methylQA and G4 dodecylQA dendrimers at (A) 0, (B) 20, (C) 24, (D) 28, and (E) 32 min after dendrimer addition. Threshold reversed for clarity.

As expected, longer QA alkyl chains (i.e., octylQA, dodecylQA) were significantly more bactericidal than the shorter alkyl chains (i.e., methylQA, butylQA) for both dendrimer generations regardless of bacterial strain. The increased efficacy of octylQA- and dodecylQA-modified dendrimers against *S. aureus* and *P. aeruginosa* is likely due to insertion of the longer alkyl chain groups into the peptidoglycan layer, resulting in physical disruption of the cell membrane.[11] Furthermore, the greater hydrophobicity of the octyl and dodecyl groups versus the shorter alkyl chains may allow for enhanced association of the dendrimers with the bacteria cell membranes. This is evident in the confocal microscopy images of RITC-tagged dendrimers with both *P. aeruginosa* and *S. aureus*, with G4 dodecylQA dendrimers associating to a greater extent in a shorter period of time than the G4 methylQA dendrimers (Figures 3.1 and 3.2). The increased association efficiency combined with the potential for greater membrane damage results in dramatically enhanced killing for these biocides. While the dodecylQA-modified dendrimers are slightly more effective than the octylQA-modified dendrimers for both generations, this trend does not apply to the methylQA- and butylQA-modified dendrimers. For G1 dendrimers, the butylQA modification was more effective than methylQA against *S. aureus*, with a decrease in MBC_{4h} from >8.0 to 3.5 mg/mL, respectively. These results indicate that the slight increase in alkyl chain length may allow for better association of the G1 butylQA dendrimers, resulting in greater antibacterial activity against *S. aureus*.

The same trend in bactericidal efficacy was not observed for the G4 scaffold. In fact, G4 methylQA dendrimers were almost twice as effective as G4 butylQA against both *S. aureus* and *P. aeruginosa*. The lowered bactericidal efficacy is attributed to decreased dendrimer-bacteria association for the G4 butylQA dendrimers relative to the G4 methylQA system (Figure 3.3). A number of factors may play a role in this decreased association. Normally, the positively charged

ammonium group enhances association of the biocide with the bacteria membrane. However, back-folding of the peripheral functional groups toward the dendrimer interior may shield the QA from the bacterial membrane, resulting in less membrane damage.[27] Shielding effect are often further amplified for the G4 scaffold (as compared to G1) due to the closer proximity of terminal functional groups. Although the bactericidal concentration of G4 butylQA was below the CVC (>5.0 mg/mL), a decrease in surface tension was still observed at these concentrations, which may be indicative of dendrimers assembling at the air-water interface instead of associating with bacteria in solution.[28, 29] We hypothesize that the slightly longer alkyl chain amplifies both QA shielding and the formation of supramolecular assemblies for the G4 butylQA scaffold, reducing its bactericidal action from that of the methylQA system.

The co-administration of active-releasing antibacterial agents with contact-based QA biocides has been shown to result in a more effective antibacterial treatment.[14, 15] We thus sought to combine active NO release, itself a multi-mechanistic antimicrobial, with the contact-based biocidal attributes of QA-modified dendrimers. The combination of NO release with the short QA alkyl chains dramatically increased the bactericidal efficacy for both G1 and G4 scaffolds, resulting in a 2 – 7 fold decrease in MBC_{4h} values over single-action QA-modified dendrimers. For most of the scaffolds, the bactericidal NO doses required to kill *S. aureus* was nearly twice that required for *P. aeruginosa* (Table 3.1). The larger NO dose for *S. aureus* killing is attributed to the more robust peptidoglycan layer inhibiting NO diffusion into the bacteria, while for *P. aeruginosa* the outer membrane and thinner peptidoglycan layer do not impede NO diffusion as efficiently. The addition of NO release to the octylQA- and dodecylQA-modified G1 dendrimers resulted in increased bactericidal efficacy against *P. aeruginosa* compared to their non-NO-releasing counterparts, but had no effect on their bactericidal action against *S. aureus.* Imparting

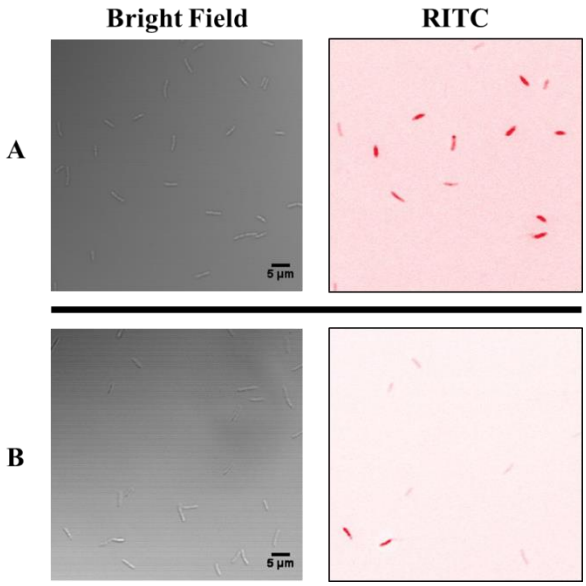

Figure 3.3. Confocal microscopy images of *P. aeruginosa* exposed to 50 µg/mL RITC-tagged (A) G4 methylQA and (B) G4 butylQA dendrimers after 20 min exposure. Threshold reversed for clarity.

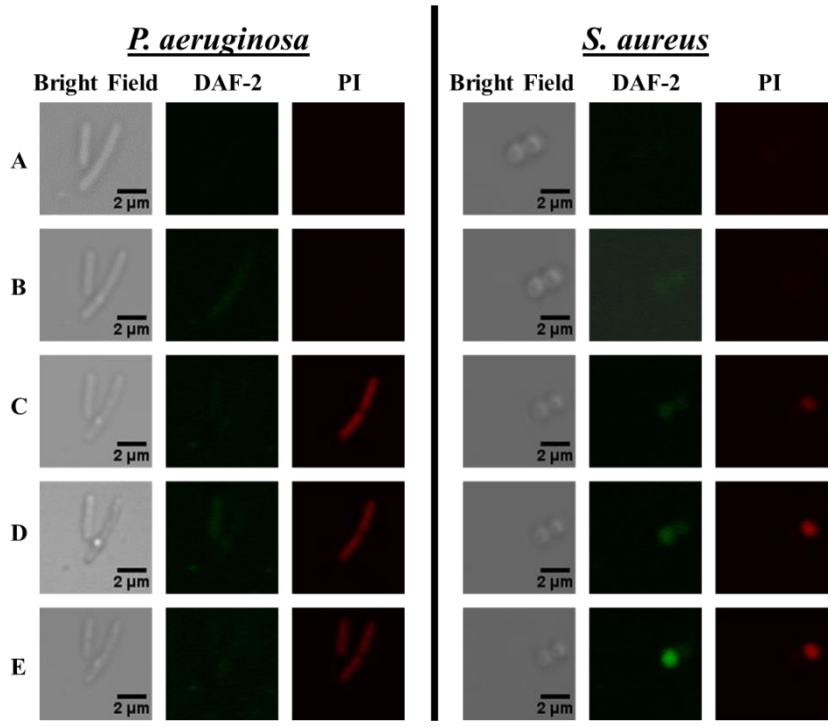

Figure 3.4. Confocal microscopy images of *P. aeruginosa* and *S. aureus* exposed to 20 µg/mL G4 dodecylQA/NO dendrimers at (A) 0, (B) 25, (C) 35, (D) 45, and (E) 60 min after dendrimer addition. DAF-2 green fluorescence designates the presence of intracellular NO, while PI red fluorescence indicates compromised membranes (cell death).

NO release to the G4 dodecylQA dendrimers did not affect the efficacy against either pathogen; both the single- and dual-action dendrimers exhibited bactericidal action against *S. aureus* and *P. aeruginosa* at equivalent concentrations (10 μg/mL). For this system, the long dodecyl chains likely cause increased physical disruption of the cell membrane, precluding intracellular NO buildup. Intracellular NO levels and membrane disruption caused by the scaffolds were qualitatively assessed via confocal microscopy of bacterial suspensions stained with specific fluorescence probes (i.e., DAF-2 and PI). In cases where NO serves as the lone antibacterial, a bright green fluorescent signal from DAF-2 (indicative of intracellular NO buildup) is generally observed prior to red fluorescence (PI), signifying membrane disruption and subsequent cell death.[7] As this red fluorescence increases, the green fluorescence is concomitantly diminished as the DAF-2 diffuses out of the membrane-compromised bacteria. Bacteria incubated with G4 dodecylQA/NO, however, exhibited considerable membrane disruption before any significant NO accumulation (Figure 3.4). For both *P. aeruginosa* and *S. aureus*, some intracellular NO was briefly observed after 25 min, but the significant membrane disruption observed for both strains shortly thereafter (at 35 min) supports our hypothesis that the dodecylQA modification compromises the cell membrane to such an extent it precludes the buildup of intracellular NO.

Finally, we compared the bactericidal action of NO-releasing QA-modified dendrimers against unmodified G1 and G4 PAMAM scaffolds to determine if the combinatorial effects were indeed more efficacious. The unmodified G1 and G4 dendrimers were significantly more effective against *P. aeruginosa* than *S. aureus* (Table 3.1). For the G1 scaffold, both individual and dual action octylQA- and dodecylQA-modified dendrimers were more bactericidal than G1 PAMAM against both pathogens. A similar result was obtained for the G4 modifications, with the exception of the individual and dual action G4 octylQA dendrimers, which exhibited equivalent bactericidal

efficacy as the G4 scaffold against *P. aeruginosa*. Modifying the G1 and G4 scaffolds with short QA alkyl chains (i.e., methylQA and butylQA) greatly decreased their antibacterial action, with only G1 butylQA dendrimers exhibiting greater bactericidal efficacy against *S. aureus* than their corresponding PAMAM scaffold. Efficacy of the NO-releasing methylQA and butylQA systems compared to the G1 and G4 scaffolds was dependent on bacterial Gram designation. G4 methylQA/NO and G4 butylQA/NO exhibited an almost 10-fold reduction in bactericidal action against *P. aeruginosa* from the G4 scaffold, while G1 methylQA/NO and G1 butylQA/NO maintained relatively similar antibacterial efficacy as G1 PAMAM. However, all of the dual action QA-modified dendrimers displayed significantly greater bactericidal efficacy against Gram-positive *S. aureus* than the unmodified PAMAM scaffolds, demonstrating the utility of these dual action dendrimers as broad-spectrum antibacterial agents.

3.3.2 Antibacterial action of alkyl chain-modified PAMAM dendrimers

As the bactericidal action of the QA-modified dendrimers was found to be highly dependent on alkyl chain length, we sought to investigate the effects of dendrimer hydrophobicity (i.e., alkyl chain length) on antibacterial action in the absence of the positively charged quaternary ammonium. The antibacterial action of the alkyl chain-modified dendrimers was evaluated against the nosocomial pathogens *P. aeruginosa*, *S. aureus*, and methicillin-resistant *S. aureus* (MRSA). The use of these bacteria allowed us to further understand the effects of bacterial Gram class and antibiotic resistance on the bactericidal efficacy of the dendrimer biocides. Similar to evaluation of QA-modified dendrimer antibacterial action, planktonic bacteria viability assays were performed under static conditions to determine the minimum dendrimer concentration required to elicit a 3-log reduction in bacterial viability over 24 h (MBC_{24h}).

Table 3.2 Minimum bactericidal concentrations (MBC_{24h}) for single- and dual-action alkyl chain-modified dendrimers against planktonic *P. aeruginosa*, *S. aureus*, and MRSA.[a]

	P. aeruginosa **MBC_{24h} (μg/mL)**	***S. aureus*** **MBC_{24h} (μg/mL)**	**MRSA** **MBC_{24h} (μg/mL)**
Vancomycin		25	12.5
G1 butyl	2000	3000	6000
G1 butyl/NO	1000	2000	1000
G1 hexyl	50	100	100
G1 hexyl/NO	25	100	100
G1 octyl	25	25	25
G1 octyl/NO	25	25	25
G1 dodecyl	25	25	25
G1 dodecyl/NO	25	25	25
G2 butyl	25	1000	1000
G2 butyl/NO	50	2000	1000
G2 hexyl	25	100	100
G2 hexyl/NO	25	100	100
G3 butyl	25	500	250
G3 butyl/NO	50	1000	250
G3 hexyl	10	50	50
G3 hexyl/NO	25	50	100
G4 butyl	50	500	500
G4 butyl/NO	50	500	500
G4 hexyl	25	100	100
G4 hexyl/NO	25	50	100

[a]Each parameter was analyzed with multiple replicates ($n \geq 3$).

Both the butyl- and hexyl-modified G1 dendrimers were more effective at eradicating planktonic *P. aeruginosa* than either *S. aureus* or MRSA (Table 3.2), corroborating our previous observations in which QA-modified dendrimers containing short alkyl chains exhibited greater bactericidal action against *P. aeruginosa* over *S. aureus*.[30] The more effective killing was attributed to faster dendrimer association with *P. aeruginosa* bacteria and the inability of the shorter alkyl chains to effectively disrupt the thick peptidoglycan layer of Gram-positive *S. aureus* bacterial cells.[26] As expected, the longer octyl and dodecyl alkyl chain modifications were more bactericidal than the shorter alkyl chains, especially against the Gram-positive bacterial strains. However, the G1 octyl and dodecyl dendrimers were equally effective at eradicating all three bacterial strains regardless of Gram designation, a discernable difference than the QA-modified system. Of note, no increase in efficacy was observed for the dodecyl modifications over the octyl-modified dendrimers. G1 hexyl dendrimers exhibited similar efficacy against *P. aeruginosa* as the longer alkyl chain modifications, suggesting a limit to the benefits of increasing alkyl chain length, particularly for these longer bactericidal assays.

Similar to previous observations, the addition of NO release was more beneficial for the shorter butyl and hexyl modifications than the longer octyl- and dodecyl-modified dendrimers. Indeed, G1 butyl/NO dendrimers exhibited greater bactericidal efficacy against all three bacterial strains compared to single-action G1 butyl, while G1 hexyl/NO dendrimers were slightly more effective at killing *P. aeruginosa* than G1 hexyl. Neither the octyl nor dodecyl modifications benefited from the addition of NO-release capabilities against any of the strains tested. Similar to the QA-modified dendrimers, this was attributed to these longer alkyl chains causing sufficient membrane damage to preclude the buildup of intracellular NO to bactericidal concentrations.[30]

The antibacterial action of G2 though G4 butyl- and hexyl-modified dendrimers was next evaluated to determine the effects of dendrimer generation on bactericidal action. Following the trend observed for the G1 dendrimers, single-action (i.e., non-NO-releasing) butyl and hexyl modifications were more efficacious against *P. aeruginosa* regardless of generation. The majority of the single-action biocides were equally effective against both Gram-positive bacteria strains, with only the G1 and G3 butyl biocides exhibiting dissimilar biocidal concentrations between *S. aureus* and MRSA. The bactericidal concentration for G1 butyl was found to be double for MRSA over *S. aureus* (6 and 3 mg/mL, respectively) while the MBC_{24h} for G3 butyl was greater for *S. aureus* over MRSA (500 and 250 μg/mL, respectively). As such, bacterial antibiotic resistance was determined to have little effect on the bactericidal action of alkyl chain-modified dendrimers, most likely due to the contact-based killing mechanism of membrane disruption exhibited by the hydrophobic dendrimers.

The hexyl-modified dendrimers were characterized by increased bactericidal activity over the butyl modifications against all three bacteria strains, likely due to greater membrane intercalation and cell membrane damage by the slightly longer hexyl chains. Further, while the butyl-modified dendrimers exhibited a sizeable increase in antibacterial action at higher generations, the bactericidal action of the hexyl-modified dendrimers varied little with dendrimer generation. G2–G4 butyl dendrimers proved more biocidal against each bacterial strain than G1 butyl, suggesting that short alkyl chain modifications benefit substantially from greater functional group density. Within the higher generations, G3 butyl dendrimers exhibited the greatest bactericidal action, requiring the lowest concentrations to eradicate each bacterial strain. Likewise, the G3 hexyl dendrimers were more effective at eradicating planktonic bacteria compared to other generations, even though the hexyl-modified dendrimers demonstrated little variation in biocidal

activity with generation. These observations suggest that the G3 scaffold may represent an optimal balance between size and functional group density, maximizing bactericidal action against both Gram-positive and Gram-negative bacteria.

With the addition of NO release, the resultant biocidal action of the now dual-action dendrimer biocides was largely dependent on dendrimer generation. The G1 scaffold benefited most from NO donor modification, with both G1 butyl/NO and G1 hexyl/NO dendrimers exhibiting greater efficacy than their non-NO-releasing counterparts. In contrast, a slightly antagonistic effect was observed upon the addition of NO release to the G2 and G3 scaffolds. Indeed, G2 butyl/NO, G3 butyl/NO, and G3 hexyl/NO dendrimers all required similar or greater dendrimer concentrations to eradicate Gram-positive and Gram-negative bacteria versus controls (i.e., single-action biocides). Little difference in bactericidal efficacy was observed between the single- and dual-action G4 dendrimers against any of the bacteria strains, suggesting that the increased functional group density of the larger scaffolds results in significant membrane damage, precluding any beneficial effects of NO release.

3.3.3 In vitro cytotoxicity

The relative toxicity against mammalian cells at bactericidal doses is critical to the design of any new antibacterial agent. Although the clinical utility of long chain quaternary ammonium salts has been somewhat limited to topical applications due to their inherent toxicity, tethering QA moieties to larger scaffolds has been shown to mitigate their toxic effects.[13, 31] The toxicity of the QA-modified dendrimers prepared herein was thus evaluated against L929 mouse fibroblast cells. The resulting dendrimer cytotoxicity was dependent on dendrimer generation, QA alkyl chain length, and biocide concentration (Figure 3.5). While the G4 methylQA dendrimers were non-toxic at 500 μg/mL (4% decrease in cell viability), increasing the biocide concentration four-fold

to 2.0 mg/mL reduced L929 cell viability by 20%. In contrast, the toxicity of G4 butylQA dendrimers was generally independent of concentration (both 1.0 and 3.5 mg/mL reduced cell viability by 40%). However, the toxicity of the butylQA functionality was generation dependent, with the G4 scaffold causing an additional 10% decrease in cell viability versus the G1 butylQA system at 3.5 mg/mL. Of significance, the low (but highly antibacterial) concentrations (i.e., 10 μg/mL) of the dodecylQA-modified dendrimers were relatively non-toxic, only reducing L929 cell viability by 15 and 2% for G1 and G4, respectively.

While the large initial NO burst characteristic of these macromolecular scaffolds may yield toxic levels of NO at higher concentrations (i.e., those required to eradicate biofilms), the concentrations tested herein did not exhibit significant toxicity to mammalian cells. Indeed, the NO-releasing QA-modified dendrimers proved to be relatively non-toxic, exhibiting >80% L929 cell viability at the effective bactericidal concentrations. Furthermore, NO release resulted in increased cell viability versus controls for nearly all of the QA modifications, demonstrating a substantial improvement over previously reported silica-based systems.[8] For several of the scaffolds that exhibited the same bactericidal concentration for both the single- and dual-action QA-modified dendrimers, the addition of NO release resulted in increased fibroblast cell viability. For example, the G4 octylQA and G4 octylQA/NO dendrimers resulted in cell viabilities of 90 and 101%, respectively, at 30 μg/mL doses. These results indicate that the combination of low NO concentrations with QA moieties may be beneficial in decreasing the overall toxicity of QA scaffolds to mammalian cells. It is important to note that the bactericidal doses for all of the NO-releasing QA-modified dendrimers resulted in greater L929 cell viability than the unmodified G1 and G4 PAMAM dendrimers, demonstrating the advantage of dual action therapeutics in reducing scaffold toxicity.

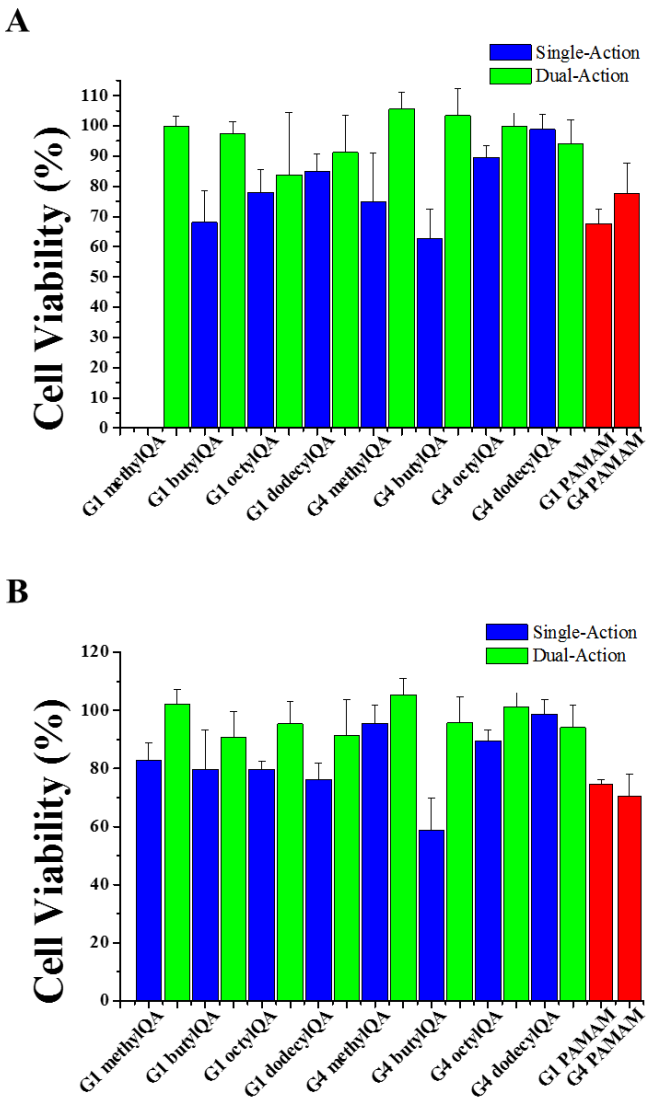

Figure 3.5. Viability (%) of L929 mouse fibroblast cells following 4 h exposure to single- (blue) and dual-action (green) QA-modified dendrimers, as well as unmodified PAMAM dendrimers (red), at the MBC_{4h} against (A) *S. aureus* and (B) *P. aeruginosa* compared to untreated control cells. For all measurements, $n \geq 3$ pooled experiments with error bars representing standard deviation of the mean.

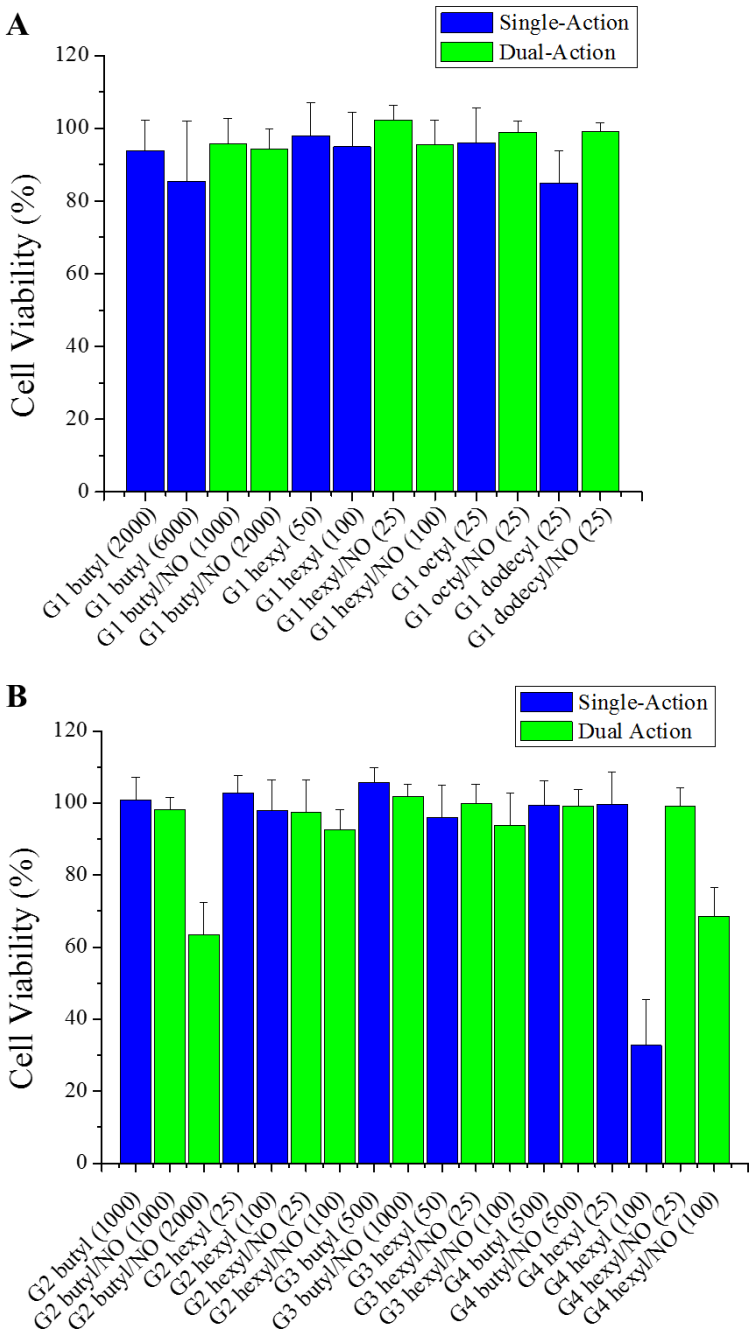

Figure 3.6. Viability (%) of L929 mouse fibroblast cells following 24 h exposure to single- (blue) and dual-action (green) alkyl chain-modified dendrimers compared to untreated control cells. Values in parenthesis represent dendrimer concentration in μg/mL. For all measurements, $n \geq 3$ pooled experiments with error bars representing standard deviation of the mean.

The toxicity of alkyl chain-modified dendrimers was evaluated against L929 fibroblast cells at the highest and lowest bactericidal concentrations over 24 h. In general, the alkyl chain-modified dendrimers were overall less toxic than their QA counterparts. All of the G1 alkyl chain dendrimers were relatively non-toxic at their highest bactericidal concentrations against planktonic bacteria, resulting in >80% cell viability compared to untreated controls (Figure 3.6 A). For the most toxic G1 modifications (i.e., 6 mg/mL G1 butyl and 25 μg/mL G1 dodecyl), the addition of NO release resulted in improved cell viability. While the decrease in toxicity for G1 butyl/NO dendrimers is likely due to the lower bactericidal concentration required, the dodecyl-modified dendrimers were tested at the same concentration with and without NO release. Similar to the long alkyl chain QA modifications, the low levels of NO released by G1 dodecyl/NO dendrimers appear to mitigate some of the toxicity inherent to the dodecyl-modified scaffold, decreasing the reduction in cell viability from 15% to <1% at 25 μg/mL doses.

Increasing the dendrimer generation appeared to have little impact on the toxicity of butyl- and hexyl-modified dendrimers at bactericidal concentrations. Indeed, single-action butyl-modified dendrimers exhibited >90% cell viability at concentrations up to 2 mg/mL regardless of dendrimer generation (Figure 3.6 B). Within the hexyl modifications only the G4 hexyl scaffold exhibited significant toxicity, reducing cell viability by 67% at a concentration of 100 μg/mL. As the G1 and G2 hexyl scaffolds reduced cell viability by <5% at similar concentrations, the dramatic increase in G4 hexyl toxicity is attributed to the increased functional group density afforded by the G4 scaffold. Of note, butyl- and hexyl-modified G3 dendrimers, which exhibited the greatest bactericidal action, were non-toxic to mammalian cells (>94% viability at all concentrations tested).

The addition of NO release to the alkyl chain-modified scaffolds had mixed effects on dendrimer toxicity. For most of the dendrimer modifications, the single- and dual-action dendrimers exhibited similar toxicity at the concentrations tested. Nitric oxide-releasing G2 butyl dendrimers exhibited a concentration-dependent toxicity, with 1 and 2 mg/mL dendrimer concentrations resulting in 2 and 37% reductions in cell viability, respectively. Alternatively, adding NO-release capabilities to the G4 hexyl scaffold decreased the toxicity by half, improving cell viability from 33 to 69% at 100 μg/mL. These results suggest that NO toxicity is highly dose-dependent. While low NO concentrations help to mitigate some of the toxic effects of the dendrimer scaffold, larger NO doses (~2 μmol/mL and greater) detrimentally impact mammalian cells.

3.4 Conclusions

Both single and dual-action QA-modified PAMAM dendrimers exhibited biocidal activity against *P. aeruginosa* and *S. aureus*, with longer QA alkyl chains (i.e., octylQA, dodecylQA) proving more effective than shorter chain (i.e., methylQA, butylQA) modifications for both G1 and G4 dendrimer scaffolds. While previous work has suggested that QA compounds are more potent against Gram-positive versus Gram-negative bacteria due to the additional outer membrane barrier characteristic of Gram-negative bacteria, this observation has lacked a mechanistic understanding.[12, 20] This work indicates that the potency of QA moieties against Gram-positive and Gram-negative bacteria is highly dependent on both the QA alkyl chain length and functional group density. In contrast to a prior report,[21] G4 dendrimers modified with shorter QA alkyl chains demonstrate reasonable bactericidal action against both *P. aeruginosa* and *S. aureus*, albeit at higher concentrations than those required for longer QA alkyl chain lengths. While the addition of NO release markedly improves the bactericidal action of short alkyl chain QA-modified G1 and

G4 dendrimers against both bacteria strains, the longer alkyl chain QA dendrimers do not benefit from NO release in the same manner. For these systems, the long alkyl chains induce significant damage to the bacteria membrane, greatly increasing their biocidal action but precluding the buildup of intracellular NO.

The alkyl chain-modified dendrimers exhibited similar trends in bactericidal action as the QA modifications, with the shorter alkyl chains proving more effective against *P. aeruginosa* than *S. aureus*. However, the longer octyl and dodecyl modifications were equally effective against each of the strains tested, suggesting the longer assay times allow for greater membrane damage to the bacterial cell regardless of Gram designation. The addition of NO release had mixed effects on both the bactericidal action and cytotoxicity of the alkyl chain-modified dendrimers, with short alkyl chain-modified G1 dendrimers exhibiting greater bactericidal action with NO-release capabilities and the low levels of NO release from G4 hexyl dendrimers mitigating scaffold toxicity. While the dual-action biocides did not exhibit dramatically improved bactericidal efficacy over the single-action dendrimers against planktonic bacteria, all systems were carried forward into biofilm assays due to the known challenges of eradicating these bacterial communities. The majority of these dual-action QA- and alkyl chain-modified antibacterial agents continue to hold great therapeutic potential as they exhibit minimal toxicity to mammalian cells at the dendrimer concentrations required to elicit a three-log reduction in bacterial viability.

REFERENCES

(1) Boucher, H. W., Talbot, G. H., Bradley, J. S., Edwards, J. E., Gilbert, D., Rice, L. B., Scheld, M., Spellberg, B., and Bartlett, J. "Bad bugs, no drugs: No eskape! An update from the infectious diseases society of america" *Clinical Infectious Diseases* **2009**, *48*, 1-12.

(2) Cottarel, G., and Wierzbowski, J. "Combination drugs, an emerging option for antibacterial therapy" *Trends in Biotechnology* **2007**, *25*, 547-555.

(3) Eliopoulos, G., and Eliopoulos, C. "Antibiotic combinations: Should they be tested?" *Clinical Microbiology Reviews* **1988**, *1*, 139-156.

(4) Fischbach, M. A. "Combination therapies for combating antimicrobial resistance" *Current Opinion in Microbiology* **2011**, *14*, 519-523.

(5) Fang, F. C. "Perspectives series: Host/pathogen interactions. Mechanisms of nitric oxide-related antimicrobial activity" *Journal of Clinical Investigation* **1997**, *99*, 2818.

(6) Fang, F. C. "Antimicrobial reactive oxygen and nitrogen species: Concepts and controversies" *Nature Reviews Microbiology* **2004**, *2*, 820-832.

(7) Hetrick, E. M., Shin, J. H., Stasko, N. A., Johnson, C. B., Wespe, D. A., Holmuhamedov, E., and Schoenfisch, M. H. "Bactericidal efficacy of nitric oxide-releasing silica nanoparticles" *ACS Nano* **2008**, *2*, 235-246.

(8) Carpenter, A. W., Worley, B. V., Slomberg, D. L., and Schoenfisch, M. H. "Dual action antimicrobials: Nitric oxide release from quaternary ammonium-functionalized silica nanoparticles" *Biomacromolecules* **2012**, *13*, 3334-3342.

(9) Privett, B. J., Deupree, S. M., Backlund, C. J., Rao, K. S., Johnson, C. B., Coneski, P. N., and Schoenfisch, M. H. "Synergy of nitric oxide and silver sulfadiazine against gram-negative, gram-positive, and antibiotic-resistant pathogens" *Molecular Pharmaceutics* **2010**, *7*, 2289-2296.

(10) Sun, B., Slomberg, D. L., Chudasama, S. L., Lu, Y., and Schoenfisch, M. H. "Nitric oxide-releasing dendrimers as antibacterial agents" *Biomacromolecules* **2012**, *13*, 3343-3354.

(11) Simoncic, B., and Tomsic, B. "Structures of novel antimicrobial agents for textiles-a review" *Textile Research Journal* **2010**, *80*, 1721-1737.

(12) Chen, C. Z., Beck-Tan, N. C., Dhurjati, P., van Dyk, T. K., LaRossa, R. A., and Cooper, S. L. "Quaternary ammonium functionalized poly (propylene imine) dendrimers as effective antimicrobials: Structure-activity studies" *Biomacromolecules* **2000**, *1*, 473-480.

(13) Thorsteinsson, T., Másson, M., Kristinsson, K. G., Hjálmarsdóttir, M. A., Hilmarsson, H., and Loftsson, T. "Soft antimicrobial agents: Synthesis and activity of labile environmentally friendly long chain quaternary ammonium compounds" *Journal of Medicinal Chemistry* **2003**, *46*, 4173-4181.

(14) Li, Z., Lee, D., Sheng, X., Cohen, R. E., and Rubner, M. F. "Two-level antibacterial coating with both release-killing and contact-killing capabilities" *Langmuir* **2006**, *22*, 9820-9823.

(15) Song, J., Kang, H., Lee, C., Hwang, S. H., and Jang, J. "Aqueous synthesis of silver nanoparticle embedded cationic polymer nanofibers and their antibacterial activity" *ACS Applied Materials & Interfaces* **2011**, *4*, 460-465.

(16) Duncan, R., and Izzo, L. "Dendrimer biocompatibility and toxicity" *Advanced Drug Delivery Reviews* **2005**, *57*, 2215-2237.

(17) Tomalia, D. A. "Birth of a new macromolecular architecture: Dendrimers as quantized building blocks for nanoscale synthetic polymer chemistry" *Progress in Polymer Science* **2005**, *30*, 294-324.

(18) Jevprasesphant, R., Penny, J., Attwood, D., McKeown, N. B., and D'Emanuele, A. "Engineering of dendrimer surfaces to enhance transepithelial transport and reduce cytotoxicity" *Pharmaceutical Research* **2003**, *20*, 1543-1550.

(19) Wiwattanapatapee, R., Carreño-Gómez, B., Malik, N., and Duncan, R. "Anionic pamam dendrimers rapidly cross adult rat intestine in vitro: A potential oral delivery system?" *Pharmaceutical Research* **2000**, *17*, 991-998.

(20) Chen, C. Z., Cooper, S., and Tan, N. B. "Incorporation of dimethyldodecylammonium chloride functionalities onto poly (propylene imine) dendrimers significantly enhances their antibacterial properties" *Chemical Communications* **1999**, 1585-1586.

(21) Charles, S., Vasanthan, N., Kwon, D., Sekosan, G., and Ghosh, S. "Surface modification of poly (amidoamine)(PAMAM) dendrimer as antimicrobial agents" *Tetrahedron Letters* **2012**.

(22) Breed, R. S., and Dotterrer, W. "The number of colonies allowable on satisfactory agar plates" *Journal of Bacteriology* **1916**, *1*, 321-331.

(23) Lu, Y., Slomberg, D. L., Shah, A., and Schoenfisch, M. H. "Nitric oxide-releasing amphiphilic poly (amidoamine)(PAMAM) dendrimers as antibacterial agents" *Biomacromolecules* **2013**, *14*, 3589-3598.

(24) Slomberg, D. L., Lu, Y., Broadnax, A. D., Hunter, R. A., Carpenter, A. W., and Schoenfisch, M. H. "Role of size and shape on biofilm eradication for nitric oxide-releasing silica nanoparticles" *ACS Applied Materials & Interfaces* **2013**, *5*, 9322-9329.

(25) Bjarnsholt, T., Kirketerp-Møller, K., Jensen, P. Ø., Madsen, K. G., Phipps, R., Krogfelt, K., Høiby, N., and Givskov, M. "Why chronic wounds will not heal: A novel hypothesis" *Wound Repair and Regeneration* **2008**, *16*, 2-10.

(26) Beveridge, T. J. "Structures of gram-negative cell walls and their derived membrane vesicles" *Journal of Bacteriology* **1999**, *181*, 4725-4733.

(27) Maiti, P. K., Cagin, T., Wang, G., and Goddard, W. A. "Structure of PAMAM dendrimers: Generations 1 through 11" *Macromolecules* **2004**, *37*, 6236-6254.

(28) Fréchet, J. M. "Dendrimers and supramolecular chemistry" *Proceedings of the National Academy of Sciences* **2002**, *99*, 4782-4787.

(29) Schenning, A. P., Elissen-Roman, C., Weener, J.-W., Baars, M. W., van der Gaast, S. J., and Meijer, E. "Amphiphilic dendrimers as building blocks in supramolecular assemblies" *Journal of the American Chemical Society* **1998**, *120*, 8199-8208.

(30) Worley, B. V., Slomberg, D. L., and Schoenfisch, M. H. "Nitric oxide-releasing quaternary ammonium-modified poly(amidoamine) dendrimers as dual action antibacterial agents" *Bioconjugate Chemistry* **2014**, *25*, 918-927.

(31) Lv, H., Zhang, S., Wang, B., Cui, S., and Yan, J. "Toxicity of cationic lipids and cationic polymers in gene delivery" *Journal of Controlled Release* **2006**, *114*, 100-109.

CHAPTER 4:

Anti-Biofilm Efficacy of Dual-Action Dendrimers

4.1 Introduction

Nosocomial infections present a tremendous challenge to society, representing the fourth leading cause of death in the U.S. alone and resulting in over $5 billion in medical costs annually.[1] Approximately 10% of hospitalized patients acquire infections from opportunistic pathogens such as *Pseudomonas aeruginosa* and *Staphylococcus aureus*, which are notorious for forming chronic biofilms that resist standard antibiotic treatment.[2] Biofilms form after planktonic bacteria irreversibly attach to a surface and produce an exopolysaccharide (EPS) matrix that surrounds and protects the bacterial community.[3-5] Biofilm-based infections exhibit increased resistance to antibacterial agents, often requiring therapeutic doses 3–4 orders of magnitude greater than those required to eradicate planktonic bacteria.[3] The inability of antibiotics to effectively eradicate biofilms is attributed to: 1) the EPS matrix limiting the diffusion of antibacterial agents into the biofilm; 2) slower bacterial metabolism reducing the efficacy of antibiotics; and, 3) the biofilm chemical microenvironment (e.g. pH, pCO_2, pO_2) adversely affecting antibacterial activity.[3] The inherent resistance of biofilms to traditional therapeutics combined with the increasing prevalence of antibiotic-resistant bacteria in clinical settings necessitates the development of new antibacterial agents that are capable of eradicating biofilms without fostering resistance.[1, 6]

Combination therapies, or the co-administration of two mechanistically different antibacterial agents, have been demonstrated to increase the bactericidal efficacy of individual biocides while reducing the emergence of bacterial resistance.[7, 8] Specifically, the combination

of a non-depleting, contact-based biocide with releasable antibacterial agents prolongs bactericidal action while increasing the overall antibacterial sphere of influence.[9, 10] The enhanced bactericidal efficacy of the dual-action scaffold should lower the required therapeutic dose and concomitantly reduce any toxicity to healthy cells and tissue.[7]

Nitric oxide (NO), an endogenously produced free radical, holds great potential as a releasable antibacterial agent due to its central role in the body's immune response to infection.[11, 12] The broad-spectrum antibacterial action of NO is attributed to the production of reactive byproducts (e.g., dinitrogen trioxide and peroxynitrite) that compromise bacterial cell function and lead to membrane disruption through both nitrosative and oxidative stresses.[11-13] Furthermore, the multi-mechanistic killing of NO makes it unlikely to foster bacterial resistance.[14] Alternatively, contact-based biocides such hydrophobic alkyl chains can exert antibacterial activity through direct interactions, such as intercalating into and disrupting the hydrophobic cell membrane.[15-17] Our laboratory has developed a toolbox of large molecular frameworks capable of storing and controllably releasing NO for use as novel antibacterial agents.[13, 18-22] Benefits of these macromolecular scaffolds include controllable NO release rates and payloads as well as allowing for the combination of multiple biocides on a single scaffold.[23, 24]

Of the NO-releasing macromolecular scaffolds pioneered by our lab, poly(amidoamine) (PAMAM) dendrimers are a particularly promising candidate for the development of anti-biofilm agents. Dendrimers are hyperbranched macromolecular polymers exhibiting unique multivalent architectures and modifiable peripheral functional groups, making them excellent scaffolds for drug delivery.[25-27] The dendrimer exterior can be altered by modifying the terminal primary amines with various functional groups, allowing for specific targeting of bacterial cell membranes.[25, 28] Increasing the dendrimer generation allows for facile synthetic control over

scaffold size and increases the number of terminal primary amines, resulting in greater functional group density.[26, 27] Combining these factors with their ability to associate with and/or cross bacterial cell membranes makes dendrimers ideal candidates for use as anti-biofilm agents.[29, 30] Indeed, initial investigations into the anti-biofilm activity of dendrimer scaffolds have yielded promising results. Johansson et al. functionalized peptide dendrimer scaffolds with LecB ligands and found that the multivalency afforded by the dendrimer scaffold increased LecB binding over monovalent ligands, inhibiting *P. aeruginosa* biofilm growth.[31] Similarly, Hou et al. found that antimicrobial dendrimeric peptides reduced the formation of *Escherichia coli* biofilms by 93% compared to untreated controls.[32] In our lab, Lu et al. reported increased killing of *P. aeruginosa* biofilms with hydrophobic dendrimers; unfortunately, these dendrimers were toxic to L929 mouse fibroblast cells at low concentrations (i.e., 10–30 μg/mL).[33] The use of more hydrophilic amphiphiles provided to be less toxic at therapeutic levels while demonstrating greater anti-biofilm activity with NO release, indicating the benefit of combining multiple biocides on a single macromolecular scaffold. Herein, we describe the anti-biofilm action of single- and dual-action generation 1 (G1) through generation 4 (G4) butyl- and hexyl-modified PAMAM dendrimers to determine the effects of exterior hydrophobicity (i.e., alkyl chain length), dendrimer size (generation), and NO release against both Gram-positive and Gram-negative biofilms. We further evaluate the efficacy of NO-releasing G3 dendrimers in concert with the traditional antibiotic vancomycin against Gram-positive *S. aureus* and methicillin-resistant *S. aureus* biofilms.

4.2 Materials and Methods

Phenazine methosulfate (PMS), fetal bovine serum (FBS) trypsin, 3-(4,5-dimethylthiazol-2-yl)-5-(3-carboxymethoxyphenyl)-2-(4-sulfophenyl)-2H-tetrazolium inner salt (MTS), penicillin streptomycin (PS), triethylamine (TEA), rhodamine B isothiocyanate (RITC), propidium iodide

(PI), and vancomycin hydrochloride (from *Streptomyces orientalis*) were purchased from Sigma-Aldrich (St. Louis, MO). Dulbecco's modified Eagle's medium (DMEM) and Dulbecco's phosphate buffered saline (PBS) were obtained from Lonza Group (Basel, Switzerland). 4,5-Diaminofluorescein diacetate (DAF-2 DA) was purchased from Calbiochem (San Diego, CA). Tryptic soy broth (TSB) and tryptic soy agar (TSA) were obtained from Becton, Dickinson and Company (Franklin Lakes, NJ). *Pseudomonas aeruginosa* (*P. aeruginosa*; ATCC #19143), *Staphylococcus aureus* (*S.aureus*; ATCC #29213), and methicillin-resistant *S. aureus* (MRSA; ATCC #33591) were obtained from American Type Tissue Culture Collection (Manassas, VA). L929 mouse fibroblasts were obtained from the UNC Tissue Culture Facility (Chapel Hill, NC). The Centers for Disease Control and Prevention (CDC) bioreactor was purchased from BioSurface Technologies Corporation (Bozeman, MT). Medical grade silicone rubber (1.45 mm thick) was purchased from McMaster Carr (Atlanta, GA) and doubled in thickness using Superflex Clear RTV silicone adhesive sealant (Loctite, Westlake, OH) to fabricate coupons to fit the CDC bioreactor (thickness ~4 mm; diameter ~12.7 mm). Carbon dioxide (CO_2) was purchased from National Welders (Raleigh, NC). Collagen-coated glass bottom microscopy dishes were received from MatTek Corporation (Ashland, MA). Common laboratory salts and solvents were purchased from Fisher Scientific (Fair Lawn, NJ). Distilled water was purified using a Millipore Milli-Q UV Gradient A-10 system (Bedford, MA), resulting in a total organic content of ≤6 ppb and a final resistivity of 18.2 mΩ·cm. Unless noted otherwise, these and all other materials were analytical-reagent grade and used as received without further purification.

4.2.1 Biofilm eradication assays

Lyophilized *P. aeruginosa*, *S. aureus*, and MRSA were reconstituted in tryptic soy broth (TSB) and cultured overnight at 37 °C. A 0.5 mL aliquot of culture was grown in 50 mL TSB to

a concentration of 10^8 colony forming units per mL (cfu/mL), collected by centrifugation (2355×*g*), resuspended in 15% glycerol (v/v in PBS), and stored at -80 °C in 1 mL aliquots. For daily experiments, colonies of bacteria culture were inoculated in 2 mL TSB overnight at 37 °C and recultured in fresh TSB (50 mL) the next day.

A CDC bioreactor was used to grow *P. aeruginosa*, *S. aureus*, and MRSA biofilms over 48 h.[34] Growth conditions (e.g., nutrient concentrations, additives, flow rate) were optimized for each biofilm system (bacterial strain). Briefly, medical grade silicone rubber substrates were added to the coupon holders within the CDC bioreactor. After autoclaving, the reactor effluent line was clamped and 500 mL sterile media (*P. aeruginosa*: 0.3 g/L TSB; *S. aureus*: 3.0 g/L TSB + 0.1% glucose; MRSA: 4.0 g/L TSB) was added aseptically. Bacteria were cultured in TSB to a concentration of 10^8 cfu/mL. The bioreactor was then inoculated with either 1 mL (*P. aeruginosa*, *S. aureus*) or 2 mL (MRSA) of the resulting 10^8 cfu/mL bacterial suspension. The completed assembly was incubated at 37 °C for 24 h with stirring (150 rpm; Reynolds number: 5000). Following this batch phase growth, the effluent line was opened, resulting in an effective volume of ~350 mL, and the reactor was continuously refreshed with new media (*P. aeruginosa*: 0.33% (v/v) TSB, 6 mL/min; *S. aureus*: 1% (v/v) TSB, 2 mL/min; MRSA: 5% TSB, 6 mL/min) for another 24 h to complete biofilm growth. Premeasured samples of single- or dual-action dendrimer in methanol were added to a 2 dram glass vial and dried under vacuum for 2 h prior to the bacteria assays. Biofilms grown on silicone rubber substrates were exposed immediately after 48 h growth to these single- or dual-action dendrimers in 3 mL PBS supplemented with 1% glucose and 0.5% TSB at 37 °C for 24 h with slight agitation. Of note, the addition of TSB did not influence the NO-release totals (i.e., NO totals were 4.5 ± 1.8% lower in TSB-supplemented PBS; $n \geq 3$). For each experiment, 3 biofilms were untreated and incubated in glucose- and TSB-supplemented PBS

to confirm biofilm viability. After 24 h incubation, the samples were sonicated (Elma Lab-Line 9331, Melrose Park, IL;10 min, 60% power) and vortexed to disrupt the biofilm. The blank and dendrimer-treated biofilm solutions were then spiral-plated at 10-, 100-, 1000-, and 10,000-fold dilutions on tryptic soy agar plates using an Eddy Jet spiral plater (IUL; Farmingdale, NY). Bacterial viability was assessed by counting the number of colonies formed on the agar plate using a Flash & Go colony counter (IUL; Farmingdale, NY). The minimum biofilm eradication concentration ($MBEC_{24h}$) was determined as the minimum concentration of dendrimer to reduce the viability of the biofilm to below the limit of detection for the plate counting method (2.5×10^3 cfu/mL).[35]

An adapted checkerboard assay[36] was used to evaluate any possible synergistic effects between alkyl chain-modified dendrimers and the antibiotic vancomycin against Gram-positive biofilms. Tested concentrations started at half the $MBEC_{24h}$ values for the dendrimer and vancomycin and were subsequently halved. Premeasured samples of single- or dual-action dendrimer in methanol were added to a 2 dram glass vial and dried under vacuum for 2 h prior to the bacteria assays. The appropriate amount of vancomycin was weighed out in a separate 2 dram glass vial. To expose biofilms, 1.5 mL of PBS supplemented with 1% glucose and 0.5% TSB were added to each vial and then added to the biofilm sample in a 15 mL falcon tube for a final exposure volume of 3 mL PBS supplemented with 1% glucose and 0.5% TSB. After exposure at 37 °C for 24 h, biofilms were sonicated and plated as described above.

4.2.2 Confocal microscopy to assess penetration into S. aureus biofilms

Fluorescently-labeled G1 – G4 PAMAM dendrimers were synthesized as described previously.[33, 37, 38] Briefly, 100 mg G1 through G4 PAMAM were added to separate vials containing one molar equivalent of RITC per mole dendrimer (G1: 37.5 mg; G2: 16.5 mg; G3: 7.8

mg; G4: 3.8 mg) in 2 mL methanol. One equivalent of triethylamine (with respect to the molar amount of primary amines) was then added to the vial. The solution was stirred for 24 h in the dark, after which solvent was removed in vacuo. Dendrimers were dissolved in water, dialyzed against water (1–3 d), and then lyophilized. The procedure for alkyl chain modification described in Section 2.2.2 was performed in the dark to modify the fluorescently-labeled G1 – G4 PAMAM with butyl and hexyl moieties.

The visualization of RITC-tagged dendrimers penetrating into *S. aureus* biofilms was adapted from a previously reported assay.[39] *S. aureus* was cultured in TSB to a concentration of 10^8 cfu/mL, and 3 mL of the resulting bacteria suspension in TSB was added to a collagen-coated glass bottom confocal dish. The bacteria were then incubated for 48 h at 37 °C with no agitation. After 2 d biofilm growth, the remaining TSB solution was removed, and the biofilms were washed with 1 mL sterile water and then kept in 1.5 mL PBS until exposure. Solutions of RITC-labeled dendrimers (100 μg/mL) in PBS (1.5 mL) were added to the biofilm solutions to achieve a final concentration of 50 μg/mL. A Zeiss 510 Meta inverted laser scanning confocal microscope with a 543 nm HeNe excitation laser (1.0 mW, 25.0% intensity) and a BP 560 – 615 nm filter was used to obtain fluorescence images of the RITC-modified dendrimers. Z-stack fluorescence images were collected in 2 μm slices using an N.A. 1.2 C-apochromat water immersion lens with a 40× objective. Images were collected every 10 min to temporally monitor dendrimer penetration into the biofilms.

4.2.3 Confocal microscopy for detection of intracellular NO and cell death

P. aeruginosa and *S. aureus* biofilms were grown on glass substrates (Biosurface Technologies) in the CDC bioreactor as described above. *P. aeruginosa* and *S. aureus* biofilms were exposed to NO-releasing G1 butyl or G1 hexyl dendrimers (100 μg/mL) in PBS containing

10 μM DAF-2 DA and 30 μM PI for 1 – 2 h. *S. aureus* biofilms were also exposed to NO-releasing G1 hexyl or G2 hexyl dendrimers (250 μg/mL) in PBS containing 10 μM DAF-2 DA and 30 μM PI for 2 – 3 h. Before imaging, the substrates were dipped in PBS to remove excess dye and loosely adhered cells. A Zeiss 510 Meta inverted laser scanning confocal microscope with a 488 nm Ar excitation laser (30.0 mW, 2.0% intensity) and a BP 505 – 530 nm filter was used to obtain DAF-2 (green) fluorescence images. A 543 nm HeNe exciation laser (1.0 mW, 25.0% intensity) with a BP 560 – 615 nm filter was used to obtain PI (red) fluorescence images. Z-stack fluorescence images were collected in 5 μm slices using a Zeiss 1.2 C-apochromat lens with a 20× objective.

4.2.4 In vitro cytotoxicity

L929 mouse fibroblasts were grown in DMEM supplemented with 10 vol% FBS and 1 wt% PS and incubated in 5 vol% CO_2 under humidified conditions at 37 °C. After reaching 80% confluency, the cells were trypsinized, seeded onto tissue culture-treated polystyrene 96-well plates at a density of 2 x 10^4 cells/mL, and incubated at 37 °C for 72 h. The supernatant was then aspirated and replaced with 200 μL of fresh growth medium and 50 μL of varying concentrations of dendrimer in PBS. Dimethyl sulfoxide (10%) and 50 μL PBS were used as positive and negative controls, respectively. After 24 h incubation at 37 °C, the supernatant was aspirated and 120 μL of a mixture of DMEM/MTS/PMS (105/20/1, v/v/v) was added to each well. After 1.5 h incubation at 37 °C, the absorbance of the colored solutions was quantified at 490 nm using a Thermoscientific Multiskan EX plate reader (Waltham, MA). The mixture of DMEM/MTS/PMS and untreated cells were used as a blank and control, respectively. Results were expressed as percentage of relative cell viability as follows:

$$\% \text{ Cell Viability} = [(Abs_{490} - Abs_{blank})/(Abs_{control} - Abs_{blank})] \times 100\% \qquad \textbf{Eq. 4.1}$$

A killing curve was constructed for the single- and dual-action alkyl chain-modified dendrimers for each generation by plotting % cell viability vs dendrimer concentration. IC_{50} values were determined for each curve, corresponding to the dendrimer concentration that resulted in a 50% reduction in cell viability.

To assess the toxicity of single- and dual-action dendrimers in tandem with vancomycin, pre-measured samples of dendrimer and vancomycin were added to separate 1 dram glass vials. Each sample was dissolved separately in 100 µL PBS. After aspirating the supernatant, the wells were filled with 200 µL of fresh growth medium, 25 µL of dendrimer sample, and 25 µL of vancomycin. The cells were incubated for 24 h at 37 °C, and cell viability was determined as described above using Equation 4.1.

4.3 Results and Discussion

4.3.1 Anti-biofilm efficacy of alkyl chain-modified PAMAM dendrimers

Although evaluation of antibacterial action against planktonic bacteria represents a viable screening method, the ability to eradicate pathogenic biofilms is more relevant for assessing the clinical utility of novel antibacterial agents. *P. aeruginosa*, *S. aureus*, and MRSA biofilms grown on medical-grade silicone rubber substrates in a CDC bioreactor were exposed to varying concentrations of single- and dual-action dendrimer biocides in PBS (pH 7.4) to determine the minimum dendrimer concentration required to eradicate biofilms over 24 h ($MBEC_{24h}$). Of note, untreated biofilms resulted in average bacterial viabilities of 3×10^9, 7×10^7, and 2×10^7 cfu/mL for *P. aeruginosa*, *S. aureus*, and MRSA biofilms, respectively. As the inherent detection limit of the plate counting method is 2.5×10^3 cfu/mL,[35] total biofilm killing corresponded to 6- and 4-log reductions in bacterial viability against *P. aeruginosa* and *S. aureus* biofilms, respectively.

Analogous to planktonic studies, nearly all of the dendrimer biocides were more effective against *P. aeruginosa* than *S. aureus* (including MRSA) biofilms, with only the longer alkyl chains exhibiting equivalent action regardless of bacterial strain (Table 4.1). The increased efficacy of both NO and short alkyl chain modifications against *P. aeruginosa* planktonic cultures has previously been attributed to both the thicker peptidoglycan layer present in *S. aureus* bacteria inhibiting NO diffusion and membrane disruption and the cytoprotective defenses exhibited by *S. aureus* against NO's bactericidal activity.[38, 40] However, the large disparity between the anti-biofilm action of the butyl-modified dendrimers against Gram-negative and Gram-positive biofilms suggests differences in the biofilm architecture may further contribute to the increased NO tolerance of *S. aureus* biofilms over *P. aeruginosa*. To elucidate the mechanism of dendrimer action against these biofilms, DAF-2 DA and PI fluorescent probes were utilized to visualize intracellular NO and cell membrane damage, respectively, via confocal microscopy. After only 2 h, G1 hexyl/NO dendrimers initiated substantial membrane damage to *P. aeruginosa* biofilms, while almost no intracellular NO or compromised membranes were observed for *S. aureus* biofilms (Figure 4.1). The inability of G1 hexyl/NO dendrimers to cause damage to the *S. aureus* biofilms during a similar exposure to *P. aeruginosa* biofilms supports the hypothesis that differences in the biofilm architecture between these two bacterial strains affect the efficiency of dendrimer diffusion into the biofilm. Of note, *S. aureus* biofilms produce copious amounts of extracellular proteins, DNA, and polysaccharides in their exopolysaccharide matrix,[41] which may result in slower diffusion of dendrimer biocides into the biofilm. Specifically, polycationic exopolysaccharides characteristically present in *S. aureus* biofilms may also electrostatically repel the cationic dendrimers, inhibiting biofilm penetrations.[42] Further, *P. aeruginosa* and *S. aureus* biofilms exhibit distinct planktonic dispersal mechanisms, likely influencing their susceptibility to

antibacterial agents. For example, several forms of *P. aeruginosa* biofilms demonstrate swarming dispersal, in which the outer wall of the biofilm consists of stationary bacteria exhibiting a biofilm phenotype while bacteria deeper within the biofilm remain planktonic cells, making them more vulnerable to the action of antibacterial agents.[41] In contrast, *S. aureus* biofilms employ a clumping dispersal mechanism, shedding aggregates of bacteria from the biofilms instead of single cells. These smaller biofilm aggregates retain their exopolysaccharide matrix, and thus exhibit similar resistance to antibacterial agents as the parent biofilms.[41] A combination of these architectural factors most likely contributes to the increased activity of the dendrimer biocides against *P. aeruginosa* biofilms over *S. aureus*.

The hexyl-modified dendrimers exhibited superior anti-biofilm activity against *P. aeruginosa* biofilms regardless of dendrimer generation. Neither the size of the dendrimer nor the functional group density affected hexyl chain-induced membrane damage or cell death against *P. aeruginosa* biofilms. The hexyl-modified dendrimers also did not exhibit an improvement in anti-biofilm efficacy with the addition of NO release, suggesting that significant membrane damage initiated by the hexyl chains precludes the buildup of intracellular NO to bactericidal concentrations.[38] In contrast, the butyl-modified dendrimers demonstrated greater anti-biofilm action with both increasing generation and NO-release capabilities, indicating the greater functional group density afforded by the higher generations improves the biocidal action of these shorter butyl chains.

The addition of NO release enhanced the anti-biofilm capabilities of all of the butyl-modified dendrimers against *P. aeruginosa* biofilms. The improved anti-biofilm efficacy of the dual-action butyl-modified dendrimers suggests the lack of membrane damage at lower concentrations (i.e., below the biocidal concentrations for single-action butyl-modified dendrimers) allows for the buildup of intracellular NO to bactericidal concentrations and NO-

Table 4.1 Minimum biofilm eradication concentrations ($MBEC_{24h}$) for single- and dual-action alkyl chain-modified dendrimers against *P. aeruginosa*, *S. aureus*, and MRSA biofilms.[a]

	***P. aeruginosa* Biofilms**	***S. aureus* Biofilms**	**MRSA Biofilms**
	$MBEC_{24h}$ (μg/mL)	**$MBEC_{24h}$ (μg/mL)**	**$MBEC_{24h}$ (μg/mL)**
Vancomycin		2000	5000
G1 butyl	8000	>30,000	>30,000
G1 butyl/NO	2000	10,000	20,000
G1 hexyl	100	1000	2000
G1 hexyl/NO	100	1000	1000
G1 octyl	50	100	200
G1 octyl/NO	50	100	200
G1 dodecyl	100	100	200
G1 dodecyl/NO	100	100	200
G2 butyl	6000	>30,000	>30,000
G2 butyl/NO	2000	5000	20,000
G2 hexyl	150	4000	>10,000
G2 hexyl/NO	150	2000	>10,000
G3 butyl	2000	>30,000	>30,000
G3 butyl/NO	1000	5000	20,000
G3 hexyl	200	100	100
G3 hexyl/NO	100	100	100
G4 butyl	2000	>30,000	>30,000
G4 butyl/NO	1000	20,000	20,000
G4 hexyl	200	100	100
G4 hexyl/NO	200	100	100

[a]Each parameter was analyzed with multiple replicates ($n \geq 3$).

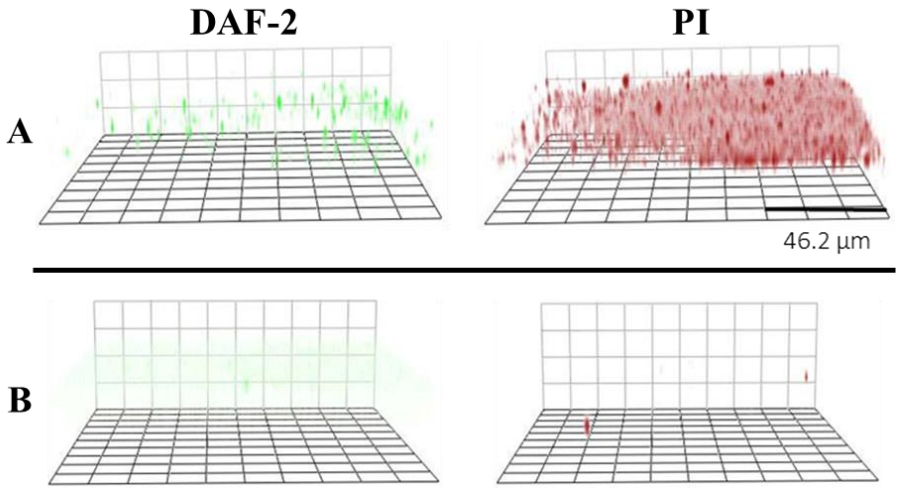

Figure 4.1. Confocal microscopy images of (A) *P. aeruginosa* and (B) *S. aureus* biofilms exposed to 100 µg/mL G1 hexyl/NO dendrimers for 2 h. DAF-2 green fluorescence designates the presence of intracellular NO, while PI red fluorescence indicates compromised membranes. Threshold reversed for clarity.

mediated killing. Confocal microscopy was used confirm this hypothesis by visualizing the buildup of intracellular NO and cell membrane damage (Figure 4.2). A substantial amount of intracellular NO was noted after only 1 h upon exposure of *P. aeruginosa* biofilms to G1 butyl/NO. After 2 h, the bacteria membranes appear extensively compromised, indicating substantial cell death. At this point, intracellular NO is no longer observed due to diffusion of DAF-2 out of the fully compromised membranes.[13] Upon exposure to G1 hexyl/NO dendrimers, however, *P. aeruginosa* biofilms exhibited considerable membrane damage at 1 h, likely the result of the intercalation of the hexyl chains and not the bactericidal action of NO.

Similar to G1 hexyl, octyl- and dodecyl-modified G1 dendrimers proved bactericidal against *P. aeruginosa* biofilms. While G1 octyl dendrimers were slightly more effective at killing *P. aeruginosa* biofilms ($MBEC_{24h}$ = 50 μg/mL), the dodecyl-modified dendrimers exhibited similar efficacy as the hexyl modifications ($MBEC_{24h}$ = 100 μg/mL). The decrease in anti-biofilm action observed for the dodecyl-modified dendrimers corroborates previous reports where hydrophobic decene-modified dendrimers were slightly less effective at eradicating *P. aeruginosa* biofilms than amphiphilic dendrimers, which was attributed to the increased hydrophobicity of the longer alkyl chains reducing efficient penetration into the biofilm exopolysaccharide matrix.[33, 43] The lessened anti-biofilm action as a function of hydrophobicity was only apparent against *P. aeruginosa* biofilms, as both octyl- and dodecyl-modified dendrimers exhibited similar action against *S. aureus* ($MBEC_{24h}$ = 100 μg/mL). The addition of NO release did not improve the anti-biofilm action of the octyl and dodecyl modifications against either bacterial strain, likely due to the increased membrane damage initiated by the longer alkyl chains precluding the buildup of intracellular NO.

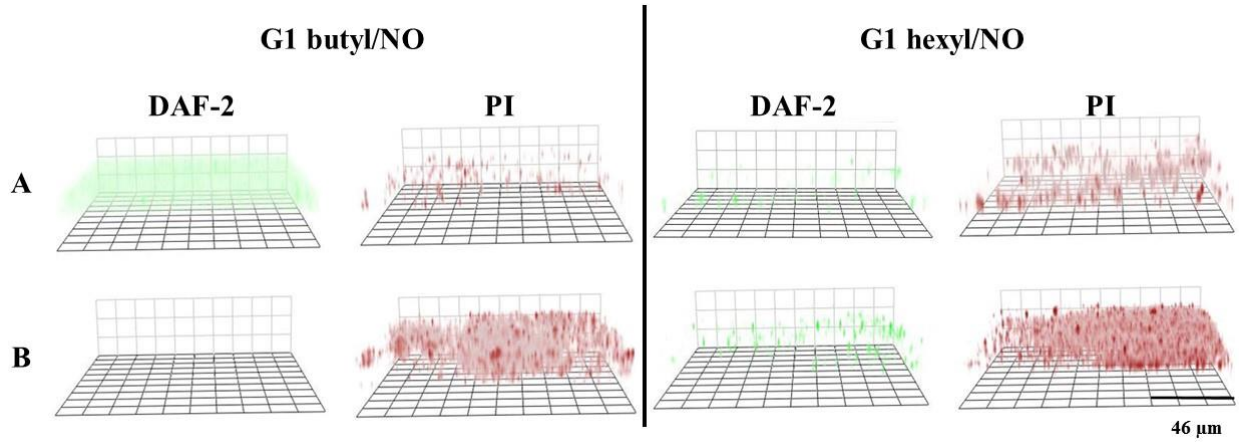

Figure 4.2. Confocal microscopy images of *P. aeruginosa* biofilms exposed to 100 µg/mL G1 butyl/NO and G1 hexyl/NO dendrimers for (A) 1 h and (B) 2 h. DAF-2 green fluorescence designates the presence of intracellular NO, while PI red fluorescence indicates compromised membranes. Threshold reversed for clarity.

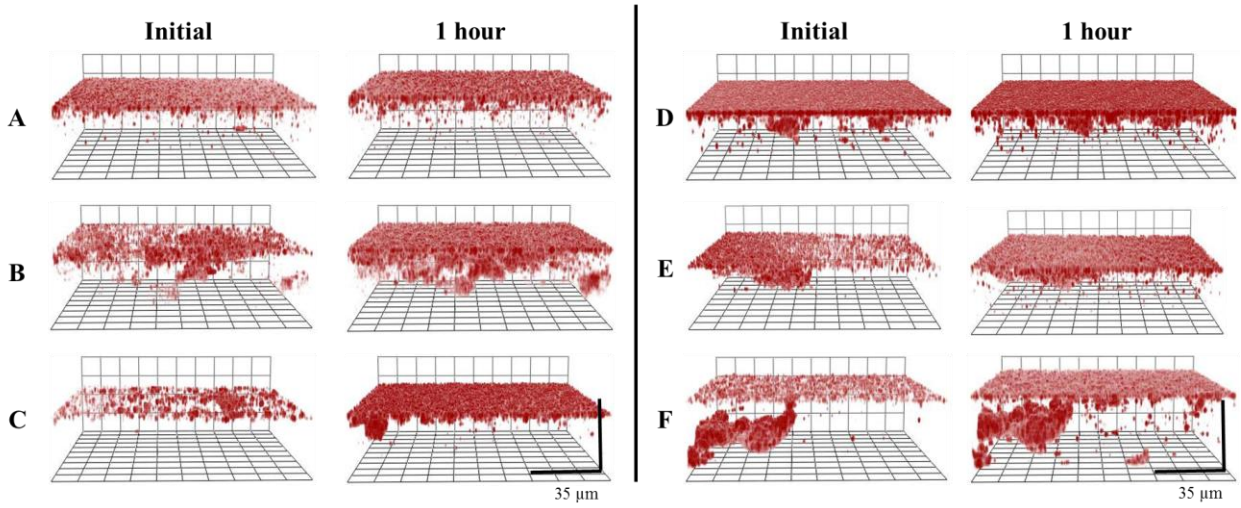

Figure 4.3. Confocal microscopy images of *S. aureus* biofilms exposed to 50 µg/mL RITC-tagged (A) G1 butyl, (B) G2 butyl, (C) G4 butyl, (D) G1 hexyl, (E) G2 hexyl, and (F) G4 hexyl dendrimers for 1 h. Threshold reversed for clarity.

The hexyl-modified dendrimers were more effective against *S. aureus* biofilms than the butyl modifications regardless of generation (Table 4.1), exhibiting at least an order of magnitude. Indeed, the butyl-modified dendrimers proved incapable of eradicating *S. aureus* biofilms at concentrations up to 30 mg/mL. To elucidate why the hexyl-modified dendrimers exhibited a dramatic enhancement in anti-biofilm action over their butyl counterparts, confocal microscopy was used to visualize the extent to which RITC-tagged butyl- and hexyl-modified dendrimers associated with and penetrated into *S. aureus* biofilms. As expected, both G1 hexyl (Figure 4.3 D) and G4 hexyl (Figure 4.3 F) dendrimers exhibited extensive biofilm penetration relative to either G1 butyl (Figure 4.3 A) or G4 butyl (Figure 4.3 C) dendrimers. These results indicate at least some of the increased anti-biofilm action of the hexyl modifications is due to their ability to infiltrate deeper into the biofilm at a faster rate than the butyl-modified dendrimers, in addition to hexyl chain-initiated membrane destruction.

Nitric oxide release greatly improved the biocidal action of the butyl-modified dendrimers against *S. aureus* biofilms. Increasing the dendrimer generation from G1 to G2 or G3 doubled the anti-biofilm action of the butyl system, with an $MBEC_{24h}$ value of 5 mg/mL for G2 and G3 butyl/NO dendrimers versus 10 mg/mL for G1 butyl/NO. The enhanced biofilm eradication is attributed to the greater functional group density of these larger scaffolds, facilitating more membrane disruption and biofilm-dendrimer association than the smaller G1 system. However, the advantages of increased functional group density were mitigated for the G4 butyl/NO dendrimers, which demonstrated less anti-biofilm action than any of the dual-action butyl-modified dendrimers against *S. aureus* biofilms ($MBEC_{24h}$ = 20 mg/mL). While initially surprising as the G4 butyl/NO scaffold was effective against *P. aeruginosa* biofilms, the larger size of the dendrimers may limit diffusion into the *S. aureus* biofilms. Confocal microscopy visualization of

biofilm penetration for RITC-tagged G1 butyl, G2 butyl, and G4 butyl dendrimers confirmed this hypothesis (Figure 4.3 A-C). The G2 butyl dendrimers infiltrated the biofilm to a greater extent after 1 h, while G1 butyl dendrimers exhibited little dispersion, remaining mostly associated with the outermost region of the biofilm. As such, the biofilm-penetrating G2 butyl scaffold allows for both cell membrane damage and internal NO release, resulting in more efficient biofilm eradication at lower dendrimer concentrations. Alternatively, less association with the biofilm and decreased biofilm penetration was observed with the G4 butyl dendrimer system. The accumulation of G4 butyl dendrimers at the biofilm surface (Figure 4.3 C) confirms the inability of this system to effectively breach the exopolysaccharide matrix.

While the hexyl-modified dendrimers were more effective at eradicating *S. aureus* biofilms, the overall anti-biofilm action proved dependent on dendrimer generation. As expected for highly antibacterial scaffolds, NO release provided little additional benefits on the anti-biofilm action of nearly all the hexyl modifications. While G1 hexyl and G1 hexyl/NO dendrimers exhibited moderate anti-biofilm efficacy ($MBEC_{24h}$ = 1 mg/mL), both single- and dual-action G3 and G4 hexyl dendrimers were appreciably more bactericidal and eradicated *S. aureus* biofilms at concentrations an order of magnitude lower ($MBEC_{24h}$ = 100 μg/mL). The enhanced biofilm eradication capabilities are attributed to the increased functional group density of the G3 and G4 scaffolds leading to greater membrane intercalation and biofilm penetration (Figure 4.3 F). Of note, confocal microscopy further reveals the size of the G4 scaffold no longer inhibits its penetration into the biofilm when modified with hexyl alkyl chains, likely due to the increased hydrophobicity of the hexyl chains enabling improved association with and disruption of the exopolysaccharide matrix and bacterial cell membranes.

Single-action G2 hexyl dendrimers required a concentration four times greater than G1 hexyl for biofilm eradication ($MBEC_{24h}$ = 4 and 1 mg/mL, respectively), making it the least effective hexyl-modified scaffold for biofilm eradication. Confocal microscopy using RITC-tagged dendrimers revealed comparable biofilm penetration after 1 h between the G1 and G2 hexyl scaffolds (Figure 4.3 D-E). Thus, the reduced anti-biofilm activity is more likely the result of poor intercalation or membrane damage by the hexyl chains rather than hindered biofilm penetration of the scaffold. Further, NO release increased the antibacterial action of the G2 hexyl scaffold, supporting the hypothesis that the membrane damage caused by the hexyl chains does not prevent the buildup of intracellular NO. As shown in Figure 4.4 A, biofilms exposed to G1 hexyl/NO dendrimers exhibit compromised cell membranes after 3 h with almost no intracellular NO present. In contrast, considerable intracellular NO and negligible membrane damage were noted for biofilms exposed to G2 hexyl/NO dendrimers (Figure 4.4 B), verifying decreased membrane damage as the cause of reduced anti-biofilm action. Factors that may be contributing to the decreased biocidal action of the G2 hexyl dendrimers include vesicle formation and backfolding of pendant functional groups towards the interior of the scaffold, reducing the exterior functional group density.[38, 44-46]

Both single- and dual-action dendrimers exhibited similar bactericidal trends against MRSA biofilms, albeit mostly at higher bactericidal concentrations than for non-resistant *S. aureus*. While butyl-modified dendrimers proved ineffective up to 30 mg/mL, the addition of NO-release capabilities only moderately improved the anti-biofilm action of the butyl systems. Contrary to the results observed for *S. aureus* biofilms a generation dependence was not observed for the dual-action scaffolds, with all of the butyl/NO dendrimers eradicating MRSA biofilms at 20 mg/mL. The similar anti-biofilm action across all generations for the dual-action butyl modifications suggests that neither increased size nor functional group density influences the

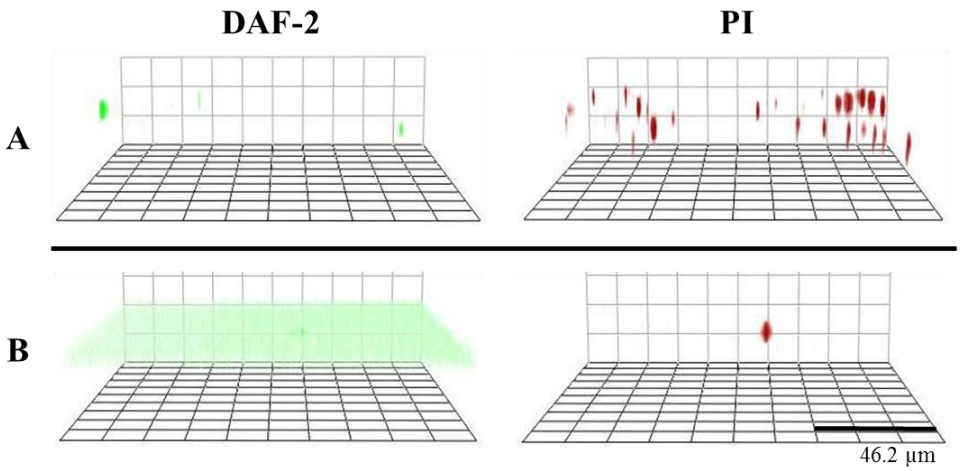

Figure 4.4. Confocal microscopy images of *S. aureus* biofilms exposed to 250 µg/mL (A) G1 hexyl/NO and (B) G2 hexyl/NO dendrimers for 3 h. DAF-2 green fluorescence designates the presence of intracellular NO, while PI red fluorescence indicates compromised membranes. Threshold reversed for clarity.

biocidal action of the dendrimers against MRSA biofilms. Rather, a NO dose of ~20 μmol/mL is necessary for MRSA biofilm eradication in the absence of membrane damage.

The generation dependence of the hexyl-modified dendrimers followed the same general trend as observed for *S. aureus* biofilms, with G3 and G4 hexyl dendrimers exhibiting greater efficacy against MRSA biofilms than either the G1 or G2 hexyl systems. The concentrations of single- and dual-action G3 and G4 hexyl were identical for eradicating both MRSA and *S. aureus* biofilms ($MBEC_{24h}$ = 100 μg/mL). Although G1 hexyl dendrimers were less effective against MRSA versus *S. aureus* ($MBEC_{24h}$ = 2 and 1 mg/mL, respectively), the addition of NO release increased their anti-biofilm action to similar levels ($MBEC_{24h}$ = 1 mg/mL). G2 hexyl and G2 hexyl/NO again represented the least effective anti-biofilm systems, with both being incapable of eradicating MRSA biofilms at concentrations up to 10 mg/mL. Finally, the anti-biofilm action of the octyl- and dodecyl-modified dendrimers was reduced almost two-fold against MRSA biofilms from *S. aureus* ($MBEC_{24h}$ = 200 μg/mL and 100 μg/mL, respectively). These results suggest that biofilms comprised of antibiotic-resistant bacteria decrease the anti-biofilm action of all but the most effective dendrimer biocides.

As biofilms can often require therapeutic doses 3–4 orders of magnitude greater than those required to eradicate planktonic bacteria,[3] we next compared the biofilm eradication concentrations for each strain to their corresponding planktonic bactericidal doses. Against *P. aeruginosa* biofilms, all of the single- and dual-action G1 dendrimers only exhibited a 2–4-fold increase in therapeutic dose from planktonic bacteria. A more substantial increase was observed for the higher generations, ranging from a 4-fold increase for G3 hexyl/NO to 240-fold for single-action G2 butyl dendrimers. The G2 butyl/NO dendrimers represented the largest gap in *P. aeruginosa* planktonic and biofilm eradication for the NO-releasing dendrimers with a 40-fold

concentration difference. Similarly, the NO-releasing dendrimers exhibited a 2–40-fold increase in concentration against *S. aureus* biofilms and a 1–100-fold increase against MRSA biofilms. Alternatively, treatment of Gram-positive biofilms with vancomycin resulted in 80- and 400-fold increases in therapeutic dose over planktonic bacteria for *S. aureus* and MRSA, respectively, indicating another benefit of using NO as an anti-biofilm agent over traditional antibiotics.

4.3.2 In vitro cytotoxicity

Regardless of effective biocidal action, the utility of new antibacterial agents is ultimately dictated by their toxicity to mammalian cells. Killing curves were constructed for the single- and dual-action alkyl chain-modified dendrimers for each generation by plotting % cell viability vs dendrimer concentration, and the concentration corresponding to a 50% reduction in L929 cell viability compared to untreated controls represented the inhibitory concentration at 50% viability (IC_{50}). Toxicity was assessed using a therapeutic index (TI) by comparing the IC_{50} against L929 mouse fibroblasts to the biofilm eradication concentrations for each dendrimer system, allowing the evaluation of the clinical utility for each biocide. A higher TI index indicates a better toxicity ratio (i.e., greater bactericidal action with minimal toxicity to mammalian cells), while a TI below 1 signifies extreme toxicity at biocidal concentrations.

As expected, G1 octyl and dodecyl dendrimers exhibited significant toxicity (IC_{50} = 75 and 40 μg/mL, respectively) due to the increased membrane intercalation and cell damage of the long alkyl chains (Table 4.2). Similarly, hexyl-modified dendrimers were substantially more toxic than the butyl modifications, most likely due to the increased membrane disruption caused by the longer hexyl chains. The toxicity of the hexyl-modified dendrimers increased with size (higher generations), as G4 hexyl dendrimers exhibited greater toxicity than the G1 scaffold (IC_{50} = 75 and 1150 μg/mL, respectively). Within each generation, however, the addition of NO release had

very little effect on the toxicity of the hexyl modifications. The toxicity of the butyl-modified dendrimers was also dependent on dendrimer generation, with the G3 and G4 scaffolds (IC_{50} ~3 mg/mL) exhibiting almost twice the toxicity of G1 or G2 butyl (IC_{50} values of ~8 and ~6 mg/mL, respectively). Despite the generation dependence of the single-action dendrimers, dual-action butyl modifications resulted in similar toxicity regardless of dendrimer size (IC_{50} ~3 mg/mL), suggesting an NO dose of ~3 μmol/mL is relatively toxic to mouse fibroblast cells irrespective of functional group density.

The overall therapeutic utility of the dendrimers as broad-spectrum antibacterial agents was determined by comparing the IC_{50} values against L929 cells for each system to their biofilm eradication concentrations and determining their TI. Nearly all of the dendrimer biocides were capable of eradicating Gram-negative *P. aeruginosa* biofilms at non-toxic concentrations (i.e., TI > 1.00), with the exception of G1 butyl, G1 dodecyl, G1 dodecyl/NO, G4 hexyl, and G4 hexyl/NO (Table 4.3). The greatest therapeutic utility was demonstrated by the G1 and G2 hexyl-modified dendrimers, which demonstrated maximal anti-biofilm action at concentrations well below their median inhibitory concentration (TI ≥ 7.50). In contrast, the biofilm eradication concentrations for most of the single- and dual-action dendrimers against Gram-positive biofilms were greater than their corresponding IC_{50} values (TI < 1.00), limiting their clinical utility as broad-spectrum antibacterial agents. The only scaffold capable of eradicating both Gram-negative and Gram-positive biofilms at non-toxic concentrations was the G3 hexyl dendrimer system, with both single-action and NO-releasing dendrimers eradicating biofilms at concentrations well below the IC_{50} values (G3 hexyl TI ≥ 2.25; G3 hexyl/NO TI = 4.50). These data suggest that the G3 scaffold, combined with the increased biocidal action of the hexyl modification, provides an optimal balance between dendrimer size and functional group density to maximize broad-spectrum antibacterial

Table 4.2 Inhibitory concentrations at 50% cell viability (IC_{50}) for single- and dual-action alkyl chain-modified dendrimers against L929 mouse fibroblast cells.[a]

	IC_{50} (μg/mL)
G1 butyl	7700
G1 butyl/NO	3000
G1 hexyl	1150
G1 hexyl/NO	750
G1 octyl	75
G1 octyl/NO	75
G1 dodecyl	40
G1 dodecyl/NO	40
G2 butyl	6000
G2 butyl/NO	2400
G2 hexyl	1150
G2 hexyl/NO	1150
G3 butyl	2900
G3 butyl/NO	2700
G3 hexyl	450
G3 hexyl/NO	450
G4 butyl	3100
G4 butyl/NO	3800
G4 hexyl	75
G4 hexyl/NO	150

[a]Each parameter was analyzed with multiple replicates ($n \geq 3$).

Table 4.3 Calculated therapeutic index (TI) for each dendrimer biocide against *P. aeruginosa*, *S. aureus*, and MRSA biofilms.

	***P. aeruginosa* Biofilms**	***S. aureus* Biofilms**	***MRSA* Biofilms**
G1 butyl	0.96	<0.26	<0.26
G1 butyl/NO	1.50	0.30	0.15
G1 hexyl	11.50	1.15	0.58
G1 hexyl/NO	7.50	0.75	0.75
G1 octyl	1.50	0.75	0.38
G1 octyl/NO	1.50	0.75	0.38
G1 dodecyl	0.40	0.40	0.20
G1 dodecyl/NO	0.40	0.40	0.20
G2 butyl	1.00	<0.26	<0.26
G2 butyl/NO	1.20	0.48	0.12
G2 hexyl	7.67	0.29	<0.12
G2 hexyl/NO	7.67	0.58	<0.12
G3 butyl	1.45	<0.26	<0.26
G3 butyl/NO	2.70	0.54	0.14
G3 hexyl	2.25	4.50	4.50
G3 hexyl/NO	4.50	4.50	4.50
G4 butyl	1.55	<0.26	<0.26
G4 butyl/NO	3.80	0.19	0.19
G4 hexyl	0.38	0.75	0.75
G4 hexyl/NO	0.75	1.50	1.50

action while minimizing toxicity to mammalian cells. As such, both G3 hexyl and G3 hexyl/NO represent the most viable options for developing broad-spectrum anti-biofilm agents against the bacterial strains investigated herein.

4.3.3 Synergy of dual-action dendrimers with vancomycin

Another important aspect in the evaluation of combination therapies is the ability to demonstrate additive or synergistic bactericidal action with established therapeutics, namely traditional antibiotics. The evaluation of potential synergy not only ensures that the combination of new and conventional therapies exhibits increased bactericidal activity, but also that the combination is not antagonistic, reducing the antibacterial action of the individual biocides.[7] Decreasing the required therapeutic concentration with increased biocidal action should mitigate toxic side effects to mammalian cells. We thus sought to evaluate any possible synergistic effects between NO-releasing dendrimers and vancomycin in the eradication of both *S. aureus* and MRSA biofilms.

Dual-action G3 butyl/NO and G3 hexyl/NO dendrimers were selected as test agents to evaluate the combined efficacy of NO release with vancomycin. Single-action (i.e., non-NO-releasing) G3 hexyl dendrimers were used as a control as they exhibited similar anti-biofilm efficacy as their NO-releasing counterparts,[47] allowing us to evaluate any additional benefits of NO release. The Gram-positive biofilms were exposed to single- or dual-action dendrimers concurrently with vancomycin using an adapted checkerboard assay, starting with concentrations at half the $MBEC_{24h}$ values for the dendrimer and vancomycin, and then subsequently halving them.[36] Any resulting synergistic effects were determined by calculating the fractional bactericidal concentration index (FBC_{24h}) using equation 4.2, where $MBEC_{24hA}$ and $MBEC_{24hB}$ represent the individual biofilm eradication concentrations for agents A and B, respectively, and $MBEC_{24hAB}$

and $MBEC_{24hBA}$ are the concentrations of agents A and B constituting the most effective bactericidal combination as determined by the adapted checkerboard assay.

$$FBC_{24h} = \frac{MBEC_{24hAB}}{MBEC_{24hA}} + \frac{MBEC_{24hBA}}{MBEC_{24hB}} \quad \textbf{Eq. 4.2}$$

For each strain, FBC_{24h} values between 0.50 and 1.00 indicate greater-than-additive (or moderately synergistic) bactericidal action, while an $FBC_{24h} \leq 0.50$ is defined as synergistic and $FBC_{24h} \leq 0.25$ is highly synergistic.[36, 48-50]

While G3 butyl/NO dendrimers were highly synergistic with vancomycin against *S. aureus* biofilms (FBC_{24h} = 0.18), only moderate synergy with vancomycin was observed for MRSA biofilms (FBC_{24h} = 0.63), most likely due to the inability of the G3 butyl scaffold to effectively penetrate MRSA biofilms. Indeed, G3 butyl/NO dendrimers required four times the concentrations to eradicate MRSA over *S. aureus* biofilms.[47] Combining G3 butyl/NO dendrimers with vancomycin resulted in an 8-fold decrease in dendrimer concentration (20 to 2.5 mg/mL) for the eradication of MRSA biofilms, indicating a marked improvement over G3 butyl/NO dendrimers alone. Both G3 hexyl and G3 hexyl/NO demonstrated synergy (FBC_{24h} = 0.50) with vancomycin against *S. aureus* biofilms, though the addition of NO release had no effect on the combined efficacy of the dual-action dendrimers (Table 4.4). Alternatively, only G3 hexyl/NO dendrimers resulted in synergy with vancomycin against MRSA biofilms (FBC_{24h} value of 0.50 compared to 0.75 for G3 hexyl dendrimers), suggesting that NO improves the antibacterial action of the hexyl-modified dendrimer scaffold in concert with vancomycin against MRSA biofilms.

To establish the utility of combining NO-releasing dendrimers and traditional antibiotics as anti-biofilm agents, the toxicity of the antibacterial combinations was evaluated against L929 mouse fibroblast cells and compared to that of the individual biocides. All of the combined dendrimer and vancomycin doses required to eradicate *S. aureus* biofilms demonstrated negligible

Table 4.4 Combined biofilm eradication concentrations and calculated fractional bactericidal concentration index (FBC_{24h}) against *S. aureus* and MRSA biofilms.[a]

***S. aureus* Biofilms**	**Dendrimer (μg/mL)**	**Vancomycin (μg/mL)**	**FBC_{24h}**
G3 butyl/NO	250	250	0.18
G3 hexyl	25	500	0.50
G3 hexyl/NO	25	500	0.50
MRSA Biofilms	**Dendrimer (μg/mL)**	**Vancomycin (μg/mL)**	**FBC_{24h}**
G3 butyl/NO	2500	2500	0.63
G3 hexyl	50	1250	0.75
G3 hexyl/NO	25	1250	0.50

[a]Each parameter was analyzed with multiple replicates ($n \geq 3$).

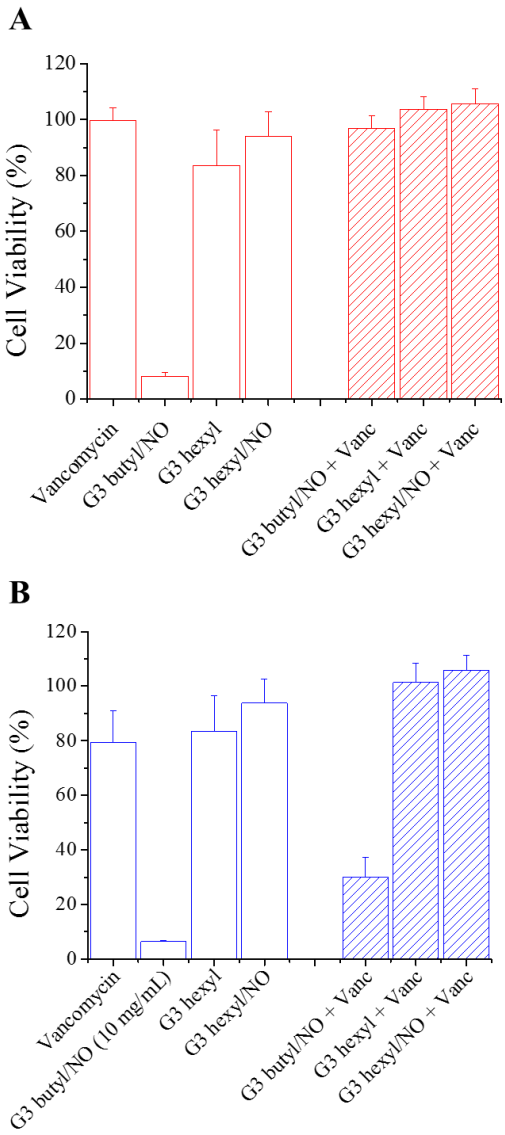

Figure 4.5. Viability (%) of L929 mouse fibroblast cells following 24 h exposure to individual (solid) and combined (hashed) dendrimer and vancomycin biofilm eradication concentrations against (A) *S. aureus* and (B) MRSA biofilms.

toxicity (>95% viability) to fibroblast cells (Figure 4.5). Although the combination of G3 hexyl and G3 hexyl/NO dendrimers with vancomycin only improved cell viability by 10–20%, the synergistic effects exhibited by G3 butyl/NO with vancomycin significantly reduced the toxicity of G3 butyl/NO dendrimers at therapeutic concentrations with an increase in cell viability from ~8 to ~97%. For the concentrations required to eradicate MRSA biofilms, both control and NO-releasing G3 hexyl dendrimers exhibited insignificant toxicity in concert with vancomycin (~100% cell viability). However, the combination of G3 butyl/NO and vancomycin required against MRSA biofilms still proved relatively toxic, only improving the cell viability of G3 butyl/NO dendrimers from ~6 to 30%. Such toxicity is attributed to the larger concentrations of G3 butyl/NO required to eradicate MRSA biofilms ($MBEC_{24h}$ = 2.5 mg/mL G3 butyl/NO + 2.5 mg/mL vancomycin).

4.4 Conclusions

The utility of alkyl chain-modified PAMAM dendrimers as broad-spectrum anti-biofilm agents was assessed through the systematic evaluation of eradication efficiency as a function of dendrimer generation, alkyl chain length, and bacterial Gram class. The anti-biofilm efficacy of alkyl chain-modified dendrimers was highly dependent on the biocide's ability to penetrate into the biofilm and compromise cell membranes. Hexyl-modified dendrimers were considerably more effective at biofilm eradication than the butyl systems, likely a result of greater membrane intercalation, cell membrane damage, and biofilm penetration. While increased membrane damage precludes the buildup of intracellular NO to bactericidal concentrations for these modifications, the addition of NO release enhanced the anti-biofilm action of dendrimer biocides that did not adequately compromise cell membranes, indicating the utility of dual-action dendrimers as broad-spectrum antibacterial agents. The G3 dendrimer scaffold represented the

ideal balance of dendrimer size and functional group density for optimal biofilm eradication due to its limited toxicity to mammalian cells, making these systems the most promising option for the design of broad-spectrum anti-biofilm agents. Indeed, NO-releasing alkyl chain-modified G3 dendrimers demonstrated moderate to high synergy with vancomycin in the eradication of Gram-positive biofilms, indicating the possible clinical utility of these scaffolds.

REFERENCES

(1) Bryers, J. D. "Medical biofilms" *Biotechnology and Bioengineering* **2008**, *100*, 1-18.

(2) Bjarnsholt, T., Kirketerp-Møller, K., Jensen, P. Ø., Madsen, K. G., Phipps, R., Krogfelt, K., Høiby, N., and Givskov, M. "Why chronic wounds will not heal: A novel hypothesis" *Wound Repair and Regeneration* **2008**, *16*, 2-10.

(3) Donlan, R. M. "Biofilm formation: A clinically relevant microbiological process" *Clinical Infectious Diseases* **2001**, *33*, 1387-1392.

(4) Dunne, W. M. "Bacterial adhesion: Seen any good biofilms lately?" *Clinical Microbiology Reviews* **2002**, *15*, 155-166.

(5) Lindsay, D., and Von Holy, A. "Bacterial biofilms within the clinical setting: What healthcare professionals should know" *Journal of Hospital Infection* **2006**, *64*, 313-325.

(6) Boucher, H. W., Talbot, G. H., Bradley, J. S., Edwards, J. E., Gilbert, D., Rice, L. B., Scheld, M., Spellberg, B., and Bartlett, J. "Bad bugs, no drugs: No eskape!" *Clinical Infectious Diseases* **2009**, *48*, 1-12.

(7) Cottarel, G., and Wierzbowski, J. "Combination drugs, an emerging option for antibacterial therapy" *Trends in Biotechnology* **2007**, *25*, 547-555.

(8) Eliopoulos, G., and Eliopoulos, C. "Antibiotic combinations: Should they be tested?" *Clinical Microbiology Reviews* **1988**, *1*, 139-156.

(9) Li, Z., Lee, D., Sheng, X., Cohen, R. E., and Rubner, M. F. "Two-level antibacterial coating with both release-killing and contact-killing capabilities" *Langmuir* **2006**, *22*, 9820-9823.

(10) Song, J., Kang, H., Lee, C., Hwang, S. H., and Jang, J. "Aqueous synthesis of silver nanoparticle embedded cationic polymer nanofibers and their antibacterial activity" *ACS Applied Materials & Interfaces* **2011**, *4*, 460-465.

(11) Fang, F. C. "Perspectives series: Host/pathogen interactions. Mechanisms of nitric oxide-related antimicrobial activity" *The Journal of Clinical Investigation* **1997**, *99*, 2818.

(12) Fang, F. C. "Antimicrobial reactive oxygen and nitrogen species: Concepts and controversies" *Nature Reviews Microbiology* **2004**, *2*, 820-832.

(13) Hetrick, E. M., Shin, J. H., Stasko, N. A., Johnson, C. B., Wespe, D. A., Holmuhamedov, E., and Schoenfisch, M. H. "Bactericidal efficacy of nitric oxide-releasing silica nanoparticles" *ACS Nano* **2008**, *2*, 235-246.

(14) Privett, B. J., Broadnax, A. D., Bauman, S. J., Riccio, D. A., and Schoenfisch, M. H. "Examination of bacterial resistance to exogenous nitric oxide" *Nitric Oxide* **2012**, *26*, 169-173.

(15) Gilbert, P., and Moore, L. "Cationic antiseptics: Diversity of action under a common epithet" *Journal of Applied Microbiology* **2005**, *99*, 703-715.

(16) Thorsteinsson, T., Másson, M., Kristinsson, K. G., Hjálmarsdóttir, M. A., Hilmarsson, H., and Loftsson, T. "Soft antimicrobial agents: Synthesis and activity of labile environmentally friendly long chain quaternary ammonium compounds" *Journal of Medicinal Chemistry* **2003**, *46*, 4173-4181.

(17) Simoncic, B., and Tomsic, B. "Structures of novel antimicrobial agents for textiles-a review" *Textile Research Journal* **2010**, *80*, 1721-1737.

(18) Hetrick, E. M., Shin, J. H., Paul, H. S., and Schoenfisch, M. H. "Anti-biofilm efficacy of nitric oxide-releasing silica nanoparticles" *Biomaterials* **2009**, *30*, 2782-2789.

(19) Lu, Y., Sun, B., Li, C., and Schoenfisch, M. H. "Structurally diverse nitric oxide-releasing poly(propylene imine) dendrimers" *Chemistry of Materials* **2011**, *23*, 4227-4233.

(20) Stasko, N. A., Fischer, T. H., and Schoenfisch, M. H. "S-nitrosothiol-modified dendrimers as nitric oxide delivery vehicles" *Biomacromolecules* **2008**, *9*, 834-841.

(21) Stasko, N. A., Johnson, C. B., Schoenfisch, M. H., Johnson, T. A., and Holmuhamedov, E. L. "Cytotoxicity of polypropylenimine dendrimer conjugates on cultured endothelial cells" *Biomacromolecules* **2007**, *8*, 3853-3859.

(22) Stasko, N. A., and Schoenfisch, M. H. "Dendrimers as a scaffold for nitric oxide release" *Journal of the American Chemical Society* **2006**, *128*, 8265-8271.

(23) Carpenter, A. W., and Schoenfisch, M. H. "Nitric oxide release: Part II. Therapeutic applications" *Chemical Society Reviews* **2012**, *41*, 3742-3752.

(24) Riccio, D. A., and Schoenfisch, M. H. "Nitric oxide release: Part I. Macromolecular scaffolds" *Chemical Society Reviews* **2012**, *41*, 3731-3741.

(25) Duncan, R., and Izzo, L. "Dendrimer biocompatibility and toxicity" *Advanced Drug Delivery Review* **2005**, *57*, 2215-2237.

(26) Tomalia, D., Baker, H., Dewald, J., Hall, M., Kallos, G., Martin, S., Roeck, J., Ryder, J., and Smith, P. "A new class of polymers: Starburst-dendritic macromolecules" *Polymer Journal* **1985**, *17*, 117-132.

(27) Tomalia, D. A. "Birth of a new macromolecular architecture: Dendrimers as quantized building blocks for nanoscale synthetic polymer chemistry" *Progress in Polymer Science* **2005**, *30*, 294-324.

(28) Meyers, S. R., Juhn, F. S., Griset, A. P., Luman, N. R., and Grinstaff, M. W. "Anionic amphiphilic dendrimers as antibacterial agents" *Journal of the American Chemical Society* **2008**, *130*, 14444-14445.

(29) Jevprasesphant, R., Penny, J., Attwood, D., McKeown, N. B., and D'Emanuele, A. "Engineering of dendrimer surfaces to enhance transepithelial transport and reduce cytotoxicity" *Pharmaceutical Research* **2003**, *20*, 1543-1550.

(30) Wiwattanapatapee, R., Carreño-Gómez, B., Malik, N., and Duncan, R. "Anionic pamam dendrimers rapidly cross adult rat intestine in vitro: A potential oral delivery system?" *Pharmaceutical Research* **2000**, *17*, 991-998.

(31) Johansson, E., Crusz, S. A., Kolomiets, E., Buts, L., Kadam, R. U., Cacciarini, M., Bartels, K.-M., Diggle, S. P., Cámara, M., and Williams, P. "Inhibition and dispersion of *Pseudomonas aeruginosa* biofilms by glycopeptide dendrimers targeting the fucose-specific lectin lecb" *Chemistry & Biology* **2008**, *15*, 1249-1257.

(32) Hou, S., Zhou, C., Liu, Z., Young, A. W., Shi, Z., Ren, D., and Kallenbach, N. R. "Antimicrobial dendrimer active against *Escherichia coli* biofilms" *Bioorganic & Medicinal Chemistry Letters* **2009**, *19*, 5478-5481.

(33) Lu, Y., Slomberg, D. L., Shah, A., and Schoenfisch, M. H. "Nitric oxide-releasing amphiphilic poly (amidoamine)(PAMAM) dendrimers as antibacterial agents" *Biomacromolecules* **2013**, *14*, 3589-3598.

(34) Goeres, D. M., Loetterle, L. R., Hamilton, M. A., Murga, R., Kirby, D. W., and Donlan, R. M. "Statistical assessment of a laboratory method for growing biofilms" *Microbiology* **2005**, *151*, 757-762.

(35) Breed, R. S., and Dotterrer, W. "The number of colonies allowable on satisfactory agar plates" *Journal of Bacteriology* **1916**, *1*, 321-331.

(36) Privett, B. J., Deupree, S. M., Backlund, C. J., Rao, K. S., Johnson, C. B., Coneski, P. N., and Schoenfisch, M. H. "Synergy of nitric oxide and silver sulfadiazine against gram-negative, gram-positive, and antibiotic-resistant pathogens" *Molecular Pharmaceutics* **2010**, *7*, 2289-2296.

(37) Sun, B., Slomberg, D. L., Chudasama, S. L., Lu, Y., and Schoenfisch, M. H. "Nitric oxide-releasing dendrimers as antibacterial agents" *Biomacromolecules* **2012**, *13*, 3343-3354.

(38) Worley, B. V., Slomberg, D. L., and Schoenfisch, M. H. "Nitric oxide-releasing quaternary ammonium-modified poly(amidoamine) dendrimers as dual action antibacterial agents" *Bioconjugate Chemistry* **2014**, *25*, 918-927.

(39) Jefferson, K. K., Goldmann, D. A., and Pier, G. B. "Use of confocal microscopy to analyze the rate of vancomycin penetration through *Staphylococcus aureus* biofilms" *Antimicrobial Agents and Chemotherapy* **2005**, *49*, 2467-2473.

(40) Richardson, A. R., Libby, S. J., and Fang, F. C. "A nitric oxide–inducible lactate dehydrogenase enables S*taphylococcus aureus* to resist innate immunity" *Science* **2008**, *319*, 1672-1676.

(41) Hall-Stoodley, L., Costerton, J. W., and Stoodley, P. "Bacterial biofilms: From the natural environment to infectious diseases" *Nature Reviews Microbiology* **2004**, *2*, 95-108.

(42) Flemming, H.-C., and Wingender, J. "The biofilm matrix" *Nature Reviews Microbiology* **2010**, *8*, 623-633.

(43) Wicke, D., Böckelmann, U., and Reemtsma, T. "Environmental influences on the partitioning and diffusion of hydrophobic organic contaminants in microbial biofilms" *Environmental Science & Technology* **2008**, *42*, 1990-1996.

(44) Boas, U., and Heegaard, P. M. "Dendrimers in drug research" *Chemical Society Reviews* **2004**, *33*, 43-63.

(45) Maiti, P. K., Cagin, T., Wang, G., and Goddard, W. A. "Structure of PAMAM dendrimers: Generations 1 through 11" *Macromolecules* **2004**, *37*, 6236-6254.

(46) Schenning, A. P., Elissen-Roman, C., Weener, J.-W., Baars, M. W., van der Gaast, S. J., and Meijer, E. "Amphiphilic dendrimers as building blocks in supramolecular assemblies" *Journal of the American Chemical Society* **1998**, *120*, 8199-8208.

(47) Worley, B. V., Schilly, K. M., and Schoenfisch, M. H. "Anti-biofilm efficacy of dual-action nitric oxide-releasing alkyl chain modified poly (amidoamine) dendrimers" *Molecular Pharmaceutics* **2015**, *12*, 1573-1583.

(48) Berenbaum, M. C. "Minor synergy and antagonism may be clinically important" *Journal of Antimicrobial Chemotherapy* **1987**, *19*, 271-273.

(49) Elion, G. B., Singer, S., and Hitchings, G. H. "Antagonists of nucleic acid derivatives VIII. Synergism in combinations of biochemically related antimetabolites" *Journal of Biological Chemistry* **1954**, *208*, 477-488.

(50) Storm, W. L., Johnson, J. A., Worley, B. V., Slomberg, D. L., and Schoenfisch, M. H. "Dual action antimicrobial surfaces via combined nitric oxide and silver release" *Journal of Biomedical Materials Research Part A* **2015**, *103*, 1974-1984.

CHAPTER 5:

Nitric Oxide-Releasing Single-Component Electrospun Polyurethane Fibers

5.1 Introduction

Chronic wounds, including diabetic foot ulcers, pressure ulcers, and venous leg ulcers, pose a serious health risk, with successful treatment often hindered by inefficient eradication of opportunistic infectious pathogens such as *Pseudomonas aeruginosa* and *Staphyloccocus aureus*.[1-3] Characteristics of an ideal wound dressing thus include facile gaseous and fluid exchange, the absorption of excess wound exudates, and protection against infectious microorganisms.[4] Electrospun fibers are inherently porous and possess high effective surface areas, which protect the wound from bacterial infections and allow for increased water absorption capabilities, making them excellent alternatives to traditional wound dressings.[4] Khil et al. demonstrated improved wound healing capabilities of electrospun polyurethane fibers over the commercially-available wound dressing Tegaderm (3M Health Care; St. Paul, Minnesota) in adult male guinea pigs.[5] The electrospun dressings were found to increase the rate of epithelialization, as well as prevent both infectious microorganism permeation and fluid accumulation. Electrospun fibers can also be modified to exhibit antibacterial action through the incorporation of therapeutic compounds into a blended, all-in-one dressing.[4, 6, 7] Initial work in the development of antibacterial electrospun wound dressings has investigated the ability to achieve controlled release of antibiotics[6-8] or silver ions[9, 10] from electrospun fibers composed of a range of polymers (e.g., polyurethane, polylactic acid, gelatin). However, the use of such antimicrobial agents continues to pose bacterial resistance

concerns that warrant the development of wound dressings capable of delivering antibacterial agents that are unlikely to foster resistance.

Nitric oxide (NO) is a promising antibacterial agent for the treatment of chronic wounds as it exhibits broad-spectrum antibacterial activity.[11] Further, NO has been shown to play a significant role in the wound healing process.[12] Indeed, the application of exogenous gaseous NO was found to improve the healing of skin wounds in rats from the inflammatory to the reparation phase, leading to faster scar tissue remodeling with less inflammation.[13] Further, the treatment of *S. aureus*-infected wounds with gaseous NO substantially improved wound healing over untreated infected wounds, with complete wound healing occurring nine days faster for the NO-treated wound.[13] Unfortunately, the direct application of gaseous NO to a wound is not trivial, necessitating the development of alternative methods for NO delivery.

In this regard, Weller et al. applied a NO-generating acidified nitrite cream to incision wounds two days after injury and found significant improvements in wound healing in both control (i.e., non-diabetic) and diabetic mice.[14] Balkus and coworkers have developed zeolite-containing and acrylonitrile-based electrospun fibers capable of NO release, but did not evaluate the antibacterial activity or wound healing characteristics of these materials.[15, 16] Wold et al. covalently modified polymers with thiol functionalities prior to electrospinning to yield *S*-nitrosothiol-modified electrospun fibers with NO release characteristics dependent on the identity of the thiol precursor.[17] The NO-releasing fibers were found to reduce *Acinetobacter baumannii* viability by 96% after 2 h.[17] Similarly, Vogt et al. reported the design of a light-triggered NO-releasing nanofibrous gelatin matrix using *S*-nitrosothiol NO donors that was capable of *S. aureus* growth inhibition.[18]

Our lab has developed macromolecular scaffolds capable of controllable NO storage and release, including silica nanoparticles and dendrimers. Indeed, Koh et al. doped silica nanoparticles modified with either *N*-diazeniumdiolate or *S*-nitrosothiol NO donors into electrospun fibers as a function of polyurethane water uptake capabilities.[19] The resulting NO-releasing fibers exhibited average release durations of ~15 and ~300 h for *N*-diazeniumdiolate- and *S*-nitrosothiol-containing fibers, respectively. The incorporation of dual-action dendrimers combining a contact-based biocide with NO release instead of the inert silica scaffold may improve the antibacterial properties of NO-releasing electrospun fibers.[20-23] Herein, we describe the fabrication of single-component electrospun polyurethane fibers doped with dual-action poly(amidoamine) dendrimers and evaluation of their in vitro antibacterial action as a function of dendrimer modification.

5.2 Materials and Methods

Triethylamine (TEA), rhodamine B isothiocyanate (RITC), dimethyloctylamine, epichlorohydrin, phenazine methosulfate (PMS), fetal bovine serum (FBS), trypsin, 3-(4,5-dimethylthiazol-2-yl)-5-(3-carboxymethoxyphenyl)-2-(4-sulfophenyl)-2H-tetrazolium inner salt (MTS), penicillin streptomycin (PS), and glutaraldehyde solution were purchased from Sigma-Aldrich (St. Louis, MO). Methyl acrylate, 1,2-epoxyhexane, 1,2-epoxyoctane, 1,2-epoxydodecane, and ethylenediamine (EDA) were purchased from the Aldrich Chemical Company (Milwaukee, WI). Sodium methoxide (5.4 M solution in methanol) was purchased from Acros Organics (Geel, Belgium). Cellulose ester dialysis membranes (500-1000 MWCO) were purchased from Spectrum Laboratories, Inc. (Rancho Dominguez, CA). Tecoflex (SG-80A) polyurethane was a gift from Thermedics (Woburn, MA). Hydrothane (AL 25-80A) polyurethane was a gift from AdvanSource Biomaterials Corp. (Willmington, MA). Tecoplast (TP-470)

polyurethane was a gift from Lubrizol (Cleveland, OH). Dispensing needles for electrospinning (JG22-1.0P) were obtained from Howard Electronic Instruments, Inc (El Dorado, KS). Dulbecco's modified Eagle's medium (DMEM) and Dulbecco's phosphate buffered saline (PBS) were obtained from Lonza Group (Basel, Switzerland). Tryptic soy broth (TSB) and tryptic soy agar (TSA) were obtained from Becton, Dickinson and Company (Franklin Lakes, NJ). *Pseudomonas aeruginosa* (*P. aeruginosa*; ATCC #19143) and *Staphylococcus aureus* (*S.aureus*; ATCC #29213) were obtained from American Type Tissue Culture Collection (Manassas, VA). L929 mouse fibroblasts were obtained from the UNC Tissue Culture Facility (Chapel Hill, NC). Nitrogen (N_2), argon (Ar), carbon dioxide (CO_2), and nitric oxide (NO) calibration (25.87 PPM, balance N_2) gases were purchased from National Welders (Raleigh, NC). Pure nitric oxide (NO) gas (99.5%) was purchased from Praxair (Sanford, NC). Common laboratory salts and solvents were purchased from Fisher Scientific (Fair Lawn, NJ). Distilled water was purified using a Millipore Milli-Q UV Gradient A-10 system (Bedford, MA), resulting in a total organic content of ≤6 ppb and a final resistivity of 18.2 mΩ·cm. Unless noted otherwise, these and all other materials were analytical-reagent grade and used as received without further purification.

5.2.1 Synthesis of QA- and alkyl chain-modified PAMAM dendrimers

Poly(amidoamine) **(**PAMAM) scaffolds were synthesized as described previously[20, 24, 25] by repeated alkylation/amidation steps using methyl acrylate and EDA from an EDA core. G4 PAMAM dendrimers were then modified with either hexyl, octyl, and dodecyl alkyl chains or octylQA moieties. To form alkyl-modified dendrimers,[22] G4 PAMAM (100 mg) was dissolved in either 2 mL (hexyl modifications) or 5 mL (octyl and dodecyl modifications) methanol, and one equivalent of triethylamine (e.g., with respect to the molar amount of primary amines) and 1 molar equivalent of epoxide (i.e., epoxyhexane, epoxyoctane, or epoxydodecane) were then added to the

vial. The solution was stirred at room temperature for 3 d. After reaction completion, excess epoxide was removed in vacuo. To ensure the removal of any unreacted epoxide, the single-action dendrimers were re-dissolved in 5 mL methanol before being kept under vacuum overnight. Complete removal of the epoxide was verified via ^{1}H NMR spectroscopy (Bruker 400 MHz spectrometer).

Representative ^{1}H NMR data of alkyl chain-modified G4 PAMAM included the following peaks. G4 hexyl: ^{1}H NMR (400 MHz, MeOD, δ) 2.28 (s, $NCH_2\mathit{CH_2}C(O)NH$), 1.34–1.20 (m, $NHCH_2CH(OH)(C\mathit{H_2})_3CH_3$), 0.85–0.81 (t, $NHCH_2CH(OH)C(H_2)_3C\mathit{H_3}$). G4 octyl: ^{1}H NMR (400 MHz, MeOD, δ) 2.29 (s, $NCH_2\mathit{CH_2}C(O)NH$), 1.35–1.23 (m, $NHCH_2CH(OH)(C\mathit{H_2})_5CH_3$), 0.83–0.80 (t, $NHCH_2CH(OH)C(H_2)_5C\mathit{H_3}$). G4 dodecyl: ^{1}H NMR (400 MHz, MeOD, δ) 2.27 (s, $NCH_2\mathit{CH_2}C(O)NH$), 1.34–1.20 (m, $NHCH_2CH(OH)(C\mathit{H_2})_9CH_3$), 0.82–0.78 (t, $NHCH_2CH(OH)(CH_2)_9C\mathit{H_3}$).

To form QA-modified dendrimers, quaternary ammonium epoxides (octylQA-epoxide) were synthesized as described previously.[23, 26] Briefly, 0.04 mmol epichlorohydrin was reacted with 0.01 mmol *N*,*N*-dimethyloctylamine at room temperature overnight (~18 h). The mixture was then added dropwise to cold ether while sonicating, and the solid/viscous liquid octylQA-epoxide was collected via centrifugation (810×*g*, 5 min). The supernatant was decanted, and the octylQA-epoxide was washed with 50 mL of cold ether and sonicated extensively. This washing procedure was repeated three times before drying the product in vacuo. A ring-opening reaction was then carried out between the octylQA-epoxide and the terminal primary amines of the PAMAM dendrimers. G4 PAMAM (100 mg) was dissolved in 5 mL of methanol. One equivalent of triethylamine (e.g., with respect to the molar amount of primary amines) and 2.5 molar equivalents of octylQA-epoxide were then added to the vial. The solution was stirred at room

temperature for 4 d. Solvent was then removed in vacuo. The dendrimers were subsequently dissolved in water, followed by dialysis against water overnight and lyophilization.

Representative ^{1}H NMR data of QA-modified G4 PAMAM included the following peaks. G4 octylQA: ^{1}H NMR (400 MHz, CD_3OD, δ) 2.31 (s, $NCH_2\mathit{CH_2}C(O)NH$), 1.80 (s, $CH_2N^+(CH_3)_2CH_2C\mathit{H_2}(CH_2)_5CH_3$), 1.31–1.23 (m, $CH_2N^+(CH_3)_2CH_2CH_2(C\mathit{H_2})_5CH_3$), 0.83 (t, $CH_2N^+(CH_3)_2CH_2CH_2(CH_2)_5C\mathit{H_3}$).

5.2.2 N-Diazeniumdiolation of QA- and alkyl chain-modified PAMAM dendrimers

To form *N*-diazeniumdiolate NO donors on the modified dendrimer scaffolds, single-action G4 PAMAM (30 mg) were dissolved in 1 mL of varying ratios of anhydrous methanol (MeOH) and tetrahydrofuran (THF) depending on the modification as follows: 8:2 MeOH:THF (G4 hexyl) or 1:1 MeOH:THF (G4 octyl, G4 dodecyl, G4 octylQA). The solutions were vortexed and then one molar equivalent (e.g., with respect to the molar amount of primary amines) of sodium methoxide was added.

The dendrimer solutions were placed in a stainless steel reactor with continuous magnetic stirring and connected to an in-house NO reactor. The vessel was flushed with Ar three times to a pressure of 7 bar, followed by three longer Ar purges (10 min) to remove trace oxygen from the solutions. Following deoxygenation, the reactor was then pressurized to 10 bar with NO gas pre-scrubbed with KOH. The pressure was maintained at 10 bar for 4 d, after which the solutions were again purged with Ar three times at short durations followed by extended purges (3 × 10 min) to remove unreacted NO. Solvent was removed in vacuo, and the resulting dual-action, NO-releasing dendrimers were dissolved in anhydrous methanol in a 1 dram glass vial, capped and parafilmed, and stored at -20 °C.

5.2.3 Fabrication of single-component electrospun polyurethane fibers

All polyurethane solutions (Tecoplast, Tecoflex, and Hydrothane) used herein were 12 wt% (120 mg/mL) in 3:1:1 THF:DMF:MeOH. Polyurethane solutions containing control and NO-releasing dendrimers (10 mg/mL; 1 wt%) were prepared by first dissolving the polyurethane in THF and DMF, followed by the addition of dendrimer solution in the remaining equivalent of methanol.

Electrospun fibrous mats were fabricated using a custom electrospinning apparatus[27] consisting of a ES20P-20W High Voltage power supply (Gamma High Voltage Research, Ormond Beach, FL), a Kent Scientific Genie Plus syringe pump (Torrington, CT), and grounded steel collector plate covered in aluminum foil. All fibers were fabricated using an applied voltage of 15 kV, 15 cm tip-to-collector distance, and 20 μL/min flow rate. For all Tecoflex and Hydrothane fibers, 1.0 mL of polyurethane solution was electrospun and collected on aluminum foil, while 2.0 mL of solution was required to obtain similar masses for the Tecoplast fibers. After collection, fibers were cut using a 1.27 cm-diameter hole-punch to yield individual samples with a resultant surface area of 1.267 cm^2.

5.2.4 Characterization of NO storage and release

Real-time NO release in deoxygenated PBS (pH 7.4, 37 °C) was monitored using a Sievers NOA 280i chemiluminescence NO analyzer (NOA, Boulder, CO). Prior to analysis, the NO analyzer was calibrated with air passed through a NO zero filter (0 ppm NO) and a 25.87 ppm NO standard gas (balance N_2). Fibrous mat coupons (surface area: 1.267 cm^2) or 0.5 mg aliquots of *N*-diazeniumdiolate-functionalized PAMAM in methanol were added to 30 mL deoxygenated PBS to initiate NO release. Nitrogen was flowed through the solution at a flow rate of 80 mL/min to carry the liberated NO to the analyzer. Additional nitrogen flow was supplied to the flask to match

the collection rate of the instrument at 200 mL/min. Nitric oxide analysis was terminated when NO levels decreased to below 1 pmol/cm^2 for fibers (9.7 ppb) or 10 ppb NO/mg dendrimer. Total amount of dendrimer incorporated per milligram of fiber were determined by measuring total NO release in 50 mM HCl at 37 °C.

5.2.5 Characterization of electrospun polyurethane fibers

Fiber diameter and morphology were assessed using either an environmental scanning electron microscope (ESEM; FEI Quanta 200 field emission gun, Hillsboro, OR) or a FEI Helios 600 Nanolab Dual Beam System (Hillsboro, OR) without additional metal coating. Fiber diameters were determined using NIH ImageJ software (Bethesda, MD) and were averaged for at least 150 measurements over three separate fiber samples.

Water absorption of the electrospun fibrous mats was assessed by comparing weights of the dry and hydrated samples. Dry electrospun fibers were weighed before soaking in Milli-Q water overnight at room temperature. The hydrated samples were removed from water, and the excess surface water was removed by dabbing with a Kimwipe before weighing the samples again. Water absorption was calculated by the following equation, where W_H is the weight of the hydrated sample and W_D is the initial weight of the dry fibrous mat:

$$\text{Water Absorption (\%)} = [(W_H - W_D)/W_D] \times 100\% \qquad \textbf{Eq. 5.1}$$

The porosity of electrospun fibrous mats was determined using the liquid intrusion method.[28, 29] Fiber mats were weighed prior to immersion in 100% ethanol at room temperature overnight to allow diffusion of ethanol into the void volume. After incubation, fibers were removed from ethanol, dabbed with a Kimwipe, and weighed again. Porosity was calculated by dividing the volume of intruded ethanol (determined by the change in mass and the density of

ethanol, 0.789 g/mL) by the total volume after intrusion (volume of ethanol + volume of fibers, determined by initial fiber mass and polyurethane density, 1.1 g/mL).

Quantitation of dendrimer delivery was performed using electrospun fibers doped with RITC-tagged G4 PAMAM dendrimers. Fluorescently-labeled G4 PAMAM dendrimers were synthesized as described previously.[21-23] Briefly, 100 mg G4 PAMAM were added to a vial containing one molar equivalent of RITC per mole dendrimer (3.8 mg) in 2 mL methanol. One equivalent of triethylamine (with respect to the molar amount of primary amines) was then added to the vial. The solution was stirred for 24 h in the dark, after which solvent was removed in vacuo. Dendrimers were dissolved in water, dialyzed against water (3 d), and then lyophilized. The above procedures for dendrimer modification and fiber mat fabrication were performed in the dark to yield RITC-tagged electrospun fibrous mats. Individual fiber mats were incubated in 500 μL PBS (pH 7.4, 37 °C) for 2 h, 1 d, and 7 d. After incubation, 100 μL of each solution was transferred to a black 96-well plate in triplicate and fluorescence intensity was measured using a BMG PolarStar Omega fluorescence plate reader (Ortenberg, Germany). Calibration standards were prepared at concentrations ranging from 0 – 100 μg/mL in triplicate. Dendrimer delivery was reported as percent dendrimer leached based on the experimental amount of dendrimer per milligram of fiber (calculated from the total dendrimer incorporation determined by NO release in 50 mM HCl) and mass of the fiber mat sample. Fluorescence images of single-component RITC-tagged fibers were obtained on a Zeiss 200M inverted microscope with an XBO 75 Xe arc lamp, single band filter set (Omega Optical), and cascade 1 K CCD camera (Photometrics) with Micromanager software using a 40× objective and 50 ms exposure time.

5.2.6 In vitro cytotoxicity

L929 mouse fibroblasts were grown in DMEM supplemented with 10 vol% FBS and 1 wt% PS and incubated in 5 vol% CO_2 under humidified conditions at 37 °C. After reaching 80% confluency, the cells were trypsinized, seeded onto tissue culture-treated polystyrene 24-well plates at a density of 10^5 cells/mL, and incubated at 37 °C for 72 h. The supernatant was then aspirated and replaced with 1 mL of fresh growth medium and the electrospun fiber mats. Dimethyl sulfoxide (10%) and 50 µL PBS were used as positive and negative controls, respectively. After incubation for 2 or 24 h at 37 °C, the supernatant was aspirated and 500 µL of a mixture of DMEM/MTS/PMS (105/20/1, v/v/v) was added to each well. After 1.5 h incubation at 37 °C, 100 µL of the colored solution was transferred to a 96-well plate in triplicate and the absorbance was quantified at 490 nm using a Thermoscientific Multiskan EX plate reader (Waltham, MA). The mixture of DMEM/MTS/PMS and untreated cells were used as a blank and control, respectively. Results were expressed as percentage of relative cell viability as follows:

$$\% \text{ Cell Viability} = [(Abs_{490} - Abs_{blank})/(Abs_{control} - Abs_{blank})] \times 100\% \qquad \textbf{Eq. 5.2}$$

5.2.7 In vitro cell proliferation

L929 mouse fibroblasts were grown in DMEM supplemented with 10 vol% FBS and 1 wt% PS and incubated in 5 vol% CO_2 under humidified conditions at 37 °C. After reaching 80% confluency, the cells were trypsinized, seeded onto electrospun fiber mats in tissue culture-treated polystyrene 24-well plates at a density of 10^5 cells/mL. After incubation at 37 °C for 24 h, fiber mats were dipped once in sterile water to remove non-adhered cells then transferred to a 15 mL falcon tube containing 500 µL of a mixture of DMEM/MTS/PMS (105/20/1, v/v/v). The solutions were then sonicated for 5 min at 60% power (Elma Lab-Line 9331, Melrose Park, IL). For wells containing positive (10% DMSO) and negative controls, the supernatant was aspirated and

replaced with 500 µL of a mixture of DMEM/MTS/PMS. After 1.5 h incubation at 37 °C, 100 µL of the colored solution was transferred to a 96-well plate in triplicate and the absorbance was quantified at 490 nm using a Thermoscientific Multiskan EX plate reader (Waltham, MA). The mixture of DMEM/MTS/PMS and untreated cells (i.e., cells seeded in a well without fibers) were used as a blank and control, respectively. The viability of cells adhered to blank fibers was calculated using Equation 5.2 and normalized to 100%. The viability of cells adhered to control and NO-releasing fibers was then reported as a percentage of the cells adhered to blank fibers.

To prepare fibers for imaging, blank, control, and NO-releasing G4 octyl-doped Tecoflex fibrous mats were exposed to L929 mouse fibroblast cells as described above. After 24 h incubation, fibers were dipped once in sterile water then fixed in 1 mL 2.5% glutaraldehyde in Milli-Q water for 45 min. After fixation, fibers were rinsed in sterile water (3 × 10 min) before dehydration in solutions of increasing percent ethanol (25, 50, 75, 95, 100%). Fibers were fully dehydrated with a Tousimis Semidri PVT-3 critical point dryer and coated with 5 nm gold using a Cressington 108 Auto Sputter Coater. Images were obtained using a FEI Helios 600 Nanolab Dual Beam System (Hillsboro, OR).

5.2.8 Bacterial adhesion assays on single-component fibers

Lyophilized *P. aeruginosa* and *S. aureus* were reconstituted in tryptic soy broth (TSB) and cultured overnight at 37 °C. A 0.5 mL aliquot of culture was grown in 50 mL TSB to a concentration of 10^8 colony forming units per mL (cfu/mL), collected by centrifugation (2355×*g*), resuspended in 15% glycerol (v/v in PBS), and stored at -80 °C in 1 mL aliquots. For daily experiments, colonies of bacteria culture were inoculated in 2 mL TSB overnight at 37 °C and recultured in fresh TSB (50 mL) the next day.

To assess the antibacterial action of the electrospun fibrous mats, *P. aeruginosa* and *S. aureus* were cultured in TSB to a concentration of 10^8 cfu/mL, collected by centrifugation (1045×*g*), and resuspended in simulated wound fluid (SWF; 25% FBS in PBS, pH 7.4) at 10^8 cfu/mL. Individual fiber mat samples (blank, control, and NO-releasing) were added to 1 dram glass vials and sterilized under UV light for 2 h prior to the bacteria assays. Fibers were exposed to 500 µL 10^8 cfu/mL bacteria in SWF for either 2 or 6 h at 37 °C with light agitation. Untreated controls (blanks) were included in each experiment to ensure the bacteria remained viable over the 2 or 6 h assays. After exposure, fibers were removed from the bacteria solutions, dipped once in sterile water to remove non-adhered cells, and transferred to a 15 mL falcon tube containing 3 mL sterile water. The solutions were then sonicated for 5 min at 60% power (Elma Lab-Line 9331, Melrose Park, IL). The resulting solutions were vortexed and then spiral-plated at 100-, 1000-, and 10,000-fold dilutions on tryptic soy agar plates using an Eddy Jet spiral plater (IUL; Farmingdale, NY). Bacterial viability was assessed by counting the number of colonies formed on the agar plate using a Flash & Go colony counter (IUL; Farmingdale, NY).

5.3 Results and Discussion

5.3.1 Synthesis and characterization of NO-releasing G4 dendrimers

To evaluate the effects of dendrimer modification on fiber NO-release characteristics, generation 4 (G4) poly(amidoamine) (PAMAM) dendrimers were modified with alkyl chains (i.e., hexyl, octyl, dodecyl) or octylQA moieties through a ring-opening reaction at the peripheral primary amines as described previously.[22, 23] Addition of the functional groups was confirmed using ^{1}H NMR spectroscopy. On average, 46 functional groups were added to the G4 scaffold, resulting in ~70% functionalization of the terminal primary amines (Table 5.1).

The secondary amines were subsequently converted to *N*-diazeniumdiolate NO donors under high pressures of NO. Nitric oxide storage was tuned by increasing the ratio of THF:methanol with increasing alkyl chain length, resulting in similar NO payloads of ~1 μmol/mg (Table 5.1). All of the alkyl chain-modified dendrimers exhibited similar initial maximum fluxes and durations (~10 h). However, a slight increase in NO-release half-life was observed with increasing alkyl chain length (~20 to ~34 min), likely due to decreased water diffusion to the proton-labile *N*-diazeniumdiolate NO donor. The QA-modified dendrimer (G4 octylQA) exhibited an initial max flux about half that of the alkyl chain-modified dendrimers and an extended NO-release half-life (115 min) and duration (16 h). The longer NO-release half-life exhibited by the QA-modified dendrimers suggests that the permanent positive charge of the QA moiety stabilizes the *N*-diazeniumdiolate group, extending NO release. Fabrication of electrospun polyurethane fibers doped with dendrimers exhibiting a range of exterior modifications and NO-release half-lives allows for the evaluation of fiber and NO-release characteristics as a function of dendrimer modification.

5.3.2 Fabrication and characterization of single-component electrospun polyurethane fibers

We have previously fabricated electrospun polyurethane fibers with NO-release capabilities through the incorporation of NO-releasing proline (PROLI/NO), silica nanoparticles, and poly(amidoamine) (PAMAM) dendrimers.[19, 27, 30, 31] Nitric oxide-release kinetics were dependent on the dopant NO-release kinetics (i.e., PROLI/NO-doped fibers exhibited much faster release kinetics than either of the macromolecular scaffolds) and polyurethane hydrophobicity. Fibers comprised of NO-releasing dendrimers and silica nanoparticles demonstrated similar NO-release totals and kinetics, but the dendrimer scaffolds were better retained within the polyurethane fibers. Indeed, dendrimer-doped Tecoplast fibers exhibited <20% leaching after one week while

Table 5.1 Characterization and NO-release properties of G4 dendrimers in PBS (pH 7.4, 37 °C) as measured by a chemiluminescence NO analyzer.[a]

	No. Modified End Groups[b]	% Modified	$[NO]_{max}$[c] (ppb/mg)	t_{max}[d] (min)	t[NO][e] (μmol/mg)	$t_{1/2}$[f] (min)	t_d[g] (h)
G4 hexyl/NO	51 ± 4	80 ± 6	3800 ± 1160	1.3 ± 0.3	0.94 ± 0.07	20 ± 1	10 ± 4
G4 octyl/NO	47 ± 3	74 ± 5	4930 ± 780	2.7 ± 0.4	0.93 ± 0.05	23 ± 3	9 ± 1
G4 dodecyl/NO	46 ± 7	71 ± 11	3880 ± 640	1.8 ± 0.4	0.90 ± 0.07	34 ± 3	10 ± 1
G4 octylQA/NO	39 ± 5	61 ± 8	1570 ± 150	2.0 ± 0.3	1.03 ± 0.06	115 ± 6	16 ± 1

[a]For all measurements, $n \geq 3$ pooled experiments. [b]Determined by ^{1}H NMR. [c]Maximum flux of NO release. [e]Time required to reach maximum flux. [e]Total NO payload released. [f]NO release half-life. [g]Duration of NO release.

70–100% of NO-releasing silica nanoparticles leached from electrospun fibers regardless of polyurethane hydrophobicity.[19, 31]

To fabricate single-component (i.e., composed of one polyurethane) electrospun fibers, three polyurethanes (Tecoplast, Tecoflex, and Hydrothane) exhibiting distinct hydrophobicity and water uptake properties were chosen for study. Of these, Tecoplast was the most hydrophobic and Hydrothane exhibited the greatest water uptake, allowing us to evaluate the effects of polyurethane hydrophobicity on fiber formation and NO-release characteristics. For these studies, control and NO-releasing G4 octyl dendrimers were doped into polyurethane solutions prior to electrospinning. Blank (no dendrimer dopant), control (non-NO-releasing), and NO-releasing electrospun fibers were fabricated for each of the individual polyurethanes. The resulting semi-porous mats contained fibers exhibiting smooth morphology with little to no bead formation (Figure 5.1). Fiber diameter was dependent on both the polyurethane composition and presence of dendrimer dopant (Table 5.2). Blank Tecoplast and Hydrothane fibers exhibited similar diameters of ~630 nm, while blank Tecoflex fibers were larger (~930 nm), demonstrating no trend between fiber diameter and polyurethane hydrophobicity. The effects of dendrimer dopant also varied with polyurethane composition. Although Hydrothane fibers exhibited no significant variation in fiber diameter with the addition of control or NO-releasing G4 octyl dendrimers, the diameters of dendrimer-doped Tecoplast and Tecoflex fibers were decreased from blank fibers by approximately 300 and 150 nm, respectively.

A critical characteristic for wound dressings is the allowance of gaseous and fluid exchanges.[4] A porous nanofiber structure with high surface area allows for cell respiration, maintains an appropriately moist environment for the wound, and prevents stagnation at the wound site by absorbing excess wound exudate. In this regard, the porosity of dendrimer-doped

electrospun fibrous mats was characterized via liquid intrusion by measuring the ability of a non-wetting liquid to permeate the pores.[28, 29] In general, porosity of the electrospun fibers trended with polyurethane hydrophobicity. Blank Tecoplast fibers (most hydrophobic) exhibited the greatest porosity (~70%), which decreased upon addition of the dendrimer dopant by ~10% (Table 5.2). Blank, control, and NO-releasing electrospun fibers exhibited similar porosities of approximately 50 and 43% for Tecoflex and Hydrothane, respectively. As expected, blank electrospun fibers exhibited greater water absorption with decreasing polyurethane hydrophobicity, most likely due to the increase in water uptake. While blank, control, and NO-releasing electrospun Tecoflex and Hydrothane fibers absorbed water at similar rates, both dendrimer-doped Tecoplast fibers exhibited significantly enhanced water absorption values (~750%) compared to blank Tecoplast fibers (~100%) (Table 5.2). This increase in water absorption is surprising considering the hydrophobicity of the Tecoplast composition. Indeed, it is likely connected to the decrease in fiber diameter and porosity observed for the dendrimer-doped fibers, leading to greater fiber surface area and allowing for increased water absorption.

Nitric oxide release from electrospun polyurethane fibers was evaluated via chemiluminescence in PBS (pH 7.4, 37 °C). Electrospun fibers were cut into coupons to yield fiber samples with a consistent surface area of 1.267 cm^2. Due to the proton-labile nature of *N*-diazeniumdiolate NO donors, the maximum NO flux was expected to increase with decreasing polyurethane hydrophobicity with a concomitant decrease in the time to reach the maximum. Surprisingly, both values were similar for each of the polyurethanes regardless of hydrophobicity (Table 5.3). Similarly, we expected the NO-release half-life ($t_{1/2}$) to decrease with increasing polyurethane water uptake. However, the most hydrophobic Tecoplast fibers exhibited the fastest NO-release half-life (17.5 min) and duration (1.4 h). Although initially surprising, these values

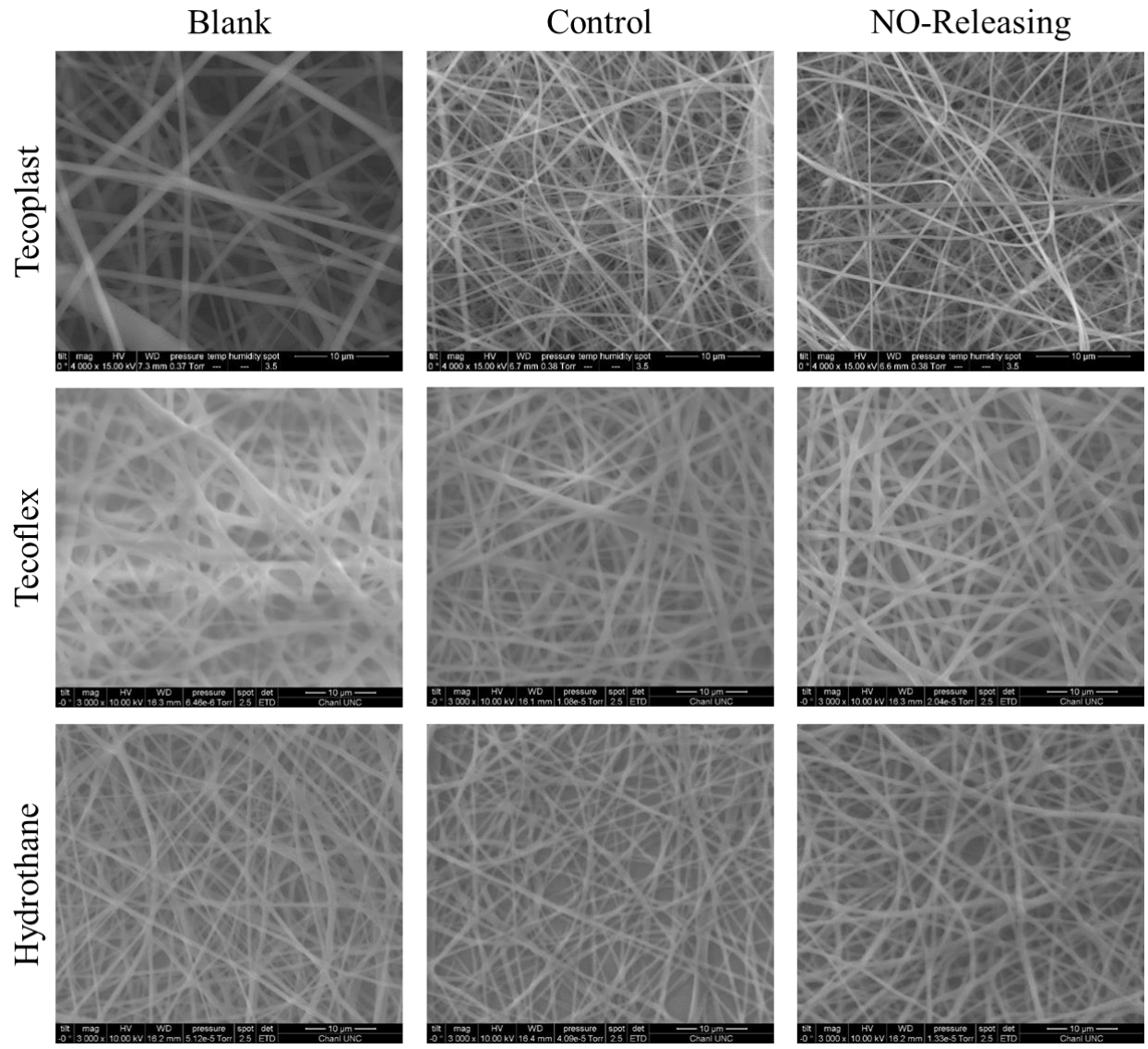

Figure 5.1 Scanning electron micrographs of blank, control, and NO-releasing G4 octyl-doped electrospun Tecoplast, Tecoflex, and Hydrothane fibers.

Table 5.2 Characterization of single-component electrospun polyurethane fibers.[a]

	Fiber Diameter (nm)	Porosity (%)	Water Absorption (%)
Tecoplast	623 ± 253	71.0 ± 4.5	102 ± 67
Tecoplast-G4 octyl	342 ± 95	63.1 ± 4.8	765 ± 166
Tecoplast-G4 octyl/NO	336 ± 107	59.1 ± 5.7	747 ± 149
Tecoflex	927 ± 310	50.4 ± 7.6	116 ± 37
Tecoflex-G4 octyl	771 ± 247	54.6 ± 5.6	112 ± 35
Tecoflex-G4 octyl/NO	798 ± 266	49.4 ± 13.7	89 ± 29
Hydrothane	636 ± 199	43.0 ± 9.3	173 ± 40
Hydrothane-G4 octyl	603 ± 237	41.7 ± 10.5	167 ± 49
Hydrothane-G4 octyl/NO	543 ± 151	44.6 ± 9.9	155 ± 37

[a]For all measurements, $n \geq 3$ pooled experiments.

were found to scale proportionally with total NO released (Figure 5.2 A). Nitric oxide-releasing Tecoflex fibers exhibited the longest half-life (36.5 min) and greatest NO payload (0.037 μmol/mg), while NO-releasing Tecoplast fibers only released 0.018 μmol NO/mg. Both the half-life (20.9 min) and total NO storage (0.027 μmol/mg) of NO-releasing Hydrothane fibers fell between these two, suggesting that polyurethane hydrophobicity has little effect on the NO-release kinetics of single-component electrospun fibers. As evidenced by the variation in NO storage, the amount of dendrimer doped into the electrospun fibers varied greatly with polyurethane identity. Total dendrimer incorporation was calculated per mass of electrospun fiber by determining the total NO released under acidic conditions (50 mM HCl). While electrospun Tecoflex-G4 octyl/NO fibers incorporated the greatest amount of dendrimer (~60 μg/mg), the more hydrophobic Tecoplast fibers exhibited much lower dendrimer incorporation (~20 μg/mg), indicating polyurethane hydrophobicity greatly affects dendrimer incorporation during electrospinning.

While previous reports have attempted to minimize dopant leaching for in vivo applications,[19, 31] active release of dual-action dendrimers is expected to increase the antibacterial action of electrospun fibers. To quantitate the amount of dendrimer delivered from each of the electrospun polyurethane fiber compositions, dendrimer leaching into solution over time was determined in PBS (pH 7.4, 37 °C) after 2 h, 1 d, and 7 d. The G4 dendrimer scaffold was labeled with the fluorescent tag RITC prior to modification with octyl alkyl chains, and the resulting RITC-tagged dendrimers were used to fabricate fluorescent electrospun fibers (Figure 5.3). Total dendrimer delivery (%) was determined after 2 h, 1 d, and 7 d using the total amount of incorporated dendrimer determined from NO release totals in acidic conditions.

Table 5.3 Nitric oxide-release properties for G4 octyl/NO-doped electrospun polyurethane fibers in PBS (pH 7.4, 37 °C).[a]

	$[NO]_{max}$[b] ($pmol/cm^2$)	t_{max}[c] (min)	t[NO][d] ($\mu mol/cm^2$)	t[NO][e] ($\mu mol/mg$)	$t_{1/2}$[f] (min)	t_d[g] (h)	t(dopant)[h] ($\mu g/mg$)
Tecoplast	13.0 ± 4.0	3.9 ± 1.6	0.017 ± 0.006	0.018 ± 0.002	17.5 ± 2.1	1.4 ± 0.3	22 ± 2
Tecoflex	11.7 ± 3.6	4.3 ± 2.1	0.036 ± 0.011	0.037 ± 0.008	36.5 ± 4.3	2.3 ± 0.4	61 ± 8
Hydrothane	15.7 ± 5.4	4.3 ± 2.4	0.027 ± 0.010	0.027 ± 0.006	20.9 ± 4.8	1.6 ± 0.4	52 ± 4

[a]For all measurements, $n \geq 3$ pooled experiments. [b]Maximum flux of NO release. [c]Time required to reach maximum flux. [d]Total NO payload released per surface area. [e]Total NO payload released per mg. [f]NO release half-life. [g]Duration of NO release. [h]Total amount of dendrimer incorporated as determined by total NO release in 50 mM HCl.

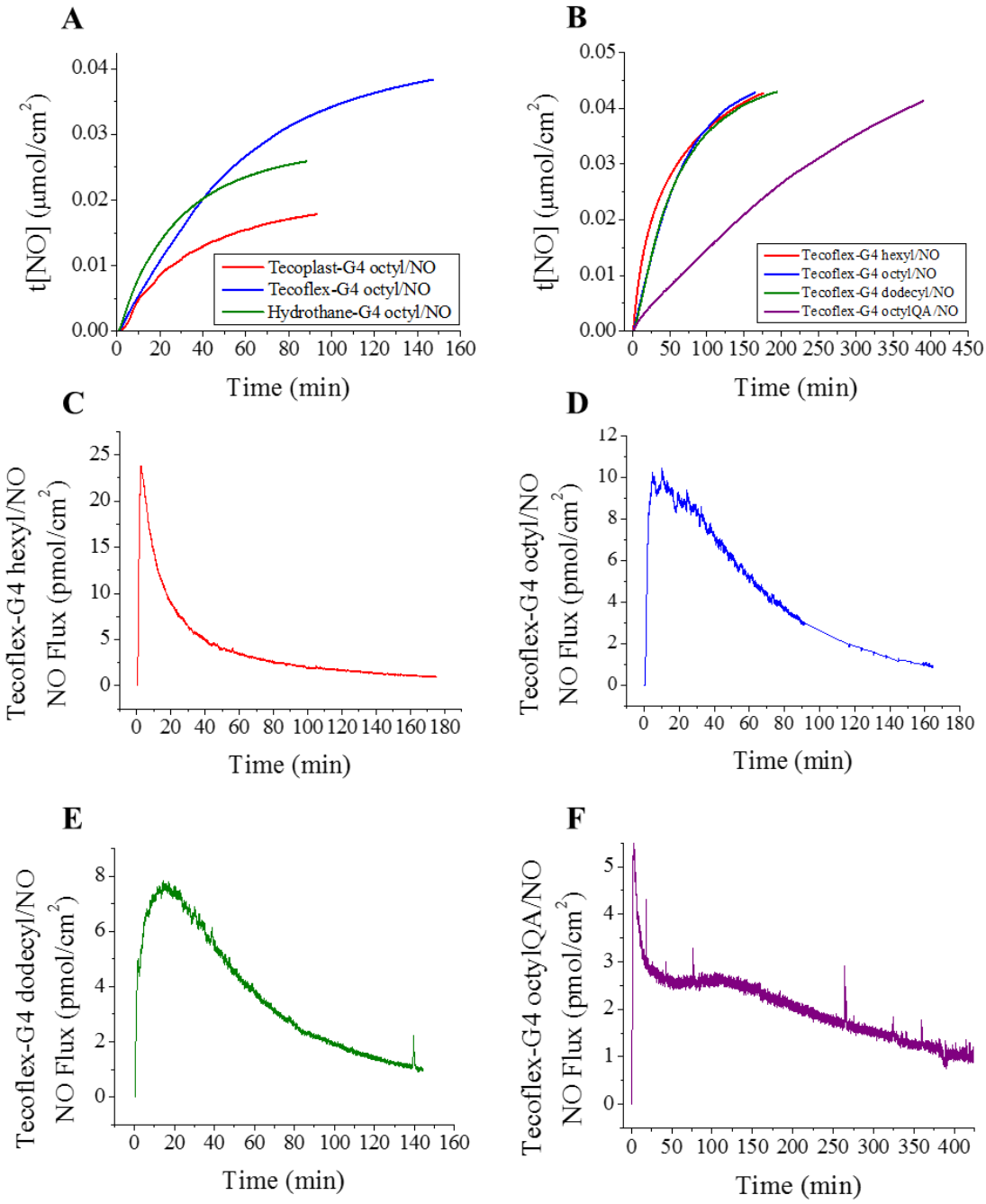

Figure 5.2 Representative total NO-release curves for (A) G4 octyl/NO-doped electrospun Tecoplast, Tecoflex, and Hydrothane fibers and (B) NO-releasing dendrimer-doped electrospun Tecoflex fibers. Representative NO-release curves for (C) G4 hexyl/NO, (D) G4 octyl/NO, (E) G4 dodecyl/NO, and (F) G4 octylQA/NO-doped electrospun Tecoflex fibers.

Although total dendrimer release slightly increased over time, the majority of dendrimer delivery occurred in the first 24 hours (Figure 5.4). As expected, dendrimer delivery was dependent on the hydrophobicity of the polyurethane, with the hydrophilic Tecoflex and Hydrothane polyurethanes exhibiting greater dendrimer release than the more hydrophobic Tecoplast fibers. After 7 d, control and NO-releasing Tecoplast fibers exhibited 35 and 26% dendrimer release, respectively, with both fiber compositions delivering approximately 20% of the total dendrimer payload in the first day. At each timepoint, the NO-releasing Tecoflex and Hydrothane fibers exhibited greater drug delivery than control (non-NO-releasing) fibers. Although control and NO-releasing Hydrothane fibers demonstrated similar dendrimer delivery after 7 d (72 and 76%, respectively), the NO-releasing fibers exhibited more rapid dendrimer release than their non-NO-releasing counterparts after 1 d (59 versus 69% for control and NO-releasing fibers, respectively). Furthermore, NO-releasing Tecoflex fibers were characterized as having faster and greater dendrimer delivery than control fibers after 7 d, exhibiting 48 and 65% release for control and NO-releasing fibers, respectively. The faster release kinetics exhibited by the NO- releasing fibers suggests that dendrimer delivery is dependent on charge, with the zwitterionic *N*-diazeniumdiolate resulting in faster release rates.

5.3.3 Fabrication and characterization of electrospun Tecoflex fibers with various dendrimer dopants

Due to the lower NO totals and dendrimer incorporation exhibited by Hydrothane and Tecoplast fibers, Tecoflex fibers were selected for further study to evaluate the effects of dendrimer exterior modification on NO-release and material characteristics. Control and NO-releasing G4 PAMAM dendrimers modified with hexyl, octyl, dodecyl, and octylQA functional groups were individually doped into electrospun Tecoflex fibers (Figures 5.1, 5.5). While the

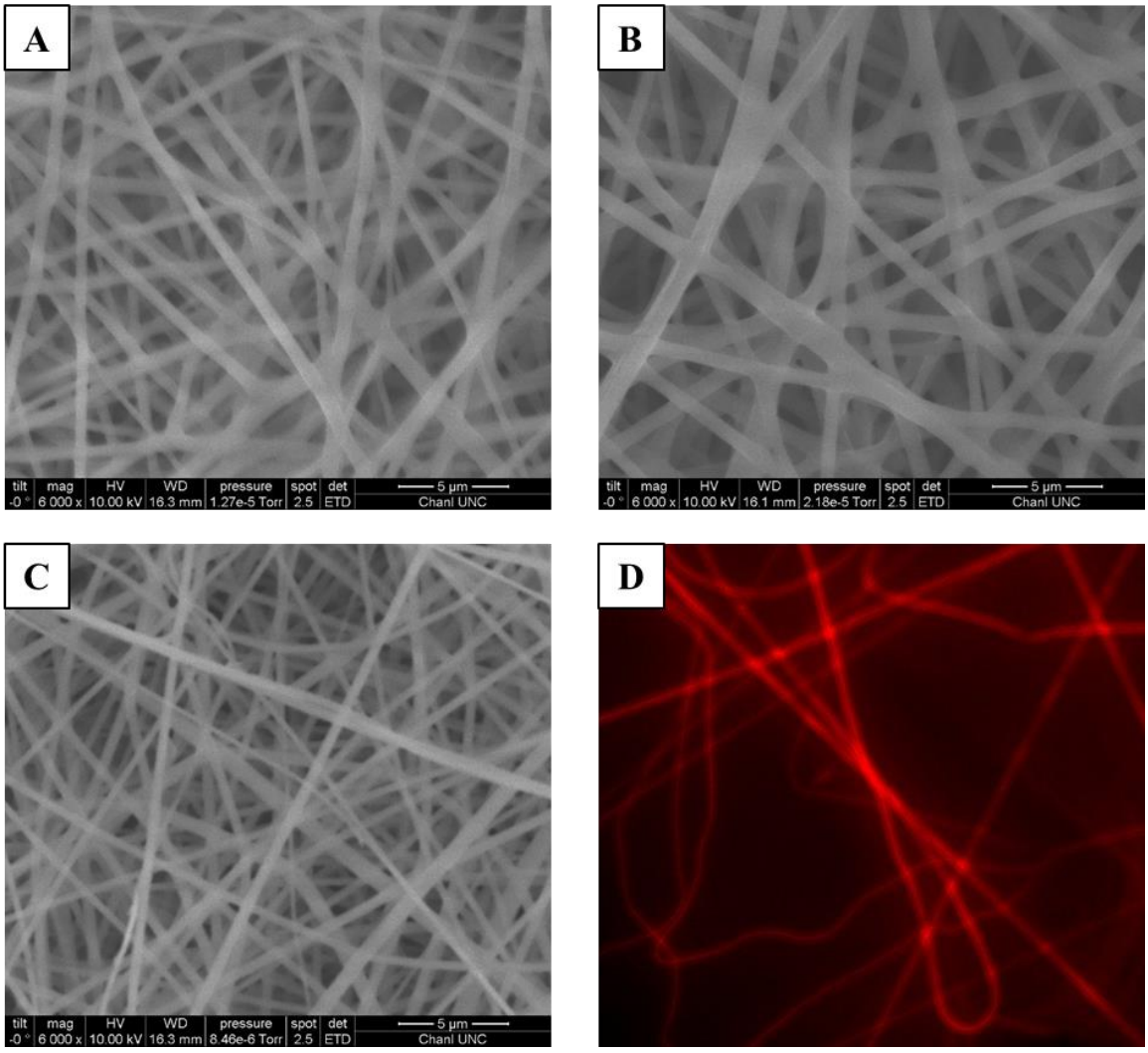

Figure 5.3 Electron micrographs of G4 RITC octyl-doped (A) Tecoplast, (B) Tecoflex, and (C) Hydrothane fibers. (D) Fluorescence image of Tecoplast-G4 RITC octyl fibers.

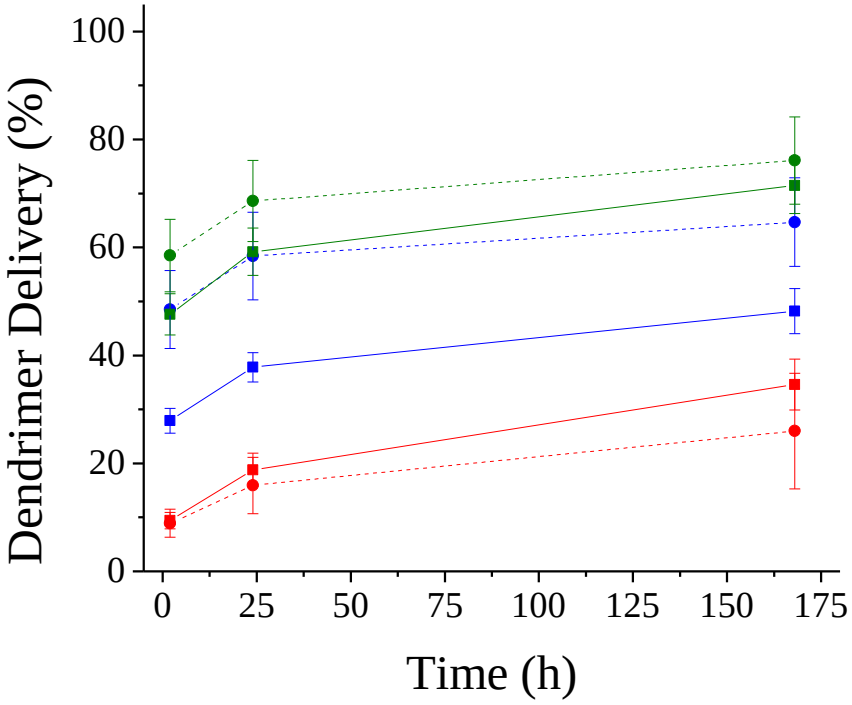

Figure 5.4 Dendrimer delivery (%) for control (solid line) and NO-releasing (dashed line) G4 octyl-doped electrospun Tecoplast (red), Tecoflex (blue), and Hydrothane (green) fibers after 2 h, 1 d, or 7 d soaking in PBS (pH 7.4, 37 °C). For all measurements, $n \geq 3$ pooled experiments with error bars representing standard deviation of the mean.

addition of control and NO-releasing dendrimer dopant decreased the average fiber diameter from blank Tecoflex fibers (~930 nm), changes in the dendrimer exterior modification had little effect on the resulting fiber diameters, with average diameters ranging from 600–800 nm (Table 5.4).

To evaluate the potential of these fibers to allow for gas and fluid exchange,[4] the porosity and water absorption of the electrospun Tecoflex fibers were evaluated as a function of dendrimer modification. As expected due to the similarity of the exterior modifications, the porosity of the fibrous mats containing alkyl chain-modified dendrimers (i.e., G4 hexyl, G4 octyl, G4 dodecyl) were unchanged from blank fibers (Table 5.4). The QA-containing Tecoflex fibers exhibited the greatest porosities (62 and 68% for control and NO-releasing, respectively), possibly due to electrostatic repulsions from the QA moiety limiting fiber interactions. For all modifications, the water absorption levels were less for the dendrimer-doped versus blank Tecoflex fibers, with almost all of the control and NO-releasing fibers exhibiting less than 100% water absorption (Table 5.4). Although control and NO-releasing G4 octyl-doped Tecoflex fibers exhibited >90% water absorption values, water uptake by the other modifications (i.e., hexyl, dodecyl, octylQA) was less (55–77%). This result was somewhat unexpected due to the similarity in fiber diameters and porosities and identical polyurethane composition (Tecoflex).

Nitric oxide release from electrospun polyurethane fibers (surface area: 1.267 cm^2) was evaluated as described above (Figure 5.2 C-F). The magnitude of the initial NO burst ($[NO]_{max}$) decreased with increasing alkyl chain length (20 to 9 $pmol/cm^2$) (Table 5.5). Similarly, the time required to reach the maximum flux increased with alkyl chain length (3.8 to 13.8 min), suggesting the hydrophobicity of the dendrimer exterior influences initial water diffusion to the NO donor within the electrospun fibers. Yet, all of the alkyl chain-doped Tecoflex fibers exhibited similar

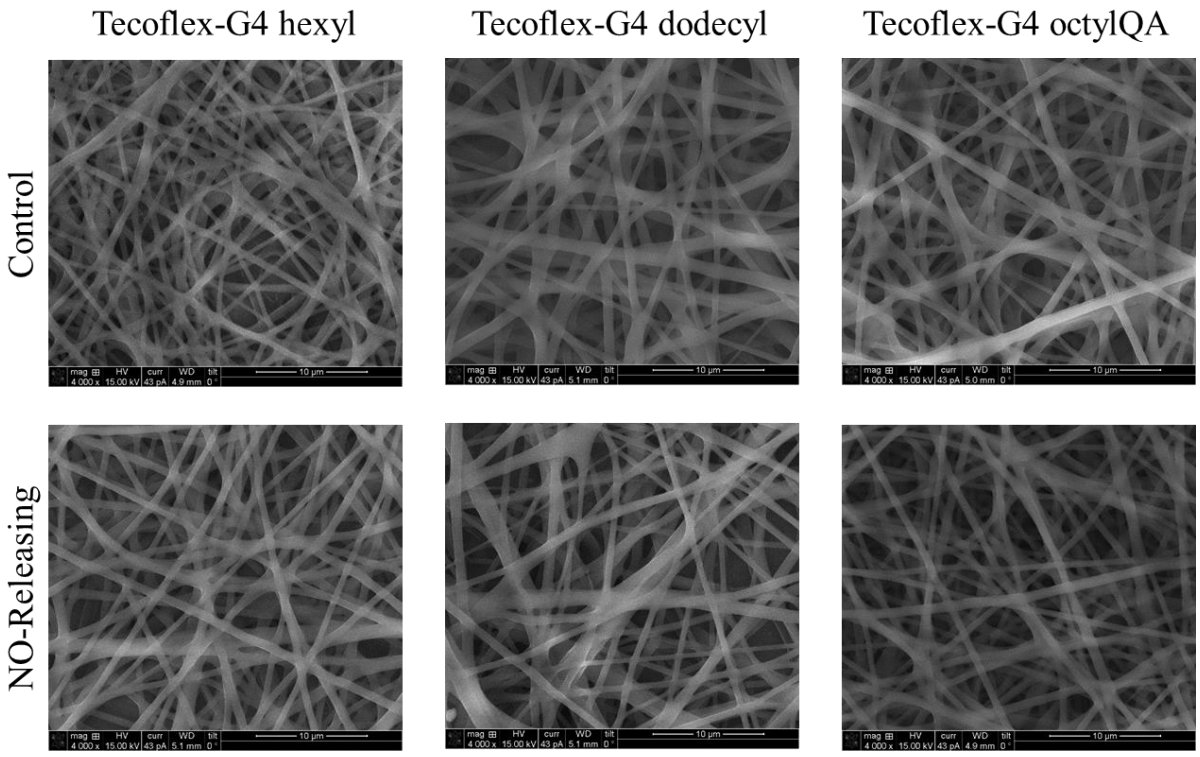

Figure 5.5 Scanning electron micrographs of control and NO-releasing G4 hexyl-, G4 dodecyl-, and G4 octylQA-doped electrospun Tecoflex fibers.

Table 5.4 Characterization of electrospun Tecoflex fibers.[a]

	Fiber Diameter (nm)	Porosity (%)	Water Absorption (%)
Tecoflex	927 ± 310	50.4 ± 7.6	116 ± 37
Tecoflex-G4 hexyl	617 ± 187	57.0 ± 8.7	64 ± 21
Tecoflex-G4 hexyl/NO	649 ± 202	52.2 ± 8.8	66 ± 27
Tecoflex-G4 octyl	771 ± 247	54.6 ± 5.6	112 ± 35
Tecoflex-G4 octyl/NO	798 ± 266	49.4 ± 13.7	89 ± 29
Tecoflex-G4 dodecyl	691 ± 249	60.9 ± 8.2	77 ± 19
Tecoflex-G4 dodecyl/NO	564 ± 183	53.1 ± 13.3	73 ± 32
Tecoflex-G4 octylQA	595 ± 194	62.3 ± 10.1	55 ± 16
Tecoflex-G4 octylQA/NO	646 ± 202	67.6 ± 13.5	59 ± 18

[a]For all measurements, $n \geq 3$ pooled experiments.

NO-release half-lives (30–40 min), totals (~0.038 μmol/mg), and durations (~2.5 h) regardless of alkyl chain modification. In contrast, the QA-containing Tecoflex fibers exhibited a lower max flux (4.8 pmol/cm^2) with extended NO-release half-life (151 min) and duration (6 h) (Figure 5.2). The longer NO release exhibited by G4 octylQA-containing fibers parallels the extended release of the QA dendrimers over the alkyl-modification systems in solution, suggesting the NO-release kinetics of the NO donor dopant may have greater influence over the NO-release characteristics of the electrospun fibers than the polyurethane identity. While all of the dendrimer modifications incorporated similar amounts of dendrimer (60–70 μg/mg), the overall NO-release totals for Tecoflex-G4 octylQA/NO fibers were slightly lower than the alkyl chain modifications (0.027 μmol/mg). This behavior is most likely the result of unaccounted for NO release below the threshold (1 pmol/cm^2) due to the extended release kinetics of these fibers at pH 7.4. Of note, the 1.267 cm^2 fiber mats exhibited similar NO-release totals (~0.36 μmol/cm^2).

Dendrimer delivery into solution was determined in PBS (pH 7.4, 37 °C) at 2 h, 1 d, and 7 d as a function of dendrimer modification. The majority of dendrimer release occurred within the first 24 h (Figure 5.6). As expected, the most hydrophobic dendrimer (G4 dodecyl) was better retained within the fibers, with control Tecoflex-G4 dodecyl fibers exhibiting only 38% dendrimer release after 7 d compared to ~48% for the other dendrimer systems. Similar to observations in Section 5.3.2, the NO-releasing fibers demonstrated greater dendrimer release than their non-NO-releasing counterparts due to increased instability of the zwitterionic *N*-diazeniumdiolate within the fibers. Of note, the Tecoflex-G4 octylQA/NO fibers exhibited the greatest levels of dendrimer delivery after 7 d (~80%), supporting the hypothesis that increased scaffold charged leads to faster and greater dendrimer release from electrospun fibers.

Table 5.5 Nitric oxide-release properties for NO-releasing electrospun Tecoflex fibers in PBS (pH 7.4, 37 °C).[a]

	$[NO]_{max}$[b] (pmol/cm^2)	t_{max}[c] (min)	t[NO][d] (μmol/cm^2)	$t[NO]_{2h}$[e] (μmol/cm^2)	t[NO][f] (μmol/mg)	$t_{1/2}$[g] (min)	t_d[h] (h)	t[dopant][i] (μg/mg)
G4 hexyl/NO	19.8 ± 6.8	3.8 ± 1.7	0.043 ± 0.014	0.039 ± 0.013	0.038 ± 0.007	30.5 ± 4.4	2.9 ± 0.4	68 ± 1
G4 octyl/NO	11.7 ± 3.6	4.3 ± 2.1	0.036 ± 0.011	0.034 ± 0.010	0.037 ± 0.008	36.5 ± 4.3	2.3 ± 0.4	61 ± 8
G4 dodecyl/NO	8.9 ± 2.4	13.8 ± 3.5	0.032 ± 0.010	0.030 ± 0.007	0.039 ± 0.004	38.3 ± 5.1	2.5 ± 0.4	65 ± 8
G4 octylQA/NO	4.8 ± 1.1	2.3 ± 0.3	0.034 ± 0.010	0.014 ± 0.004	0.027 ± 0.005	151.0 ± 22.1	6.0 ± 0.9	72 ± 4

[a]For all measurements, $n \geq 3$ pooled experiments. [b]Maximum flux of NO release. [c]Time required to reach maximum flux. [d]Total NO payload released per surface area. [e]NO payload released after 2 h. [f]Total NO payload released per mg. [g]NO release half-life. [h]Duration of NO release. [i]Total amount of dendrimer incorporated as determined by total NO release in 50 mM HCl.

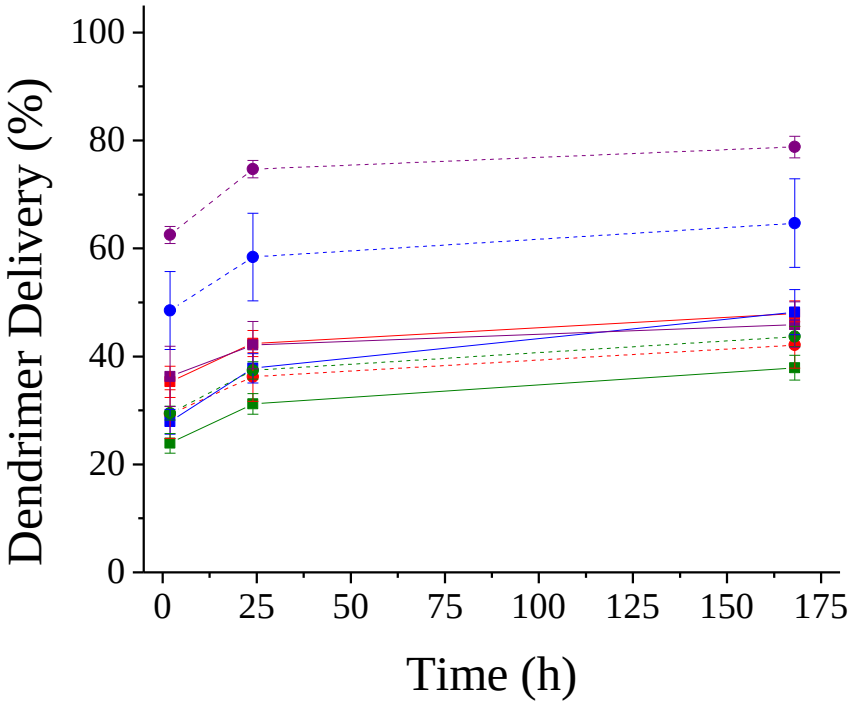

Figure 5.6 Dendrimer delivery (%) for control (solid line) and NO-releasing (dashed line) G4 hexyl- (red), G4 octyl- (blue), G4 dodecyl- (green), and G4 octylQA- (purple) doped electrospun Tecoflex fibers after 2 h, 1 d, or 7 d soaking in PBS (pH 7.4, 37 °C). For all measurements, $n \geq 3$ pooled experiments with error bars representing standard deviation of the mean.

5.3.4 In vitro cytotoxicity and cell proliferation

The toxicity of blank, control, and NO-releasing electrospun polyurethane fibers was evaluated against L929 mouse fibroblast cells over 2 and 24 h. Each of the G4 octyl-doped polyurethane fibers were non-toxic at both timepoints (>80% cell viability compared to untreated controls), with variations in toxicity dependent on polyurethane identity (Figure 5.7 A-B). Blank, control, and NO-releasing Tecoflex fibers exhibited no toxicity (~100% viability) regardless of dendrimer dopant or NO release (Figure 5.7 C-D). Control Tecoplast fibers were slightly more toxic at 24 than 2 h (96 and 88% viability, respectively), while NO-releasing Tecoplast fibers exhibited similar toxicity (~95% viability) at both timepoints. Electrospun Hydrothane fibers were characterized as having the highest toxicity, with control and NO-releasing fibers reducing cell viability to 87 and 81%, respectively, after 2 h exposure. This may be attributed to the slightly higher dendrimer release exhibited by the Hydrothane fibers. However, the lack of toxicity exhibited by control and NO-releasing Tecoflex fibers despite relatively similar concentrations of dendrimer delivery makes this unlikely. Alternatively, the greater toxicity of the G4 octyl-doped Hydrothane fibers is likely due to the bulk characteristics of the fiber mat itself leading to fiber-cell interactions and cell removal (from the well) upon removal of the fiber mat.

The ability of L929 cells to proliferate on dendrimer-doped electrospun Tecoflex fibers was next evaluated upon direct cell seeding onto the fibrous mats. While some prior studies have correlated the ability of cells to integrate into and proliferate on electrospun fibrous mats with wound healing capabilities,[7, 32] Lalani et al. reported that a lack of cell adhesion on the fibers is more beneficial for use as removable wound dressings.[10] Decreased cell adhesion on the wound dressings would allow for easier, painless dressing removal without harming the newly formed skin underneath.[10] Along these lines, the ability of L929 cells to adhere to blank, control, and NO-

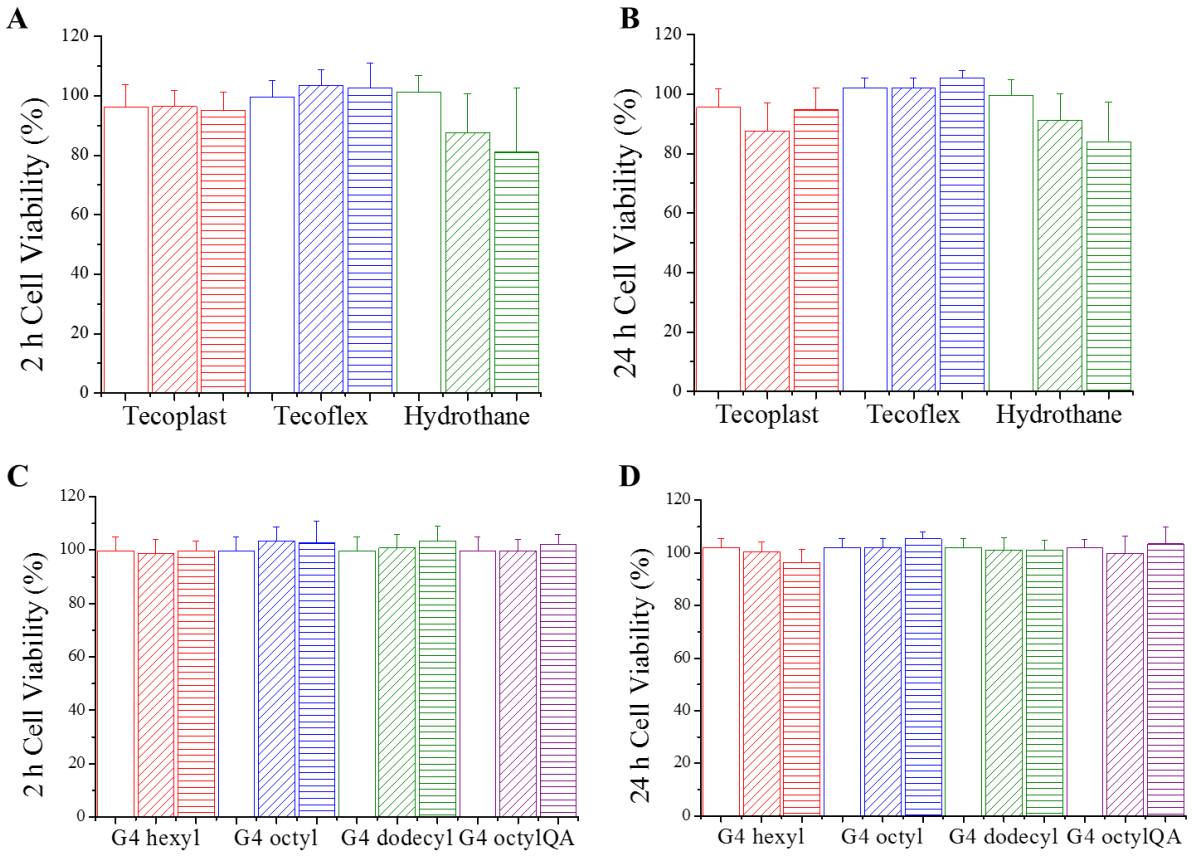

Figure 5.7 Viability (%) of L929 mouse fibroblast cells following (A,C) 2 h or (B,D) 24 h exposure to blank (solid), control (diagonal lines), and NO-releasing (horizontal lines) (A,B) G4 octyl-doped electrospun fibers or (C,D) dendrimer-doped electrospun Tecoflex fibers. For all measurements, n $\geq$ 3 pooled experiments with error bars representing standard deviation of the mean.

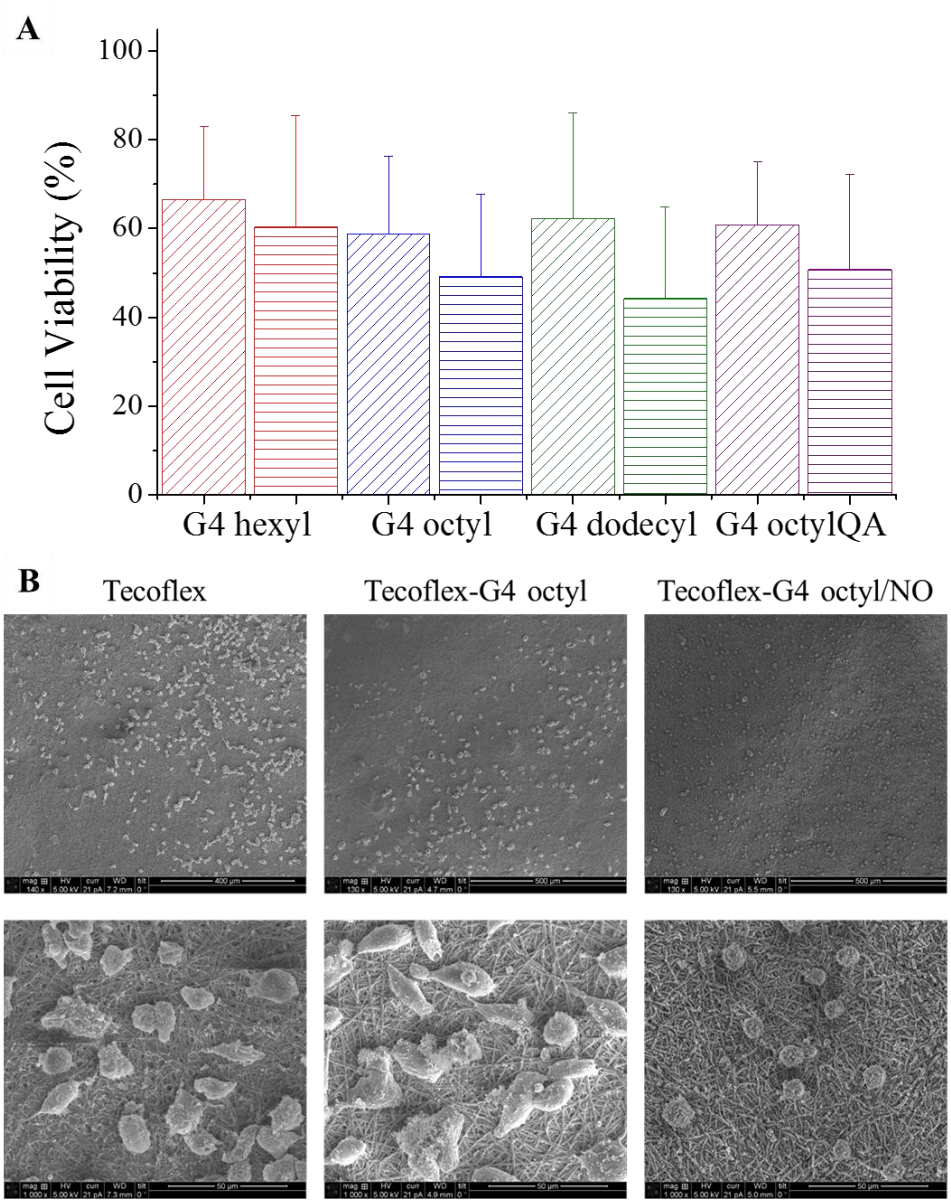

Figure 5.8 (A) Viability (%) of L929 mouse fibroblast cells adhered to control (diagonal lines) and NO-releasing (horizontal lines) dendrimer-doped Tecoflex electrospun fibers following 24 h exposure. For all measurements, $n \geq 3$ pooled experiments with error bars representing standard deviation of the mean. (B) Scanning electron micrographs of L929 mouse fibroblast cells adhered to blank, control, and NO-releasing G4 octyl-doped Tecoflex electrospun fibers following 24 h exposure.

releasing electrospun Tecoflex fibers was evaluated with the idea that decreased adhesion would indicate greater potential for wound dressing compatibility.

To assess any reductions in cell adhesion, the number of viable L929 cells adhered to blank Tecoflex fibers after 24 h (~10% of the total cells in the well) was normalized to 100%. The percent viability of cells adhered to control and NO-releasing Tecoflex fibers was determined in relation to the blank fibers (Figure 5.8 A). For each of the dendrimer dopants, control Tecoflex fibers exhibited a statistically significant decrease in adhered cell viability (~60% compared to blank fibers). With the exception of Tecoflex-G4 hexyl/NO fibers, the remaining NO-releasing Tecoflex fibers further decreased cell viability (~50% compared to blank fibers). While statistically significant from the blank Tecoflex fibers ($p < 0.05$ using two-tailed student's t-test), this behavior was not significant from control fibers. The lack of toxicity exhibited by the leached dendrimer, NO dose, and electrospun fibers to L929 cells above (Figure 5.7) indicates that these decreases in cell viability are most likely attributed to reduced cell adhesion and not cell death. To confirm this, L929 cells were fixed with glutaraldehyde after 24 h exposure and imaged via scanning electron microscopy. For both the control and NO-releasing G4 octyl-doped Tecoflex fibers, L929 cells appear to be less densely adhered to the electrospun fibers than for the blank fibers (Figure 5.8 B). Of note, the L929 fibroblast cells in contact with NO-releasing fibers exhibited a morphology distinct from those adhered to blank or control fibrous mats. This spherical morphology is often indicative of non-adhered cells, as opposed to spread-out, spindle shaped cells (as those adhered to the control fibers).[33] While both control and NO-releasing Tecoflex fibers reduced L929 cell adhesion compared to blank fibers, cells in contact with NO-releasing fibrous mats exhibited the morphology of non-adhered cells, indicating the benefits of NO release in further reducing cell adhesion and integration into electrospun fiber mats.

5.3.5 Antibacterial action of NO-releasing single-component electrospun fibers

P. aeruginosa and *S. aureus* represent two of the most commonly isolated species in chronic wounds.[2] Antibacterial action of single-component NO-releasing fibers was thus carried out to further assess the potential of these materials as wound dressings. Electrospun fibers were cut into coupons to yield fiber samples with similar surface area (1.267 cm^2) and NO payloads. Bacterial adhesion studies were performed in simulated wound fluid (SWF) composed of 25% fetal bovine serum in PBS (pH 7.4, 37 °C) for 2 or 6 h, corresponding to the duration of NO release for the Tecoflex-G4 octyl/NO and Tecoflex-G4 octylQA/NO fibers, respectively. Log reductions in bacterial viability were determined by comparing the bacterial viability on control or NO-release fibers to that on blank Tecoflex fibers.

Both control and NO-releasing electrospun Tecoflex fibers were found to reduce the viability of adhered *P. aeruginosa* and *S. aureus* compared to blank Tecoflex fibers after 2 and 6 h exposures (Figure 5.9). After 2 h exposure, the control G4 octyl-doped Tecoflex fibers proved more effective at reducing bacterial adhesion (both strains) than their NO-releasing counterparts, (Table 5.6). In contrast, both control and NO-releasing Tecoflex-G4 octyl fibers exhibited similar reductions in adhered bacterial viability at 6 h, likely due to the inability of the dendrimers to eradicate the larger concentrations of bacteria resulting from bacterial growth. Similar trends were observed for the G4 octylQA-doped Tecoflex fibers, with control fibers exhibiting greater reductions in adhered bacterial viability after 2 h exposure but similar reductions at 6 h as the NO-releasing fibers against both bacterial strains. As a result of the negligible killing by both control and NO-releasing Tecoflex fibers (≤1-log reduction), the evaluation of single-component electrospun fibers was abandoned. The fabrication of composite electrospun polyurethane fibers

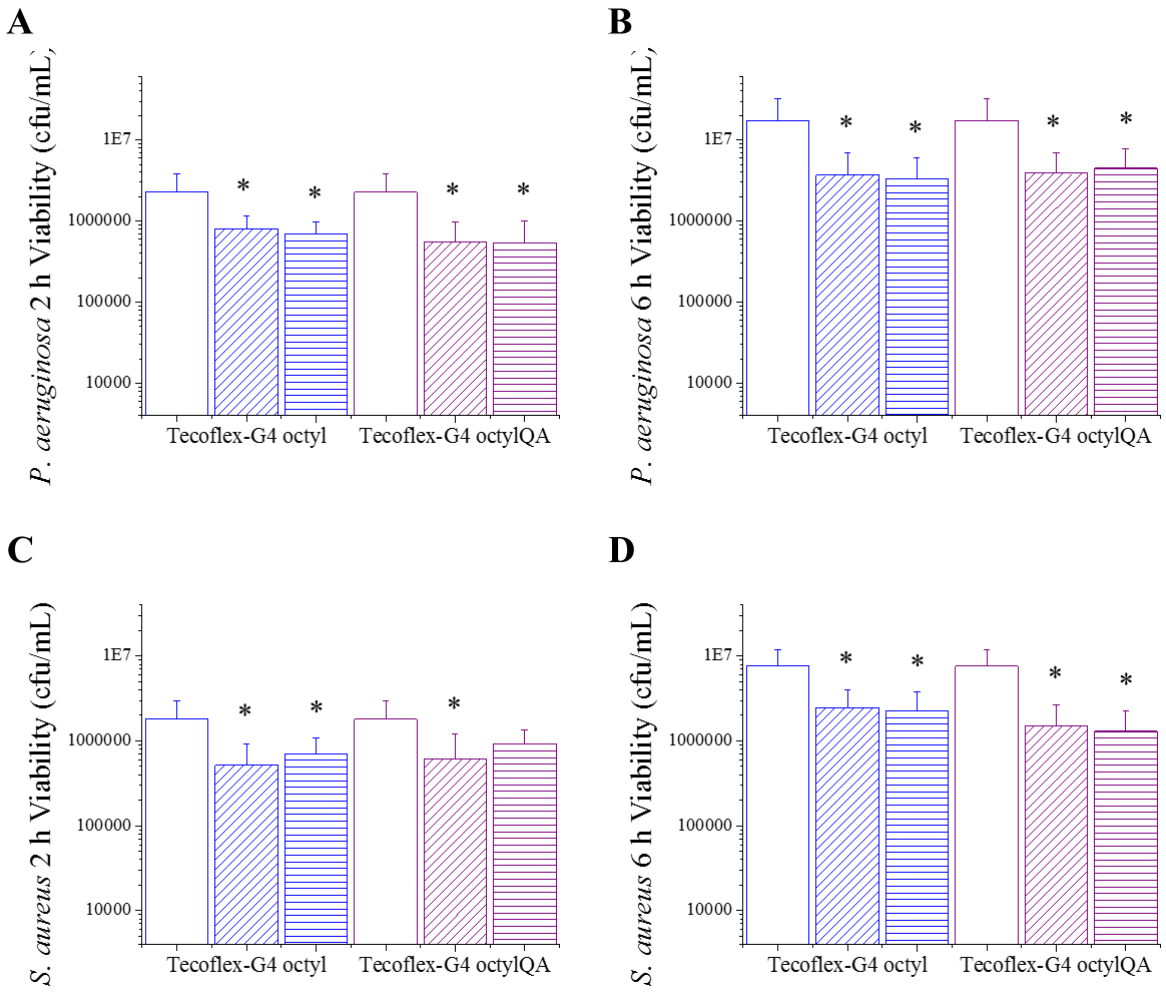

Figure 5.9 Viability of (A,B) *P. aeruginosa* or (C,D) *S. aureus* adhered to blank (solid), control (diagonal lines), and NO-releasing (horizontal lines) dendrimer-doped Tecoflex electrospun fibers following 2 or 6 h exposure. For all measurements, $n \geq 3$ pooled experiments with error bars representing standard deviation of the mean. Asterisk indicates significant differences from blank ($p < 0.05$) using two-tailed student's t-test.

Table 5.6 Average log reduction of adhered bacterial viability.[a]

	P. aeruginosa		*S. aureus*	
	2 h	6 h	2 h	6 h
Tecoflex-G4 octyl	0.9 ± 0.6	0.8 ± 0.4	1.0 ± 0.6	0.6 ± 0.3
Tecoflex-G4 octyl/NO	0.5 ± 0.2	0.9 ± 0.5	0.5 ± 0.2	0.6 ± 0.3
Tecoflex-G4 octylQA	1.2 ± 0.5	0.8 ± 0.3	1.1 ± 0.9	0.9 ± 0.5
Tecoflex-G4 octylQA/NO	0.9 ± 0.8	0.7 ± 0.4	0.4 ± 0.3	0.9 ± 0.3

[a]For all measurements, $n \geq 3$ pooled experiments.

formed using a co-axial electrospinning setup was thus investigated (Chapter 6), as the distinct core-sheath structure of these fibers should allow for greater dendrimer incorporation and control over both dendrimer- and NO-release characteristics.

5.4 Conclusions

Three distinct polyurethanes were electrospun into single-component fibers doped with control or NO-releasing G4 octyl dendrimers. While the fiber diameter, porosity, water absorption, and dendrimer incorporation were dependent on the polyurethane identity, NO-release proved independent of polyurethane hydrophobicity. Electrospun Tecoflex fibers prepared using dendrimer dopants with a range of exterior modifications exhibited tunable NO-release kinetics and durations, indicating the dendrimer modification greatly influences the NO-release properites. Both control and NO-releasing dendrimer-doped electrospun Tecoflex fibers exhibited decreased L929 cell adhesion from blank Tecoflex fibers, with the fibroblasts exposed to NO-releasing fibers demonstrating non-adhesive morphologies. However, the low antibacterial action of the NO-releasing Tecoflex fibers against planktonic bacteria required a new direction for the development of electrospun fibers to allow for enhanced dendrimer storage, NO release, and bactericidal action.

REFERENCES

(1) James, G. A., Swogger, E., Wolcott, R., Secor, P., Sestrich, J., Costerton, J. W., and Stewart, P. S. "Biofilms in chronic wounds" *Wound Repair and Regeneration* **2008**, *16*, 37-44.

(2) Bjarnsholt, T., Kirketerp-Møller, K., Jensen, P. Ø., Madsen, K. G., Phipps, R., Krogfelt, K., Høiby, N., and Givskov, M. "Why chronic wounds will not heal: A novel hypothesis" *Wound Repair and Regeneration* **2008**, *16*, 2-10.

(3) Blakytny, R., and Jude, E. "The molecular biology of chronic wounds and delayed healing in diabetes" *Diabetic Medicine* **2006**, *23*, 594-608.

(4) Zahedi, P., Rezaeian, I., Ranaei-Siadat, S. O., Jafari, S. H., and Supaphol, P. "A review on wound dressings with an emphasis on electrospun nanofibrous polymeric bandages" *Polymers for Advanced Technologies* **2010**, *21*, 77-95.

(5) Khil, M. S., Cha, D. I., Kim, H. Y., Kim, I. S., and Bhattarai, N. "Electrospun nanofibrous polyurethane membrane as wound dressing" *Journal of Biomedical Materials Research Part B: Applied Biomaterials* **2003**, *67*, 675-679.

(6) Jannesari, M., Varshosaz, J., Morshed, M., and Zamani, M. "Composite poly (vinyl alcohol)/poly (vinyl acetate) electrospun nanofibrous mats as a novel wound dressing matrix for controlled release of drugs" *International Journal of Nanomedicine* **2011**, *6*, 993-1003.

(7) Unnithan, A. R., Barakat, N. A., Pichiah, P. T., Gnanasekaran, G., Nirmala, R., Cha, Y.-S., Jung, C.-H., El-Newehy, M., and Kim, H. Y. "Wound-dressing materials with antibacterial activity from electrospun polyurethane–dextran nanofiber mats containing ciprofloxacin HCl" *Carbohydrate Polymers* **2012**, *90*, 1786-1793.

(8) Thakur, R., Florek, C., Kohn, J., and Michniak, B. "Electrospun nanofibrous polymeric scaffold with targeted drug release profiles for potential application as wound dressing" *International Journal of Pharmaceutics* **2008**, *364*, 87-93.

(9) Dongargaonkar, A. A., Bowlin, G. L., and Yang, H. "Electrospun blends of gelatin and gelatin–dendrimer conjugates as a wound-dressing and drug-delivery platform" *Biomacromolecules* **2013**, *14*, 4038-4045.

(10) Lalani, R., and Liu, L. "Electrospun zwitterionic poly (sulfobetaine methacrylate) for nonadherent, superabsorbent, and antimicrobial wound dressing applications" *Biomacromolecules* **2012**, *13*, 1853-1863.

(11) Hetrick, E. M., Shin, J. H., Stasko, N. A., Johnson, C. B., Wespe, D. A., Holmuhamedov, E., and Schoenfisch, M. H. "Bactericidal efficacy of nitric oxide-releasing silica nanoparticles" *ACS Nano* **2008**, *2*, 235-246.

(12) Schäffer, M. R., Tantry, U., Gross, S. S., Wasserkrug, H. L., and Barbul, A. "Nitric oxide regulates wound healing" *Journal of Surgical Research* **1996**, *63*, 237-240.

(13) Shekhter, A. B., Serezhenkov, V. A., Rudenko, T. G., Pekshev, A. V., and Vanin, A. F. "Beneficial effect of gaseous nitric oxide on the healing of skin wounds" *Nitric Oxide* **2005**, *12*, 210-219.

(14) Weller, R., and Finnen, M. J. "The effects of topical treatment with acidified nitrite on wound healing in normal and diabetic mice" *Nitric Oxide* **2006**, *15*, 395-399.

(15) Liu, H. A., and Balkus Jr, K. J. "Novel delivery system for the bioregulatory agent nitric oxide" *Chemistry of Materials* **2009**, *21*, 5032-5041.

(16) Lowe, A., Deng, W., Smith Jr, D. W., and Balkus Jr, K. J. "Acrylonitrile-based nitric oxide releasing melt-spun fibers for enhanced wound healing" *Macromolecules* **2012**, *45*, 5894-5900.

(17) Wold, K. A., Damodaran, V. B., Suazo, L. A., Bowen, R. A., and Reynolds, M. M. "Fabrication of biodegradable polymeric nanofibers with covalently attached NO donors" *ACS Applied Materials & Interfaces* **2012**, *4*, 3022-3030.

(18) Vogt, C., Xing, Q., He, W., Li, B., Frost, M. C., and Zhao, F. "Fabrication and characterization of a nitric oxide-releasing nanofibrous gelatin matrix" *Biomacromolecules* **2013**, *14*, 2521-2530.

(19) Koh, A., Carpenter, A. W., Slomberg, D. L., and Schoenfisch, M. H. "Nitric oxide-releasing silica nanoparticle-doped polyurethane electrospun fibers" *ACS Applied Materials & Interfaces* **2013**, *5*, 7956-7964.

(20) Lu, Y., Slomberg, D. L., Shah, A., and Schoenfisch, M. H. "Nitric oxide-releasing amphiphilic poly (amidoamine)(PAMAM) dendrimers as antibacterial agents" *Biomacromolecules* **2013**, *14*, 3589-3598.

(21) Sun, B., Slomberg, D. L., Chudasama, S. L., Lu, Y., and Schoenfisch, M. H. "Nitric oxide-releasing dendrimers as antibacterial agents" *Biomacromolecules* **2012**, *13*, 3343-3354.

(22) Worley, B. V., Schilly, K. M., and Schoenfisch, M. H. "Anti-biofilm efficacy of dual-action nitric oxide-releasing alkyl chain modified poly(amidoamine) dendrimers" *Molecular Pharmaceutics* **2015**, *12*, 1573-1583.

(23) Worley, B. V., Slomberg, D. L., and Schoenfisch, M. H. "Nitric oxide-releasing quaternary ammonium-modified poly(amidoamine) dendrimers as dual action antibacterial agents" *Bioconjugate Chemistry* **2014**, *25*, 918-927.

(24) Tomalia, D., Baker, H., Dewald, J., Hall, M., Kallos, G., Martin, S., Roeck, J., Ryder, J., and Smith, P. "A new class of polymers: Starburst-dendritic macromolecules" *Polymer Journal* **1985**, *17*, 117-132.

(25) Tomalia, D. A. "Birth of a new macromolecular architecture: Dendrimers as quantized building blocks for nanoscale synthetic polymer chemistry" *Progress in Polymer Science* **2005**, *30*, 294-324.

(26) Carpenter, A. W., Worley, B. V., Slomberg, D. L., and Schoenfisch, M. H. "Dual action antimicrobials: Nitric oxide release from quaternary ammonium-functionalized silica nanoparticles" *Biomacromolecules* **2012**, *13*, 3334-3342.

(27) Koh, A., Lu, Y., and Schoenfisch, M. H. "Fabrication of nitric oxide-releasing porous polyurethane membranes-coated needle-type implantable glucose biosensors" *Analytical Chemistry* **2013**, *85*, 10488-10494.

(28) Pham, Q. P., Sharma, U., and Mikos, A. G. "Electrospun poly (ε-caprolactone) microfiber and multilayer nanofiber/microfiber scaffolds: Characterization of scaffolds and measurement of cellular infiltration" *Biomacromolecules* **2006**, *7*, 2796-2805.

(29) Savoji, H., Rana, D., Matsuura, T., Tabe, S., and Feng, C. "Development of plasma and/or chemically induced graft co-polymerized electrospun poly (vinylidene fluoride) membranes for solute separation" *Separation and Purification Technology* **2013**, *108*, 196-204.

(30) Coneski, P. N., Nash, J. A., and Schoenfisch, M. H. "Nitric oxide-releasing electrospun polymer microfibers" *ACS Applied Materials & Interfaces* **2011**, *3*, 426-432.

(31) Storm, W. L. "Combined bactericidal/bacterial adhesion-resistant coating through nitric oxide release" *Department of Chemistry*, University of North Carolina-Chapel Hill **2013**.

(32) Yari, A., Yeganeh, H., and Bakhshi, H. "Synthesis and evaluation of novel absorptive and antibacterial polyurethane membranes as wound dressing" *Journal of Materials Science: Materials in Medicine* **2012**, *23*, 2187-2202.

(33) Shinmoto, H., Sato, K., and Dosako, S. "Inhibition by bovine lactoferrin of adhesion of L929 cells cultured in serum-free git medium" *Bioscience, Biotechnology, and Biochemistry* **1992**, *56*, 965-966.

CHAPTER 6:

Active Release of Dual-Action Dendrimers from Co-Axial Electrospun Polyurethane Fibers

6.1 Introduction

The successful treatment of chronic wounds such as diabetic foot ulcers, pressure ulcers, and venous leg ulcers is often hindered by the inefficient eradication of opportunistic pathogens such as *Pseudomonas aeruginosa* and *Staphyloccocus aureus*.[1-3] Left untreated, the proliferation of infectious bacteria and biofilms in chronic wounds often leads to significant morbidity (e.g., limb amputation).[3] While the use of wound dressings may facilitate some wound healing, the presence of bacteria hinders complete wound closure. An ideal wound dressing wound provide facile gaseous and fluid exchange, absorb excess wound exudates, and act as a physical barrier to infectious microorganisms, while also reducing the bacterial burden in the wound site.[4]

Polyurethane materials are often used as wound dressings because they exhibit adequate barrier properties, oxygen permeability, and tissue compatibility.[5-8] Commercially-available wound dressings such as semi-permeable polyurethane films and foams have demonstrated utility as physical barriers, inhibiting the migration of bacteria to the wound and promoting wound closure.[4, 9, 10] Incorporating silver ions into these polyurethane wound dressings as an active release antimicrobial agent further improved wound healing and reduced pain-related symptoms.[11-13] However, significant accumulation of wound fluid beneath the bandage continues to be a disadvantage of these dressings, requiring frequent wound aspiration to prevent leakage and infection.[5, 14, 15] The fabrication of porous wound dressing materials via electrospinning has been proposed to further improve the wound healing capabilities of polyurethane wound dressings. The

electrospinning technique, consisting of the application of a high potential difference between the head of a syringe needle containing a polymer solution and a grounded collector, produces nonwoven nanofibrous polymer webs.[4, 16, 17] These mats demonstrate properties essential for wound healing due to their inherent porosity and large effective surface area. Indeed, the high surface area to volume ratio allows for increased water absorption, while the semi-permeability and porous architecture of such materials allows for cell respiration and protects the wound from bacterial infection.[4] Khil et al. reported improved wound healing capabilities of electrospun polyurethane fibers in adult male guinea pigs over the conventional Tegaderm (3M Health Care; St. Paul, Minnesota), a commercially-available polyurethane wound dressing.[5] The electrospun dressings both increased the rate of epithelialization and prevented the permeation of infectious microorganisms with little observed fluid accumulation.

Electrospun fibers have also been modified to exhibit antibacterial action via the incorporation of therapeutic compounds blended into an all-in-one dressing.[4, 18, 19] Initial studies in the development of antibacterial electrospun wound dressings have demonstrated the controlled release of antibiotics[18-20] and silver ions[21, 22] from electrospun fibers. However, bacterial resistance to both antibiotics and silver[23-25] warrants the development of dressings capable of delivering next generation antibacterial agents that are unlikely to foster resistance.

Nitric oxide (NO) is a promising antibacterial agent that exhibits both broad-spectrum antibacterial and wound-healing actions.[26-28] Our lab has pioneered the development of antibacterial macromolecular scaffolds capable of controllable NO storage and release,[29, 30] with dendrimers representing an excellent scaffold for the design of novel antibacterial agents.[31-33] Combining antibacterial NO release with a non-depleting, contact-based biocide (i.e., quaternary ammonium moieties or alkyl chains) has proven especially effective at producing broad-spectrum

dual-action antibacterial agents.[34-37] The co-administration of two mechanistically different biocides in this manner is expected to reduce the emergence of bacterial resistance and improve the bactericidal efficacy of the scaffold, thereby lowering the required therapeutic dose.[38, 39] We have previously reported on the ability of NO-releasing alkyl chain-modified dendrimers to eradicate both Gram-negative and Gram-positive biofilms as a function of dendrimer generation (i.e., size) and modification.[35, 36] Herein, we report both the fabrication of electrospun composite polyurethane fibers doped with NO-releasing alkyl chain- or quaternary ammonium (QA)-modified poly(amidoamine) dendrimers and evaluation of the antibacterial action of the resulting dendrimer- and NO-releasing fibers against both Gram-negative and Gram-positive bacteria. Our study investigated the promise of dual-action dendrimer biocide release from electrospun polyurethane fibers as potential antibacterial wound dressings.

6.2 Materials and Methods

Triethylamine (TEA), rhodamine B isothiocyanate (RITC), dimethyloctylamine, epichlorohydrin, phenazine methosulfate (PMS), fetal bovine serum (FBS), trypsin, 3-(4,5-dimethylthiazol-2-yl)-5-(3-carboxymethoxyphenyl)-2-(4-sulfophenyl)-2H-tetrazolium inner salt (MTS), penicillin streptomycin (PS), and propidium iodide (PI) were purchased from Sigma-Aldrich (St. Louis, MO). Methyl acrylate, 1,2-epoxyoctane, and ethylenediamine (EDA) were purchased from the Aldrich Chemical Company (Milwaukee, WI). Sodium methoxide (5.4 M solution in methanol) was purchased from Acros Organics (Geel, Belgium). Colloidal silica in methanol was obtained from Nissan Chemical America Corporation (Houston, TX). Cellulose ester dialysis membranes (500-1000 MWCO) were purchased from Spectrum Laboratories, Inc. (Rancho Dominguez, CA). Tecophilic (HP-93A-100) and Tecoflex (SG-80A) polyurethanes were obtained from Thermedics (Woburn, MA). Tecoplast (TP-470) polyurethane was a gift from Lubrizol (Cleveland, OH).

Dulbecco's modified Eagle's medium (DMEM) and Dulbecco's phosphate buffered saline (PBS) were obtained from Lonza Group (Basel, Switzerland). 4,5-Diaminofluorescein diacetate (DAF-2 DA) was purchased from Calbiochem (San Diego, CA). Tryptic soy broth (TSB), tryptic soy agar (TSA), Luria-Bertani (LB) broth, LB, and Mueller Hinton agar were obtained from Becton, Dickinson and Company (Franklin Lakes, NJ). *Pseudomonas aeruginosa* (*P. aeruginosa*; ATCC #19143), *Eschericia coli* (*E. coli*; ATCC #35150), *Staphylococcus aureus* (*S. aureus*; ATCC #29213), and methicillin-resistant *Staphylococcus aureus* (MRSA; ATCC #33591) were obtained from American Type Tissue Culture Collection (Manassas, VA). L929 mouse fibroblasts were obtained from the UNC Tissue Culture Facility (Chapel Hill, NC). Nitrogen (N_2), argon (Ar), carbon dioxide (CO_2), and nitric oxide (NO) calibration (25.87 PPM, balance N_2) gases were purchased from National Welders (Raleigh, NC). Pure nitric oxide (NO) gas (99.5%) was purchased from Praxair (Sanford, NC). Common laboratory salts and solvents were purchased from Fisher Scientific (Fair Lawn, NJ). Distilled water was purified using a Millipore Milli-Q UV Gradient A-10 system (Bedford, MA), resulting in a total organic content of ≤6 ppb and a final resistivity of 18.2 mΩ·cm. Unless noted otherwise, all materials were analytical-reagent grade and used as received without further purification.

6.2.1 Synthesis of QA- and alkyl chain-modified PAMAM dendrimers

Poly(amidoamine) **(**PAMAM) scaffolds were synthesized as described previously,[35, 40, 41] by repeated alkylation/amidation steps using methyl acrylate and EDA from an EDA core. G4 PAMAM dendrimers were then modified with either octyl or octylQA moieties. To form octyl-modified dendrimers,[36] G4 PAMAM (100.0 mg) was dissolved in 5 mL methanol, and one equivalent of triethylamine (with respect to the molar amount of primary amines) and one molar equivalent of epoxyoctane were then added to the vial. This solution was stirred at room

temperature for 3 d. After reaction completion, excess epoxide was removed in vacuo. To ensure removal of any unreacted epoxide, dendrimers were re-dissolved in 5 mL methanol and kept under vacuum overnight. Complete removal of the epoxide was verified via ^{1}H NMR spectroscopy (Bruker 400 MHz spectrometer; Billerica, MA).

To form octyl QA-modified dendrimers, quaternary ammonium epoxides (octylQA-epoxide) were first synthesized as described previously.[34, 37] Briefly, 0.04 mmol epichlorohydrin was reacted with 0.01 mmol *N*,*N*-dimethyloctylamine at room temperature overnight (~18 h). The mixture was then added dropwise to cold ether while sonicating, and the solid/viscous liquid octylQA-epoxide was collected via centrifugation (810×*g*, 5 min). The supernatant was decanted, and the octylQA-epoxide was washed with 50 mL of cold ether and sonicated extensively. This washing procedure was repeated three times before drying the product in vacuo. A ring-opening reaction was then carried out between the octylQA-epoxide and the terminal primary amines of the PAMAM dendrimers. G4 PAMAM (100.0 mg) was dissolved in 5 mL of methanol. One equivalent of triethylamine (with respect to the molar amount of primary amines) and 2.5 molar equivalents of octylQA-epoxide were then added to the vial. The solution was stirred at room temperature for 4 d. Solvent was then removed in vacuo. The dendrimers were subsequently dissolved in water, followed by dialysis against water overnight and lyophilization.

Representative ^{1}H NMR data of modified G4 PAMAM included the following peaks. G4 octyl: ^{1}H NMR (400 MHz, MeOD, δ) 2.29 (s, $NCH_2\mathit{CH_2}C(O)NH$), 1.35–1.23 (m, $NHCH_2CH(OH)(C\mathit{H_2})_5CH_3$), 0.83–0.80 (t, $NHCH_2CH(OH)C(H_2)_5C\mathit{H_3}$). G4 octylQA: ^{1}H NMR (400 MHz, CD_3OD, δ) 2.31 (s, $NCH_2\mathit{CH_2}C(O)NH$), 1.80 (s, $CH_2N^+(CH_3)_2CH_2C\mathit{H_2}(CH_2)_5CH_3$), 1.31–1.23 (m, $CH_2N^+(CH_3)_2CH_2CH_2(C\mathit{H_2})_5CH_3$), 0.83 (t, $CH_2N^+(CH_3)_2CH_2CH_2(CH_2)_5C\mathit{H_3}$).

6.2.2 N-Diazeniumdiolation of QA- and alkyl chain-modified PAMAM dendrimers

To form *N*-diazeniumdiolate NO donors on the modified dendrimer scaffold, single-action G4 PAMAM (30 mg) were added to 1 mL solutions of 1:1 MeOH:THF. One molar equivalent (e.g., with respect to the molar amount of primary amines) of sodium methoxide was added after mixing (vortexing) the solutions. The resulting dendrimer solutions were placed in a stainless steel reactor with continuous magnetic stirring and connected to an in-house NO reactor. The vessel was flushed with Ar three times to a pressure of 7 bar, followed by three longer Ar purges (10 min) to remove trace oxygen from the solutions. Following deoxygenation, the reactor was pressurized to 10 bar with NO gas pre-scrubbed with KOH. The pressure was maintained at 10 bar for 4 d, after which the solutions were again purged with Ar three times for short durations followed by extended purges (3 × 10 min) to remove unreacted NO. Solvent was removed in vacuo, and the NO-releasing dendrimers were dissolved in anhydrous methanol in a 1 dram glass vial, capped and parafilmed, and stored at -20 °C.

6.2.3 Fabrication of electrospun polyurethane fibers

All polyurethane solutions used were prepared at a concentration of 10 wt% (100 mg/mL) in 3:1:1 THF:DMF:MeOH. Polyurethane solutions containing control and NO-releasing dendrimers (5, 15, or 25 mg/mL) were prepared by first dissolving the polyurethane in THF and DMF, followed by the addition of dopant solution in the remaining equivalent of methanol.

Electrospun fibrous mats were fabricated using a custom electrospinning apparatus[42, 43] consisting of a ES20P-20W High Voltage power supply (Gamma High Voltage Research, Ormond Beach, FL), two Kent Scientific Genie Plus syringe pumps (Torrington, CT), and a grounded steel collector plate covered in aluminum foil placed at a 45° angle to the needle. All fibers were fabricated using an applied voltage of 15 kV and 15 cm tip-to-collector distance. Composite polyurethane fibers were formed using a co-axial needle (Ramè-Hart; Succasunna, NY) composed

of two concentric needles (inner gauge: 22, outer gauge: 13). The co-axial needle was supplied by both individual core and sheath solutions, each connected to a separate syringe pump (Appendix). Core solutions were composed of either 10 wt% Tecophilic (HP 93A) or Tecoflex (SG 80A) polyurethanes doped with control or NO-releasing dendrimer (blank fibers contained no dendrimer dopant in the core solution). Sheath solutions were composed of 10 wt% Tecoplast (TP 470) or Tecoflex (SG 80A) polyurethanes with no dendrimer dopant. Fibers prepared with a SG 80A sheath and HP 93A core were doped with either 5, 15, or 25 mg/mL dendrimer, while the core solutions for all fibers prepared using a TP 470 sheath were doped with 25 mg/mL dendrimer. To form fibrous mats, 0.5 mL core solution (10 μL/min flow rate) and 1.5 mL sheath solutions (30 μL/min flow rate) were electrospun and collected on aluminum foil. After collection, fibers were cut using a 1.27 cm-diameter hole-punch to yield individual "coupon" samples with a resultant surface area of 1.267 cm^2. Each fiber sample was weighed, and any sample with a mass below 1 mg or above 3.5 mg was excluded.

6.2.4 Characterization of NO storage and release

Nitric oxide release was evaluated in real-time in deoxygenated PBS (pH 7.4, 37 °C) using a Sievers NOA 280i chemiluminescence NO analyzer (NOA, Boulder, CO).[44] Prior to analysis, the NO analyzer was calibrated with air passed through a NO zero filter (0 ppm NO) and a 25.87 ppm NO standard gas (balance N_2). Fibrous mat coupons (surface area: 1.267 cm^2) or 0.5 mg aliquots of *N*-diazeniumdiolate-functionalized PAMAM in methanol were added to 30 mL deoxygenated PBS to initiate NO release. Nitrogen was flowed through the solution at a flow rate of 80 mL/min to carry the liberated NO to the analyzer. Additional nitrogen flow was supplied to the flask to match the collection rate of the instrument at 200 mL/min. Nitric oxide analysis was

terminated when NO levels decreased to below 1 pmol NO/cm^2 for fibers (9.7 ppb) or 10 ppb NO/mg dendrimer.

Nitric oxide release was also measured in 50 mM HCl at 37 °C to calculate the mass of dendrimer encapsulated within the fiber (μg dendrimer/mg fiber). The total amount of dendrimer dopant incorporated into the fibers (t[dendrimer]) was determined by the following equation, where $t[NO]_{dendrimer}$ is the total NO payload released per milligram of dendrimer scaffold and $t[NO]_{HCl}$ is the total NO payload released per milligram of fiber in 50 mM HCl:

$$t[\text{dendrimer}] = t[NO]_{HCl} / t[NO]_{dendrimer} \times 1000 \qquad \textbf{Eq. 6.1}$$

6.2.5 Characterization of electrospun polyurethane fibers

Fiber diameter and morphology were assessed using a FEI Helios 600 Nanolab Dual Beam System (Hillsboro, OR) without additional metal coating. Fiber diameters were determined using NIH ImageJ software (Bethesda, MD) and averaged for at least 300 measurements over three separate fiber samples.

Water absorption capabilities of the electrospun fibrous mats were assessed by comparing weights of the dry and hydrated samples. Dry electrospun fibers were weighed before soaking in Milli-Q water overnight at room temperature. The hydrated samples were removed from water, and the excess surface water was removed by dabbing with a Kimwipe before weighing the samples again. Water absorption was calculated by the following equation, where W_H is the weight of the hydrated sample and W_D is the initial weight of the dry fiber mat:

$$\text{Water Absorption (\%)} = [(W_H - W_D)/W_D] \times 100\% \qquad \textbf{Eq. 6.2}$$

The porosity of the electrospun fibrous mats was determined using the liquid intrusion method.[45, 46] Fiber mats were weighed prior to immersion in 100% ethanol at room temperature overnight to allow diffusion of ethanol into the void volume. After this incubation, fibers were

removed from ethanol, dabbed with a Kimwipe, and weighed again. Porosity was calculated by dividing the volume of intruded ethanol (determined by the change in mass and the density of ethanol, 0.789 g/mL) by the total volume after intrusion (volume of ethanol and fibers, determined by initial fiber mass and polyurethane density, 1.1 g/mL).

Leaching assays for determining dendrimer delivery were performed by doping RITC-tagged G4 PAMAM dendrimers into the fibers. Fluorescently-labeled G4 PAMAM dendrimers were synthesized as described previously.[36, 37, 47] Briefly, 100 mg G4 PAMAM was added to a vial containing one molar equivalent of RITC per mole dendrimer (3.8 mg) in 2 mL methanol. One equivalent of triethylamine (with respect to the molar amount of primary amines) was then added to the vial. The solution was stirred for 24 h in the dark, followed by solvent removal in vacuo. Dendrimers were dissolved in water, dialyzed against water (3 d), and then lyophilized. The above procedures for dendrimer modification and fiber mat fabrication were performed in the dark to yield RITC-tagged electrospun fibrous mats. Individual fiber mats were incubated in 500 µL PBS (pH 7.4, 37 °C) for 30 min, 2 h, 6 h, and 24 h. After incubation, 100 µL of each solution was transferred to a black 96-well plate in triplicate. The fluorescence intensity was measured using a BMG PolarStar Omega fluorescence plate reader (Ortenberg, Germany). Calibration standards were prepared at concentrations ranging from 0 – 200 µg/mL in triplicate.

6.2.6 Zone of inhibition assays

Lyophilized *P. aeruginosa*, *E. coli*, *S. aureus*, and MRSA were reconstituted in tryptic soy broth (TSB) or Luria-Bertani (LB) broth (*E. coli*) and cultured overnight at 37 °C. A 0.5 mL aliquot of culture was grown in 50 mL TSB or LB broth to a concentration of 10^8 colony forming units per mL (cfu/mL), collected by centrifugation (2355×*g*), resuspended in 15% glycerol (v/v in PBS), and stored at -80 °C in 1 mL aliquots. For daily experiments, colonies of bacteria culture

were inoculated in 2 mL TSB or LB broth overnight at 37 °C and recultured in fresh TSB or LB broth (50 mL) the next day.

The antibacterial action of the electrospun fibers was evaluated using a corrected zone of inhibition test.[48] Briefly, *P. aeruginosa*, *E. coli*, *S. aureus*, and MRSA were cultured in TSB or LB broth (*E. coli*) to a concentration of 10^8 cfu/mL, and 50 µL of the bacterial suspension in broth was spared over Mueller Hinton agar plates. Individual fiber mat samples (blank, control, and NO-releasing) were placed on the bacteria-containing agar. The plates were then incubated at 37 °C overnight. Zones of growth inhibition (ZOI) surrounding the fibers were measured (in mm) from the edge of the sample using calipers. Of note, no plate dehydration was observed. All zone of inhibition tests were repeated in triplicate.

6.2.7 Bacterial log reduction assays

An adapted time-kill kinetic log reduction assay was also employed to further assess the antibacterial action of the electrospun fibrous mats.[48] Briefly, *P. aeruginosa*, *E. coli*, *S. aureus*, and MRSA were cultured in TSB or LB broth (*E. coli*) to a concentration of 10^8 cfu/mL. Individual fiber mat samples (blank, control, and NO-releasing) were added to 1 dram glass vials and sterilized under UV light for 2 h prior to the bacteria assays. Fibers were exposed to 200 µL 10^8 cfu/mL bacteria in broth for either 2 or 24 h at 37 °C with light agitation. Untreated controls (blanks) were included in each experiment to ensure the bacteria remained viable over the 2 or 24 h assays. After 2 h exposure, the bacteria solutions were vortexed and a 10 µL aliquot was removed for dilution and plating on tryptic soy agar (TSA) or LB agar (*E. coli*) plates. The bacteria and fiber solutions were then returned to 37 °C with light agitation for the remainder of the 24 h incubation. After exposure, the bacteria solutions were vortexed and then spiral-plated at 100-, 1000-, and 10,000-fold dilutions on TSA or LB agar plates using an Eddy Jet spiral plater (IUL;

Farmingdale, NY). Bacterial viability was assessed by counting the number of colonies formed on the agar plate using a Flash & Go colony counter (IUL; Farmingdale, NY). Log reductions in bacterial viability were determined by the following equation, where Blank Viability is the viability of the unexposed bacterial blank solution and Exposed Viability is the resulting viability of bacteria solutions exposed to either blank, control, or NO-releasing electrospun fibers:

$$\text{Log Reduction} = \log_{10} \frac{Blank\ Viability\ (cfu/mL)}{Exposed\ Viability\ (cfu/mL)} \qquad \textbf{Eq. 6.3}$$

6.2.8 Fluorescence microscopy for detection of intracellular NO and cell death

P. aeruginosa was cultured in TSB to a concentration of 10^8 cfu/mL, collected by centrifugation (2355×*g*), and resuspended in PBS containing 30 μM PI and 20 μM DAF-2 DA at 10^8 cfu/mL. Nitric oxide-releasing fibers were exposed to 200 μL *P. aeruginosa* in PBS/PI/DAF-2 DA for 30 min. Every 5 min, a 10 μL aliquot of the bacteria solution was deposited on a glass slide with a coverslip for wide-field fluorescence imaging. An Olympus iX80 inverted microscope with an Olympus light source (Chroma) and Hamamatsu ORCA detector were used to image bacteria on slides. Fluorescent PI images (red) were obtained using a BP 542 – 582 nm excitation and BP 604 – 644 nm emission filters. Green DAF-2 images were obtained using BP 464 – 500 nm emission and BP 516 – 556 nm excitation filters. Images were acquired using Metamorph software and a 0.45 NA lens with a 20× objective.

6.2.9 In vitro cytotoxicity

L929 mouse fibroblasts were grown in DMEM supplemented with 10 vol% FBS and 1 wt% PS and incubated in 5 vol% CO_2 under humidified conditions at 37 °C. After reaching 80% confluency, cells were trypsinized and seeded onto tissue culture-treated polystyrene. To assess fiber cytotoxicity, L929 cells were seeded onto tissue culture-treated polystyrene 24-well plates at a density of 10^5 cells/mL, and incubated at 37 °C for 72 h. The supernatant was then aspirated and

replaced with 1 mL of fresh growth medium and the electrospun fiber mats. Dimethyl sulfoxide (10%) was used as a positive control. After incubation for 2 or 24 h at 37 °C, the fiber mats were removed from the wells and the supernatant was aspirated. Next, 500 µL of a mixture of DMEM/MTS/PMS (105/20/1, v/v/v) was added to each well. After 1.5 h incubation at 37 °C, 100 µL of the colored solution was transferred to a 96-well plate in triplicate. The absorbance was quantified at 490 nm using a Thermoscientific Multiskan EX plate reader (Waltham, MA), with the DMEM/MTS/PMS mixture and untreated cells used as blanks and controls, respectively. Results were expressed as percentage of relative cell viability as follows:

$$\% \text{ Cell Viability} = [(Abs_{490} - Abs_{blank})/(Abs_{control} - Abs_{blank})] \times 100\% \qquad \textbf{Eq. 6.4}$$

To determine dendrimer toxicity, L929 cells were seeded onto tissue culture-treated polystyrene 96-well plates at a density of 2×10^4 cells/mL, and incubated at 37 °C for 72 h. The supernatant was then aspirated and replaced with 200 µL of fresh growth medium and 50 µL of varying concentrations of dendrimer in PBS. Dimethyl sulfoxide (10%) and 50 µL PBS were used as positive and negative controls, respectively. After 2 or 24 h incubation at 37 °C, the supernatant was aspirated and 120 µL of a mixture of DMEM/MTS/PMS (105/20/1, v/v/v) was added to each well. After 1.5 h incubation at 37 °C, the absorbance of the colored solutions was quantified at 490 nm with percent cell viability determined using Eq. 4. A killing curve was constructed for each dendrimer modification by plotting % cell viability versus dendrimer concentration. IC_{50} values, defined as the dendrimer concentration that corresponded to a 50% reduction in cell viability, were determined from each plot.

6.3 Results and Discussion

6.3.1 Synthesis and characterization of NO-releasing G4 dendrimers

Generation 4 (G4) poly(amidoamine) (PAMAM) dendrimers were modified with octyl alkyl chains or octylQA moieties through a ring-opening reaction at the peripheral primary amines as described previously (Scheme 1).[36, 37] Covalent chemical modifications were confirmed using ^{1}H NMR spectroscopy. On average, 40 – 50 functional groups were added to the G4 scaffold, resulting in ~70% functionalization of the terminal primary amines (Appendix).

The resulting secondary amines were converted to *N*-diazeniumdiolate NO donors under high pressures of NO. Nitric oxide storage was tuned by adjusting the ratio of THF:methanol, resulting in similar NO payloads of ~1 μmol/mg for each scaffold (Appendix). The NO-releasing octyl-modified dendrimers exhibited a half-life ($t_{1/2}$) of ~25 min and duration of 9 h. In contrast, G4 octylQA/NO dendrimers were characterized by slower NO-release kinetics, with an initial max flux about half that of the G4 octyl/NO dendrimers and extended NO-release ($t_{1/2}$ of 115 min and duration exceeding 16 h). This longer NO release suggests that the permanent positive charge of the QA moiety stabilizes the *N*-diazeniumdiolate group. The effects of dendrimer NO-release kinetics on the NO-release characteristics of electrospun polyurethane fibers could thus be evaluated due to the variation of dendrimer half-lives.

6.3.2 Fabrication and characterization of electrospun polyurethane fibers

To fabricate antibacterial wound dressings, electrospun fibers were formed from three medical grade thermoplastic polyurethanes. Tecoplast (TP 470), a rigid, aromatic polyurethane, was the most hydrophobic system evaluated. Tecoflex (SG 80A) and Tecophilic (HP 93A) represent hydrophilic aliphatic polyurethanes, with HP 93A, a polyether-based polyurethane, demonstrating the greatest water uptake capabilities. The dendrimer-containing core solution was

Scheme 6.1 Reaction of G4 PAMAM scaffold with either (A) octyl alkyl chain or (B) octylQA epoxides to yield G4 octyl and G4 octylQA dendrimers, respectively, followed by reaction with high pressures of NO to generate NO-releasing dendrimers.

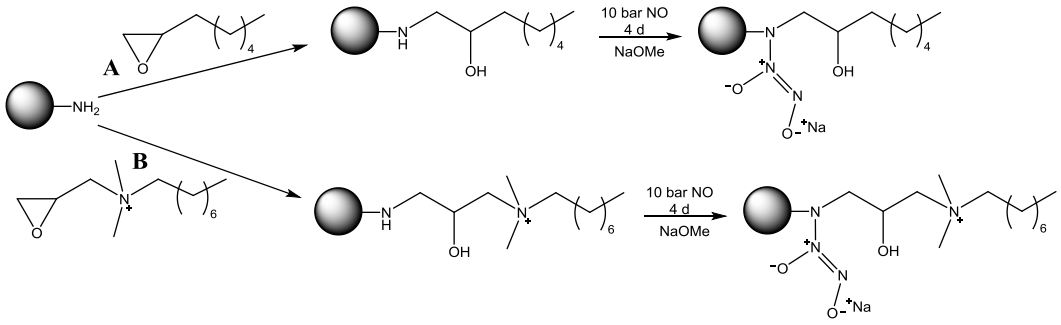

composed of either SG 80A or HP 93A aliphatic polyurethanes, while the outer (non-dendrimer-containing) sheath polymer was either SG 80A or TP 470. For clarity, the polymer compositions are denoted Sheath/Core-Dopant; for example, a G4 octyl-doped HP 93A core combined with a TP 470 sheath is referred to as TP 470/HP 93A-G4 octyl. Fibers were fabricated using a custom electrospinning apparatus with a co-axial setup using concentric needles to introduce both core and sheath polymer solutions (Appendix).

Blank (no dendrimer dopant), control (non-NO-releasing), and NO-releasing composite electrospun polyurethane fibers were prepared using three polymer compositions (i.e., SG 80A/HP 93A, TP 470/SG 80A, and TP 470/HP 93A) and two dendrimer modifications (i.e., G4 octyl and G4 octylQA). The resulting semi-porous electrospun fibrous mats exhibited smooth morphology with little to no bead formation (Figure 6.1). Altering the polyurethane composition greatly influenced the macroscopic physical characteristics of the electrospun fiber mats (Figure 6.2). Fiber mats fabricated using SG 80A as either the core or sheath polyurethane were elastic and adhered to each other. Alternately, the TP 470/HP 93A electrospun fibers maintained good shape over time and were easier to handle. Fiber diameter distributions for polyurethane compositions were more dependent on the identity of the sheath polyurethane rather than the core (Figure 6.3). The SG 80A/HP 93A fiber diameters skewed larger, averaging around 600 nm compared to 400 – 450 nm for both TP 470 sheath compositions. These differences in fiber diameter were attributed to greater kinematic viscosity of the Tecoflex polyurethane solutions.[43]

The allowance of gaseous and fluid exchanges represents an important characteristic for wound dressings.[4] A porous nanofiber structure allows for adequate wound respiration and helps maintain an appropriately moist environment. The porosity of dendrimer-doped electrospun fibrous mats was evaluated via liquid intrusion by measuring the ability of a non-wetting liquid to

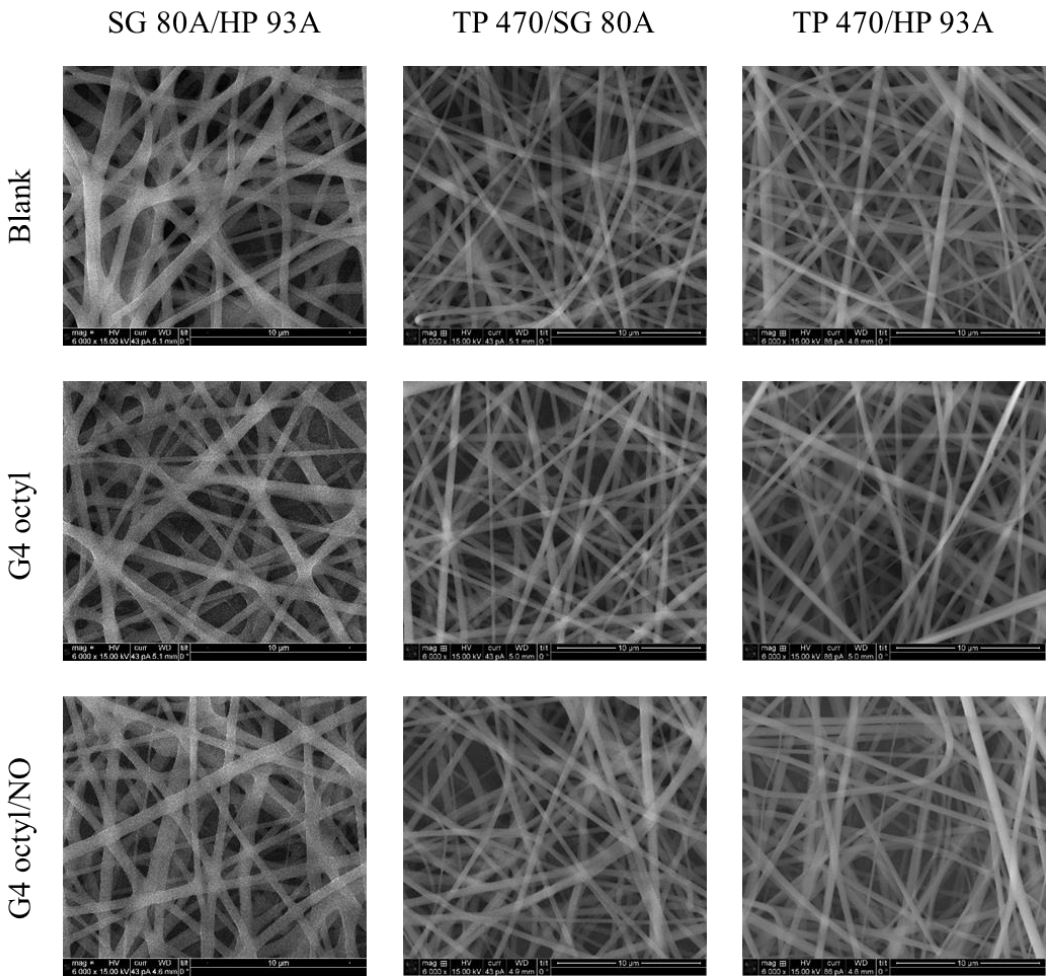

Figure 6.1 Scanning electron micrographs of blank, control, and NO-releasing G4 octyl-doped electrospun SG 80A/HP 93A, TP 470/SG 80A, and TP 470/HP 93A fibers.

Figure 6.2 Image of electrospun fiber substrates (1.267 cm^2). From left to right: SG 80A/HP 93A, TP 470/SG 80A, and TP 470/HP 93A.

permeate the pores.[45, 46] The SG 80A/HP 93A fibers exhibited greater mat porosity compared to fibers containing a TP 470 sheath (Table 6.1). The cause of this substantial decrease in porosity, from ~70 to 30 – 50%, when moving from the SG 80A to TP 470 sheath polyurethane is unclear but most likely the result of larger fiber diameter distributions of the SG 80A/HP 93A fibers. Further, composite fibers containing TP 470 exhibited similar porosities regardless of core polyurethane. While adding dendrimers to the TP 470/SG 80A fibers increased fiber mat porosity by ~10%, control and NO-releasing TP 470/HP 93A fibers exhibited porosities ~10% lower than blank fibers. Overall, the electrospun fiber characteristics were more influenced by the composition of the sheath polymer than either the core polyurethane or dendrimer dopant.

The absorption of water by electrospun fibers is an indicator of how efficiently the wound dressings can remove fluid from highly exuding wounds, preventing wound stagnation.[4, 22] Although all of the fiber samples demonstrated sufficient water uptake capabilities (>100%), SG 80A/HP 93A fibers absorbed roughly half the water as fibers prepared using a TP 470 sheath (Table 6.1). This result was initially surprising due to the greater hydrophobicity of the TP 470 polyurethane compared to SG 80A. However, the water absorption capabilities of the electrospun polyurethane fibers correlated directly with the percent porosity exhibited by the fibrous mat. Electrospun SG 80A/HP 93A fiber mats demonstrated both the largest porosity (~70%) and modest water absorption (~130%), while fibers prepared using a TP 470 sheath had lower porosities (30 – 50%) and absorbed more water (>300%). Control and NO-releasing TP 470/HP 93A fibers exhibited ~10% lower porosity than the blank fibers with enhanced water absorption (150 to ~350%). The increased water uptake with lower fiber mat porosity is attributed to the greater surface area available per volume allowing for more efficient absorption of water into the individual fibers.

Total NO and dendrimer storage were determined by measuring the NO release under acidic conditions (50 mM HCl). Despite doping the core polyurethane solution with the same dendrimer concentration (25 mg/mL), total dendrimer incorporation varied dramatically between polyurethane compositions (Table 6.2). SG 80A/HP 93A-G4 octyl/NO fibers demonstrated the largest dendrimer storage (~110 μg/mg), followed by the TP 470/SG 80A-G4 octyl/NO (~80 μg/mg) and the TP 470/HP 93A-G4 octyl/NO (~60 μg/mg) fibers. Additionally, dendrimer incorporation varied between dendrimer modifications, with the TP 470/HP 93A-G4 octylQA/NO fibers exhibiting the second largest storage (~95 μg/mg). The identity of the core or sheath polyurethane had no clear effect on the amount of dendrimer incorporated into the fibers, suggesting the dendrimer loading cannot be projected prior to fiber fabrication due to potential dendrimer loss during the electrospinning process. However, the total dendrimer incorporation could be tuned by varying the concentration of dendrimer in the initial core polyurethane solution. Doping G4 octyl/NO dendrimers into SG 80A/HP 93A fibers at initial concentrations of 5, 15, and 25 mg/mL led to greater total dendrimer incorporation with increasing dendrimer concentration, highlighting the tunability of dendrimer loading within electrospun fibers. Due to the low dendrimer loading within the 5 mg/mL SG 80A/HP 93A-G4 octyl/NO fibers (~5 μg/mg), only the 15 and 25 mg/mL compositions were further evaluated.

To evaluate dendrimer delivery from composite polyurethane fibers, control and NO-releasing dendrimers were modified with a fluorescent RITC tag prior to electrospinning. The resulting RITC-containing electrospun fiber mats (Appendix) were soaked in PBS to quantify the amount of dendrimer released over 24 h. Impact of the fluorescent label on the scaffold was minimized by limiting the amount of RITC incorporated to one molecule per dendrimer scaffold (~3% of G4 PAMAM mass). For all of the composite polyurethane fibers, most of the dendrimer

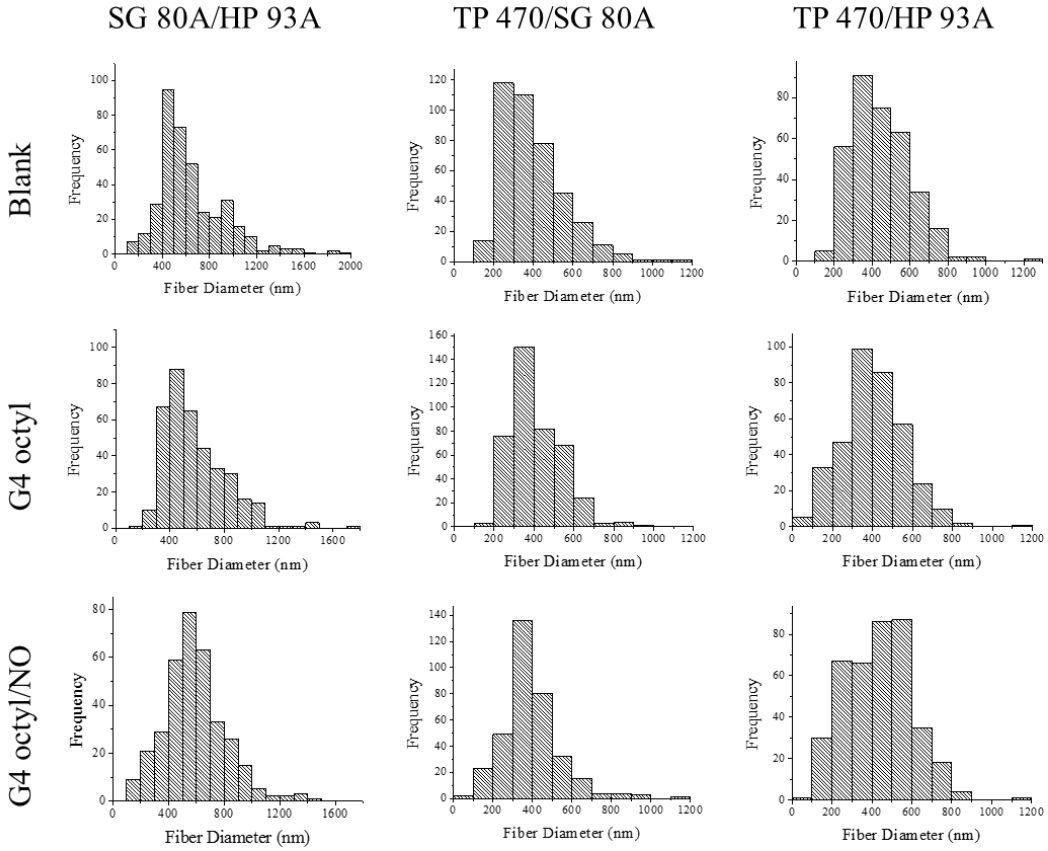

Figure 6.3 Histograms depicting fiber diameter distribution (nm) for blank, control, and NO-releasing G4 octyl-doped electrospun SG 80A/HP 93A, TP 470/SG 80A, and TP 470/HP 93A fibers.

Table 6.1 Characterization of co-axial electrospun polyurethane fibers.[a]

	Substrate Mass (mg)	Fiber Diameter (nm)	Porosity (%)	Water Absorption (%)
SG 80A/HP 93A	1.41 ± 0.40	645 ± 292	71.4 ± 8.3	128 ± 41
SG 80A/HP 93A-G4 octyl	1.58 ± 0.34	585 ± 228	78.0 ± 4.0	145 ± 26
SG 80A/HP 93A-G4 octyl/NO	1.63 ± 0.60	590 ± 217	70.1 ± 7.4	120 ± 42
TP 470/SG 80A	1.41 ± 0.25	394 ± 156	29.4 ± 5.0	306 ± 40
TP 470/SG 80A-G4 octyl	1.74 ± 0.52	412 ± 127	40.3 ± 3.8	397 ± 44
TP 470/SG 80A-G4 octyl/NO	1.36 ± 0.35	393 ± 157	42.6 ± 4.0	210 ± 48
TP 470/HP 93A	1.77 ± 0.43	443 ± 152	51.3 ± 4.0	156 ± 70
TP 470/HP 93A-G4 octyl	1.40 ± 0.28	409 ± 176	37.1 ± 5.0	333 ± 107
TP 470/HP 93A-G4 octyl/NO	1.99 ± 0.78	433 ± 165	37.4 ± 8.3	379 ± 80
TP 470/HP 93A-G4 octylQA	1.68 ± 0.36	440 ± 182	45.9 ± 5.3	435 ± 68
TP 470/HP 93A-G4 octylQA/NO	1.82 ± 0.55	418 ± 155	39.0 ± 10.5	335 ± 90

[a]For all measurements, $n \geq 3$ pooled experiments.

Table 6.2 Total nitric oxide storage and dendrimer encapsulation by fiber mass.[a]

	[Dendrimer][b] (mg/mL)	t[NO][c] (nmol/mg)	$t[NO]_{HCl}$[d] (nmol/mg)	t[dendrimer][e] (μg/mg)
SG 80A/HP 93A-G4 octyl/NO	5	1.8 ± 0.8	3.8 ± 0.4	5 ± 1
SG 80A/HP 93A-G4 octyl/NO	15	26.0 ± 3.6	35.0 ± 5.2	42 ± 6
SG 80A/HP 93A-G4 octyl/NO	25	72.3 ± 9.0	93.8 ± 7.4	111 ± 10
TP 470/SG 80A-G4 octyl/NO	25	42.4 ± 4.4	71.1 ± 8.3	81 ± 6
TP 470/HP 93A-G4 octyl/NO	25	27.3 ± 4.1	51.0 ± 12.7	63 ± 13
TP 470/HP 93A-G4 octylQA/NO	25	44.7 ± 11.0	88.8 ± 18.9	94 ± 23

[a]For all measurements, $n \geq 3$ pooled experiments. [b]Dendrimer concentration in the original polymer solution. [c]Total NO payload released per mg of fiber in PBS (pH 7.4). [d]Total NO payload released per mg of fiber in 50 mM HCl. [e]Total amount of dendrimer encapsulated per mg of fiber (determined by total NO release in 50 mM HCl).

delivery occurred over the first 2 h, with only a slight increase in dendrimer release over the remaining 24 h (Figure 6.4). Of note, an insignificant increase in dendrimer delivery was observed after 7 d, indicating the majority of dendrimer release is achieved during the first 24 h (data not shown).

The polyurethane composition dramatically influenced the rate of control dendrimer delivery from composite electrospun fibers. Fibers containing a SG 80A sheath were characterized by greater delivery of control dendrimers than either of the corresponding fibers with TP 470 as the sheath polyurethane (Figure 6.4 A-B). Both the 15 and 25 mg/mL SG 80A/HP 93A-G4 octyl fibers exhibited similar dendrimer release (~30 μg/mL), although it corresponded to 65 and 30% of the total incorporated dendrimer, respectively. Alternately, control TP 470/HP 93A and TP 470/SG 80A fibers release dendrimer doses corresponding to ~10 and ~20% of the total incorporated dendrimer, respectively, indicating both core and sheath polyurethane identity influence the rate of dendrimer delivery. The decreased dendrimer release exhibited by the TP 470/SG 80A and TP 470/HP 93A fibers compared to the fibers containing an SG 80A sheath is attributed to the more rigid and hydrophobic TP 470 polyurethane acting as a more effective barrier layer compared to the aliphatic SG 80A. Further, the greater release of control G4 octyl dendrimers from TP 470/SG 80A fibers compared to TP 470/HP 93A fibers is attributed to greater charge stabilization of the dendrimers within the more hydrophilic, polyether-based HP 93A polyurethane.

Release of the NO-releasing dendrimers was dependent on the amount of dendrimer incorporated and sheath polyurethane, with the fibers containing an SG 80A polyurethane sheath resulting in greater dendrimer release. Indeed, the 25 mg/mL SG 80A/HP 93A-G4 octyl/NO fibers delivered the largest total dendrimer dose (~60 μg/mg), representing ~50% of the total dendrimer

storage. While the remaining G4 octyl/NO-doped fibers exhibited similar dendrimer release (~40 μg/mg), this amount corresponded to ~55% of the total incorporated dendrimer for the fibers composed using a TP 470 sheath and ~100% delivery for the 15 mg/mL SG 80A/HP 93A-G4 octyl/NO fibers, again demonstrating that the aliphatic SG 80A provides a less effective barrier layer than the hydrophobic TP 470 polyurethane.

Larger doses of NO-releasing dendrimer were delivered than control dendrimers for all of the polyurethane compositions. The *N*-diazeniumdiolate NO donor is zwitterionic and thus may destabilize the dendrimer scaffold within the polyurethane fibers relative to control dendrimers due to an overall increase in electrostatic charge.[49] In a similar manner, control and NO-releasing TP 470/HP 93A-G4 octylQA fibers delivered greater dendrimer doses compared to the G4 octyl system (Figure 6.4 C), which lacks a cationic QA moiety. Dendrimer release rates were clearly dependent on the resulting charge of the dendrimer scaffold after modification (e.g., QA moiety or *N*-diazeniumdiolate), with increased charge resulting in decreased dendrimer stability within the polyurethane fibers and faster delivery.

Similar to dendrimer delivery, NO-release kinetics of the composite electrospun fibers was found to be dependent on both the polyurethane identity and dendrimer modification. To evaluate NO-release kinetics from composite electrospun fibers under physiological conditions (pH 7.4, 37 °C), fiber mats were cut into circular coupons with a standard surface area (1.27 cm^2), and NO release was measured in real-time via chemiluminescence.

Regardless of polyurethane composition, all of the NO-releasing fibers demonstrated an initial maximum burst of NO followed by a steady decline in release (Appendix). The initial NO burst for both of the SG 80A/HP 93A-G4 octyl/NO fiber compositions was higher than that for either of the fibers containing a TP 470 sheath (Table 6.3). This difference in initial NO flux was

attributed to the aliphatic SG 80A polyurethane being a less effective barrier layer to both water and dendrimers, leading to a faster release of dendrimers in solution and greater water access for *N*-diazeniumdiolate dissociation. Further, while the 15 mg/mL SG 80A/HP 93A-G4 octyl/NO fibers exhibited similar NO totals as the G4 octyl/NO-doped fibers containing a TP 470 sheath (~45 nmol/cm^2), they demonstrated faster NO-release kinetics. Indeed, the SG 80A/HP 93A-G4 octyl/NO fibers had a shorter half-life (22 min) and duration (2.2 h) than either of the fibers fabricated using a TP 470 sheath (half-life ~40 min, duration ~3 h), indicating the sheath polyurethane has a greater influence on fiber release kinetics than the core polyurethane identity. Between the two SG 80A/HP 93A-G4 octyl/NO compositions, both NO-release totals and kinetics were dependent on total dendrimer incorporation. The 25 mg/mL composition exhibited larger total NO storage (87 versus 45 nmol/cm^2) and longer NO-release half-life (36 versus 22 min) and duration (4.2 versus 2.2 h) than the 15 mg/mL fibers, demonstrating the ability to tune NO-release characteristics as well as dendrimer delivery for the electrospun fibers. Similarly, the TP 470/HP 93A-G4 octylQA/NO fibers exhibited both a greater NO-release half-life (102 min) and duration (~7 h) relative to the G4 octyl/NO-containing fibers. This was attributed to the extended NO-release properties characteristic of the G4 octylQA/NO scaffold (NO-release half-life ~115 min), indicating that fiber NO-release kinetics are highly dependent on the dendrimer modification.

6.3.3 Zone of inhibition

P. aeruginosa, *E. coli*, and *S. aureus* (including methicillin-resistant strains) are among the most commonly isolated species in chronic wounds.[2, 50, 51] These pathogens were thus selected to evaluate the potential antibacterial action of control and NO-releasing electrospun fibers. The use of two Gram-negative (*P. aeruginosa*, *E. coli*) and two Gram-positive (*S. aureus*, MRSA) bacterial

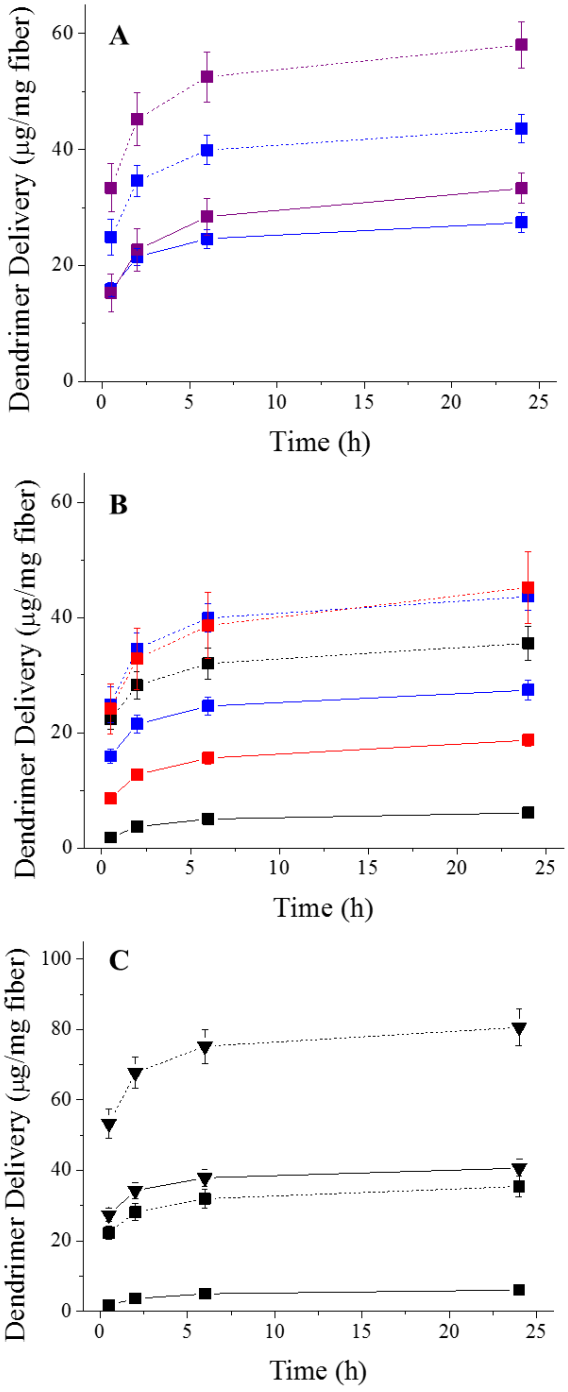

Figure 6.4 (A) Delivery of control (solid line) and NO-releasing (dashed line) G4 octyl dendrimers from electrospun SG 80A/HP 93A fibers at 15 (blue) and 25 (purple) mg/mL initial dendrimer concentration. (B) Delivery of control (solid line) and NO-releasing (dashed line) G4 octyl dendrimers from electrospun SG 80A/HP 93A (blue), TP 470/SG 80A (red), TP 470/HP 93A (black) fibers. (C) Delivery of control (solid line) and NO-releasing (dashed line) G4 octyl (square) and G4 octylQA (triangle) dendrimers from electrospun TP 470/HP 93A fibers. For all measurements, n ≥ 3 pooled experiments with error bars representing standard deviation of the mean.

Table 6.3 Nitric oxide-release properties for NO-releasing electrospun fibers in PBS (pH 7.4, 37 °C).[a]

	[Dendrimer][b] (mg/mL)	[NO]max[c] (pmol/cm^2)	t_{max}[d] (min)	t[NO][e] (nmol/cm^2)	$t[NO]_{2h}$[f] (nmol/cm^2)	$t_{1/2}$[g] (min)	t_d[h] (h)
SG 80A/HP 93A-G4 octyl/NO	15	21.8 ± 5.7	6.1 ± 2.9	44.6 ± 11.1	43.7 ± 10.2	22.4 ± 3.3	2.2 ± 0.3
SG 80A/HP 93A-G4 octyl/NO	25	27.6 ± 11.7	6.2 ± 2.2	87.2 ± 19.1	71.2 ± 17.3	35.7 ± 3.9	4.2 ± 0.8
TP 470/SG 80A-G4 octyl/NO	25	14.0 ± 2.1	3.3 ± 0.6	46.7 ± 9.5	38.3 ± 7.2	47.8 ± 6.9	3.6 ± 0.5
TP 470/HP 93A-G4 octyl/NO	25	17.2 ± 6.2	4.0 ± 1.6	44.3 ± 10.1	39.9 ± 9.1	39.0 ± 4.5	2.9 ± 0.4
TP 470/HP 93A-G4 octylQA/NO	25	10.6 ± 1.5	4.3 ± 0.6	66.5 ± 16.5	36.2 ± 5.6	102.4 ± 24.6	6.8 ± 1.5

[a]For all measurements, $n \geq 3$ pooled experiments. [b]Dendrimer concentration in the original polymer solution. [c]Maximum flux of NO release. [d]Time required to reach maximum flux. [e]Total NO payload released per surface area. [f]NO payload released after 2 h. [g]NO release half-life. [h]Duration of NO release.

strains allowed for an initial evaluation of the effect of Gram designation on antibacterial action.

As expected, electrospun composite polyurethane fibers prepared without dendrimers (i.e., blanks) were void of antibacterial action. Nearly every control and NO-releasing polyurethane composition exhibited low antibacterial activity (ZOI <1 mm) against each of the Gram-negative strains, with only the TP 470/SG 80A-G4 octyl/NO fibers displaying an inhibition zone of 1.7 mm (Table 6.4). Moderate bactericidal action was observed against Gram-positive bacteria. Both control and NO-releasing SG 80A/HP 93A-G4 octyl fibers resulted in inhibition zones of ~1 mm, while the TP 470/SG 80A-G4 octyl/NO fibers again exhibited greater inhibition zones of 2.0 and 1.6 mm against *S. aureus* and MRSA, respectively. While NO-releasing TP 470/HP 93A fibers (i.e., G4 octyl and G4 octylQA) resulted in low to moderate antibacterial action against both Gram-positive strains (ZOI 0.4 – 0.7 mm), the control TP 470/HP 93A fibers exhibited little to no bactericidal activity against either Gram-negative or Gram-positive bacteria (ZOI ≤0.2 mm). Despite small inhibition zones, bacterial growth was not observed beneath any of the control or NO-releasing fiber samples (Appendix). The larger zones of inhibition (ZOI >0.6 mm) agree with results published by Vogt et al. who demonstrated the antibacterial efficacy of NO-releasing nanofibers against *S. aureus* (ZOI 0.75 – 1.2 mm).[52] However, as NO diffuses in all directions, not just along the agar surface,[52] we evaluated the reduction of bacterial growth in solution in conjunction with the zone of inhibition assay to fully assess the antibacterial action of NO-releasing electrospun polyurethane fiber mats.

6.3.4 Bacterial log reduction

For log reduction tests, a compound is considered bactericidal if it reduces bacterial viability by at least three orders of magnitude.[48, 53] Using this assay, we evaluated the ability of blank, control, and NO-releasing TP 470/HP 93A fibers to reduce the viability of *P. aeruginosa*,

Table 6.4 Average zone of inhibition against planktonic bacteria.[a]

	P. aeruginosa ZOI (mm)	*E. coli* ZOI (mm)	*S. aureus* ZOI (mm)	MRSA ZOI (mm)
SG 80A/HP 93A-G4 octyl	0.4 ± 0.3	0.5 ± 0.1	1.0 ± 0.1	1.2 ± 0.3
SG 80A/HP 93A-G4 octyl/NO	0.5 ± 0.3	0.4 ± 0.1	0.9 ± 0.3	0.6 ± 0.1
TP 470/SG 80A-G4 octyl	0.4 ± 0.5	0.4 ± 0.3	0.2 ± 0.3	0.0 ± 0.0
TP 470/SG 80A-G4 octyl/NO	1.7 ± 0.3	1.8 ± 0.3	2.0 ± 0.1	1.6 ± 0.2
TP 470/HP 93A-G4 octyl	0.1 ± 0.3	0.1 ± 0.2	0.2 ± 0.3	0.2 ± 0.3
TP 470/HP 93A-G4 octyl/NO	0.4 ± 0.5	0.1 ± 0.2	0.7 ± 0.2	0.6 ± 0.1
TP 470/HP 93A-G4 octylQA	0.0 ± 0.0	0.0 ± 0.0	0.0 ± 0.0	0.0 ± 0.0
TP 470/HP 93A-G4 octylQA/NO	0.3 ± 0.5	0.6 ± 0.4	0.6 ± 0.2	0.4 ± 0.2

[a]For all measurements, $n \geq 3$ pooled experiments.

E. coli, *S. aureus*, or MRSA planktonic cultures as a function of NO-release kinetics and dendrimer modification. These studies were performed under growth conditions (i.e., in nutrient broth) over 2 and 24 h to determine both the short- and long-term bactericidal action of control and NO-releasing polyurethane fibers. Fiber mats displayed high antibacterial activity if they exhibited at least a 3-log reduction in bacterial viability, moderate activity for a 1- to 3-log reduction, and low activity for <1-log reduction.[48]

As expected, blank TP 470/HP 93A fibers did not eradicate bacteria (Appendix), while the antibacterial activity of control (i.e., non-NO-releasing) fibers was dependent on the dendrimer dopant. Similar to the zone of inhibition studies, TP 470/HP 93A-G4 octylQA fibers demonstrated little to no antibacterial action against any of the pathogens at either timepoint (Table 6.5). Alternatively, TP 470/HP 93A-G4 octyl fibers were moderately antibacterial against the majority of bacterial strains tested (≥1-log reduction), only exhibiting low antibacterial action against *S. aureus* (<1-log reduction). The increased bactericidal action of the G4 octyl-doped fibers over their G4 octylQA counterparts was surprising due to the lower corresponding dendrimer dose, but corroborates our previous observations that alkyl chains are more potent biocides than the QA moieties.[36, 37] The G4 octyl-doped fibers were generally more effective at shorter timescales, with an average 2-log bacterial reduction after 2 h and only a 1-log reduction after 24 h. This result was expected, however, as the majority of the low dendrimer dose is delivered over the first 2 h. Nitric oxide-releasing electrospun fibers proved to have greater antibacterial action than either blank or control fibers. Indeed, moderate to high antibacterial activity was consistently observed against the bacterial strains evaluated. The TP 470/HP 93A-G4 octyl/NO fibers demonstrated greater bactericidal action against Gram-negative pathogens while TP 470/HP 93A-G4 octylQA/NO fibers were more effective against the Gram-positive strains, although the differences

in efficacy were modest (~1-log difference between the two dendrimer modifications). In contrast to control fibers, the NO-releasing TP 470/HP 93A fibers were more effective at reducing bacterial viability at extended time periods (24 h), suggesting the greater doses provided by the NO-releasing polyurethane fibers allows for continued bactericidal action of the dendrimer scaffold in solution. Of note, at least one of the NO-releasing fiber formulations displayed high antibacterial activity against each bacterial strain, with an average 4-log reduction in bacterial viability observed at 24 h. However, as TP 470/HP 93A-G4 octylQA/NO fibers deliver almost twice as much dendrimer per milligram of fiber (~35 and 80 μg/mg for G4 octyl/NO and G4 octylQA/NO fibers, respectively), the TP 470/HP 93A-G4 octyl/NO fibers exhibited greater broad-spectrum bactericidal activity with less antibacterial dendrimer delivery. The broad-spectrum antibacterial action exhibited by the NO-releasing electrospun fibers is noteworthy, particularly in comparison to certain commercially available silver-releasing dressings that do not exhibit adequate bactericidal action against Gram-positive bacteria.[48]

To elucidate the mechanism of antibacterial action for the NO-releasing electrospun fibers, DAF-2 DA and PI fluorescent probes were used to visualize intracellular NO and cell membrane damage, respectively. After 5 min exposure to TP 470/HP 93A-G4 octyl/NO fibers, planktonic *P. aeruginosa* bacteria show evidence of both intracellular NO and substantial membrane damage (Figure 6.5). Almost no overlap between the bacterial cells with compromised membranes and the localization of intracellular NO was noted, however, indicating the biocidal actions of G4 octyl-modified dendrimers and NO are exerted independently from one another. The diminished intracellular NO levels after 15 min and undetectable DAF-2 fluorescence at later timepoints suggests that any antibacterial activity derived from NO release is only observed at short timescales. As such, the majority of bactericidal action exhibited by the NO-releasing fibers is the

Table 6.5 Average log reduction against planktonic bacteria.[a]

	P. aeruginosa		*E. coli*		*S. aureus*		MRSA	
	2 h	24 h	2 h	24 h	2 h	24 h	2 h	24 h
TP 470/HP 93A	0.4 ± 0.8	0.6 ± 0.7	0.0 ± 0.2	0.2 ± 0.2	0.0 ± 0.1	-0.2 ± 0.2	0.0 ± 0.1	0.7 ± 0.8
G4 octyl	2.0 ± 0.6	1.2 ± 1.4	2.5 ± 0.5	1.1 ± 1.0	0.7 ± 1.0	0.4 ± 0.9	1.5 ± 0.8	2.4 ± 1.5
G4 octyl/NO	4.0 ± 0.8	3.7 ± 0.4	3.0 ± 0.6	4.2 ± 0.8	2.7 ± 0.8	4.3 ± 1.4	2.6 ± 0.6	4.4 ± 1.0
G4 octylQA	0.5 ± 0.9	0.1 ± 0.5	0.0 ± 0.3	0.2 ± 0.3	0.2 ± 0.4	-0.2 ± 0.1	0.5 ± 0.5	0.4 ± 0.8
G4 octylQA/NO	4.1 ± 0.9	3.5 ± 1.3	2.3 ± 0.5	2.6 ± 0.8	3.4 ± 0.7	4.7 ± 1.2	3.2 ± 1.0	4.7 ± 0.9

[a]For all measurements, $n \geq 3$ pooled experiments.

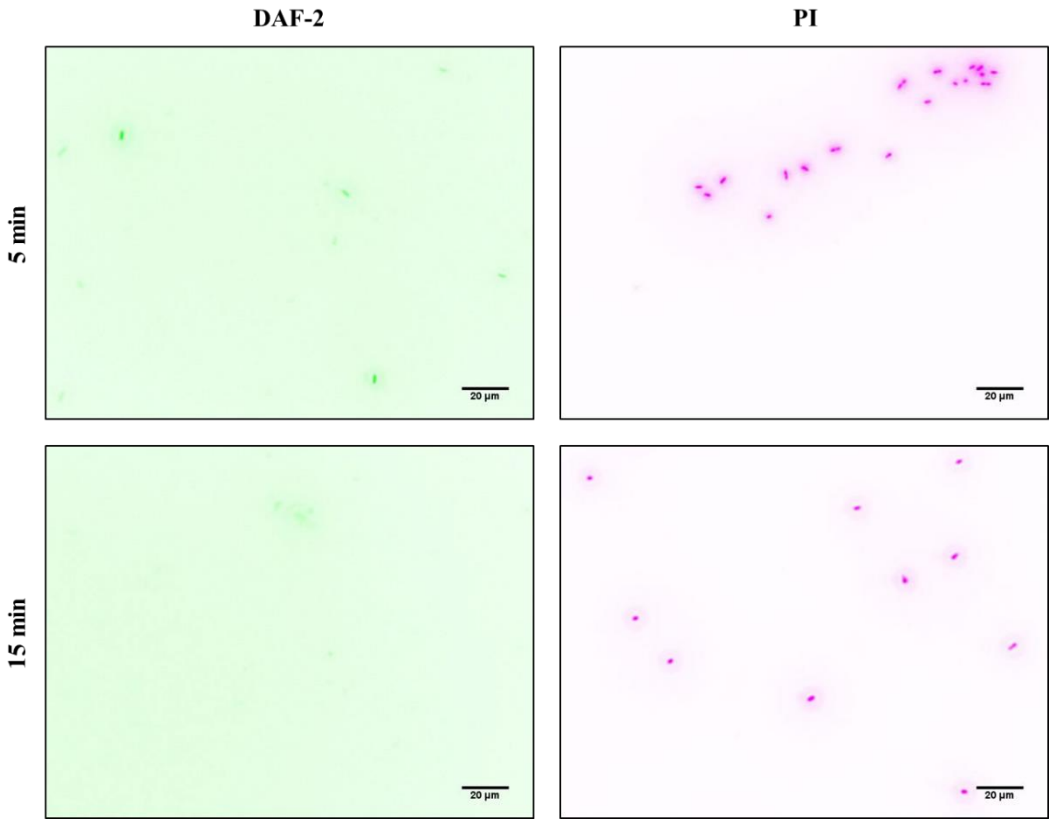

Figure 6.5 Fluorescence microscopy images of *P. aeruginosa* exposed to TP 470/HP 93A-G4 octyl/NO fibers for 5 and 15 minutes. DAF-2 green fluorescence depicts intracellular NO, while PI red fluorescence indicates compromised membranes. Threshold inverted for clarity.

result of dendrimer-induced bacterial killing, corroborating our observation that greater dendrimer delivery from NO-releasing fibers increases bactericidal action compared to control fibers.

6.3.5 In vitro cytotoxicity

Toxicity of the electrospun fibers was assessed against L929 mouse fibroblast cells over 2 and 24 h. For comparison, the inhibitory concentrations at 50% cell viability (IC_{50}) against L929 mouse fibroblasts were evaluated for each of the control and NO-releasing dendrimers at both timepoints. As expected, both control and NO-releasing dendrimers were significantly more toxic at longer timescales, with IC_{50} values ranging from 200 – 360 and 40 – 100 μg/mL after 2 and 24 h, respectively (Appendix). Due to this toxicity of octyl- and octylQA-modified dendrimers alone at relatively low concentrations, we hypothesized that the NO-releasing polyurethane fibers would exhibit substantial toxicity to L929 cells after 24 h exposure. Yet, all of the fiber formulations were relatively non-toxic (≥ 80% cell viability) at both timepoints (Figure 6.6, Appendix). The most significant toxicity was observed for the blank and control SG 80A/HP 93A fibers after 24 h (86 and 82% cell viability, respectively), while the SG 80A/HP 93A-G4 octyl/NO fibers exhibited no reduction in viability. The reduction in cell viability observed for the blank fibers is attributed to cell adhesion to the fiber mat and subsequent removal from the culture plate. All of NO-releasing fibers demonstrated at least ~95% cell viability or greater, suggesting that releasing antibacterial dendrimers from electrospun fibers over time reduces their toxicity compared to direct exposure.

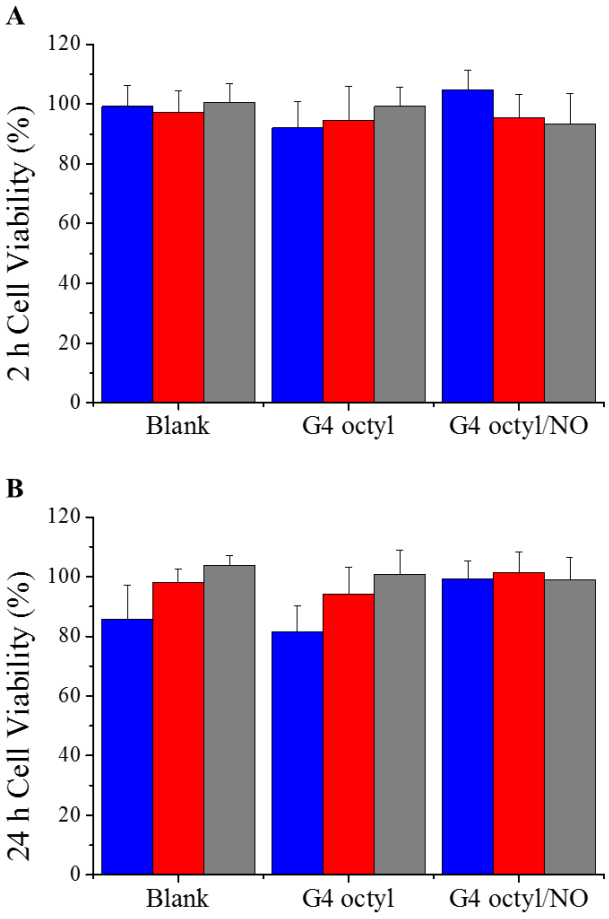

Figure 6.6 Viability (%) of L929 mouse fibroblast cells following (A) 2 h or (B) 24 h exposure to blank, control, and NO-releasing electrospun SG 80A/HP 93A (blue), TP 470/SG 80A (red), and TP 470/HP 93A (gray) fibers. For all measurements, $n \geq 3$ pooled experiments with error bars representing standard deviation of the mean.

6.4 Conclusions

The utility of dendrimer- and NO-releasing electrospun polyurethane fibers as potential antibacterial wound dressings was evaluated as a function of polyurethane composition and dendrimer modification. The dendrimer-doped electrospun fibers exhibited adequate porosity and water absorption capabilities that should enable dynamic gas and fluid exchange in a chronic wound setting. The release of antibacterial dendrimers and NO were tuned by adjusting the sheath polyurethane hydrophobicity, dendrimer modification, and amount of dendrimer incorporated into the fibers. Fibers fabricated using a less hydrophobic sheath polyurethane were characterized by faster dendrimer and NO release, while the charged dendrimer modifications (e.g., *N*-diazeniumdiolate or QA moieties) resulted in greater dendrimer delivery. Similarly, NO-release kinetics were dependent on the dendrimer modification, reflecting the relative kinetics of the NO-releasing dendrimers in solution. The NO-releasing TP 470/HP 93A fibers demonstrated moderate to high antibacterial activity against several Gram-negative and Gram-positive species at both short and long timescales, averaging a 4-log reduction in bacterial viability after 24 h exposure. Finally, the release of the control and NO-releasing dendrimers from the electrospun fibers reduced the overall toxicity of the dendrimer scaffold to mammalian cells, demonstrating the utility of these fibers as broad-spectrum antibacterial dressings with minimal cytotoxic effects.

REFERENCES

(1) James, G. A., Swogger, E., Wolcott, R., Secor, P., Sestrich, J., Costerton, J. W., and Stewart, P. S. "Biofilms in chronic wounds" *Wound Repair and Regeneration* **2008**, *16*, 37-44.

(2) Bjarnsholt, T., Kirketerp-Møller, K., Jensen, P. Ø., Madsen, K. G., Phipps, R., Krogfelt, K., Høiby, N., and Givskov, M. "Why chronic wounds will not heal: A novel hypothesis" *Wound Repair and Regeneration* **2008**, *16*, 2-10.

(3) Blakytny, R., and Jude, E. "The molecular biology of chronic wounds and delayed healing in diabetes" *Diabetic Medicine* **2006**, *23*, 594-608.

(4) Zahedi, P., Rezaeian, I., Ranaei-Siadat, S. O., Jafari, S. H., and Supaphol, P. "A review on wound dressings with an emphasis on electrospun nanofibrous polymeric bandages" *Polymers for Advanced Technologies* **2010**, *21*, 77-95.

(5) Khil, M. S., Cha, D. I., Kim, H. Y., Kim, I. S., and Bhattarai, N. "Electrospun nanofibrous polyurethane membrane as wound dressing" *Journal of Biomedical Materials Research Part B: Applied Biomaterials* **2003**, *67*, 675-679.

(6) Sabitha, M., and Rajiv, S. "Preparation and characterization of ampicillin- incorporated electrospun polyurethane scaffolds for wound healing and infection control" *Polymer Engineering & Science* **2015**, *55*, 541-548.

(7) Yao, C., Li, X., Neoh, K., Shi, Z., and Kang, E. "Surface modification and antibacterial activity of electrospun polyurethane fibrous membranes with quaternary ammonium moieties" *Journal of Membrane Science* **2008**, *320*, 259-267.

(8) Yücedag, F., Atalay-Oral, C., Erkal, S., Sirkecioglu, A., Karasartova, D., Sahin, F., Tantekin-Ersolmaz, S. B., and Güner, F. S. "Antibacterial oil-based polyurethane films for wound dressing applications" *Journal of Applied Polymer Science* **2010**, *115*, 1347-1357.

(9) Andersen, K. E., Franken, C. P. M., Gad, P., Larsen, A. M., Larsen, J. R., Franciscus, P. A., Van Neer, A., Vuerstaek, J., Wuite, J., and Martino, H. A. "A randomized, controlled study to compare the effectiveness of two foam dressings in the management of lower leg ulcers" *Ostomy Wound Management* **2002**, *48*, 34-41.

(10) Payne, W. G., Posnett, J., Alvarez, O., Brown-Etris, M., Jameson, G., Wolcott, R., Dharma, H., Hartwell, S., and Ochs, D. "A prospective, randomized clinical trial to assess

the cost-effectiveness of a modern foam dressing versus a traditional saline gauze dressing in the treatment of stage II pressure ulcers" *Ostomy Wound Management* **2009**, *55*, 50-55.

(11) Jørgensen, B., Price, P., Andersen, K. E., Gottrup, F., Bech-Thomsen, N., Scanlon, E., Kirsner, R., Rheinen, H., Roed-Petersen, J., and Romanelli, M. "The silver-releasing foam dressing, contreet foam, promotes faster healing of critically colonised venous leg ulcers: A randomised, controlled trial" *International Wound Journal* **2005**, *2*, 64-73.

(12) Lo, S. F., Chang, C. J., Hu, W. Y., Hayter, M., and Chang, Y. T. "The effectiveness of silver-releasing dressings in the management of non-healing chronic wounds: A meta-analysis" *Journal of Clinical Nursing* **2009**, *18*, 716-728.

(13) Lo, S. F., Hayter, M., Chang, C. J., Hu, W. Y., and Lee, L. L. "A systematic review of silver-releasing dressings in the management of infected chronic wounds" *Journal of Clinical Nursing* **2008**, *17*, 1973-1985.

(14) Staso, M. A., Raschbaum, M., Slater, H., and Goldfarb, I. W. "Experience with Omiderm-a new burn dressing" *Journal of Burn Care & Research* **1991**, *12*, 209.

(15) Yari, A., Yeganeh, H., and Bakhshi, H. "Synthesis and evaluation of novel absorptive and antibacterial polyurethane membranes as wound dressing" *Journal of Materials Science: Materials in Medicine* **2012**, *23*, 2187-2202.

(16) Bhardwaj, N., and Kundu, S. C. "Electrospinning: A fascinating fiber fabrication technique" *Biotechnology Advances* **2010**, *28*, 325-347.

(17) He, C. L., Huang, Z. M., Han, X. J., Liu, L., Zhang, H. S., and Chen, L. S. "Coaxial electrospun poly (L-lactic acid) ultrafine fibers for sustained drug delivery" *Journal of Macromolecular Science, Part B* **2006**, *45*, 515-524.

(18) Jannesari, M., Varshosaz, J., Morshed, M., and Zamani, M. "Composite poly (vinyl alcohol)/poly (vinyl acetate) electrospun nanofibrous mats as a novel wound dressing matrix for controlled release of drugs" *International Journal of Nanomedicine* **2011**, *6*, 993-1003.

(19) Unnithan, A. R., Barakat, N. A., Pichiah, P. T., Gnanasekaran, G., Nirmala, R., Cha, Y.-S., Jung, C.-H., El-Newehy, M., and Kim, H. Y. "Wound-dressing materials with antibacterial activity from electrospun polyurethane–dextran nanofiber mats containing ciprofloxacin HCl" *Carbohydrate Polymers* **2012**, *90*, 1786-1793.

(20) Thakur, R., Florek, C., Kohn, J., and Michniak, B. "Electrospun nanofibrous polymeric scaffold with targeted drug release profiles for potential application as wound dressing" *International Journal of Pharmaceutics* **2008**, *364*, 87-93.

(21) Dongargaonkar, A. A., Bowlin, G. L., and Yang, H. "Electrospun blends of gelatin and gelatin–dendrimer conjugates as a wound-dressing and drug-delivery platform" *Biomacromolecules* **2013**, *14*, 4038-4045.

(22) Lalani, R., and Liu, L. "Electrospun zwitterionic poly (sulfobetaine methacrylate) for nonadherent, superabsorbent, and antimicrobial wound dressing applications" *Biomacromolecules* **2012**, *13*, 1853-1863.

(23) Landsdown, A., and Williams, A. "Bacterial resistance to silver in wound care and medical devices" *Journal of Wound Care* **2007**, *16*, 15-19.

(24) Percival, S., Bowler, P., and Russell, D. "Bacterial resistance to silver in wound care" *Journal of Hospital Infection* **2005**, *60*, 1-7.

(25) Boucher, H. W., Talbot, G. H., Bradley, J. S., Edwards, J. E., Gilbert, D., Rice, L. B., Scheld, M., Spellberg, B., and Bartlett, J. "Bad bugs, no drugs: No eskape!" *Clinical Infectious Diseases* **2009**, *48*, 1-12.

(26) Hetrick, E. M., Shin, J. H., Stasko, N. A., Johnson, C. B., Wespe, D. A., Holmuhamedov, E., and Schoenfisch, M. H. "Bactericidal efficacy of nitric oxide-releasing silica nanoparticles" *ACS Nano* **2008**, *2*, 235-246.

(27) Schäffer, M. R., Tantry, U., Gross, S. S., Wasserkrug, H. L., and Barbul, A. "Nitric oxide regulates wound healing" *Journal of Surgical Research* **1996**, *63*, 237-240.

(28) Shekhter, A. B., Serezhenkov, V. A., Rudenko, T. G., Pekshev, A. V., and Vanin, A. F. "Beneficial effect of gaseous nitric oxide on the healing of skin wounds" *Nitric Oxide* **2005**, *12*, 210-219.

(29) Carpenter, A. W., and Schoenfisch, M. H. "Nitric oxide release: Part II. Therapeutic applications" *Chemical Society Reviews* **2012**, *41*, 3742-3752.

(30) Riccio, D. A., and Schoenfisch, M. H. "Nitric oxide release: Part I. Macromolecular scaffolds" *Chemical Society Reviews* **2012**, *41*, 3731-3741.

(31) Duncan, R., and Izzo, L. "Dendrimer biocompatibility and toxicity" *Advanced Drug Delivery Reviews* **2005**, *57*, 2215-2237.

(32) Malik, N., Wiwattanapatapee, R., Klopsch, R., Lorenz, K., Frey, H., Weener, J., Meijer, E., Paulus, W., and Duncan, R. "Dendrimers: Relationship between structure and biocompatibility in vitro, and preliminary studies on the biodistribution of 125I-labelled polyamidoamine dendrimers in vivo" *Journal of Controlled Release* **2000**, *65*, 133-148.

(33) Svenson, S. "Dendrimers as versatile platform in drug delivery applications" *European Journal of Pharmaceutics and Biopharmaceutics* **2009**, *71*, 445-462.

(34) Carpenter, A. W., Worley, B. V., Slomberg, D. L., and Schoenfisch, M. H. "Dual action antimicrobials: Nitric oxide release from quaternary ammonium-functionalized silica nanoparticles" *Biomacromolecules* **2012**, *13*, 3334-3342.

(35) Lu, Y., Slomberg, D. L., Shah, A., and Schoenfisch, M. H. "Nitric oxide-releasing amphiphilic poly (amidoamine)(PAMAM) dendrimers as antibacterial agents" *Biomacromolecules* **2013**, *14*, 3589-3598.

(36) Worley, B. V., Schilly, K. M., and Schoenfisch, M. H. "Anti-biofilm efficacy of dual-action nitric oxide-releasing alkyl chain modified poly(amidoamine) dendrimers" *Molecular Pharmaceutics* **2015**, *12*, 1573-1583.

(37) Worley, B. V., Slomberg, D. L., and Schoenfisch, M. H. "Nitric oxide-releasing quaternary ammonium-modified poly(amidoamine) dendrimers as dual action antibacterial agents" *Bioconjugate Chemistry* **2014**, *25*, 918-927.

(38) Cottarel, G., and Wierzbowski, J. "Combination drugs, an emerging option for antibacterial therapy" *Trends in Biotechnology* **2007**, *25*, 547-555.

(39) Eliopoulos, G., and Eliopoulos, C. "Antibiotic combinations: Should they be tested?" *Clinical Microbiology Reviews* **1988**, *1*, 139-156.

(40) Tomalia, D., Baker, H., Dewald, J., Hall, M., Kallos, G., Martin, S., Roeck, J., Ryder, J., and Smith, P. "A new class of polymers: Starburst-dendritic macromolecules" *Polymer Journal* **1985**, *17*, 117-132.

(41) Tomalia, D. A. "Birth of a new macromolecular architecture: Dendrimers as quantized building blocks for nanoscale synthetic polymer chemistry" *Progress in Polymer Science* **2005**, *30*, 294-324.

(42) Coneski, P. N., Nash, J. A., and Schoenfisch, M. H. "Nitric oxide-releasing electrospun polymer microfibers" *ACS Applied Materials & Interfaces* **2011**, *3*, 426-432.

(43) Koh, A., Carpenter, A. W., Slomberg, D. L., and Schoenfisch, M. H. "Nitric oxide-releasing silica nanoparticle-doped polyurethane electrospun fibers" *ACS Applied Materials & Interfaces* **2013**, *5*, 7956-7964.

(44) Coneski, P. N., and Schoenfisch, M. H. "Nitric oxide release: Part III. Measurement and reporting" *Chemical Society Reviews* **2012**, *41*, 3753-3758.

(45) Pham, Q. P., Sharma, U., and Mikos, A. G. "Electrospun poly (ε-caprolactone) microfiber and multilayer nanofiber/microfiber scaffolds: Characterization of scaffolds and measurement of cellular infiltration" *Biomacromolecules* **2006**, *7*, 2796-2805.

(46) Savoji, H., Rana, D., Matsuura, T., Tabe, S., and Feng, C. "Development of plasma and/or chemically induced graft co-polymerized electrospun poly (vinylidene fluoride) membranes for solute separation" *Separation and Purification Technology* **2013**, *108*, 196-204.

(47) Sun, B., Slomberg, D. L., Chudasama, S. L., Lu, Y., and Schoenfisch, M. H. "Nitric oxide-releasing dendrimers as antibacterial agents" *Biomacromolecules* **2012**, *13*, 3343-3354.

(48) Gallant-Behm, C. L., Yin, H. Q., Liu, S., Heggers, J. P., Langford, R. E., Olson, M. E., Hart, D. A., and Burrell, R. E. "Comparison of in vitro disc diffusion and time kill-kinetic assays for the evaluation of antimicrobial wound dressing efficacy" *Wound Repair and Regeneration* **2005**, *13*, 412-421.

(49) Soto, R. J., Privett, B. J., and Schoenfisch, M. H. "In vivo analytical performance of nitric oxide-releasing glucose biosensors" *Analytical Chemistry* **2014**, *86*, 7141-7149.

(50) Bryers, J. D. "Medical biofilms" *Biotechnology and Bioengineering* **2008**, *100*, 1-18.

(51) Costerton, J. W., Stewart, P. S., and Greenberg, E. "Bacterial biofilms: A common cause of persistent infections" *Science* **1999**, *284*, 1318-1322.

(52) Vogt, C., Xing, Q., He, W., Li, B., Frost, M. C., and Zhao, F. "Fabrication and characterization of a nitric oxide-releasing nanofibrous gelatin matrix" *Biomacromolecules* **2013**, *14*, 2521-2530.

(53) Hall, R. E., Bender, G., and Marquis, R. E. "Inhibitory and cidal antimicrobial actions of electrically generated silver ions" *Journal of Oral and Maxillofacial Surgery* **1987**, *45*, 779-784.

CHAPTER 7:

Summary and Future Directions

7.1 Summary

The synthesis and subsequent microbiological evaluation of dual-action poly(amidoamine) (PAMAM) dendrimer biocides, followed by the design and preparation of nitric oxide (NO)-releasing electrospun polyurethane fibers, represented the focus of my dissertation research. Chapter 1 provided an overview of the formation and protective mechanisms of biofilm-based infections, current research into anti-biofilm therapies, and the need for novel therapeutic agents capable of eradicating biofilms. This introduction chapter further highlighted the benefits of combining multiple biocidal mechanisms to create dual-action antibacterial agents with increased bactericidal action while minimizing the emergence of bacterial resistance.

Chapter 2 focused on modifying PAMAM dendrimers of varying generation (i.e., size and functional group density) with either quaternary ammonium (QA) moieties or alkyl chains of varying chain lengths. Nitric oxide-release kinetics were dependent on the type of modification (e.g., QA moiety or alkyl chain) and alkyl chain length but independent of dendrimer generation. Quaternary ammonium-modified PAMAM dendrimers exhibited longer NO-release half-lives than their alkyl chain-modified counterparts, suggesting stabilization of the zwitterionic *N*-diazeniumdiolate by the cationic QA moiety. While half-lives for the QA-modified dendrimers were dependent on the alkyl chain length due to bilayer vesicle formation in solution, the NO-release characteristics of the alkyl chain modifications were successfully controlled to yield dual-

action dendrimers with similar NO totals and release kinetics. The antibacterial and anti-biofilm actions of the resulting single- and dual-action dendrimers were evaluated in subsequent chapters.

In Chapter 3, the antibacterial activity of QA- and alkyl chain-modified dendrimers was determined against planktonic cultures of pathogenic bacteria. Both single and dual-action QA-modified PAMAM dendrimers exhibited biocidal activity against *P. aeruginosa* and *S. aureus*, with longer QA alkyl chains (i.e., octylQA and dodecylQA) proving more effective than shorter chain (i.e., methylQA and butylQA) modifications for both G1 and G4 dendrimer scaffolds. This work established the mechanism of biocidal action for the QA-modified dendrimers as a function of alkyl chain length and Gram designation that was lacking in previous research.[1-3] The NO-releasing octylQA- and dodecylQA-modified dendrimers exhibited similar bactericidal efficacy as their single-action counterparts due to the membrane damage inflicted on bacterial cell membranes by the long alkyl chains, greatly increasing their biocidal action but precluding the buildup of intracellular NO. However, the addition of NO-release capabilities both improved the antibacterial action of short alkyl chain QA-modified dendrimers markedly and lessened the overall toxicity of the dendrimer scaffolds to mouse fibroblast cells, indicating the benefits of the dual-action system. The alkyl chain-modified dendrimers exhibited similar trends in bactericidal action as the QA modifications, with the shorter alkyl chains proving more effective against *P. aeruginosa* than *S. aureus*. The addition of NO release, however, had mixed effects on both the bactericidal action and cytotoxicity of the alkyl chain-modified dendrimers. Although the short alkyl chain-modified G1 dendrimers were more bactericidal with NO release, the antibacterial action for most of the remaining dendrimer biocides was not affected by NO release. However, low levels of NO release from the more effective scaffolds were found to mitigate toxicity to mammalian cells, regardless of improvements to bactericidal action.

These studies were expanded in Chapter 4 to evaluate the ability of dual-action alkyl chain-modified dendrimers to eradicate pathogenic biofilms as a function of dendrimer generation, alkyl chain length, and bacterial Gram class. Single- and dual-action dendrimers were significantly more bactericidal against *P. aeruginosa* than Gram-positive *S. aureus* or MRSA biofilms. Using confocal microscopy, this increased efficacy was attributed to the inability of the dendrimer biocides to effectively damage cell membranes in *S. aureus* biofilms compared to *P. aeruginosa*, most likely due to differences in the biofilm architecture. Dendrimer anti-biofilm efficacy was found to be highly dependent on the biocide's ability to penetrate into the biofilm and compromise cell membranes, which was corroborated using confocal microscopy. Hexyl-modified dendrimers were considerably more effective at biofilm eradication than the butyl system, likely due to a combination of greater membrane intercalation, cell membrane damage, and biofilm penetration. Furthermore, the addition of NO release enhanced the anti-biofilm action of dendrimer biocides incapable of efficient membrane disruption and biofilm penetration. While the majority of dendrimer biocides were toxic at concentrations required to eradicate Gram-positive biofilms, single- and dual-action G3 hexyl dendrimers were characterized as having a clinically relevant therapeutic index against all bacterial strains tested, suggesting the G3 dendrimer scaffold represents the ideal balance of dendrimer size and functional group density for optimal biofilm eradication with minimal cytotoxicity. Indeed, NO-releasing alkyl chain-modified G3 dendrimers demonstrated moderate to high synergy with vancomycin in the eradication of Gram-positive biofilms, reducing the toxicity of the therapy to mouse fibroblasts and indicating the possible clinical utility of these scaffolds.

In Chapter 5, G4 PAMAM dendrimers with various exterior modifications were incorporated into single component electrospun polyurethane fibers. Control and NO-releasing

G4 octyl dendrimers were first doped into fibers fabricated from one of three polyurethanes exhibiting distinct water uptake capabilities. While the fiber characteristics (i.e., fiber diameter, porosity, water absorption, and electrospinning efficiency) were dependent on polyurethane composition, the NO-release characteristics were overall independent of polyurethane hydrophobicity. Electrospun fibers composed of a moderately hydrophilic polyurethane (Tecoflex) were doped with dendrimers exhibiting various exterior modifications (e.g., alkyl chains and QAs) and a range of NO-release kinetics. The NO-release properties of the resulting electrospun fibers reflected those of the dendrimer dopant, indicating the dendrimer modification has greater influence on the NO-release characteristics of single component electrospun fibers than the polyurethane composition. Both control and NO-releasing dendrimer-doped electrospun Tecoflex fibers exhibited decreased L929 cell adhesion from blank Tecoflex fibers, with the fibroblasts exposed to NO-releasing fibers demonstrating non-adhesive morphologies, suggesting NO-releasing electrospun fibers will allow for easy, painless wound dressing removal without harming the newly formed skin underneath. However, the NO-releasing Tecoflex fibers exhibited low antibacterial and anti-adhesive action against *P. aeruginosa* and *S. aureus* bacteria, limiting the clinical utility of these fibers and necessitating the development of fibers capable of greater NO storage to allow for enhanced bactericidal action.

To improve the antibacterial action of NO-releasing electrospun fibers, antibacterial dendrimers were incorporated into electrospun composite polyurethane fibers in Chapter 6. Composite electrospun fibers were formed from three medical grade thermoplastic polyurethanes using a co-axial electrospinning method. The dendrimer dopant (i.e., G4 octyl or G4 octylQA) and polyurethane composition were varied to evaluate the effects of dendrimer modification and polyurethane hydrophobicity on fiber mat characteristics, including leaching of the dual-action

antibacterial scaffold into solution. Release of antibacterial dendrimers from the fibrous mats was influenced by the polyurethane composition and dendrimer modification. Increased hydrophobicity of the sheath polyurethane slowed dendrimer release from the electrospun fibers, while charged dendrimer modifications resulted in greater overall dendrimer release. While the identity of the core polyurethane had little effect on NO-release kinetics, the use of a more hydrophilic sheath polyurethane led to faster NO release due to the sheath polyurethane being a less effective barrier layer to both water and dendrimer leaching. Similar to the results in Chapter 5, NO-release kinetics were dependent on the dendrimer modification and reflected the kinetics of the dendrimers alone in solution. Nitric oxide-releasing fibers demonstrated moderate to high broad-spectrum antibacterial activity against four pathogenic species at both short (2 h) and long (24 h) timescales. The long-term bactericidal action was due to the release of greater dual-action dendrimer concentrations from the NO-releasing fibers, averaging a 4-log reduction in bacterial viability after 24 h exposure. Finally, release of the control and NO-releasing dendrimers from electrospun fibers reduced their overall toxicity to mammalian cells, demonstrating the utility of these fibers as broad-spectrum antibacterial dressings with minimal cytotoxic effects.

7.2 Future Directions

The investigations described in the prior chapters established the utility of NO-releasing dendrimer scaffolds as dual-action antibacterial agents, including the first report of NO-releasing dendrimer efficacy against MRSA biofilms. Incorporation of these dendrimer biocides into electrospun polyurethane fibers proved highly antibacterial ($\geq$3-log reduction in bacterial viability) against four strains of pathogenic bacteria. While the results described herein demonstrate the utility of NO-releasing dendrimers as dual-action antibacterial agents alone and as dopants in electrospun fibers, substantial work is required before these therapeutics can be employed in a

clinical setting. In this section, techniques to improve the efficacy and utility of NO-releasing dendrimers and electrospun fibers will be discussed, as well as studies to further demonstrate the ability of these materials to eradicate pathogenic biofilms.

7.2.1 Studies to increase the antibacterial action of dual-action scaffolds

In Chapters 3 and 4, the antibacterial and anti-biofilm efficacy of dual-action dendrimer scaffolds was evaluated, with control and NO-releasing G3 hexyl dendrimers exhibiting the most efficient anti-biofilm action and minimal toxicity to mammalian cells. However, the addition of NO release had little impact on the antibacterial action of the dendrimer scaffold for many of the highly bactericidal agents discussed herein due to significant membrane disruption precluding buildup of intracellular NO. To improve the antibacterial action of NO in conjunction with these contact-based biocides, the effects of NO-release kinetics on bactericidal action must be evaluated. In previous work, the antibacterial activity of NO-releasing silica nanoparticles was found to be highly dependent on NO flux and bacterial identity.[4, 5] Lu et al. demonstrated that silica particles exhibiting faster NO-release kinetics eradicated planktonic cultures of both *S. aureus* and *P. aeruginosa* at significantly lower NO doses. Designing NO-releasing dendrimers with shorter NO-release half-lives and larger initial NO fluxes may improve the anti-biofilm action of the dual-action scaffold against these pathogenic strains.

In addition to improving the efficacy of dendrimer scaffolds, future work should evaluate the bactericidal action of NO-releasing hyperbranched polymers. While hyperbranched polymers exhibit similar multivalency as dendrimers, they can be synthesized via a one-pot reaction versus the time-consuming synthetic protocols required to form dendrimer scaffolds.[6-9] Similar to dendrimers, the scaffold exterior can be tailored through modification of the terminal end groups, although these can be either primary amines or hydroxyl groups.[6] Scaffold properties may be

altered further through backbone or hybrid modification, allowing for greater synthetic control over the hyperbranched structure and the fabrication of biocompatible or biodegradable polymers that may be less toxic to mammalian cells. The use of hyperbranched polymers may allow for the same advantages afforded by the multivalent dendrimer scaffold while reducing the overall toxicity of the therapeutic.

7.2.2 Methods to extend nitric oxide release from electrospun fibers

In Chapters 5 and 6, electrospun polyurethane fibers were fabricated to incorporate antibacterial NO-releasing dendrimer scaffolds. The resulting NO-release characteristics were highly dependent on dendrimer modification, reflecting the release kinetics of the dendrimers in solution. The release durations for these fibers were relatively short (<12 h), likely limiting the ability of NO to enhance wound healing or antibacterial action. Ideally, prolonged NO release would improve clinical utility by allowing for greater time between dressing changes (i.e., 1 – 3 days versus <1 day) while maintaining antibacterial action and wound healing.[10]

A promising method for extending NO release from electrospun fibers may be direct modification of the polyurethane with NO donors prior to electrospinning. Direct polymer functionalization has several advantages over the incorporation of NO donors, including mitigating any potential toxicity from leached NO donors and extending NO release. Direct modification of the polymer may alter its overall characteristics, which would require further investigation into polymer stability and mechanical properties. Previous work has demonstrated the modification of polyurethanes with *N*-diazeniumdiolate NO donors through two general methods: 1) incorporating amine sites pendant to the polymer backbone and subsequent reaction with gaseous NO; or, 2) modifying the polymer backbone with O^2-protected diazeniumdiolate functionalities followed by deprotection.[11-13] Several methods have been developed to tether amine sites to the polymer

backbone, including adding secondary amine-containing monomers to the synthetic solution prior to polymerization, linking secondary amines to the polyurethane amide, and integrating lysine residues into polymer chain extenders.[12-15] The resultant NO storage is dependent on the efficiencies of polymer modification and NO reaction with the derivatized polymer. However, the use of protected *N*-diazeniumdiolate functionalities may potentially allow for controlled and predictable NO payloads from the polymer.[13] Directly modifying polyurethanes with NO donors should allow for increased control over the NO-release characteristics, including NO flux, payload, and duration. To evaluate the potential synthetic control, electrospun fibers should be fabricated from secondary-amine containing polyurethanes both before and after *N*-diazeniumdiolate formation.

In all of the aforementioned studies, PAMAM dendrimers were modified with *N*-diazeniumdiolate NO donors to allow for controllable NO storage and release. In aqueous solutions at neutral or acidic pH, *N*-diazeniumdiolate moieties undergo proton-initiated dissociation to spontaneously release NO (Figure 1.4B).[16, 17] Alternatively, NO release from *S*-nitrosothiol (RSNO) donors is achieved through a number of decomposition pathways (Figure 1.4A), including homolytic cleavage of the S-NO bond by light or heat, copper ion-mediated catalytic decomposition, and reaction with reducing agents (e.g., ascorbate).[18, 19] As the RSNO-derived NO release is independent of water uptake, it may be more useful in designing wound dressings for dry, low-exuding wounds where the aqueous decomposition of *N*-diazeniumdiolate NO donors would be inhibited.[10]

Modifying electrospun fibers with RSNO-derived NO release could be accomplished through either direct polyurethane functionalization or incorporation of *S*-nitrosothiol-modified scaffolds (i.e., dendrimers, hyperbranched polyesters).[6, 7, 20] In contrast to *N*-diazeniumdiolate

moieties, RSNO donors are uncharged and should be better retained within the fibers to allow for extended NO release. Initial studies in the development of NO-releasing fibers have directly modified polymers with thiols groups for RSNO donor formation. For example, Reynolds and coworkers reported the modification of polymers with three distinct thiol functionalities prior to electrospinning, followed by nitrosation to yield NO-releasing fibers with variable NO-release kinetics and durations.[21] Similarly, Vogt et al. formed a highly porous nanofibrous gelatin matrix through phase separation fabrication.[22] This scaffold was subsequently functionalized with a thiol precursor and nitrosated to produce photoinitiated NO-releasing matrices. Coneski et al. incorporated free thiols into both the hard and soft segment polyurethane domains, with soft segment-thiol modification demonstrating retention of polyurethane characteristics and high thiol to RSNO conversion efficiencies.[23] The various methods of RSNO integration into electrospun fibers should allow for synthetic control to finely tune the duration and flux of NO release independent of water uptake.

7.2.3 Antibacterial action against polymicrobial biofilms

As discussed in Chapter 1, pathogenic biofilms are complex and diverse multi-organism communities.[24-29] As such, polymicrobial biofilm models (i.e., biofilms composed of several bacterial strains) should be used to more accurately represent in vivo biofilms as opposed to the over-simplified monomicrobial biofilms studied herein. As *P. aeruginosa* and *S. aureus* represent the most commonly isolated species in clinical infections,[24] a proper polymicrobial model would include both of these pathogens and their antibiotic-resistant strains. A more complex model of polymicrobial biofilms would include other commonly isolated bacterial strains, such as *S. epidermidis*, *E. coli*, *Klebsiella pneumoniae*, and *Enterococcus faecalis*.[27, 30]

The biggest challenge in studying polymicrobial biofilms is quantifying the individual bacterial species present before and after treatment to accurately assess the bactericidal action of dual-action antibacterial agents. Selective plating methods can provide accurate colony counts for distinct bacterial species within polymicrobial biofilms. For example, mannitol salt agar, specific for staphylococci strains, does not allow for the growth of Gram-negative bacteria (e.g., *E. coli*, *P. aeruginosa*).[31-33] The addition of a phenol red indicator further allows for differentiation between coagulase positive (e.g., *S. aureus*) and coagulase negative staphylococci.[32] Isolation of *P. aeruginosa* is achieved using agar containing triclosan, an antimicrobial agent that selectively inhibits Gram-positive and Gram-negative bacteria, excluding *Pseudomonas* strains.[34-36] While selective plating methods allow for general isolation of bacterial strains, additional evaluation is often required for further identification or quantification.

Fluorescence in situ hybridization (FISH) can be used in combination with confocal microscopy to visualize individual bacterial strains within a polymicrobial biofilm. The use of bacteria-specific probes in conjunction with FISH allows for the identification of specific pathogenic strains, including *S. aureus*, *P. aeruginosa*, *E. faecalis*, and *K. pneumoniae*.[37, 38] Fluorescence measurements can then be used to quantify specific bacterial strains within a mixed bacterial population. Additionally, the polymerase chain reaction (PCR) can be used to isolate, amplify, and selectively detect pathogens from a complex bacterial community. Species-specific primers have been developed for *P. aeruginosa*, *S. aureus*, MRSA, and *E. faecalis*, allowing for the determination of population distribution and bacterial load using quantitative, real-time PCR.[38-40]

7.3 Conclusions

The work described herein highlights the importance of complete biofilm eradication in treating infections. As NO is a broad-spectrum antibacterial agent unlikely to foster bacterial resistance, particular focus was given to establishing the utility of NO-releasing dendrimer scaffolds as dual-action antibacterial agents capable of pathogenic biofilm eradication. Higher generation (i.e., G3 or G4) hexyl-modified dendrimers demonstrated efficient and extensive biofilm penetration, eradicating biofilms at lower concentrations and mitigating toxicity to mammalian cells. The addition of NO-release capabilities significantly enhanced the anti-biofilm activity of dendrimer scaffolds incapable of good biofilm penetration, highlighting the benefits of this dual-action system. Further, the incorporation of dual-action dendrimer biocides into electrospun composite polyurethane fibers resulted in high broad-spectrum antibacterial action and lessened the toxicity of the dendrimer scaffold against mouse fibroblast cells. The observations made in the prior chapters will aid in the future design of NO-releasing dual-action therapeutics with maximal anti-biofilm action while minimizing unwanted cytotoxicity.

REFERENCES

(1) Charles, S., Vasanthan, N., Kwon, D., Sekosan, G., and Ghosh, S. "Surface modification of poly(amidoamine) (PAMAM) dendrimer as antimicrobial agents" *Tetrahedron Letters* **2012**, *53*, 6670-6675.

(2) Chen, C. Z., Beck-Tan, N. C., Dhurjati, P., van Dyk, T. K., LaRossa, R. A., and Cooper, S. L. "Quaternary ammonium functionalized poly (propylene imine) dendrimers as effective antimicrobials: Structure-activity studies" *Biomacromolecules* **2000**, *1*, 473-480.

(3) Chen, C. Z., Cooper, S. L., and Beck-Tan, N. C. "Incorporation of dimethyldodecylammonium chloride functionalities onto poly (propylene imine) dendrimers significantly enhances their antibacterial properties" *Chemical Communications* **1999**, 1585-1586.

(4) Backlund, C., Worley, B., Sergesketter, A., and Schoenfisch, M. H. "Kinetic-dependent killing of oral pathogens with nitric oxide" *Journal of Dental Research* **2015**, *94*, 1092-1098.

(5) Lu, Y., Slomberg, D. L., Sun, B., and Schoenfisch, M. H. "Shape- and nitric oxide flux-dependent bactericidal activity of nitric oxide-releasing silica nanorods" *Small* **2013**, *9*, 2189-2198.

(6) Huang, Y., Wang, D., Zhu, X., Yan, D., and Chen, R. "Synthesis and therapeutic applications of biocompatible or biodegradable hyperbranched polymers" *Polymer Chemistry* **2015**, *6*, 2794-2812.

(7) Voit, B. I., and Lederer, A. "Hyperbranched and highly branched polymer architectures-synthetic strategies and major characterization aspects" *Chemical Reviews* **2009**, *109*, 5924-5973.

(8) Tomalia, D., Baker, H., Dewald, J., Hall, M., Kallos, G., Martin, S., Roeck, J., Ryder, J., and Smith, P. "A new class of polymers: Starburst-dendritic macromolecules" *Polymer Journal* **1985**, *17*, 117-132.

(9) Tomalia, D. A. "Birth of a new macromolecular architecture: Dendrimers as quantized building blocks for nanoscale synthetic polymer chemistry" *Progress in Polymer Science* **2005**, *30*, 294-324.

(10) Zahedi, P., Rezaeian, I., Ranaei-Siadat, S. O., Jafari, S. H., and Supaphol, P. "A review on wound dressings with an emphasis on electrospun nanofibrous polymeric bandages" *Polymers for Advanced Technologies* **2010**, *21*, 77-95.

(11) Reynolds, M. M., Frost, M. C., and Meyerhoff, M. E. "Nitric oxide-releasing hydrophobic polymers: Preparation, characterization, and potential biomedical applications" *Free Radical Biology and Medicine* **2004**, *37*, 926-936.

(12) Reynolds, M. M., Hrabie, J. A., Oh, B. K., Politis, J. K., Citro, M. L., Keefer, L. K., and Meyerhoff, M. E. "Nitric oxide releasing polyurethanes with covalently linked diazeniumdiolated secondary amines" *Biomacromolecules* **2006**, *7*, 987-994.

(13) Reynolds, M. M., Saavedra, J. E., Showalter, B. M., Valdez, C. A., Shanklin, A. P., Oh, B. K., Keefer, L. K., and Meyerhoff, M. E. "Tailored synthesis of nitric oxide-releasing polyurethanes using O^2-protected diazeniumdiolated chain extenders" *Journal of Materials Chemistry* **2010**, *20*, 3107-3114.

(14) Jun, H.-W., Taite, L. J., and West, J. L. "Nitric oxide-producing polyurethanes" *Biomacromolecules* **2005**, *6*, 838-844.

(15) Taite, L. J., Yang, P., Jun, H. W., and West, J. L. "Nitric oxide-releasing polyurethane–PEG copolymer containing the yigsr peptide promotes endothelialization with decreased platelet adhesion" *Journal of Biomedical Materials Research Part B: Applied Biomaterials* **2008**, *84*, 108-116.

(16) Davies, K. M., Wink, D. A., Saavedra, J. E., and Keefer, L. K. "Chemistry of the diazeniumdiolates. 2. Kinetics and mechanism of dissociation to nitric oxide in aqueous solution" *Journal of the American Chemical Society* **2001**, *123*, 5473-5481.

(17) Dutton, A. S., Fukuto, J. M., and Houk, K. "The mechanism of NO formation from the decomposition of dialkylamino diazeniumdiolates: Density functional theory and cbs-qb3 predictions" *Inorganic Chemistry* **2004**, *43*, 1039-1045.

(18) Hogg, N. "The biochemistry and physiology of S-nitrosothiols" *Annual Review of Pharmacology and Toxicology* **2002**, *42*, 585-600.

(19) Jen, M. C., Serrano, M. C., van Lith, R., and Ameer, G. A. "Polymer- based nitric oxide therapies: Recent insights for biomedical applications" *Advanced Functional Materials* **2012**, *22*, 239-260.

(20) Stasko, N. A., Fischer, T. H., and Schoenfisch, M. H. "S-nitrosothiol-modified dendrimers as nitric oxide delivery vehicles" *Biomacromolecules* **2008**, *9*, 834-841.

(21) Wold, K. A., Damodaran, V. B., Suazo, L. A., Bowen, R. A., and Reynolds, M. M. "Fabrication of biodegradable polymeric nanofibers with covalently attached no donors" *ACS Applied Materials & Interfaces* **2012**, *4*, 3022-3030.

(22) Vogt, C., Xing, Q., He, W., Li, B., Frost, M. C., and Zhao, F. "Fabrication and characterization of a nitric oxide-releasing nanofibrous gelatin matrix" *Biomacromolecules* **2013**, *14*, 2521-2530.

(23) Coneski, P. N., and Schoenfisch, M. H. "Synthesis of nitric oxide-releasing polyurethanes with S-nitrosothiol-containing hard and soft segments" *Polymer Chemistry* **2011**, *2*, 906-913.

(24) Bjarnsholt, T., Kirketerp-Møller, K., Jensen, P. Ø., Madsen, K. G., Phipps, R., Krogfelt, K., Høiby, N., and Givskov, M. "Why chronic wounds will not heal: A novel hypothesis" *Wound Repair and Regeneration* **2008**, *16*, 2-10.

(25) Blakytny, R., and Jude, E. "The molecular biology of chronic wounds and delayed healing in diabetes" *Diabetic Medicine* **2006**, *23*, 594-608.

(26) Bryers, J. D. "Medical biofilms" *Biotechnology and Bioengineering* **2008**, *100*, 1-18.

(27) Donlan, R. M. "Biofilm formation: A clinically relevant microbiological process" *Clinical Infectious Diseases* **2001**, *33*, 1387-1392.

(28) Hall-Stoodley, L., Costerton, J. W., and Stoodley, P. "Bacterial biofilms: From the natural environment to infectious diseases" *Nature Reviews Microbiology* **2004**, *2*, 95-108.

(29) Percival, S. L., Hill, K. E., Williams, D. W., Hooper, S. J., Thomas, D. W., and Costerton, J. W. "A review of the scientific evidence for biofilms in wounds" *Wound Repair and Regeneration* **2012**, *20*, 647-657.

(30) Dunne, W. M. "Bacterial adhesion: Seen any good biofilms lately?" *Clinical Microbiology Reviews* **2002**, *15*, 155-166.

(31) Bannerman, T. L., Peacock, S., Murray, P., Baron, E., Jorgensen, J., Landry, M., and Pfaller, M. "Staphylococcus, micrococcus, and other catalase-positive cocci" *Manual of Clinical Microbiology: Volume 1* **2006**, 390-411.

(32) Chapman, G. H. "The significance of sodium chloride in studies of Staphylococci" *Journal of Bacteriology* **1945**, *50*, 201-203.

(33) Lally, R. T., Ederer, M., and Woolfrey, B. "Evaluation of mannitol salt agar with oxacillin as a screening medium for methicillin-resistant Staphylococcus aureus" *Journal of Clinical Microbiology* **1985**, *22*, 501-504.

(34) Darzins, A., and Chakrabarty, A. "Cloning of genes controlling alginate biosynthesis from a mucoid cystic fibrosis isolate of Pseudomonas aeruginosa" *Journal of Bacteriology* **1984**, *159*, 9-18.

(35) Grant, M. A., and Holt, J. G. "Medium for the selective isolation of members of the genus Pseudomonas from natural habitats" *Applied and Environmental Microbiology* **1977**, *33*, 1222-1224.

(36) King, E. O., Ward, M. K., and Raney, D. E. "Two simple media for the demonstration of pyocyanin and fluorescin" *The Journal of Laboratory and Clinical Medicine* **1954**, *44*, 301-307.

(37) Kempf, V. A., Trebesius, K., and Autenrieth, I. B. "Fluorescent in situ hybridization allows rapid identification of microorganisms in blood cultures" *Journal of Clinical Microbiology* **2000**, *38*, 830-838.

(38) Dalton, T., Dowd, S. E., Wolcott, R. D., Sun, Y., Watters, C., Griswold, J. A., and Rumbaugh, K. P. "An in vivo polymicrobial biofilm wound infection model to study interspecies interactions" *PloS one* **2011**, *6*, 1-10.

(39) Sun, Y., Dowd, S. E., Smith, E., Rhoads, D. D., and Wolcott, R. D. "In vitro multispecies lubbock chronic wound biofilm model" *Wound Repair and Regeneration* **2008**, *16*, 805-813.

(40) Warren, D. K., Liao, R. S., Merz, L. R., Eveland, M., and Dunne, W. M. "Detection of methicillin-resistant Staphylococcus aureus directly from nasal swab specimens by a real-time PCR assay" *Journal of Clinical Microbiology* **2004**, *42*, 5578-5581.

APPENDIX:

Supplemental Information for Chapter 6

Table A1. Characterization and NO-release properties of G4 dendrimers in PBS (pH 7.4, 37 °C) as measured by a chemiluminescence NO analyzer[a].

	No. Modified End Groups[a]	% Modified	Molec. Weight (Da)	$[NO]_{max}$[c] (ppb/mg)	t_{max}[d] (min)	t[NO][e] (μmol/mg)	$t_{1/2}$[f] (min)	t_d[g] (h)
G4 octyl/NO	47 ± 3	74 ± 5	25987.7	4760 ± 920	2.7 ± 0.4	0.92 ± 0.06	25 ± 6	9 ± 1
G4 octylQA/NO	39 ± 5	61 ± 8	23953.6	1570 ± 150	2.0 ± 0.3	1.03 ± 0.06	115 ± 6	16 ± 1

[a]For all measurements, n ≥ 3 pooled experiments. [b]Determined by ^{1}H NMR. [c]Maximum flux of NO release. [e]Time required to reach maximum flux. [e]Total NO payload released. [f]NO release half-life. [g]Duration of NO release.

Table A2. Inhibitory concentrations at 50% viability (IC_{50}) against L929 mouse fibroblast cells.[a]

	2h IC_{50} (µg/mL)	**24h IC_{50} (µg/mL)**
G4 octyl	200	60
G4 octyl/NO	360	100
G4 octylQA	300	60
G4 octylQA/NO	280	40

[a]For all measurements, $n \geq 3$ pooled experiments

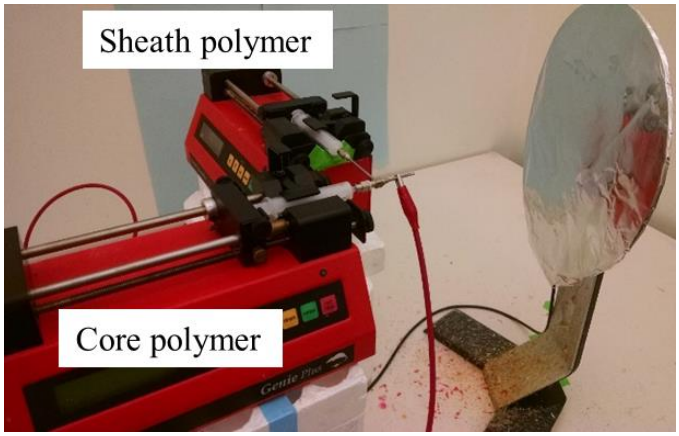

Figure A1. Custom electrospinning apparatus in co-axial configuration

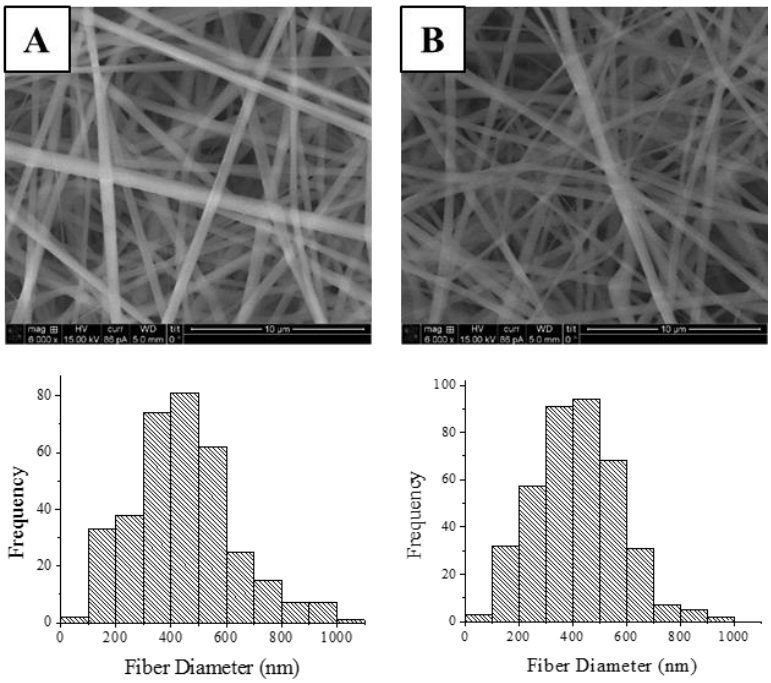

Figure A2. Scanning electron micrographs of (A) TP 470/HP 93A-G4 octylQA and (B) TP 470/HP 93A-G4 octylQA/NO electrospun fibers with corresponding fiber diameter histograms.

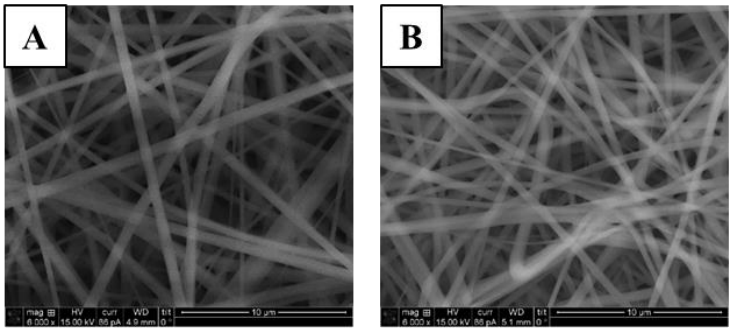

Figure A3. Scanning electron micrographs of (A) TP 470/HP 93A-G4 RITC octyl/NO and (B) TP 470/HP 93A-G4 RITC octylQA/NO electrospun fibers.

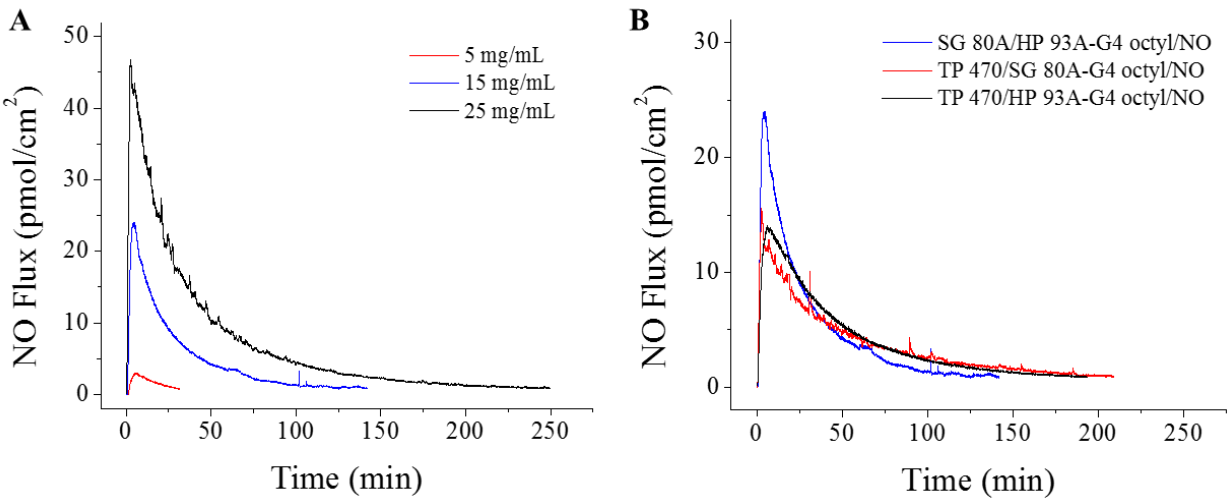

Figure A4. Representative NO-release profiles for (A) SG 80A/HP 93A-G4 octyl/NO fibers at 5 (red), 15 (blue), and 25 (black) mg/mL dendrimer concentrations, and (B) G4 octyl/NO-doped electrospun SG 80A/HP 93A (blue), TP 470/SG 80A (red), TP 470/HP 93A (black) fibers.

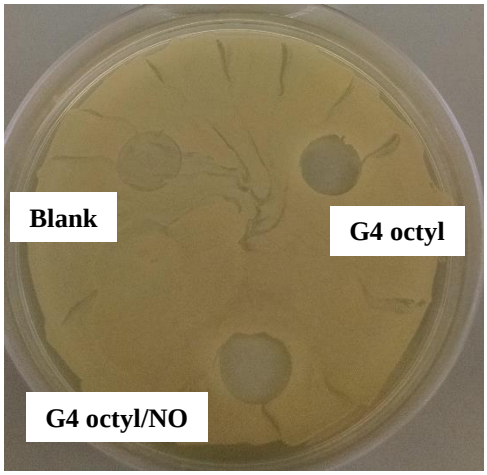

Figure A5. Zone of inhibition images against MRSA showing no bacteria growth under control and NO-releasing TP 470/SG80A-G4 octyl fibers

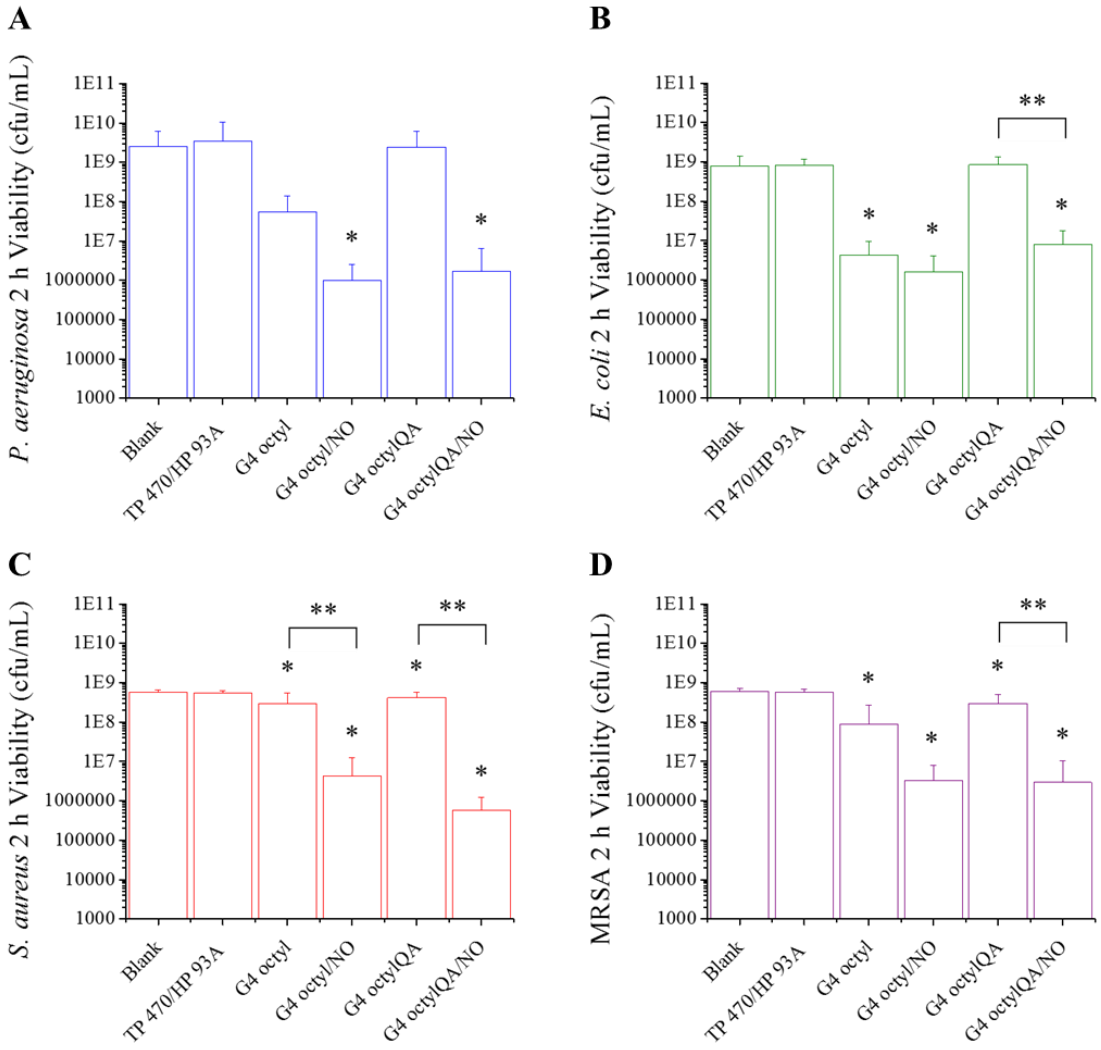

Figure A6. Viability of (A) *P. aeruginosa*, (B) *E. coli*, (C) *S. aureus*, and (D) MRSA after 2 h exposure to blank, control, and NO-releasing co-axial electrospun TP 470/HP 93A fibers. For all measurements, $n \geq 3$ pooled experiments with error bars representing standard deviation of the mean. Asterisk (*) indicates significant differences from blank ($p < 0.05$) and double asterisk (**) indicates significant differences ($p < 0.05$) using two-tailed student's t-test.

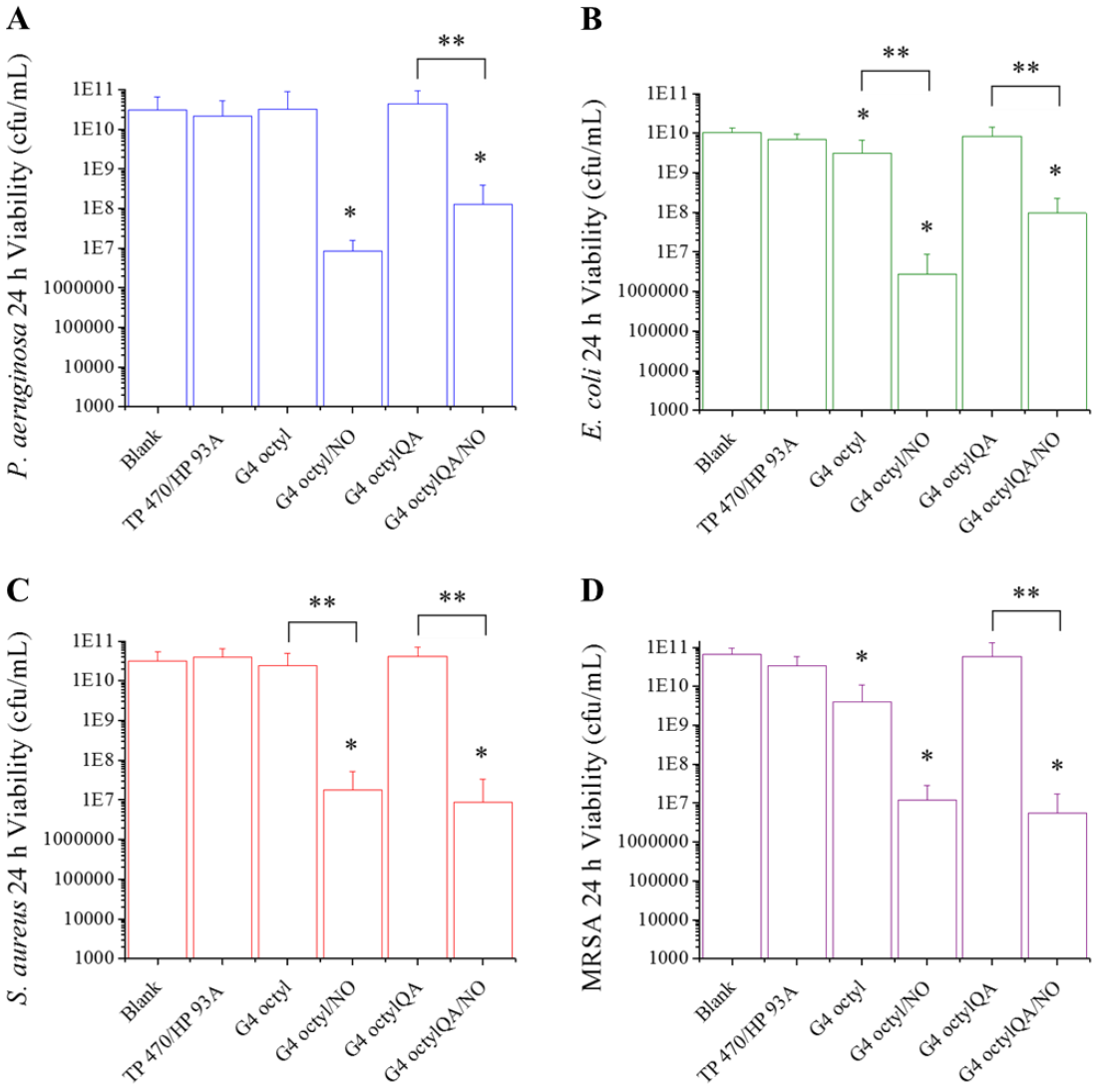

Figure A7. Viability of (A) *P. aeruginosa*, (B) *E. coli*, (C) *S. aureus*, and (D) MRSA after 24 h exposure to blank, control, and NO-releasing co-axial electrospun TP 470/HP 93A fibers. For all measurements, n ≥ 3 pooled experiments with error bars representing standard deviation of the mean. Asterisk (*) indicates significant differences from blank ($p < 0.05$) and double asterisk (**) indicates significant differences ($p < 0.05$) using two-tailed student's t-test.

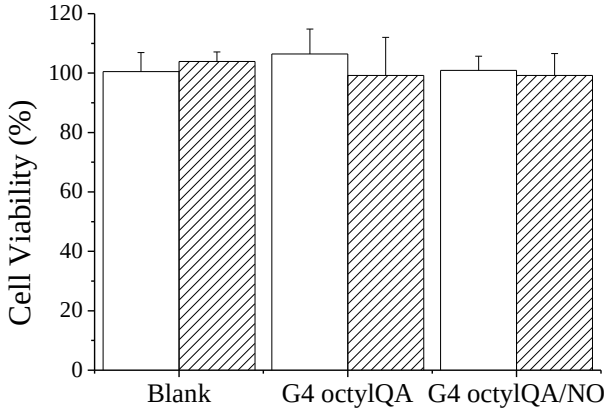

Figure A8. Viability (%) of L929 mouse fibroblast cells following 2 h (solid) or 24 h (diagonal lines) exposure to blank, control, and NO-releasing electrospun TP 470/HP 93A-G4 octylQA fibers. For all measurements, $n \geq 3$ pooled experiments with error bars representing standard deviation of the mean.